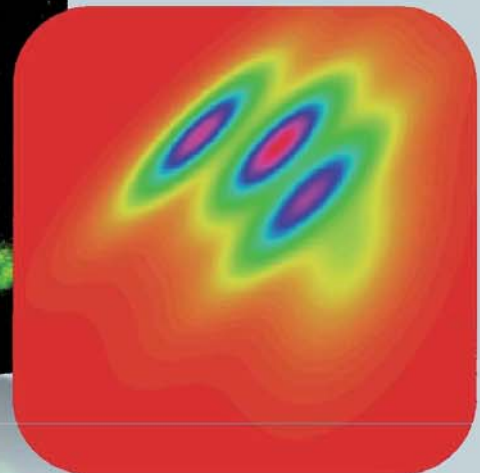
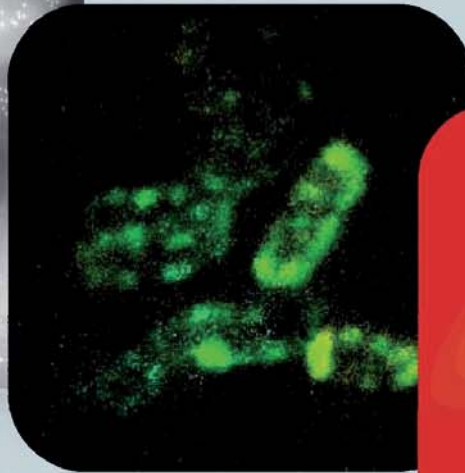
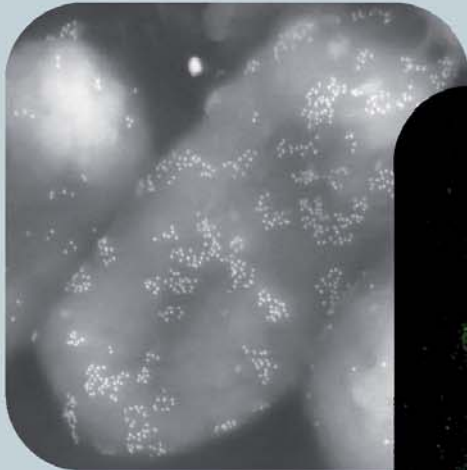




Technische  
Universität  
Braunschweig



## Holistic bioprocess engineering of antibody fragment secreting *Bacillus megaterium*

Florian David



**ibvt-Schriftenreihe**

Schriftenreihe des Institutes für Bioverfahrenstechnik  
der Technischen Universität Braunschweig

Herausgegeben von Prof. Dr. Christoph Wittmann

**Band 63**

**Cuvillier-Verlag  
Göttingen, Deutschland**



Herausgeber  
Prof. Dr. Christoph Wittmann  
Institut für Bioverfahrenstechnik  
TU Braunschweig  
Gaußstraße 17, 38106 Braunschweig  
[www.ibvt.de](http://www.ibvt.de)

**Hinweis:** Obgleich alle Anstrengungen unternommen wurden, um richtige und aktuelle Angaben in diesem Werk zum Ausdruck zu bringen, übernehmen weder der Herausgeber, noch der Autor oder andere an der Arbeit beteiligten Personen eine Verantwortung für fehlerhafte Angaben oder deren Folgen. Eventuelle Berichtigungen können erst in der nächsten Auflage berücksichtigt werden.

### **Bibliographische Informationen der Deutschen Nationalbibliothek**

Die Deutsche Nationalbibliothek verzeichnet diese Publikation in der Deutschen Nationalbibliographie; detaillierte bibliographische Daten sind im Internet über <http://dnb.d-nb.de> abrufbar.

1. Aufl. – Göttingen: Cuvillier, 2012

© Cuvillier-Verlag · Göttingen 2012

Nonnenstieg 8, 37075 Göttingen

Telefon: 0551-54724-0

Telefax: 0551-54724-21

[www.cuvillier.de](http://www.cuvillier.de)

Alle Rechte, auch das der Übersetzung, vorbehalten

Dieses Werk – oder Teile daraus – darf nicht vervielfältigt werden, in Datenbanken gespeichert oder in irgendeiner Form – elektronisch, fotomechanisch, auf Tonträger oder sonst wie – übertragen werden ohne die schriftliche Genehmigung des Verlages.

1. Auflage, 2012

Gedruckt auf säurefreiem Papier

ISBN 978-3-95404-115-2

ISSN 1431-7230



# **Holistic bioprocess engineering of antibody fragment secreting *Bacillus megaterium***

Bei der Fakultät für Maschinenbau  
der Technischen Universität Carolo-Wilhelmina zu Braunschweig

zur Erlangung der Würde  
eines Doktor-Ingenieurs (Dr.-Ing.)  
genehmigte Dissertation

von Herrn Dipl.-Biotechnol. Florian Bodo David  
aus Braunschweig

eingereicht am: 09.06.2011

mündliche Prüfung am: 21.07.2011

Prüfungsvorsitz: Prof. Dr.-Ing. Dietmar C. Hempel  
1. Referent: Jun.-Prof. Dr.-Ing. Ezequiel Franco-Lara  
2. Referent: PD Dr. Michael Hust

**2012**



## Danksagung

Hinter einer Arbeit wie dieser verbergen sich neben den gezeigten Erkenntnissen unzählige Geschichten von Tief- und Hochpunkten mit errungenen Meilensteinen und euphorische Sternstunden. Bei diesen Erlebnissen sind es neben den kleinsten Bakterien vor allem die Menschen, die mich auf diesem Weg begleiteten und zur Seite standen.

Angefangen mit meinen studentischen Mitarbeitern möchte ich mich bei Frank Hellmers, Thomas Bewersdorf und Robert Westphal für ihren unermüdlichen Einsatz auf dem Gebiet der Prozessparameter- und Medienoptimierung bedanken. Außer diesen gilt Claudia Korneli und Mandy Schön mein herzlicher Dank für ihre Diplomarbeiten im Bereich der Prozessoptimierung von *Bacillus megaterium* als Antikörperproduzent. Ihr wart ein perfektes Team. Auf dem Gebiet der Einzelzellanalyse hat Antje Berger im Rahmen Ihrer Bachelorarbeit entscheidende Ergebnisse erzielt und war stets eine eifrige Diskussionspartnerin. Ein Dankschön auch an Paul Quehl, der ebenfalls in seiner Bachelorarbeit großen Elan und Energie in die Prozessoptimierung gesteckt hat und sich auch auf neue Wege zur Produktion von alternativen Antikörperfragmenten begab. Ihr wart ohne Ausnahme klasse Mitarbeiter und jeder auf seine Art eine Bereicherung für meine Arbeit.

Nun aber zu meinen lieben Kollegen und den Mitarbeitern vom IBVT. Ohne Euch wären das Arbeiten und auch das Leben am IBVT weniger lustig, abenteuerlich und abwechslungsreich gewesen. Angefangen mit freundlichen „Hailos“ am Morgen bis hin zu schreckhaften Begegnungen auf der Kellertreppe des Nachts. Auch außerhalb des IBVTs habe ich mit vielen Kooperationspartnern im Rahmen des „Sonderforschungsbereiches 578“ zusammengearbeitet. An dieser Stelle auch meinen Dank an Euch für die stets vertrauensvolle Zusammenarbeit.

Dann natürlich ein Dankeschön an Professor Dr. Dietmar Hempel, der mich als damaliger Institutsleiter mit einem herzlichen Handschlag einstellte und netterweise den Prüfungsvorsitz übernahm.

Nun zu meinem Doktorvater: Jun.-Prof. Ezequiel Franco-Lara. Ich danke Dir für die gewährten Freiheiten, das stete Vertrauen in meine Fähigkeiten und die Unterstützung auf ganzer Linie. Dadurch war es mir erst möglich mich frei zu entfalten, meinen Weg zu finden und eigenen Zielen zu folgen.

Zum Finale dieser Danksagung noch ein paar Worte zu den wichtigsten Personen: meiner Familie und meinen Freunden. Gerade in so einer spannenden und aufreibenden Zeit wie der, der Doktorarbeit braucht man einfach Orte des Zurückziehens, Entspannens, der Ablenkung und des Luftholens.

Danke, dass Ihr für mich da wart, mir Kraft gegeben habt und an mich geglaubt habt!



## Summary

Antibodies and antibody fragments are most important tools for therapeutic and diagnostic applications. An increasing demand of these high potential drugs makes less cost intensive production systems most desirable. Compared to mammalian cell culture microbial production platforms are beneficial with regards to reaching high production titers, scale up approaches, regulatory aspects and reduced costs of goods. Amongst these production systems those that are having the ability of an additional product secretion are most advantageous as the downstream processing costs are decisively reduced.

In this work *Bacillus megaterium*, as a Gram positive model organism, was used to extensively study the production and secretion of the antibody fragment D.13 scFv. For the bioprocess optimization a holistic approach was followed. First the aim was to establish a high productive defined cultivation medium. Different media components like carbon sources, metal ions and ammonium concentrations were screened throughout various cultivation platforms ranging from micro titer plates to shaking flasks. Statistical design of experiments and a genetic algorithm approach were used to establish an appropriate defined high production medium. As a second step the process was transferred to the bioreactor scale of several liter cultivation volume. An optimal bioprocess strategy based on alternating growth and starvation phases was established to gain high product titers of antibody fragment D1.3 scFv. As a final step an up-scale to a 100 L bioreactor was done accounting for an advanced process control and considering “good manufacturing practice” guidelines. The advanced bioprocess monitoring tool of flow cytometry was used to gain deeper insights on microbial physiology at single cell level regarding cell viability, cell integrity and production intensity. This knowledge was used for a sophisticated cell physiology based bioprocess development and optimization. Furthermore culture heterogeneities were measured and characterized for *B. megaterium* producing antibody fragment D1.3 scFv under controlled bioreactor conditions. To obtain additional information about the regulatory processes occurring inside the cell on gene expression level a transcriptome analysis was performed comparing cells with an increased production and secretion status to less producing and non-producing cells. These cutting-edge technologies of flow cytometry and transcriptome analysis revealed possible bottlenecks of the overall bioprocess’ performance and product secretion of antibody fragments with *B. megaterium* as production platform and form a robust basis for rational strain optimization and advanced process designs.

**Keywords:** Antibody fragment, secretion, *Bacillus megaterium*, medium optimization, bioprocess engineering, up-scale approach, single cell analysis, transcriptome assay, bottleneck of production



## Zusammenfassung

Antikörper und Antikörperfragmente sind wichtige Werkzeuge für eine große Anzahl von diagnostischen und therapeutischen Anwendungen. Der stetig wachsende Bedarf dieser hoch spezifischen Proteine macht kostengünstige Produktionsprozesse erstrebenswert. Mikrobielle Produktionssysteme sind aufgrund von hohen Produktivitäten, Zulassungsaspekten und geringeren Herstellungskosten vorteilhafter gegenüber industriell etablierten Säugetier-Zellkulturen. In dieser Arbeit wurde die Produktion und Sekretion des Antikörperfragments D1.3 scFv mit Hilfe des Gram positiven Modellorganismus *Bacillus megaterium* intensiv untersucht. Bei der Bioprozessoptimierung wurde ein holistischer systembiotechnologischer Ansatz verfolgt. Zunächst wurde ein definiertes Minimalmedium mit erhöhten Produktionseigenschaften entwickelt. Verschiedene Mediumkomponenten, wie die verwendete Kohlenstoffquelle, Metallionen- und Ammoniumkonzentration wurden in unterschiedlichen Kultivierungsplattformen wie Mikrotiter-Platten und Schüttelkolben optimiert. Dabei kamen Methoden der statistischen Versuchsplanung und die Verwendung eines genetischen Algorithmus zum Einsatz. In einem zweiten Schritt wurde eine Maßstabsvergrößerung des Kultivierungsvolumens in den Litermaßstab erfolgreich vorgenommen. Dabei wurde eine für die Antikörperfragment-Produktion optimierte Kultivierungsstrategie mit automatisierten alternierenden Wachstums- und Hungerphasen entwickelt. In einem finalen Schritt wurde die Prozessstrategie auf den 100 l Maßstab unter der Berücksichtigung von GMP-Richtlinien zur „guten Herstellungspraxis“ erfolgreich übertragen. Prozessbegleitend wurde die Methode der Durchflussszytometrie verwendet, um auf Einzelzellebene die Zellen hinsichtlich ihrer Aktivität bzw. Vitalität und ihres Produktionsstatus zu charakterisieren. Diese Informationen wurden für eine auf der mikrobiellen Physiologie basierenden ganzheitlichen Bioprozessentwicklung und Optimierung erfolgreich angewendet. Darüber hinaus wurden Kulturheterogenitäten unter kontrollierten Bioreaktorbedingungen gemessen und mit einem angepassten Clusterverfahren ausführlich analysiert. Zusätzlich wurde eine Transkriptom-Analyse zur Charakterisierung der Genexpression des Produktionsorganismus unter Produktionsbedingungen sowie unter verstärkten Sekretionsbedingungen vergleichend zu Nicht-Produktionsbedingungen durchgeführt. Basierend auf diesen innovativen Technologien wurden die potentiellen kritischen Produktionsengpässe in der Produktion und Sekretion von Antikörperfragmenten mit *B. megaterium* aufgedeckt. Diese Ergebnisse bilden eine robuste Grundlage für eine weitere rationale Optimierung von Produktionsstämmen und den zugehörigen Bioprozessen.

**Suchbegriffe:** Antikörperfragment, Sekretion, *Bacillus megaterium*, Medienoptimierung, Bioprozessoptimierung, Maßstabsvergrößerung, Einzelzellanalyse, Transkriptomassay, Produktionsengpässe

## Vorveröffentlichungen

Teilergebnisse aus dieser Arbeit wurden mit Genehmigung der Fakultät für Maschinenbau, vertreten durch den Mentor der Arbeit, in folgenden Beiträgen vorab veröffentlicht.

## Publications

- ▶ David F., Korneli C., Schön M., Westphal R., Franco-Lara E. (2009): **Process optimization of antibody fragment-secreting *Bacillus megaterium* cultivations and its effect on the cell heterogeneity.** *New Biotechnology*, 25(1), doi:10.1016.
- ▶ David F., Westphal R., Bunk B., Jahn D., Franco-Lara E. (2010): **Optimization of antibody fragment production in *Bacillus megaterium*: the role of metal ions on protein secretion.** *Journal of Biotechnology*, 150 (1): 115-124.
- ▶ David F., Berger A., Hänsch R., Rohde M., Franco-Lara E. (2011): **Single cell analysis applied to antibody fragment production with *Bacillus megaterium*: development of advanced physiology and bioprocess state estimation tools.** *Microbial Cell Factories*, 10:23.
- ▶ Lueders S., David F., Steinwand M., Jordan E., Hust M., Dübel S., Franco-Lara E. (2011): **Influence of the hydromechanical stress and temperature on growth and antibody fragment production with *Bacillus megaterium*.** *Applied Microbiology and Biotechnology*, 91:81-90.
- ▶ Schädel F., David F., Franco-Lara E. (2011): **Evaluation of cell damage caused by cold sampling and quenching for metabolome analysis.** *Applied Microbiology and Biotechnology*, (in press).
- ▶ Korneli C., David F., Godard T., Franco-Lara E. (2011): **Influence of fructose and oxygen gradients on fed-batch recombinant protein production using *Bacillus megaterium*.** *Engineering in Life Sciences*, (in press).
- ▶ David F., Steinwand M., Hust M., Bohle K., Ross A., Dübel S., Franco-Lara E. (2011): **Antibody production in *Bacillus megaterium*: strategies and physiological implications of scaling from micro titer plates to industrial bioreactors.** *Biotechnology Journal* (in press).
- ▶ David F., Hebeisen M., Schade G., Franco-Lara E., Di Berardino M. (2011): **Viability and metabolic activity analysis of *Bacillus megaterium* cells by impedance flow cytometry.** *Biotechnology and Bioengineering*, 109 (2), 483-492.

## Conference Contributions

- ▶ David F., Franco-Lara E. (2007): Metabolic process analysis and optimization of bacterial cultivations (*Bacillus megaterium*). **1st International PhD Symposium of the Helmholtz International Research School for Infection Biology**, December 7<sup>th</sup>, 2007 Braunschweig, Germany.
- ▶ David F., Göcke Y., Bewersdorf T., Hellmers F., Lüders S., Jordan E., Hust M., Dübel S., Franco-Lara E. (2008): Bioprocess Design of Antibody Fragment-Secreting *Bacillus megaterium* MS941 Cultivations. **7<sup>th</sup> European Symposium on Biochemical Engineering Science (ESBES 7)**. 7-10 September, 2008. Faro, Portugal.
- ▶ Franco-Lara E., David F., Lüders S. (2008): Bioprocess design of the antibody fragment D1.3 scFv production. **German-Mexican Workshop on the Integration of Microbial Physiology and Bioprocess Technology**. 21-23 September, 2008. Sponsored by the Deutsche Forschungsgemeinschaft (DFG) and the Mexican Council for Research and Technology (CONACYT). Cuernavaca, Mexico.
- ▶ David F., Korneli C., Schön M., Westphal R., Lüders S., Franco-Lara E. (2009): Bioprozessdesign von Antikörperfragment sekretierendem *Bacillus megaterium*. **Vortrags- und Diskussionstagung „Biokatalyse: Neue Verfahren, Neue Produkte“**. 18-20 May 2009. Bad Schandau, Germany.
- ▶ David F., Korneli C., Schön M., Berger A., Franco-Lara E. (2009): Culture heterogeneity in *Bacillus megaterium* cultivations producing antibody fragments regarding the state of production and membrane potential. **19<sup>th</sup> Annual Conference of the German Society for Cytometry. 14-16 October, 2009**. Helmholtz-Centre for Environmental Research, Leipzig, Germany, (**oral presentation**).
- ▶ David F., Korneli C., Schön M., Westphal R., Göcke Y., Franco-Lara E. (2009): ***Bacillus megaterium*: a microbial cell factory for antibody fragments**. **12<sup>th</sup> German-American Frontiers of Engineering Symposium**. Sponsored by the Alexander von Humbolt Foundation and the National Academy of Engineering (NAE). 22-25 April 2009. Potsdam, Germany.
- ▶ David F., Korneli C., Franco-Lara E. (2009): **Cell physiology and heterogeneity in the production of antibody fragments**. **BioProScale Symposium: Inhomogeneities in large scale bioreactors**. November 24-27, 2009. Berlin, Germany, (**oral presentation (invited)**).
- ▶ David F., Korneli C., Schön M., Dübel S., Franco-Lara E. (2009). Process optimization of Antibody Fragment-Secreting *Bacillus megaterium* cultivations accompanied by investigations towards culture heterogeneity by using Flow Cytometry. **Symbiosis, the 14<sup>th</sup> European Congress on Biotechnology**. 13-16 September, 2009. Barcelona, Spain.
- ▶ Korneli C., David F., Franco-Lara E. (2010): Productivity and cell heterogeneity of *Bacillus megaterium* is a function of the control strategy in fed-batch cultures. **8<sup>th</sup> European Symposium on Biochemical Engineering Science (ESBES)**. 5-8 September, 2010. Bologna, Italy.
- ▶ David F., Franco-Lara E. (2010): Cell physiology and heterogeneity dynamics in the production of antibody fragments in *Bacillus megaterium*. **8<sup>th</sup> European Symposium on Biochemical Engineering Science (ESBES)**. 5-8 September, 2010. Bologna, Italy.
- ▶ David F., Franco-Lara E. (2011): Single-cell fingerprint dynamics of antibody fragment secreting *Bacillus megaterium* cells. **5<sup>th</sup> International Conference on Analysis of Microbial Cells at the Single Cell Level**, 5-8 November, 2011. Carry-le-Rouet, Marseille, France, (**oral presentation**).



## TABLE OF CONTENTS

<b>1</b>	<b><i>Introduction</i></b>	<b>1</b>
<b>1.1</b>	<b>Antibodies</b>	<b>2</b>
1.1.1	Benchmark analysis	2
1.1.2	Antibody formats	3
1.1.3	ABF – key benefits	6
1.1.4	Specific examples	6
1.1.5	Antibody production systems	8
<b>1.2</b>	<b><i>Bacillus megaterium</i> as production host</b>	<b>12</b>
<b>1.3</b>	<b>Objectives</b>	<b>14</b>
<b>2</b>	<b><i>Theory</i></b>	<b>15</b>
<b>2.1</b>	<b>“Omics” approach</b>	<b>15</b>
<b>2.2</b>	<b>Flow cytometry and cell heterogeneity</b>	<b>17</b>
2.2.1	Flow cytometry – history and function	17
2.2.2	Assessing cell states	18
2.2.3	Cell heterogeneities	20
<b>2.3</b>	<b>Process development</b>	<b>22</b>
<b>3</b>	<b><i>Material and methods</i></b>	<b>25</b>
<b>3.1</b>	<b>Strain and plasmid</b>	<b>25</b>
<b>3.2</b>	<b>Sampling of cultivation supernatant</b>	<b>26</b>
<b>3.3</b>	<b>High-performance liquid chromatography analysis</b>	<b>27</b>
<b>3.4</b>	<b>Biomass measurements</b>	<b>27</b>
<b>3.5</b>	<b>Quantification of the antibody fragment D1.3 scFv concentration via ELISA</b>	<b>27</b>
<b>3.6</b>	<b>Cell bank – <i>Bacillus megaterium</i></b>	<b>29</b>
<b>3.7</b>	<b>Screening in deep well plates</b>	<b>29</b>
<b>3.8</b>	<b>Cultivation conditions – deep well plates</b>	<b>30</b>
<b>3.9</b>	<b>Cultivation conditions – batch</b>	<b>31</b>



<b>3.10 Cultivation conditions – fed-batch</b>	<b>32</b>
<b>3.11 Gas analysis</b>	<b>32</b>
<b>3.12 Oscillating fed-batch strategy</b>	<b>32</b>
<b>3.13 Flow cytometry</b>	<b>34</b>
<b>3.14 Dye screening for membrane potential estimation</b>	<b>34</b>
<b>3.15 DiOC<sub>2</sub>(3) ratio analysis</b>	<b>35</b>
<b>3.16 Membrane potential calibration</b>	<b>35</b>
<b>3.17 Viability assay</b>	<b>36</b>
<b>3.18 Single cell production intensity assay</b>	<b>36</b>
<b>3.19 Immuno field emission scanning electron microscopy</b>	<b>36</b>
<b>3.20 Confocal laser scanning microscopy</b>	<b>37</b>
<b>3.21 Population cluster analysis</b>	<b>37</b>
3.21.1 DiOC <sub>2</sub> membrane potential assay (SS, EV) (FL1, FL3)	38
3.21.2 Production intensity assay (FL1, FL3) (FL1, FL3, SS, EV)	43
<b>3.22 Central composite design</b>	<b>44</b>
<b>3.23 Genetic algorithm</b>	<b>44</b>
<b>3.24 Prediction of metal-dependent enzymes of <i>Bacillus megaterium</i></b>	<b>45</b>
<b>3.25 DNA micro arrays</b>	<b>46</b>
3.25.1 RNA-preparation	46
3.25.2 One colour microarray	46
<b>3.26 Chemicals</b>	<b>46</b>
<b>4 Results and discussion</b>	<b>47</b>
<b>4.1 Aims of the work</b>	<b>47</b>
<b>4.2 Medium design</b>	<b>48</b>
4.2.1 Carbon source screening	48
4.2.2 Inducer screening	49
4.2.3 Genetic algorithm approach – optimization of metal ion concentrations	50
4.2.4 Statistical DoE – optimization of MgSO <sub>4</sub> and (NH <sub>4</sub> ) <sub>2</sub> SO <sub>4</sub> concentrations	58



<b>4.3 Single cell analysis</b>	<b>59</b>
4.3.1 Membrane potential	59
4.3.2 Cell integrity	63
4.3.3 Production intensity	64
<b>4.4 Process development</b>	<b>67</b>
4.4.1 Batch culture	67
4.4.2 Fed-batch culture	73
4.4.3 Up-scale approach	81
<b>4.5 Transcriptome analysis</b>	<b>83</b>
4.5.1 Differential gene expression dependent on recombinant ABF D1.3 scFv production/secretion in <i>Bacillus megaterium</i>	85
4.5.2 Growth phase dependent gene expression	88
4.5.3 Growth phase dependent gene expression related to recombinant ABF D1.3 scFv production	92
4.5.4 Summary	94
<b>4.6 Culture heterogeneity</b>	<b>98</b>
4.6.1 Late induction of ABF D1.3 scFv production	98
4.6.2 Batch process with 50 g/L initial carbon source	106
4.6.3 Process relevance of heterogeneities	108
<b>5 Conclusions and outlook</b>	<b>110</b>
<b>5.1 Medium design</b>	<b>110</b>
<b>5.2 Advanced process control</b>	<b>111</b>
<b>5.3 Process development and limitations</b>	<b>113</b>
<b>5.4 Era of cytomics and data modeling</b>	<b>114</b>
<b>5.5 Antibodies – a future perspective</b>	<b>115</b>
5.5.1 Potential of microbial systems	115
5.5.2 Most promising antibody formats	117
5.5.3 Future – application	118
<b>6 References</b>	<b>119</b>
<b>7 Nomenclature</b>	<b>136</b>
<b>7.1 Abbreviations</b>	<b>136</b>
<b>7.2 Symbols</b>	<b>139</b>





## 1 Introduction

Antibodies (AB) and antibody fragments (ABF) are some of the most promising therapeutic and diagnostic tools of the 21st century. Less side effects and high specificities make them to ideal drugs for treating cancer, autoimmune, cardiovascular and infectious diseases. Their mechanism of action goes back to natural principles of the human immune system and uses its autologous defense devices to cope with health threatening diseases. The production of these multifunctional drugs is done by the key technology of biotechnology. Microbial and mammalian cells undergo genetic modifications to specifically produce the desired AB formats. The current challenges are to reduce the high production costs and to meet the increasing demands of these potent therapeutic tools. Therefore creating new production systems with lesser costs and higher productivity are most desirable.

As an alternative to expensive mammalian production platforms beneficial microbial systems can be used to efficiently produce and secrete ABFs. In this work the Gram positive bacterium *Bacillus megaterium* was used to thoroughly characterize production and secretion of a model ABF regarding process characterization and transfer to industrial scale. A contemporary holistic approach of bioprocess control, monitoring and optimization was followed. Traditional methods improving the process performance like optimization of culture medium and bioprocess development towards high cell densities were combined with cutting-edge technologies of flow cytometry (FCM) and transcriptome analysis. With these two new technologies at hand new insights on the ongoing processes in the model organism could be found on single cell level (by FCM) and on the overall gene expression profile (transcriptome analysis). These will help to identify possible bottlenecks of the overall bioprocess' performance and product secretion of ABFs with *B. megaterium* as production platform.



## 1.1 Antibodies

### 1.1.1 Benchmark analysis

More than 100 years ago Nobel Prize winner Paul Ehrlich proposed in 1908 the creation of “magic bullets” (**Fig. 1**) used to fight against human diseases which nowadays have become highly specific cancer therapeutics in form of monoclonal AB (mAB) constructs. The first Food and Drug Administration (FDA)-approved mAB appeared 25 years ago and today 28 mAB-based drugs are safe and effective therapeutic agents in the treatment of cancer, inflammation, cardiovascular and infectious diseases [1].

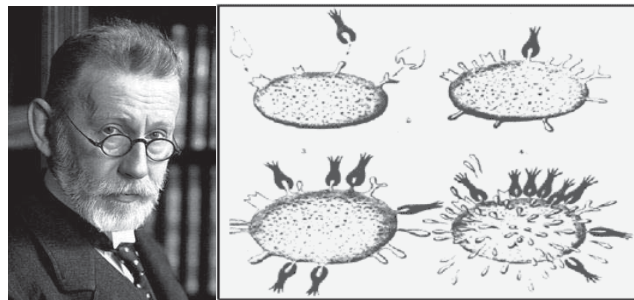


**Figure 1:** Nobel prize winner Paul Ehrlich (© The Nobel Foundation); magic bullets, side chain theory (1890) [2].

It has been projected, that in the next 10 years 135 mABs will be approved by the US FDA [3]. Being the major proportion of almost 50% of the therapeutic protein market they present the fastest growing sector in pharmaceutical industry. Predicted sales of mABs will reach \$56 billion dollars by 2012 with a compound annual growth rate (CAGR) of 13% [4]. **Figure 2** gives an overview about approved mAB products in Germany and their overall sales in the last years [5]. The increasing economic impact in Germany of mAB based products is highlighted at the corresponding growing fraction of overall biopharmaceutical products sales from 2004 to 2008.

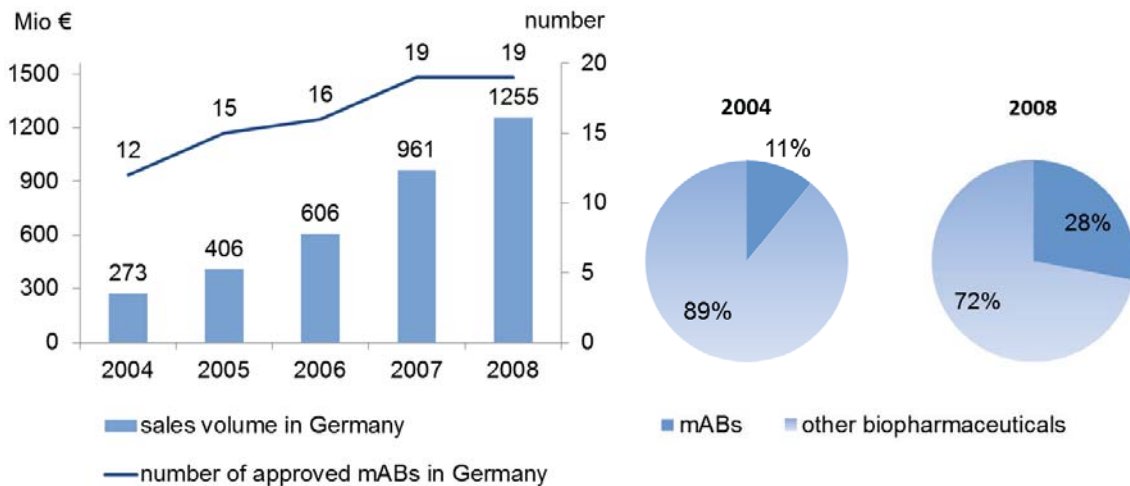


**Figure 2:** Sales volume and number of mABs based products in Germany from 2004 to 2008 [5].

Besides the therapeutic usage, mABs are intensively used for diagnostic purposes and revealing total new insights in the field of cell biology and single cell analysis. Analytical *in vitro* methods such as Enzyme-Linked-Immunosorbent-Assay (ELISA), Radio-Immuno-Assay (RIA), blotting techniques, FCM, confocal imaging, immunochemistry, diagnostic biochip sensors, bio-imaging and protein purification are highly dependent upon the use of polyclonal or monoclonal ABs [6]. As a future perspective, recombinant mABs may even be used in consumer products e. g. for toothpaste to protect against tooth decay related to caries [7-9].

To meet the need of the high demand of mAB based therapeutics and diagnostics of more than 1000 kg/year [10] host cell engineering, optimization of cultivation and purification processes are of great importance.

### 1.1.2 Antibody formats

ABs are a class of flexible molecular adaptors playing a crucial role in the adaptive immune systems of vertebrates [11]. Using them for therapeutic purposes is a nearby approach as they naturally function in vertebrates to protect the organism against infections, malignant cells and toxic molecules. They were originally discovered by Behring and Kitasato in 1890 [12] but it took another 70 years until the basic structure was determined [13]. Due to their diverse and heterogeneous structures, ABs mediate diverse humoral and cellular immune responses. Thereby they execute various biochemical mechanisms such as antigen recognition, AB-dependent cellular cytotoxicity (ADCC) and complement-dependent cellular cytotoxicity (CDC). Five distinct classes of ABs exist in most higher mammals (IgG, IgA, IgM, IgD and IgE) differing in form and function based on variances in amino acid composition, charge distribution and carbohydrate content [14].

Immunoglobulins exhibit a symmetrical Y-structure and consist of pairs of identical heavy and light chains linked together through disulfide bridges (**Fig. 3**) [15]. The heavy chain type determines the subclass of AB linked to different physiological functions. The particular chains form globular domains that are either related to the specific antigen binding (variable region) or show Fc-related properties like complement activation and lymphocyte binding being essential for the cellular immune response [16]. **Figure 3** gives an overview on such a typical whole size AB IgG structure.

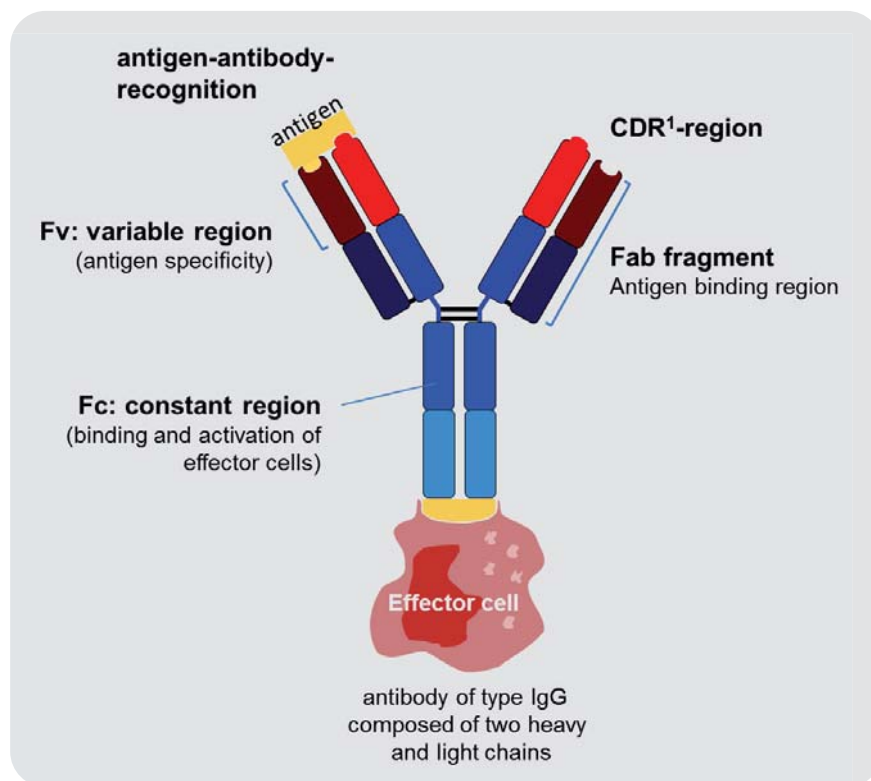


**Figure 3:** Functional parts of a whole size IgG mAB with specific effector binding and antigen binding functions, CDR<sup>1</sup> = complementarity determining region ([17] modified).

In general one has to distinguish between monoclonal and polyclonal ABs. The latter are used for detection reagents in research and are created from animal immunization activating an unspecific *in vivo* AB response. These ABs display unknown specificities and are very immunogenic, restricting their therapeutic application [6]. Monoclonal ABs instead are created by the so-called “hybridoma technology” which is based on the fusion of AB producing spleen cells from immunized mice or rats with immortal myeloma cell lines [18]. To generate fully human ABs, transgenic mice are used in which the mouse AB genes were replaced with the human equivalents [19]. In contrast to these *in vivo* techniques there are also *in vitro* AB selection methods available. Methods like phage display, yeast surface display or ribosome display are used to directly link the phenotype to the genotype and screen for higher affinity, stability and solubility of ABs derived from recombinant libraries of human VH and VL genes [6, 20, 21]. The phage display technology for



instance has been used for generating 30% of all human ABs currently in clinical development [22].

Besides natural whole size IgGs (~150 kDa) other AB formats are also developed for various applications including Fab fragments, single chain ABs (scFv) and single domain ABs (sdAB) (**Fig. 4**). AB molecules were developed exhibiting a certain biological activity e. g. at particular therapeutic and diagnostic applications [23]. The structures can be divided into two groups those being subject of major protein engineering modifications and those consisting of native components of the original IgG. The Fv fragment can be stabilized by linker polypeptide creating a single chain Fv (scFv) ABF, allowing an expression from a single gene thereby producing a single chain polypeptide [24, 25]. Additionally multimeric variants of the scFv such as dia-bodies and tri-bodies were created. An alternative approach describes the fusion of Fv fragments with leucin zipper forming amphipathic helices with leucin residues lining up on the hydrophobic face of a helix [26]. A so-called “Fab fragment” consists of the variable domain of the heavy and the light chain linked by a disulfide bond (**Fig. 4**). Different linker constructs at the hinge region facilitate various formats like single chain Fabs (scFab) [27], dimeric or even trimeric Fab constructs. Also bispecific ABs were generated at which one domain binds e. g. to a cancer specific surface and recruiting with the other domain cytotoxic T-cells inducing T-cell-dependent cytotoxicity [28]. Other AB formats like VHH/VH naturally existing in llamas and camels are lacking the light chain of ABs but still exhibiting high stabilities and affinities [29]. They display the smallest format of ABFs with a molecular weight of 15 kDa.

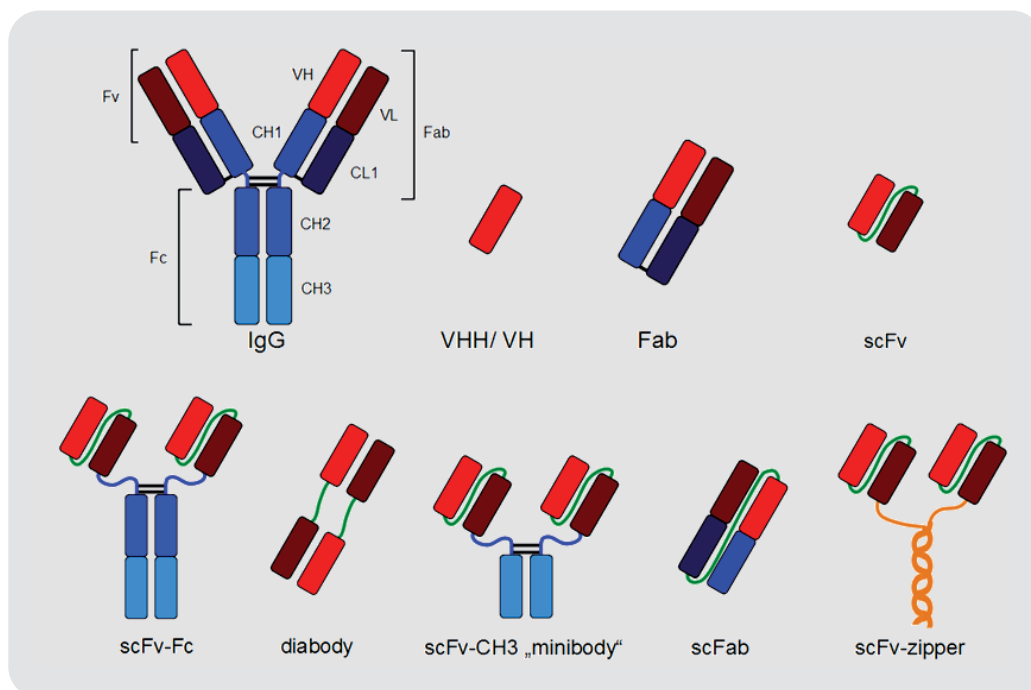


**Figure 4:** Different designs of ABFs consisting either of antigen specific (red), effector recruiting parts (blue) or both, stabilized by linker peptides (green), (Figure adapted from [6]).



### 1.1.3 ABF – key benefits

Currently most therapeutic ABs on the market are whole size IgG mABs produced in mammalian systems. They have the advantage to be fully human origin, to exhibit glycosylation patterns which are important for effector function and to have no immunogenic effects. However the production process in mammalian cell lines is rather time consuming, expensive and complex with high Cost of Goods (COG), so that new expression platforms producing highly specific, adjustable AB formats are most desirable. ABFs like Fab and scFv have multiple benefits compared to full-length IgG Abs, as the complete AB glycoprotein is not always necessary for its therapeutic function. The optimal composition might not be the whole AB structure but a distinctive fragment containing the specific antigen-binding domain. ABFs not possessing any Fc part can be advantageous for therapeutic application as they do not lead to the recruitment of effector cells or the activation of the complement system. In particular during inflammation processes only the neutralizing antigen-binding activity is desired. Due to their smaller size they show certain pharmacokinetic advances like the increased penetration into solid tumors, the possibility of local applications [30] or rapid clearance from circulating blood serum. Clearance from the blood stream is mediated by the renal pathway thus reducing the AB-half-life to hours rather than weeks [3, 31]. This may be on the one hand advantageous to avoid unspecific binding and on the other hand is beneficial for acute indications such as myocardial infarction, acute infections or intoxications. Modifications of half-life can be specifically adjusted by PEGylation (conjugation with polyethylene glycol) determining circulation time, biodistribution, immunogenicity, solubility, proteolytic degradation and storage stability [31].

A drawback of ABFs is that in some cases they consist of major protein engineering parts like peptide linker or purification tags. These may be associated with potential immunogenicity making these fragments unlikely to be used for repeated dosing therapies. However humanized ABFs and post-translational modifications (PTM) facilitate the optimal design of AB-based drugs with advanced pharmacokinetic and therapeutic function so that in contrast to standard IgG formats a greater flexibility can be achieved [32].

### 1.1.4 Specific examples

Therapeutic ABs have two modes of action. They can either work as antagonists by blocking interactions of receptor molecules or they can function as agonists by e. g. binding to cell surface receptors leading to the activation of downstream signaling cascades [31]. When recruitment of effector cells by the Fc part is not requested then AB domains containing antigen-binding properties (sdAB, scFv, Fv, Fab) are sufficient.

Possible applications of specific mABs and ABFs are being presented in the next paragraph.



- 1) Herceptin (*Trastuzumab*, Genentech (US), Roche (EU)) is one of the most prominent therapeutic mAB therapeutically used for destroying specific breast cancer tumor cells. Its development marks the beginning of a new era of designed target drugs and diagnostic tests [33]. It is a humanized monoclonal IgG AB targeting to the human epidermal growth factor receptor 2 (HER2). This receptor is overexpressed in in 20-30% of human breast cancers [34, 35]. Herceptin is produced in mammalian chinese hamster ovary (CHO) cells with a Fc part and distinctive glycosylation pattern. The potential mechanisms of how Herceptin avoids further tumor growth are versatile and comprise the following facts: degradation of HER2 receptors from the cell membrane [36], recruitment of immune cells by effector function [37], antagonizing uncontrolled growth signaling [38] and interaction with other signaling pathways [39].
- 2) The Fab fragment Cimzia (*Certolizumab* Pegol, Nektar Therapeutics, UCB Pharmaceuticals) is a humanized and PEGylated ABF recently approved by the FDA for therapeutic usage against TNF- $\alpha$  -related diseases. It is an anti TNF- $\alpha$  Fab fragment which was initially approved in 2008 for treatment of Crohn's disease but since May 2009 it is also indicated for the treatment of rheumatoid arthritis [31, 40]. It is composed of a light chain with 214 amino acids and a heavy chain with 229 amino acids and is produced in a microbial system of *Escherichia coli* cells [3]. By binding to TNF- $\alpha$  as a key proinflammatory cytokine it selectively neutralizes it and thereby inhibits further stimulation of TNF- $\alpha$  induced inflammatory reactions. The PEGylation extends the plasma half-life of the product, enabling its once-monthly subcutaneous administration [41]. As a benefit Fab units do not exhibit immunogenic parts as they consist of natural AB domains when being produced by humanized AB generation methods.
- 3) So-called "single domain ABs" (sdAB) were also shown to exhibit certain therapeutic usage possibilities. It was reported that daily oral administration of an untagged sdAB with specificity for *Staphylococcus mutans* reduced dental caries development of rats [7, 8]. Another interesting application in the field of "functional food" is an genetically engineered *Lactobacillus paracasei* strain expressing a sdAB on the surface which was shown to bind rotavirus' and thereby shortens virus-induced diarrhea in a mouse model [42, 43].



In this study, the focus of investigation is on a scFv fragment. Amongst others these formats already were shown to be effective for the antidote treatment of intoxications by ricin [44] and for neutralizing the lethal factor of *Bacillus anthracis* by inhibiting protective antigen-LF complex formation [45]. *B. megaterium* was used in the current work as the expression system for the ABF D1.3 scFv and to study the production and secretion by the bacterium itself. The ABF is directed against hen egg lysozyme which was chosen as an inexpensive antigen-model. Other fragments like anti-CRP-scFv and anti-lysozyme-Fab fragments [46-48] were also reported to be successfully produced by *B. megaterium*.



### 1.1.5 Antibody production systems

The expression of ABs and ABFs can be realized in several prokaryotic and eukaryotic production systems. All production platforms have certain advantages and disadvantages which are summarized in **Tables 1** to **3**. It has to be taken into account that optimal production hosts and parameters may vary for each generated particular AB format due to different requirements related to protein folding and posttranslational modifications, COG and regulatory acceptance [49]. The presented particular yield data is AB format and host specific and should give an idea about the efficiencies of the particular production platforms.

**Table 1:** Prokaryotic cells as productions hosts for mAB.

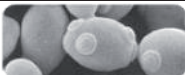
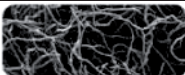
Organisms	Prokaryotic Cells	
	Gram Negative 	Gram Positive 
<b>Example</b>	<i>Escherichia coli</i>	<i>Bacillus subtilis</i> , <i>B. brevis</i> , <i>B. megaterium</i> , <i>Lactobacillus</i>
<b>Antibody Formats</b>	scFv, Fab, IgG	scFv, Fab
<b>Yield</b>	0.8 mg/L - 10 g/L (cytoplasmatic)	15 mg/L
<b>Advantages</b>	<ul style="list-style-type: none"> <li>• high cell density bioprocess with high yields</li> <li>• established host</li> <li>• minimal media</li> <li>• disulfid bond formation in periplasmatic space</li> </ul>	<ul style="list-style-type: none"> <li>• direct functional secretion</li> <li>• GRAS status</li> <li>• no endotoxins</li> <li>• reduced downstream processing</li> </ul>
	<ul style="list-style-type: none"> <li>• inclusion body formation</li> <li>• less secretion</li> <li>• no glycolisation</li> <li>• endotoxin contamination</li> </ul>	<ul style="list-style-type: none"> <li>• low product titers</li> <li>• less optimized host</li> <li>• no high production strains</li> </ul>
<b>Improvements</b>	<ul style="list-style-type: none"> <li>• coexpression: <i>GroEL/ES</i>, trigger factor, <i>DanK/J</i>, <i>FkPa</i></li> <li>• coexpression: periplasmatic chaperones <i>DsbC</i>, <i>Skp</i></li> </ul>	<ul style="list-style-type: none"> <li>• gene knock out <i>htrA</i>, <i>wprA</i> (proteases)</li> <li>• process and media optimization</li> </ul>
<b>Literature</b>	[50-56]	[47, 48, 57-61]

Prokaryotic systems like the well-established Gram negative production host *E. coli* display high production yields of up to 10 g/L heterologous produced proteins as cytoplasmatic inclusion bodies (**Tab. 1**). In the last 60 years the system was optimized to produce heterologous proteins up to 50% of the total cell protein [6]. Moreover microbial cells are inexpensive, easily grown and quickly produce small amounts of target proteins for evaluation [62]. Also systems of periplasmatic secretion and thereby functional generation of disulfide bonds and modified “leaky” *E. coli* cells were developed [63]. However those leaky strains do not provide so far enough robustness for high cell density cultivations [64].



In contrast to *E. coli*, Gram positive cells like *Bacillus subtilis* and *B. megaterium* have the big advantage of being naturally high secretors. As they lack a second outer membrane, the AB is directly secreted and functionally folded through the membrane related SecA pathway [65] and finally released by diffusion through the cell wall. Although Gram positive expression systems exhibit relatively low production titers they still display a good secretion alternative to *E. coli*. Their potential for optimizing secretion is far from being exploited yet and even may lead to concentrations in g/L range as shown for other intracellular [66] and extracellular proteins [67]. However prokaryotic systems do not display any functional glycosylation patterns which are indispensable for therapeutic effector function of ABs. Therefore other production systems like eukaryotic cells play a predominant role.

**Table 2:** Eukaryotic microbial cells as production hosts for mAB.

Organisms	Eukaryotic Cells (microorganism)	
	Yeast	Fungi
		
<b>Example</b>	<i>Saccharomyces cerevisiae</i> , <i>Pichia pastoris</i>	<i>Aspergillus</i> , <i>Trichoderma</i>
<b>Antibody Formats</b>	scFv, llama V <sub>HH</sub> , Fab, scFv-Fc fusions	IgG, Fab, scFvs, llama V <sub>HH</sub>
<b>Yield</b>	70 mg/L - 1.2 g/L	1 mg/L - 1.2 g/L
<b>Advantages</b>	<ul style="list-style-type: none"> <li>• short generation time</li> <li>• secretion, no endotoxin or virus</li> <li>• robustness, simple medium</li> <li>• postranslational modifications, effector functions</li> </ul>	<ul style="list-style-type: none"> <li>• high secretion capacities</li> <li>• GRAS status</li> </ul>
	<ul style="list-style-type: none"> <li>• incomplete proteolytic processing</li> <li>• low transformation efficiency</li> <li>• insufficient and hyper-glycosylation</li> </ul>	<ul style="list-style-type: none"> <li>• proteolytic active</li> </ul>
<b>Disadvantages</b>	<ul style="list-style-type: none"> <li>• chaperone overexpression</li> </ul>	
<b>Improvements</b>	<ul style="list-style-type: none"> <li>• coexpression: <i>BiP</i>, <i>PDI</i></li> <li>• bioprocess optimization</li> </ul>	
<b>Literature</b>	[68-76]	[72, 77, 78]

Microorganisms like yeast cells and fungi were found to efficiently secrete and at the same time glycosylate ABs and ABFs (**Tab. 2**). As a main drawback these systems sometimes show insufficient glycosylation or even hyper-glycosylation patterns. They also display increased proteolytic activity thus making production processes less reproducible and more difficult to handle. The same is true for insect cells which are based on the baculo-virus-infection system. In some cases they display a high diversity of post-translational modified products and a strong intracellular protein aggregation [31].




The current systems of choice especially for therapeutic AB production are mammalian cells like chinese hamster ovary (CHO), baby hamster kidney (BHK) or human embryonic





kidney (HEK) cell lines (**Tab. 3**). The predominant use of mammalian cell cultures has been driven by the need to obtain proteins with complex biochemical structures and resulting superior activity with native structures and function, e. g. proper folding, formation of disulfide bridges, oligomerization, proteolytic processing, phosphorylation and the addition of specific and complex carbohydrate groups [31, 79]. High extracellular product titers and an advanced secretion and folding apparatus for human glycosylation pattern make them an ideal production platform for mAB. However the overall costs for development and production are quite high compared to the other systems. As an example suspension cultures grown for 10-15 days can be used to inoculate a 10.000 L reactor followed by a subsequent cultivation of 6-14 days [3]. Here a typical cultivation process lasts at least around 25 days requiring large amounts of energy and resource consuming costs. A further challenge is the development of stable high producing cell lines and serum free media to reduce the risk of contamination. Additionally the production costs are not simply reduced by up-scaling the process. As an example for a whole cell system transgenic plants are mentioned as a most scalable production system with reduced production costs (**Tab. 3**).

**Table 3:** Eukaryotic cells and cell systems as productions hosts for mAB.

Organisms	Eukaryotic Cells		
	Insect Cells 	Mammalian Cells 	Transgenic Plants 
<b>Example</b>	<i>Drosophila melanogaster</i> "Baculo Virus" System	CHO, BHK, HEK	<i>Nicotiana tabacum</i> , <i>Arabidopsis thaliana</i>
<b>Antibody Formats</b>	IgG, scFv	IgG, scFv-Fc	IgG, scFv, Fab, V <sub>HH</sub>
<b>Yield</b>	0.4 - 25 mg/L	1.4 - 1.8 g/L	28 - 136 mg/kg
<b>Advantages</b>	<ul style="list-style-type: none"> <li>mediate effector function</li> <li>human tolerance to baculo</li> <li>secretion, correct folding</li> </ul>	<ul style="list-style-type: none"> <li>advanced folding, secretion, post translational apparatus</li> <li>highly productive</li> <li>suitable for large and complicated proteins</li> <li>established system (60-70% of all antibodies)</li> </ul>	<ul style="list-style-type: none"> <li>1-10% of hybridoma production costs</li> <li>simple scale-up</li> </ul>
	<ul style="list-style-type: none"> <li>protease inhibitors recommended</li> <li>expensive media</li> <li>virus contamination risk</li> <li>strong intracellular protein aggregation</li> <li>high diversity of post translational modified products</li> </ul>	<ul style="list-style-type: none"> <li>high production costs</li> <li>may require animal derived media components</li> <li>extensive characterization (mycoplasma, virus testing)</li> <li>long term screening for high producers</li> <li>long process times</li> </ul>	<ul style="list-style-type: none"> <li>limits at glycosylation</li> <li>containment issues</li> <li>long development times for transgenic plants</li> </ul>
<b>Improvements</b>	<ul style="list-style-type: none"> <li>overexpression of <i>BiP</i>, <i>PDI</i></li> <li><i>hsp70</i> coexpression</li> </ul>	<ul style="list-style-type: none"> <li>serum free media (avoiding e. g. viral contamination)</li> <li>efficient chromosome integration</li> <li>optimized handling and bioprocesses</li> </ul>	
<b>Literature</b>	[80-83]	[84-88]	[89-91]

Alternative expression platforms in contrast to the cost- and time-intensive production in mammalian cells are microbial systems which are already used for production of all kinds of recombinant proteins. However, in most of the microbial systems the production itself is very efficient, though being also associated with high downstream processing costs [6, 31]. The steps for getting access to the intracellularly stored products, e. g. expressed in *E. coli*, usually comprise cellular disruption, product separation and purification. Therefore *B. megaterium* is a promising alternative with it being an efficient and less cost intensive expression host with high secretion capacities. Due to its lack of the outer membrane which is well known for Gram negative bacteria like *E. coli*, produced ABFs can directly be harvested from the culture supernatant.

## 1.2 *Bacillus megaterium* as production host

The Gram positive soil bacterium *B. megaterium*, which was discovered in 1884 from Anton de Bary, got its name from “big beast” greek „megatherium” related to its big size of up to  $4 \times 1.5 \mu\text{m}$  (**Fig. 5**) [92]. The pronounced magnitude of the bacterium classifies it as an ideal model organism to study cell structures and protein localization. In the past *B. megaterium* has been intensively used to analyze sporulation, bacteriophages and biochemistry of Gram positive bacteria [93-96]. Also more than sixty years ago, Maurice Lemoigne discovered the polyester polyhydroxybutyrate in *B. megaterium* as an important storage compound in bacteria, today being a potential resource for generating bio-plastic [97].

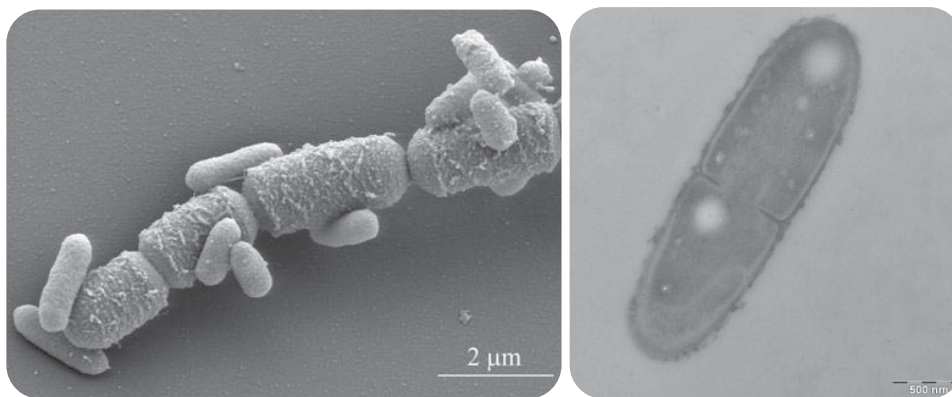


**Figure 5:** Scanning electronic microscope (SEM) pictures of *B. megaterium* ( $4 \times 1.5 \mu\text{m}$ ) and *E. coli* ( $2 \times 0.5 \mu\text{m}$ ) (left); Ultra-thin section of a dividing *B. megaterium* cell (right) [98].

*B. megaterium* can be isolated from a various habitats like soil, water, sediments and also from honey or dry food products [99], due to its high osmotic tolerance and its ability to metabolize a vast spectrum of carbon sources.

As part of the Collaborative Research Center SFB 578 the genome of *B. megaterium* strain DSM319 was sequenced and annotated [100, 101]. Thereby a phylogentic classification was done showing, according to the NCBI taxonomy database, a close relation to the *B. cereus*/*B. anthracis* group of the genus *Bacilli*.

A big advantage of *B. megaterium* compared to Gram negative organisms like *E. coli* is that it is an expression host with high secretion capacities [99]. The lack of an outer membrane allows secreted products to be directly harvested from the culture supernatant. It does not produce alkaline proteases and also has higher plasmid stability during growth [102]. To ensure the secretion of recombinant proteins signal peptides have to be added to the N-terminal end. These peptide chains are recognized by the type II secretion apparatus [65] of the SecA pathway and the protein is functionally folded upon release through the cell membrane [103, 104]. In the last years it has been shown that *B. megaterium* is able to intracellularly produce and secrete high amounts of functional

proteins [105, 106] including industrially important products like penicillin-G-acylase [107], different amylases [108], glycosyltransferases [109], dextranucrase [110], vitamin B<sub>12</sub> [111, 112], cytochrome monooxygenases [113],  $\beta$ -galactosidase, glucose dehydrogenase, formate dehydrogenase, toxin A [114, 115] and hydrolases [116, 117]. Its non-pathogen status qualifies it as an ideal industrial production strain. Besides the mentioned recombinant proteins, *B. megaterium* was shown to efficiently secrete ABFs in the surrounding medium [47, 48, 59].

The heterologous plasmid-based protein production is under the control of a xylose inducible promoter system [118] (**Fig. 6**) characterized and developed by Rygus and Hillen in 1991 [119] and is depicted in the following scheme.

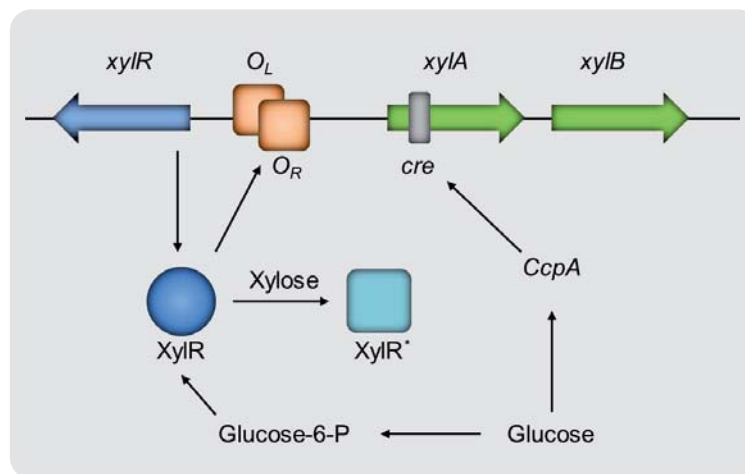


**Figure 6:** Regulation of the xylose-operon from *B. megaterium*; **CcpA**: Catabolite control protein A, (transcription factor), **cre**: DNA-sequence ("catabolite response element"), **O<sub>L</sub>/O<sub>R</sub>**: operator region of the *xyl* promoter, **xylA**: xylose isomerase gene, **xylB**: xylulokinase gene, **xylR**: xylose repressor gene, **XylR**: active xylose repressor, **XylR\***: inactive xylose repressor.

In the absence of xylose the xylose repressor protein XylR is binding to the operator region O<sub>L</sub> and O<sub>R</sub> of the xylose promoter thereby inhibiting the initiation of transcription. In presence of xylose the repressor protein conformation is changed, enabling the operator region and facilitating the RNA-polymerase mediated transcription of the controlled gene. Xylose addition increases transcription efficiency up to 150 times [120]. Furthermore transcription of the xylose operon is also controlled by other mechanisms. When glucose is present the binding affinity of CcpA (Catabolite control protein A) to an inside the *xylA* gene located *cre*-sequence (catabolite responsive element) is increased, thereby inhibiting an effective transcription. The other controlling mechanisms comprises the competition of glucose-6-monophosphat, usually generated upon glucose uptake, with xylose for binding to the active site of xylose repressor. At the presence of glucose-6-monophosphat the activation of the promoter by Xylose is being blocked and transcription cannot occur. Thereby the xylose related activation of the promoter is hindered and the actual transcription is repressed [119].

### 1.3 Objectives

In this work *B. megaterium* was used as a Gram positive model organism to extensively study the production and secretion of the ABF D.13 scFv. For the bioprocess optimization a holistic approach was followed. First the aim was to establish a defined production medium. Different media components like carbon sources, metal ions and ammonium concentrations were screened on a platform of 96 well plates of 1 ml scale and shaking flasks with a maximal cultivation volume of 100 ml. As a second step the process was transferred to the bioreactor scale of up to 4 L. Throughout this up-scaling procedure both, the production of ABF D1.3 scFv and biomass formation with *B. megaterium* as production host were optimized in a bidirectional approach. An optimal bioprocess strategy based on alternating growth and starvation phases was established to gain high product titers of ABF D1.3 scFv. As a final step a scale-up to a 100 L bioreactor was done accounting for an advanced process control and considering “Good Manufacturing Practice” (GMP) guidelines (**Fig. 7**). As an advanced bioprocess monitoring tool means of flow cytometry were used to gain deeper insights on single cell level regarding cell viability, cell integrity and production intensity. Furthermore culture heterogeneities were measured and characterized for *B. megaterium* producing ABF D1.3 scFv under controlled bioreactor conditions. These methods were used for detailed microbial physiology studies and implemented for bioprocess development and optimization. To gain further information about what was happening inside the cell on gene expression level a transcriptome analysis was performed comparing cells with an increased production and secretion status to less producing and non-producing cells.

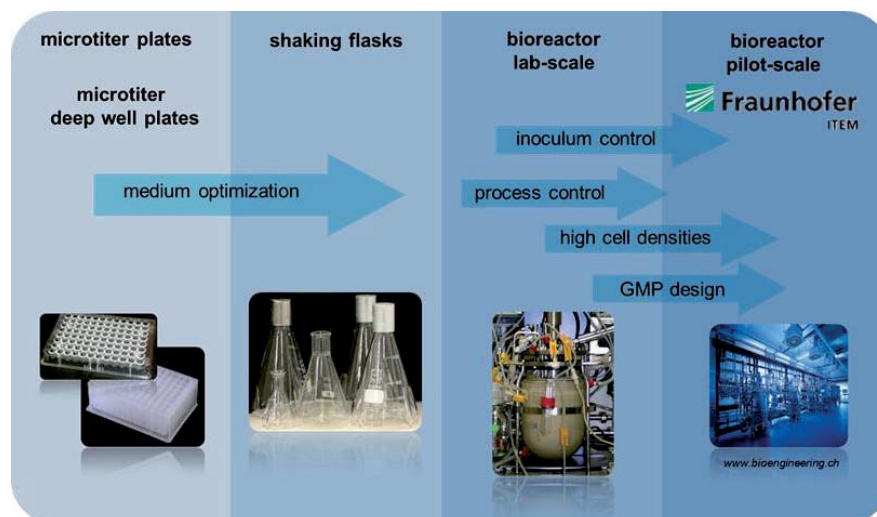


**Figure 7:** Process development of ABF producing platform with *B. megaterium* as production host.



## 2 Theory

### 2.1 “Omics” approach

The fundamental biochemical principle states that genetic information coded in DNA is first transcribed to mRNA and further translated to proteins with particular functions at least defining the phenotype of an organism. This transition of information does not function unidirectionally but shows distinctive feedback control und regulation mechanisms creating a fine tuned adapted network (**Fig. 8**). Metabolites e. g. have a primary effect on enzyme functions and regulatory proteins are directly involved in controlling transcription and translation. Particular gene expression and regulation is determined by environome conditions like physical parameters (e. g. temperature and pH), nutrient availability, toxic compounds or environmental stress conditions in general. These parameters can specifically be controlled in bioreactor cultivations with the aim to maximize the specific productivity of a bioprocess. To gain deeper insights into the system and to actually understand the parameter dependencies different high-resolution techniques are available. On the level of gene expression transcriptome analysis, based on DNA microarray technology, is used to semi-quantify mRNA expression levels under certain conditions. This is done by comparing the expression pattern of two distinctive conditions or bacterial strains. Proteome analysis reveals details about the proteins present under certain circumstances. Quantitative data can for instance be determined by labelled peptide mass fingerprinting measured with LC-MS analysis techniques. Metabolite concentrations (Metabolome) and metabolic fluxes (Fluxome) based on  $^{13}\text{C}$  labelling experiments with resulting label pattern of particular amino acids are measured by GC-MS/LC-MS technologies and reveal deeper insights on metabolic level. This “omics” approach gives a detailed fingerprint about processes inside the cell under certain environmental conditions assuming that the sample taken is homogenous in its cell population. Here the “cytomics” technique comes into play revealing possible culture heterogeneities. This technique is based on a single cell characterization finger print of a whole cell culture by means of FCM. The method also opens up the chance to sort these populations and subsequently follow the “omics” approach on the level of different populations.



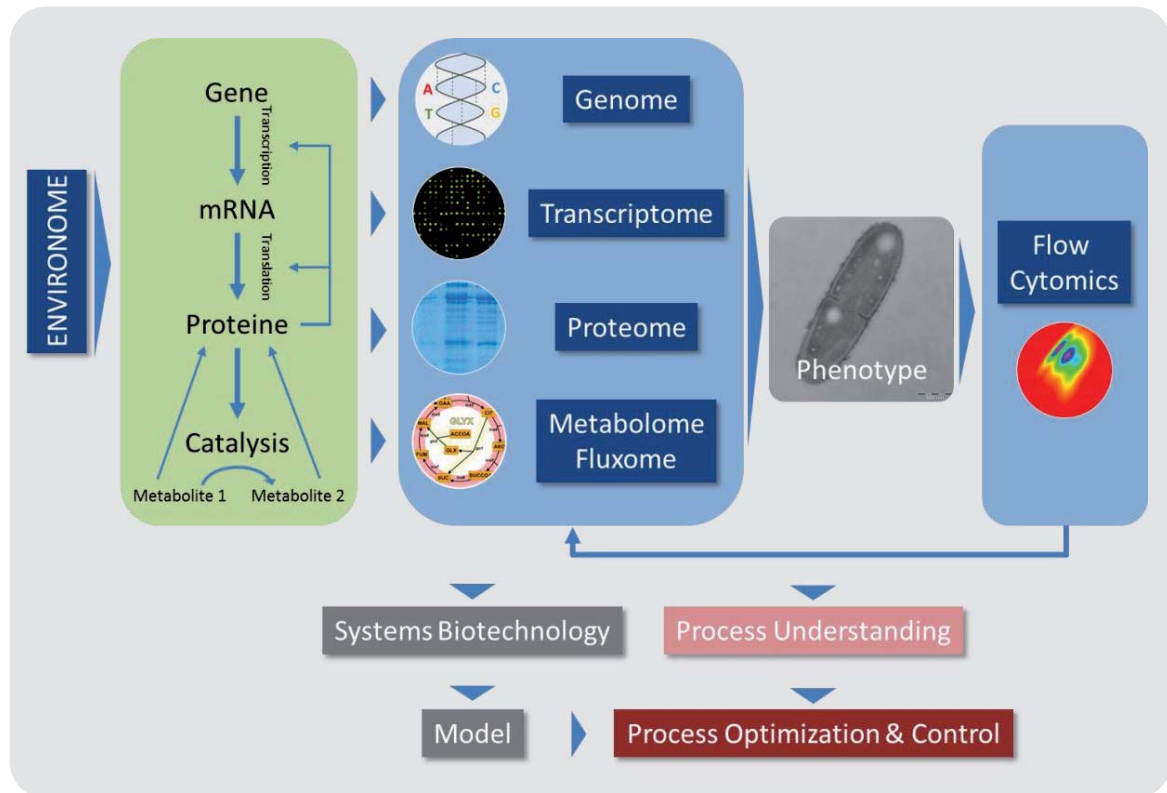


**Figure 8:** Systems Biotechnology approach; “From Environome to Phenotype” with the aim of modeling and control.

Transcriptomics, Proteomics, Metabolomics, Fluxomics and Cytomics provide a huge amount of data. The challenge for the future is to interpret all these data sets in a common holistic way. Thereby bioprocesses can be predicted and optimized combined in the discipline of systems biotechnology (**Fig. 8**). As described for a whole cell model, none of these data sets should be considered separately as distinctive interactions and regulation mechanisms exist. Still single “omics” techniques are sufficient in providing information about specific effects, reveal bottlenecks in gene expression and metabolic fluxes and are appropriate to use for rational bioprocess control and considered strain design by means of genetic engineering.



## 2.2 Flow cytometry and cell heterogeneity

Considering production processes in the biotechnological industry Process Analytical Technologies (PAT) for monitoring and evaluation of these processes are gaining more and more importance [121]. A major point is to easily decide whether a process is stable and reliable in production according FDA standards. Its central idea is to move away from quasi-final off-line product quality assessment to “real time” strategies accompanied by online measurements of critical variables. To gain a better understanding and deeper insights into the particular bioprocess, studies at single cell level are required. By this means the evaluation of single cell performances would lead with the use of appropriate methods to the characterization of the physiology of a particular bacterial population.

### 2.2.1 Flow cytometry – history and function

Originally FCM was developed as a particle analysis technique for detection of aerosolic biological weapons in 1949 [122]. First commercial instruments were released by Kamensky and Göhde in 1965 and 1969 [123]. Early microbiological publications using the FCM technique were related to plasmid content, growth rate, viability estimation and bioprocess optimization [124-127]. FCM was further established for characterizing and sorting mammalian cells (e. g. haemogram analysis) but gained recently more and more importance for the application in microbial processes [128, 129], in medicine [130-132], the dairy industry [133, 134], for alcoholic beverage production [135] and in environmental and water systems [136]. In industrial production processes, single cell analysis may give high resolution insights into whole cell cultures concerning the cell status of viability, metabolic activity or even the current state of single cell production intensities [128, 137].

For measuring single cells with FCS, at first the cells are being arranged like a string of pearls by hydrodynamic focusing, which is generated by a laminar flow. Single cells are then moving with a high velocity through a flow chamber and pass an excitation source of a laser beam (**Fig. 9**). Characteristic light scattering and refraction properties of microbial cells are used to distinguish microorganisms from non-cell particles and electronic noise signals. This approach is a so-called “trigger setting”, measuring particles only with a minimal distinctive granularity. Assessment of further parameters like cell integrity, viability and production intensities can be realized by usage of specific fluorescent dyes. After excitation by the laser beam the emission spectra are processed by dichroic mirrors and long pass (LP) and band pass (BP) filters absorbing certain wavelengths and transmitting others to particular photomultiplier tubes converting optical into electronic signals. The instrument used in this work (Quanta MPL, Beckmann Coulter, Germany) also measures the electronic volume based on the Coulter-counter principle [138]. Here the change in electrical conductance by a particle or microorganism respectively, going through a small aperture in a fluid containing cell is used to determine its electronic volume (EV). After rapid screening of up to 10.000 cells in less than one minute recorded single cell properties are analyzed through classifying histograms. Diverse parameters can be combined



such as different fluorescence values and information on cells like scatter and size properties.

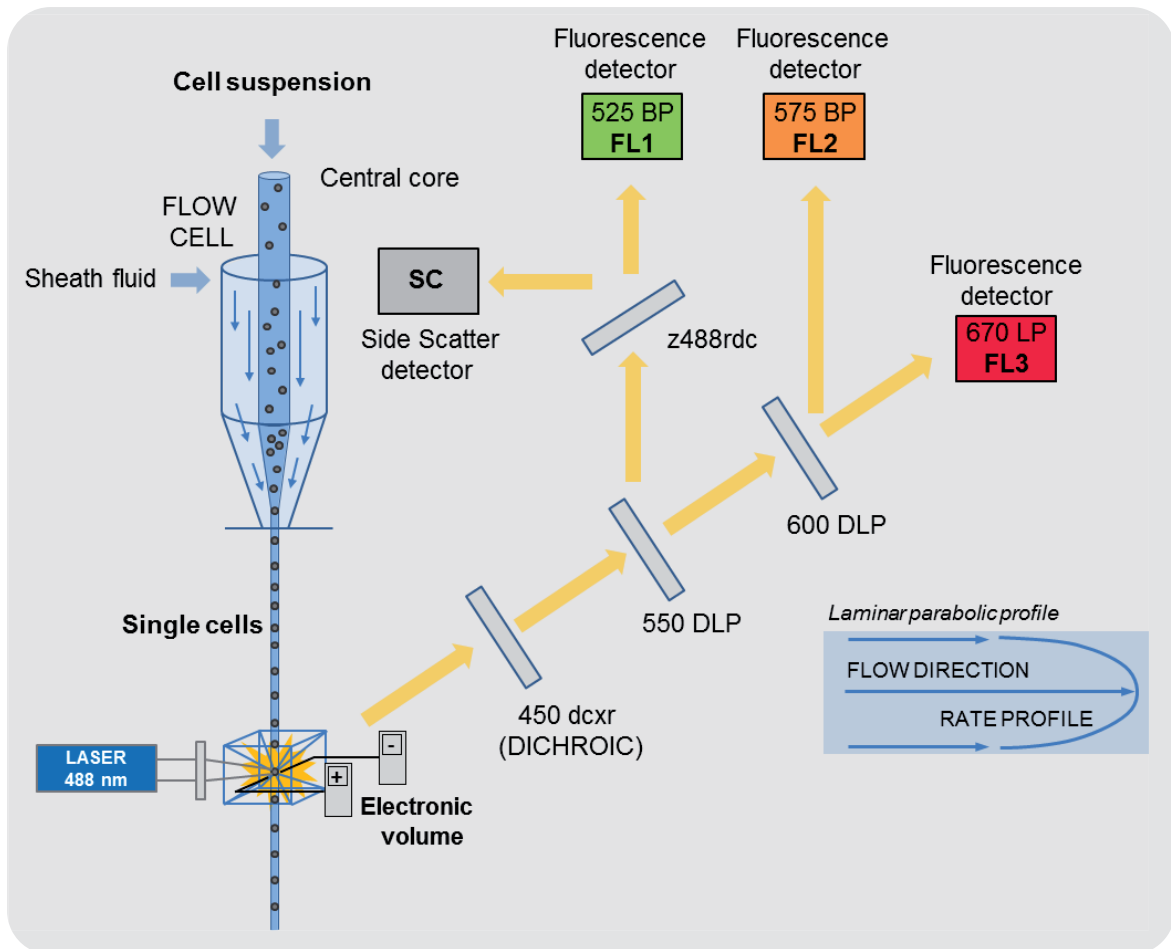


**Figure 9:** Work principle of a flow cytometer (Quanta FC Beckmann coulter), hydrodynamic focusing and subsequent fluorescence and electronic volume analysis with particular filter settings (modified according to [139]).

### 2.2.2 Assessing cell states

Different cellular states, like viable or dead cells, can be assessed by various parameters like cell growth, metabolic activity, membrane potential (MP) and membrane integrity (**Fig. 10**). The MP reflects the energetic membrane status which is an indication for the metabolic activity of every cell. Thus measuring the MP makes it possible to distinguish very precisely between active and inactive (dormant) cells. An optimal cell culture status is achieved when the majority of the cells is metabolically active thus having a high MP respectively.

In addition to that the membrane integrity is an indicator for cell death, as cells with damaged membranes cannot maintain stability of their molecular structures and eventually decompose and die. Therefore most fluorescence dyes used for cell viability



measurements are based on dye exclusion methods. Typical dyes like propidium iodide (PI) can only penetrate cells with damaged cell membranes and then emit an increased fluorescence signal after having intercalated into nucleic acid structures inside the cell.

Single cell analysis of cell viability and cell integrity mostly relies on staining procedures with fluorescence dyes. The protocols for staining and measuring therefore need to be adapted for the specific application regarding suitability of dyes, concentration and incubation times which are necessary. It is important to verify that the used method is specific and sensitive enough for measuring slight changes in the investigated physiological parameters leading to quantitative and not only to qualitative measurements. Especially for bioreactor cultivation where cell properties change over time [140-142], the robustness and applicability of a method should be assured in order to consider it suitable as appropriate at-line technique for process monitoring.

The MP and membrane integrity are suitable parameters to distinguish between living-active, living-inactive (dormant) and dead cells and have a great potential to estimate the culture status throughout a bioprocess on a single cell level as an advanced process monitoring tool.

Another process relevant parameter is the current production status of cells. By using appropriate assays based on fluorescent detection ABs it is then possible to distinguish between highly productive and less productive cells consequently revealing production and secretion heterogeneities and probable dependencies on certain cell viability states. For instance not all viable cells must exhibit the same pattern of productivity and a higher secretion efficiency may be coupled to certain transition states.

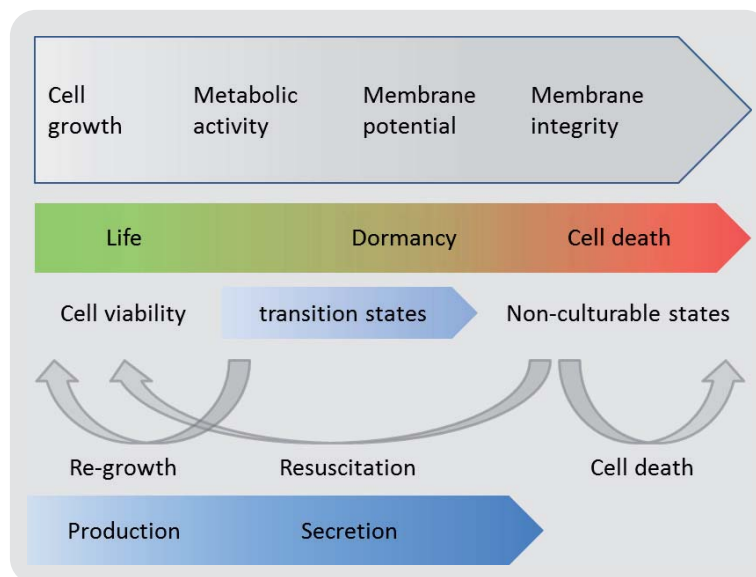


**Figure 10:** Functional criteria determining different levels of cell viability and production intensity (modified according to [139]).



### 2.2.3 Cell heterogeneities

At biotechnology process optimization and basic research-related “omics” approaches a bacterial culture is normally assumed to be in a homogenous state. In different works using FCM to monitor cells on a single level it was discovered that this homogeneity of a whole cell culture is not always present. In the following different mechanisms and principles for evolving culture heterogeneity are discussed focusing on why these culture heterogeneities evolve (2.2.3.1, 2.2.3.2) and where they may be originated from in particular (2.2.3.3, 2.2.3.4).

#### 2.2.3.1 Deterministic and stochastic processes

The evolution towards genetic networks favoring multi-stability of populations is based on the fact that phenotypic variability can be regarded as a key element to cope with changing or severe conditions [143]. A potential pre-condition for this phenotypic variability are random fluctuations in the biochemical reactions of the cell [144, 145]. Here the “noise” is most distinctive when the number of molecules is small (so-called “finite number effect”). It is speculated that stochastic processes play an important role in determining which individual cell will switch its phenotype and when [146].

#### 2.2.3.2 Heterogeneity trigger

Factors triggering the formation of heterogeneities are related to changes in environmental conditions like e. g. nutrient limitation, concentration gradients [147], toxic compounds or the induction of heterologous protein production [148]. These conditions impose selective pressure upon cells leading to a distinctive formation of different cell populations. In this sense heterogeneous populations have an increased fitness compared to homogenous populations. The basic principles and characteristics of heterogeneities in populations of microorganisms are further being discussed in the following and some examples are given.

#### 2.2.3.3 Mechanisms

Heterogeneities in bacterial cultivations are based on a variety of mechanisms ranging from cell cycle variations, changes in the micro-environment to the appearance of distinctive mutations [149].

The microbial cell division process itself may cause differentiation of cells related to so-called “replicated aging” [150], “non-symmetric cell division” [151] and the development of aged cell poles [152]. It was shown that particular cells differ in their magnitudes and DNA content. Regarding bacterial cell growth and proliferation Smith and Martin [128] postulated that the cell cycle consists of two main parts: 1) a stochastic nutrient availability dependent phase and 2) a deterministic replication and cell division related phase. At a key experiment of a phased cultivation it was shown that the duration of stochastic versus deterministic phases distinctively influenced the heterogeneity of a population [153].



Another theory for further segregation of populations is based on the assumption of a bistability state of bacterial cells [149]. It is a switch-like behavior of certain gene expression pattern as an either-or response to environmental stress conditions. An early example for bistability is the utilization of lactose of *E. coli* cells forming two distinct subpopulations related to different metabolic states [154]. Other examples for bistability based heterogeneities in bacterial populations are the competence development and sporulation behavior of *B. subtilis* cells [155]. Here two distinct populations can be distinguished within an isogenic population of stationary-phase cells into sporulating and nonsporulating cells. It was found that the signal to sporulate already occurs during the exponential growth phase and is epigenetically passed on (section 2.2.3.4). Thereby cells can rapidly react on starvation conditions and start spore formation if necessary [155]. A further example for heterogeneity in terms of extracellular enzymes is the production and secretion of exoprotease AprE (subtilisin) and Bpr (bacillopeptidase) of *B. subtilis* which are known to degrade extracellular proteins as nutrient source under nutrient-limiting conditions. The secretion of these enzymes was found to be limited only to a small part of the population [156]. Here a simple form of altruism is developed as all cells somehow benefit from the costly production of proteases of single cells.

Mutation-based subpopulations were found to be related to conditions of stress like nutrient limitation during the stationary phase. In *E. coli*, hypermutable subpopulations (HMS) are e. g. based on mechanisms of general stress response, SOS response, double-strand break (DSB) and repair [157]. This phenotypic variability ensures that at least one offspring will be adapted and fit under the given environmental conditions. Another very interesting adaptive mutation related to a certain cell type are the so-called “antibiotic resistance persister cells” [143] e. g. from biofilm formation. These persister cells can be re-grown to a form of population that once again consists of antibiotic-sensitive cells and a small subpopulation of persisters being related to its stochastic switch behavior and epigenetic nature [158].

#### 2.2.3.4 Inheritance

The information leading to the formation of distinctive subpopulations is passed on to following generations and can be described as a type of epigenetic inheritance. Mechanisms belonging to this kind of non-Mendelian inheritance are based on modifications to DNA structures like methylation, genomic imprinting, histone modification, prions and transfer of transcriptional regulators during cell division which are determining the later cell phenotype [159].

**Figure 11** summarizes different trigger factors, characteristics and epigenetic inheritance mechanisms leading to a certain selection pressure to heterogeneity formation in microbial cell populations. Measuring these heterogeneities with means of FCM and subsequent cluster analysis will give totally new insights into population dynamics in both industrial bioprocess development and optimization and basic research topics like biofilm formation. Also the systematic screening for highly producing cells becomes possible and can be combined with a sorting and “omics” approach thus revealing possible bottlenecks and heterogeneity mechanisms.

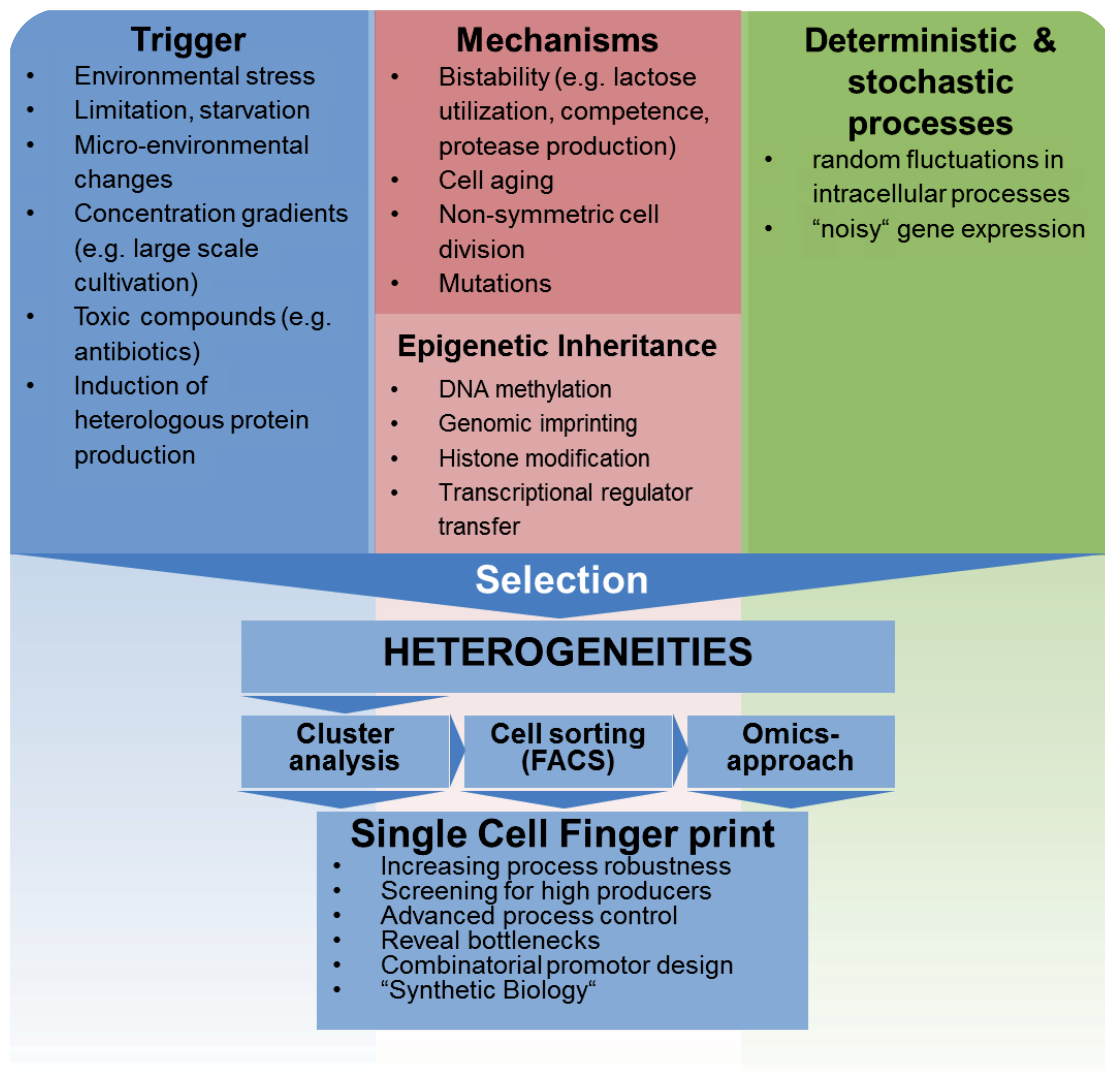


**Figure 11:** Microbial population heterogeneity; triggers, mechanisms and possible applications.

## 2.3 Process development

The production of ABs with their multimeric disulfide structure is quite complicated although the main principle is really straight forward. Cells, being microbial or mammalian systems, do what "nature" actually tells them: synthesize proteins. The biotechnologist simply exploits these micro scale cell factories to gain the desired products.

For development and optimization of an integral bioprocess it is important to account for both improving upstream and at the same time downstream processing. Upstream processing is referred to as the generation of a product by an appropriate process design. It involves suitable choices of the production strain, medium composition and process strategies to gain high titers of functional product at short time periods with at the same time low COGs. Downstream processing includes the purification and formulation of the



final product and accounts for up to 80% of overall production costs [160]. Therefore a whole process design with integration of upstream and downstream processing is most desirable.

The cultivation medium is an important parameter of the upstream processing as it has a direct influence on the process productivity as well as on the purification effort. In principle there are two media types used for biotechnological processes. The so-called “complex media” rely on undefined media components like yeast extract or peptone, consisting of less reproducible mixtures of amino acids, peptides, vitamins and minerals. In contrast minimal or defined media have a specific composition of a particular carbon- and nitrogen-source, phosphate e. g. in form of a buffer system, minerals and trace elements. Micro-elements like manganese, cobalt, copper, nickel, molybdenum, selenium, zinc and vanadium are sufficient in small amounts but have an important role for distinct enzyme functionalities. Media compositions depend on the used microorganism and can have direct effects on cell growth and product formation. Complex media are easy to handle on the one hand, but on the other hand, problems with downstream processing particularly those correlated with the separation of contaminating agents from complex ingredients, e. g. yeast extract proteins have to be taken into account. Particularly in industrial processes where criteria like GMP [161] and PAT [162] must be taken into account, complex protein rich ingredients should be avoided and are less beneficial. A minimal medium therefore is one of the most important pre-requisites to realize effective process control strategies in bioreactor cultivations and is fundamental for modeling intracellular metabolic phenomena.

The underlying project of the ABF production by *B. megaterium* is incorporated into the Collaborative Research Center (SFB 578) where exactly these considerations “From Gene to Product” are in the main focus of rational process development. From the initial strain and plasmid design to process engineering and final purification and applications of the product, all areas of a biotechnological process are involved. As a typical example to improve the overall purification process, different parameters such as the production strain, plasmid constructions and the particular medium design have to be taken into account and may influence the final product quality, production and purification costs.

Considering the process design one must not underestimate the problems occurring at taking a process from the bench to production facilities of much greater scale. Process properties being clearly different include the quantities required (scale), regulatory aspects, raw materials, equipment, process costs (economics) and formulation and stability of the final product. On the lab scale the process itself is designed to quickly perform many varying experiments for optimizing different parameters whereas the main focus of a large manufacturing process is the establishment of a robust and reproducible process which can also handle large volumes and product titers [62]. According to the FDA certain validation approaches and principles of current Good Manufacturing Practice (cGMP) have to be followed for processes designed to manufacture human or animal drugs. Especially quality, safety, efficacy and control are most important. The manufacturing should be designed and controlled to assure that in-process materials as well as the



finished product meet predetermined quality requirements and do so consistently and reliable [163]. To meet these requirements sufficient process knowledge is indispensable. Design of Experiment (DOE) studies are appropriate instruments to reveal relationships, including multivariate interactions e. g. of media components and process parameters [164]. By online measurement of process parameters e. g. biomass concentration can be estimated and used for adapted process control. This general approach involving PAT is a promising tool to further increase and control the reliability and quality of industrial bioprocesses [165].





### 3 Material and methods

#### 3.1 Strain and plasmid

In all experiments the *B. megaterium* strain YYBm1 [166] carrying the plasmid pEJBmD1.3scFv was used [46]. The strain was provided by the group of Dieter Jahn at the Technische Universität Braunschweig and is a mutant derived from *B. megaterium* MS941, which was also derived from the parental strain *B. megaterium* DSM319 [167] (German Collection of Microorganisms and Cell Cultures, Braunschweig, Germany). The ABF D1.3 scFv expression is under the control of xylose promotor system. Due to a *xylA* mutation in the strain YYBm1 the inducer xylose is not metabolized. The secretion of the ABF D1.3 scFv in the surrounding media is ensured by the signal peptide of Lipase A using the Sec-pathway combining both the actual functional folding and the secretion process through the cell membrane.

The plasmid design was done by the group of Stefan Dübel and includes several important components as described in **Figure 12** [46]. Among these are an antibiotic resistance marker gene against tetracycline (*tet*), the gene for the ABF D1.3 scFv, both chains connected by a linker region (VH-linker-VL), an origin of replication for *Bacillus* species and some components being important for cloning approaches done in the *E. coli* system.



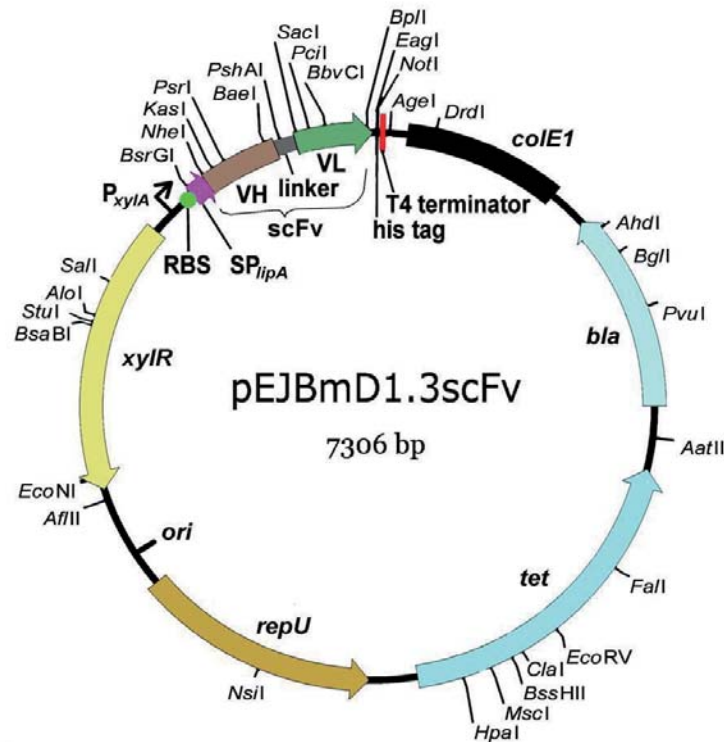


**Figure 12:** Expression plasmid pEJBmD1.3scFv [46];  $P_{xyIA}$ : xylose promotor; **VH**: coding region for variable domain of heavy chain; **VL**: coding region for variable domain of light chain; **linker**: coding region for peptide linker connecting heavy and light chain; **His-tag**: affinity tag coding for 6 histidines; **RBS**: ribosome binding site; **SP<sub>lipA</sub>**: coding region for signal peptide from extracellular lipase A gene; **tet**: tetracycline resistance gene; **repU**: origin of replication for *B. megaterium*; **ori**: origin of replication for *E. coli*; **xyIR**: xylose repressor gene [59].

For transcriptome investigations the *B. megaterium* strain YYBm1 carrying the plasmid p3Stop1623 was used as a control. This plasmid is equal to the ABF expression plasmid pEJBmD1.3scFv without the actual gene coding for the ABF and a stop codon after the promotor region to avoid any heterologous gene expression.

### 3.2 Sampling of cultivation supernatant

Samples were taken for biomass, xylose, fructose concentration measurements and single cell analysis. The cell suspension (2 mL) was centrifuged at 15.7 g, 5 min, 4 °C (5415 R Eppendorf, Hamburg, Germany). For MP measurements the centrifugation was done at 3.3 g and cells were immediately stained and subsequently measured (3.14). The supernatant was frozen at -20 °C and cell pellet was stored at 4 °C for production intensity assay (3.18). The supernatant was used for determining sugar concentration by HPLC analysis (3.3) and for quantitative ELISA test (3.5) as described below. Cell pellets were



used for determining production intensities (3.18), cell dry weight concentration (CDW) (3.4) and taking scanning electron microscope (SEM) pictures (3.19).

### 3.3 High-performance liquid chromatography analysis

Sugars (xylose, fructose) were quantified by high-performance liquid chromatography (HPLC) (Hitachi Elite LaChrom, Krefeld, Germany) equipped with a Metacarb 87 C column (Varian, Palo Alto, CA, USA) as stationary phase and Millipore H<sub>2</sub>O as mobile phase at 0.6 mL/min and 85 °C. Detection was performed using an IR detector. Organic acids were measured with means of HPLC (Hitachi Elite LaChrom, Krefeld, Germany) equipped with an Aminex HPX 87 H column (Biorad, Hercules, CA, USA) as the stationary phase and 12.5 mM H<sub>2</sub>SO<sub>4</sub> as the mobile phase at 0.5 mL/min and 45 °C. The detection was performed using an UV detector (220 nm) or a refractive index detector (RI), respectively.

Preparing the sample, 2 mL of the cultivation supernatant was sucked into a 2 mL plastic syringe and directly squeezed through a sterile filter (polyvinylidene fluoride, 0.2 µm pore size, Roth, Karlsruhe, Germany). For protein precipitation 20 µL/mL 0.5 M H<sub>2</sub>SO<sub>4</sub> were added and samples were frozen at -20 °C. After thawing and centrifuging at 15.7 g, 4 °C for 5 min (5415 R Eppendorf, Hamburg, Germany) 500 µL of supernatant was filled in HPLC vials and analyzed.

### 3.4 Biomass measurements

Cell concentration was determined as optical density at a wavelength of 578 nm using a Novespec 3 Photometer (Amersham Bioscience). CDW was measured via gravimetric analysis in triplicates. Here biomass pellets of 15 mL culture volume were washed twice with distilled water to remove salts and afterwards dried at 80 °C for 48 h.

### 3.5 Quantification of the antibody fragment D1.3 scFv concentration via ELISA

Antigen binding ELISA was done according previously established protocol [46]. Maxisorb MTPs (Nunc, Wiesbaden, Germany) were coated with 1 µg hen egg white lysozyme in 100 µL PBS per well overnight at 4 °C. BSA of same amount was used as a control for unspecific binding. Coated wells were washed three times with PBST (PBS + 0.1% (v/v) Tween 20) and blocked with 2% (w/v) skim milk powder in PBST for 1.5 h at room temperature, followed by three times washing with PBST. 50 µL ABF containing superna-

tant and several 1:3 dilutions in PBS were diluted 1:2 with blocking solution and incubated for 1.5 h, followed by three times washing with PBST. Functional ABFs were detected with monoclonal mouse anti-penta His AB (1:10000) (Qiagen, Hilden, Germany) and polyclonal goat anti-mouse IgGs conjugated with horse radish peroxidase (HRP) (Fab specific) (1:10000) (Sigma, Taufkirchen, Germany) each at an incubation time of 1.5 h and a subsequent three times washing step with PBST. The visualisation was done adding 100  $\mu$ L TMB (3,3',5,5'-tetramethylbenzidine) substrate and the staining reaction was stopped by addition of 100  $\mu$ L 1 N sulphuric acid. The absorbance at 450 nm (reference at 620 nm) was measured using a micro titer plate reader SUNRISE (Tecan, Crailsheim, Germany).

A quantitative determination of functional folded ABF D1.3 scFv was done by parallel measuring a calibration standard of purified ABF D1.3 scFv on the 96 well plates. The standard was purified from the supernatant with a protein-L column (©Pierce) and quantified by densitometric analysis of corresponding SDS gel bands related to a D1.3 scFv standard.

**Figure 13** illustrates the main steps of a Protein-L purification, visualized on a SDS-gel analysis (SDS-gel (12%), Precision Plus Protein Unstained Standard (BioRad), [168]). After centrifugation at 4 g for 15 min and sterile filtration through a 0.5  $\mu$ m sterile filter, the supernatant is concentrated via Ultrafiltration (10 kDa cut-off, Amicon Ultra, Millipore) and applied on a Protein-L column (©Pierce). Protein L is a protein derived from *Peptostreptococcus magnus* binding specifically to light chain variable regions belonging to the human gene families  $\kappa$ 1,  $\lambda$ 2 and  $\lambda$ 3 but not  $\kappa$ 4 or  $\lambda$ 1 [169]. This highly specific method selectively purifying functional folded ABFs has the drawback of harsh elution conditions at a low pH. This leads to degradation of the ABF indicated by two smaller bands corresponding to fragments of  $\sim$ 13 kDa. Subsequently the amount of functional, not degraded ABF is determined by densitometric analysis at comparing band intensities to previously quantified protein standard of same size range. Thereby it is possible to directly link the functional amount of ABF to its activity in the ELISA assay as a calibration standard. Particular samples were measured in three dilutions (1:3) and quantified according to the standard samples via logit-log plot analysis [170] (**Fig. 14**).

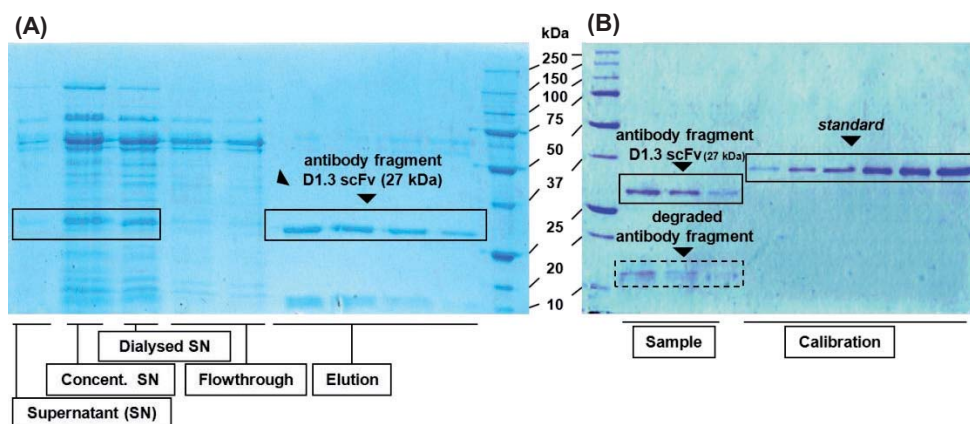


**Figure 13:** (A) Purification of ABF D1.3 scFv by Protein L (©Pierce) and (B) densitometric quantification with an adequate protein standard.

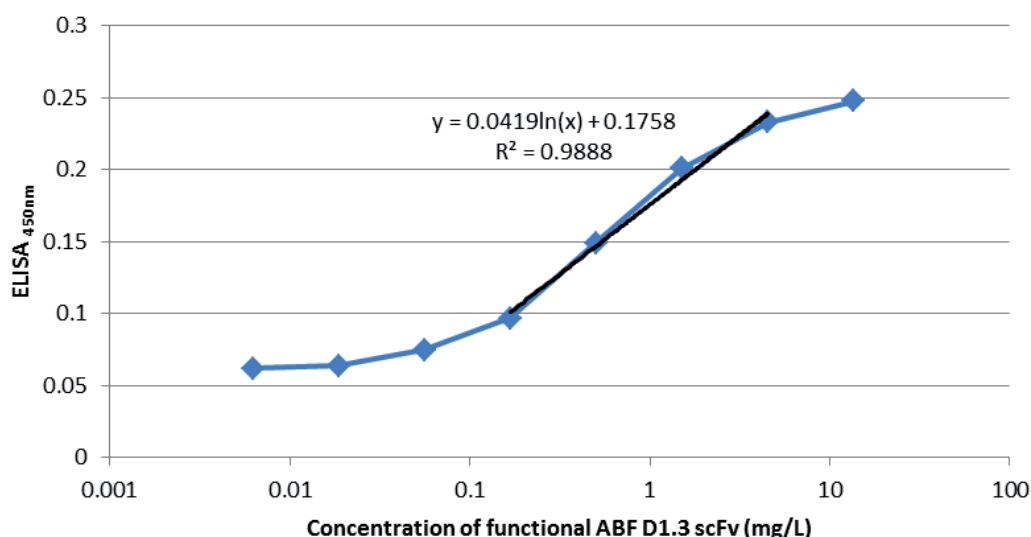


**Figure 14:** Specific binding activities of the D1.3 scFv produced in *B. megaterium* YYBm1 (EJBmD1.3scFv) determined by ELISA. Absorbance was measured at 450 nm and corrected for absorbance at 620 nm. The D1.3 scFv concentration detection limits were ~0.01 mg/L.

### 3.6 Cell bank – *Bacillus megaterium*

*B. megaterium* was stored at -80 °C in a 50% glycerol solution in cryogenic vials. For preparing cryogenic cultures *B. megaterium* was cultivated in 10 mL minimal medium at 37°C for 12 h. 100 mL minimal medium in a 1000 mL shaking flask without baffles were inoculated with this cell suspension adjusting to an OD<sub>578nm</sub> of 0.1. In the exponential phase (OD<sub>578nm</sub> = 3) 10 mL of cell suspension were mixed with 10 mL glycerol (99%) and immediately frozen in 0.5 ml aliquots in liquid nitrogen and stored at -80 °C.

### 3.7 Screening in deep well plates

Screening in micro titer plates should be done under non-oxygen limiting conditions. Oxygen concentration is influenced by the cultivation volume and the amount of generated biomass directly coupled to the amount carbon source used initially. For this reason experiments were carried out to determine the optimal concentration of fructose and the appropriate cultivation volume in micro titer deep well plates so as to prevent the limitation of oxygen. Here a minimal medium was used which composition is further explained as follows. In addition to the biomass concentration, two other parameters such as the product concentration and remaining fructose as only carbon source were measured in different cultivation volumes after 12 h of cultivation. **Figure 15** gives a brief overview of these process parameters at using a starting concentration of 5 g/L fructose. As can be seen, 900 µL of cultivation volume is ideal for screening as it shows the highest production

of ABFs accompanied by the complete consumption of fructose after 12 h, indicating that no oxygen limitation occurred. To make sure measuring growth dependent production and secretion the cultivation time was set to 11 h in subsequent experiments.

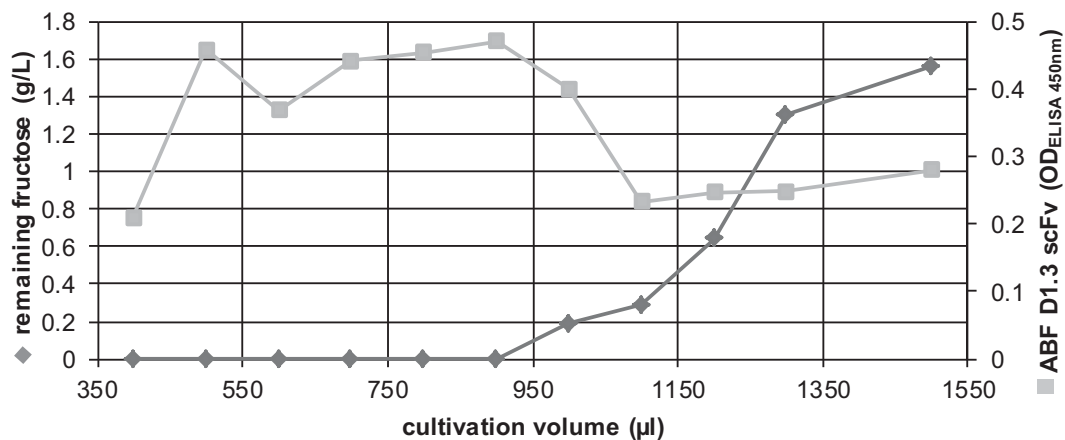


**Figure 15:** Screening of different cultivation volumes in 96-deep-well plates showing the produced ABF (■) and the remaining fructose (◆). Excess in fructose gives a hint on oxygen limitation as the carbon source is not completely depleted.

### 3.8 Cultivation conditions – deep well plates

As a starter medium, modified A5 medium [166] with pH 7.2 was applied with 5 g/L fructose, 5 g/L  $(\text{NH}_4)_2\text{SO}_4$ , 3.52 g/L  $(\text{KH}_2\text{PO}_4)$ , 6.64 g/L  $\text{Na}_2\text{HPO}_4 \times 2\text{H}_2\text{O}$  and 10 µg/mL tetracycline. 2 mL/L of sterilized filtered trace element solution was added [166, 171] consisting of 40 g/L  $\text{MnCl}_2 \times 4\text{H}_2\text{O}$ , 53 g/L  $\text{CaCl}_2 \times 2\text{H}_2\text{O}$ , 2.5 g/L  $\text{FeSO}_4 \times 7\text{H}_2\text{O}$ , 2 g/L  $(\text{NH}_4)_6\text{Mo}_7\text{O}_{24} \times 4\text{H}_2\text{O}$ , 1.091 g/L  $\text{CoCl}_2$  and 150 g/L  $\text{MgSO}_4 \times 7\text{H}_2\text{O}$ . The pre-culture was prepared in 10 mL overnight cultures in shake flasks at 37 °C and 130 rpm (CERTOMAT® BS-1; B.Braun Biotech International). Different media compositions created by the genetic algorithm were assembled by adding different volumes of stock solutions in distilled water and tested in 96 deep-well plates in triplicates. These plates were sealed with Aeraseal Sealing film (Sigma -Aldrich, A9224-50EA) and breathe easy film (Roth, T093.1) and were shaken at 37 °C, 1000 (1/min) in an orbital shaker (Titramax 1000, Heidolph, Düsseldorf). By using both sealing films and a volume of 900 µL cultivation medium evaporation and oxygen limitation were avoided and totally negligible at incubation times less than 12 h.

The samples were inoculated at an OD of 0.6 and induction was started by adding 0.5% xylose. After 11 h the cultivation was stopped, OD was measured by 50 µL sample diluted 1:2 with Millipore  $\text{H}_2\text{O}$  in a Tecan microplate reader at 620 nm. CDW was estimated by a correlation with the OD at 620 nm.



$$CDW = -0.084 + 2.13 \times OD_{620nm} - 1.30 \times (OD_{620nm})^2 + 1.77 \times (OD_{620nm})^3 \quad (1)$$

After centrifuging the sample at 15.7 g the supernatant was directly used for antigen binding ELISA.

### 3.9 Cultivation conditions – batch

For particular stages of medium optimization different media compositions were used.

The basic medium composition for carbon source screening was based on A5 medium according to Yang et al. (2007) [166] consisting of: 0.3 g/L  $MgSO_4 \times 7H_2O$ , 5 g/L  $(NH_4)_2SO_4$ , 3.52 g/L  $KH_2PO_4$ , 7.26 g/L  $Na_2HPO_4 \times 2H_2O$ , 2 mL trace element solution, 10 mg/L tetracycline, 1 g/L yeast extract, 4 g/L of the particular carbon source. Trace element composition was 40 g/L  $MnCl_2 \times 4H_2O$ , 53 g/L  $CaCl_2 \times 2H_2O$ , 2.5 g/L  $FeSO_4 \times 7H_2O$ , 2 g/L  $(NH_4)_6Mo_7O_{24} \times H_2O$ , 2 g/L  $CoCl_2 \times 6H_2O$ .

For inducer concentration screening, statistical experimental design of  $MgSO_4 \times 7H_2O$  and  $(NH_4)_2SO_4$  concentrations and bioreactor cultivations a minimal medium based on the previous metal ion optimization approach was used according to David et al. (2010) [172]. It contains fructose at 5 g/L as a sole carbon source supplemented with 3.52 g/L  $KH_2PO_4$ , 5.3 g/L  $Na_2HPO_4$ , 3 g/L  $MgSO_4 \times 7H_2O$ , 25 g/L  $(NH_4)_2SO_4$ , 0.312 g/L  $MnCl_2 \times 4H_2O$ , 0.095 g/L  $CaCl_2 \times 2H_2O$ , 5.5 mg/L  $FeSO_4 \times 7H_2O$ , 21.6 mg/L  $(NH_4)_6Mo_7O_{24} \times 4H_2O$ , 6.2 mg/L  $CoCl_2$ , 16 µg/L  $CuSO_4 \times 5H_2O$ , 155 µg/L  $H_3BO_3$ , 15 µg/L  $ZnSO_4 \times 7H_2O$  and 10 mg/L tetracycline. For the Central Composite Design (CCD), the particular  $(NH_4)_2SO_4$  and  $MgSO_4 \times 7H_2O$  concentrations were adjusted as shown in **Table 4**.

For bioreactor batch cultivations the optimized minimal medium regarding metal ions [172]  $MgSO_4 \times 7H_2O$  (3 g/L) and  $(NH_4)_2SO_4$  (25 g/L) concentration were used with 15 g/L fructose as carbon source. 1 L of minimal medium was inoculated with the pre-culture to reach an  $OD_{578nm}$  of 0.1 in a 3.7 L bioreactor (Bioengineering, Wald, Switzerland). The cultivation was carried out under constant temperature at 37 °C and controlled at pH 6.3. The DO concentration was adjusted above a value of 20% saturation, using a stepwise cascade control, increasing alternately agitation and aeration rate. Induction was done by addition of an appropriate amount of a 100 g/L xylose solution 1.5 h after inoculation if not mentioned differently to reach a final concentration of 5 g/L.

For pre-cultures, 100 µL of cryogenic culture was used as inoculum for 10 mL of the particular minimal medium with 5 g/L fructose, cultivated for 12 h and subsequently used as inoculum. As second pre-culture for bioreactor experiments, 100 mL medium was inoculated from first pre-culture adjusting to an  $OD_{578nm}$  of 0.1 and cultivated for additional 12 h.





### 3.10 Cultivation conditions – fed-batch

At fed-batch experiments the previously described minimal medium for batch cultivations at bioreactor scale was used. Changes in concentration ranges are mentioned in detail. The pre-cultures were prepared as described before. The main lab scale cultivation was carried out in a 5 L bioreactor (Bioengineering, Wald, Switzerland). For the oscillating fed-batch experiment 3 L minimal medium with an initial  $\text{MgSO}_4 \times 7\text{H}_2\text{O}$  concentration of 0.3 g/L and a fructose concentration of 2.7 g/L was inoculated with a pre-culture volume to adjust the main culture to an  $\text{OD}_{578\text{nm}}$  of 0.02. After a batch phase of approximately 12 h the feed was started indicated by a sudden DO peak. The feed composition was as follows: 225 g/L fructose, 75 g/L  $(\text{NH}_4)_2\text{SO}_4$ , 22.5 g/L  $\text{MgSO}_4 \times 7\text{H}_2\text{O}$ , 5 g/L xylose, trace elements and tetracycline concentrations were as described for optimized minimal medium before. The cultivation was carried out under constant temperature at 37 °C and controlled pH at 6.3 with 5 M NaOH and 0.5 M  $\text{H}_3\text{PO}_4$ . The DO concentration was controlled at a value of 20% saturation, using a stepwise cascade control, increasing alternately agitation and aeration rate. Induction was done by an appropriate amount of a 100 g/L xylose solution 2 h after inoculation to reach a final concentration of 5 g/L. The cultivation for upscale to 55 L cultivation volume was carried out in a 100 L bioreactor (B. Braun Biotech International, Melsungen, Germany) under same medium, process control and inoculation conditions as just described for the small scale.

### 3.11 Gas analysis

Carbon dioxide and oxygen in the exhaust gas were measured with gas sensors (Blue Sense, Herten, Germany) and the corresponding (specific) oxygen uptake rate (OUR ( $q\text{O}_2$ )) and (specific) carbon dioxide evolution rate (CER, ( $q\text{CO}_2$ )) were calculated for all cultivations considering nitrogen as inert gas.

### 3.12 Oscillating fed-batch strategy

The oscillating fed-batch strategy is based on the formula for exponential feeding strategies. The term  $e^{\mu \times t}$  is assumed to be equal to 1 as the feed is steadily adapted making the time interval going to 0.





$$F = \left( \left( \frac{\mu_{set}}{Y_{x/s}} \right) + m_E \right) \times \frac{(X \times V)}{S_0} \times \overbrace{e^{\mu \times t}}^{=1} \quad (2)$$

- X:** biomass concentration estimated by CER and  $\mu_{set-0.25}$  (g/L)  
**m:** maintenance coefficient; 0.0616 (g/g/h), calculated from chemostat cultivation  
 **$Y_{x/s}$ :** biomass yield coefficient; 0.633 (g/g)  
 **$S_0$ :** substrate concentration in the feed; 225 (g/L)  
**V:** cultivation volume (L)  
 **$\mu_{set}$ :** growth rate (time dependent) (1/h)

The specific growth rate used is time dependent based on two cosine functions leading to oscillating changes in growth and starving phases.

$$\mu_{set} = \mu_{max} \times (0.78 \times (\cos(\cos(0.5 \times (\frac{12.6}{2.4}) \times t) - 2.28) + 1)) \quad (3)$$

- t:** time (h)  
 **$\mu_{max}$ :** maximal in process growth rate; 0.3 (0.4) (1/h)

As the given specific growth rate continuously change, a consistent adaptation of the current biomass concentration  $X$  and volume  $V$  is necessary. The biomass concentration was estimated via a soft-sensor derived from the  $CO_2$  evolution rate (CER) and the particular growth rate, which is assumed to be 0.25 h time shifted before the growth rate  $\mu_{set}$  taken for the feed calculation. This was done due to experiments showing a certain delay in the growth rate which is set by the feed and the actual growth rate present. The linear correlation between CER/ $X$  and the corresponding growth rate  $\mu$  was deduced from batch data with a respiration quotient of 1.

$$\mu_{set(t-0.25)} = 0.4 \times (0.78 \times (\cos(\cos(0.5 \times (\frac{12.6}{2.4}) \times (t - 0.25)) - 2.28) + 1)) \quad (4)$$

$$X = \frac{CER}{(0.013 \times \mu_{set(t-0.25)} + 0.0024)} \quad (5)$$

- X:** biomass concentration (g/L)  
**CER:**  $CO_2$  evolution rate (mol/L/h)

The particular cultivation volume was determined by accounting for the fed volume and the sample volume taken.

$$V = \left( \frac{\text{feed}_{(\text{balance})}}{\rho_{\text{feed}}} \right) + V_{\text{start}} - \sum(V_{\text{sample}}) \quad (6)$$

<b>V:</b>	volume (L)	<b>V<sub>start</sub>:</b>	cultivation volume start (L)
<b>feed<sub>(balance)</sub>:</b>	weight of fed volume (g)	<b>V<sub>sample</sub>:</b>	sample volume (L)
<b>ρ<sub>feed</sub>:</b>	feed density (g/L)		

### 3.13 Flow cytometry

FCM studies were performed using a Quanta MPL (Beckmann Coulter, Krefeld, Germany) flow cytometer equipped with a 488 nm argon Laser. The SS signal was used as a trigger signal, green fluorescence (FL1) was detected through a dual band pass filter (525 nm,  $\pm 21$  nm bandwidth) and red fluorescence (FL3) was detected through a 670 nm long pass filter. Both fluorescence values were detected in parallel using a dichroic long pass filter for splitting. The sheath flow rate was 4.17  $\mu\text{L}/\text{min}$  and the sample rate never exceeded over 600 events 1/s at doing 10.000 counts per measurement. Signals were logarithmically amplified and photomultiplier (PMT) settings were adjusted to particular staining methods. The EV (Coulter Counter Principle, Cell Lab Quanta<sup>TM</sup> SC MPL) was used to determine cell fluorescence concentration (FL-FC: FL-Channel/ (Volume Channel)) and cell fluorescence surface density (FL-FSD: FL-Channel/ ((Volume Channel) <sup>2/3</sup>)).

### 3.14 Dye screening for membrane potential estimation

Different dyes (DiOC<sub>2</sub>(3), DiOC<sub>6</sub>(3) and DiBAC<sub>4</sub>(3)) were tested according their suitability for MP estimation. Therefore  $2 \times 10^6$  *B. megaterium* cells per mL were centrifuged (3.3 g, room temperature) and resuspended in 1 mL staining puffer (0.06 M Na<sub>2</sub>HPO<sub>4</sub>, 0.06 M NaH<sub>2</sub>PO<sub>4</sub>, 5 mM KCl, 130 mM NaCl, 1.3 mM CaCl<sub>2</sub>, 0.5 mM MgCl<sub>2</sub> adjusted to a pH 7 with NaOH, steril filtered [173]). 10  $\mu\text{L}$  of particular dye working solutions were added (DiOC<sub>2</sub>(3), DiOC<sub>6</sub>(3) in 50%/50%-DMSO/H<sub>2</sub>O, DiBAC<sub>4</sub>(3) in 100% DMSO). As a negative control 10  $\mu\text{L}$  CCCP solution (1.5 mM in DMSO) were added to depolarize cells. All dyes and CCCP were purchased from Invitrogen (Molecular Probes, USA).



### 3.15 DiOC<sub>2</sub>(3) ratio analysis

Ratio analysis of DiOC<sub>2</sub>(3) stain was done according Novo et al. 1999 and was used to estimate MP [173].

$$MP = \log \left( 10^{\frac{2}{3}} \times \left( \frac{FL3 \text{ (red fluorescence)}}{FL1 \text{ (green fluorescence)}} \right) \right) \quad (7)$$

Polarized cells show an increased staining property with the actually green fluorescent dye leading to a dye accumulation with red fluorescent properties [174].

### 3.16 Membrane potential calibration

MPs were artificially simulated by the application of the potassium ionophore valinomycin in the presence of different external potassium concentrations [173]. At particular potassium concentrations, the resulting FL3/FL1 ratios of DiOC<sub>2</sub>(3) stained cells were determined. Further MP were calculated based on the Nernst Equation ( $\Delta E = -61.54 \text{ mV} \lg (c_{\text{inside}}/c_{\text{outside}})$ ) where the potassium concentration inside the cells was assumed to be constant at 243.75 mM. Potassium concentrations outside the cells were changing according to experimental setup from 300 mM to 0 mM where the overall molarity was kept constant at 300 mM by adding an appropriate amount of sodium. Staining was done in buffer of 0.06 M Na<sub>2</sub>HPO<sub>4</sub>, 0.06 M NaH<sub>2</sub>PO<sub>4</sub>, 130 mM NaCl, 1.3 mM CaCl<sub>2</sub> and 0.5 mM MgCl<sub>2</sub> adjusted to a pH 7 with NaOH, steril filtered and addition of the appropriate amount of NaCl and KCl.



### 3.17 Viability assay

For distinguishing between live and dead cells a fluorescence dye based viability assay was evaluated. Here DiBAC<sub>4</sub>(3) and propidium iodide (PI) were used at different mixtures of live (derived from exponential phase) and heat treated cells (80 °C, 10 min). As described before, 10 µL of particular staining working solutions were added to  $2 \times 10^6$  cells in 1 mL staining puffer (PI: 1.5 mM, DiBAC<sub>4</sub>(3): 0.21 mM; end-concentrations DiBAC<sub>4</sub>(3): 2.1 µM, PI: 15 µM). Staining patterns in green and red fluorescence were subsequently analyzed by FCM.

### 3.18 Single cell production intensity assay

After sampling a cell pellet of about  $10^7$  cells, cells were re-suspended in 200 µL PBS-T (PBS (8.5 g/L NaCl, 1.34 g/L Na<sub>2</sub>HPO<sub>4</sub> × 2H<sub>2</sub>O, 0.345 g/L NaH<sub>2</sub>PO<sub>4</sub> × 2H<sub>2</sub>O), 0.05% Tween 20) and 600 µL of 4% paraformaldehyde was added. Cells were fixed for 10 min at room temperature. After centrifugation at 15.7 g for 5 min at 4 °C the cell pellet was resuspended in 900 µL PBS-T and mixed with 100 µL of particular lysozyme stock solutions (0.25 mg/mL to 5 mg/mL in PBS-T). After incubation for 10 min at room temperature and centrifugation at 15.7 g, 5 min, 4 °C cells were washed once with 500 µL PBS-T to reduce unspecific binding. Cells were first incubated with a mouse-anti-penta-His detection AB (100 µL, 1:100 in PBS-T, Qiagen 34660) at room temperature for 1.5 h and afterwards washed twice with 500 µL PBS-T. A second Alexa Fluor coupled AB (100 µL, 1:50, Alexa Fluor 488 ® goat anti-mouse IgG (H+L) highly cross-adsorbed 2 mg/mL Cat.No. A-11029 Invitrogen, USA) was added and incubated for 1 h at 4 °C in the dark. The used Alexa Dye 488 is a bright photostable conjugate being most applicable in measuring reproducible and reliable results with a high resolution [175]. Subsequently cells were washed once with 500 µL PBS-T and flow cytometric analysis was performed using the green fluorescence channel. Negative controls were established for cells treated with no lysozyme, not induced cells and leaving of first or second detection AB. As a counter stain PI was used to better visualize the data sets (end-concentrations PI: 15 µM).

### 3.19 Immuno field emission scanning electron microscopy

Preparing samples for electron microscopy cells were treated as described before (section 3.18) with the addition that as a second detection AB a 115 nm goat anti-mouse IgG coupled to 15 nm gold nanoparticles was applied. After washing with PBS samples were adsorbed onto butvar-coated 300 mesh copper grids, washed with TE buffer (20 mM TRIS, 1 mM EDTA, pH 6.9), distilled water and air-dried. Samples were then mounted



onto conductive carbon adhesive tabs on specimen mounts and were subsequently examined in a Zeiss DSM982 Gemini field emission scanning electron microscope (Zeiss, Oberkochen) at an acceleration voltage of 5 kV using the Everhart-Thornley secondary electron detector (SE-detector) and the built-in inlense Se-detector in a 75:25 ratio. Images were recorded onto MO-disk and contrast and brightness was adjusted with Adobe Photoshop CS4.

### 3.20 Confocal laser scanning microscopy

The CLSM technique was applied to directly monitor bound Alexa Fluor detection ABs at the cell surface. Here cells were resuspended in PBS and investigated with CLSM technique. Fluorescence was analyzed with a confocal laser scanning microscope CLSM-510META connected to an Axiovert 200M (Carl Zeiss, Germany) with laser excitation of 488 nm, HFT UV/488 and BP 505–530 for GFP fluorescence. All images were processed with LSM Image Browser Release 4.2 (Carl Zeiss, Germany).

### 3.21 Population cluster analysis

The technology of flowcytometry creates multiparametric datasets of fluorescence (FL), electronic volume (EV) and sideways scatter (SS) cell properties. Data analysis and data summarization have to be done in a condensed form that can explicitly be interpreted. In a multidimensional data approach the clustering of population can only hardly be achieved with simple gating tools. Gating is a process to identify homogenous cell groups which display a similar function. This process is based predominantly on the investigator's intuition than standardized statistical approaches. Therefore a model based clustering approach at the statistical platform R provided by bioconductor packages was used to identify cell populations in FCM analysis [176-178]. At a typical data analysis the number of populations is statistically ensured and the data multidimensionality is exploited guaranteeing more accurate and reproducible identification of populations. For the population analysis an appropriate model approach has to be followed. The assumption that each data set follows a Gaussian distribution is often unrealistic. Therefore an automated clustering approach based on t-mixture model with Box-Cox transformation was used [179]. Outliers have to be excluded as they may have a significant effect on the resulting clustering. The Box-Cox transformation done is defined by the Box-Cox parameter  $\lambda$ . The number of clusters is set by the Bayesian Information Criterion (BIC) number calculated for t-mixture models with Box-Cox transformation. Transformation selection, outlier identification and clustering are done simultaneously. The model-based clustering used provides both "hard" clustering (whole data separation) and soft clustering where each event may belong to more than one cluster. Here certain overlapping of



clusters become observable at the same time existing uncertainties about the event the cluster belongs to.

Open source Bioconductor packages for analysis of FCM data [180] were used to analyze and interpret particular data sets. *FlowCore* handles importing, storing, preprocessing and assessment of data from FCM experiments. *FlowViz* provides graphical methods for visualization and *FlowClust* implements mixtures to perform model based clustering algorithms of FCM data [179]. The program code used is exemplified for analyzing MP and for production intensity single cell assays of *B. megaterium* cells producing ABFs. Data sets for MP estimation by DiOC<sub>2</sub> staining and production intensity fluorescence assays were analyzed based of 4 measured parameters (SS, EV, FL1, FL3).

### 3.21.1 DiOC<sub>2</sub> membrane potential assay (SS, EV) (FL1, FL3)

# Load libraries with required methods;

```
> library (flowCore)
> library (flowViz)
> library (flowClust)
```

# Read in lmd-file into R environment;

```
> file.name <- system.file("extdata", "POPDIOC2.lmd", package = "flow-
Core")
> P1 <- read.FCS(file.name, transformation = FALSE)
```

# Summary of raw data;

```
> P1
```

#### Raw data summary

```
flowFrame object 'POPDIOC2.lmd'
```

```
with 10000 cells and 5 observables:
```

	name		Range	min	max
\$P1	SS	Side Scatter	1024	1	1023
\$P2	EV	Electronic Volume	1024	0	1023
\$P3	FL1	FL1 Fluorescence	1024	0	1023
\$P4	FL2	FL2 Fluorescence	1024	0	1023
\$P5	FL3	FL3 Fluorescence	1024	0	1023



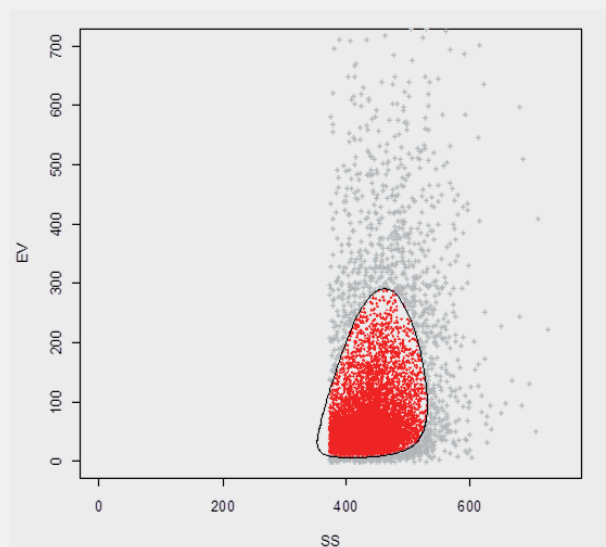
# Analysis with one cluster using SS and EV; “K” is the number of clusters; “B” is the maximum number for EM iterations, “level” sets the rule for outliers here 85% quantile, which means that a point outside the 85% quantile region of the cluster to which it is assigned will be called an outlier. Main purpose here is to identify outliers, which will be removed from the subsequent analysis.

```
> resP <- flowClust(P1, varNames = c("SS", "EV"), K = 1, B = 100,
level=0.85)
```

# Outliers and clustered data is plotted in a dot plot diagram with outliers presented as “+” and axes scaled according to “xlim” and “ylim” to control clustering.

```
> plot(resP, data=P1, pch.outliers="+", xlab="SS", ylab="EV", pch=20,
xlim=c(0,750), ylim=c(0,700))
```

Picture of plot



# The data of first clustering is loaded into P12 and outliers are removed.

```
> P12 <- P1[P1 %in% resP, ]
```

# Second clustering is done according to fluorochrome channels FL1 and FL3 on the cells selected at the first stage. The number of clusters are set from one to six, “trans” is a numeric indicating that the BOX-COX parameter  $\lambda$  is estimated from the data. The outliers are again identified by 0.85 quantile.

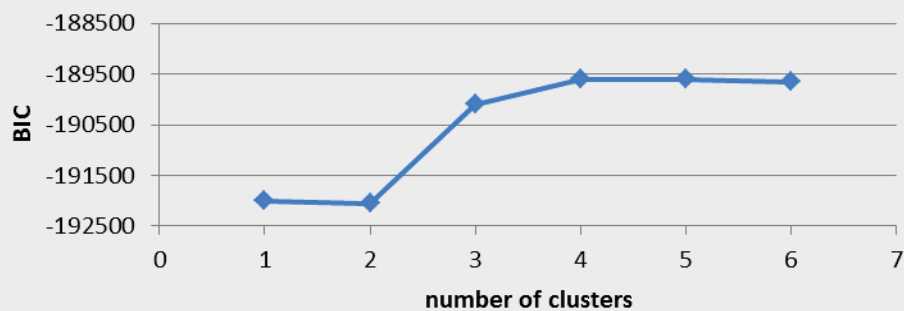


```
> resP2 <- flowClust(P12, varNames = c("FL1", "FL3"), K= 1:6, B = 100,
trans=1, level=0.85)
```

# Output of “BIC” (Bayesian Information Criterion) value, cluster number with largest or at least stable “BIC” number is selected.

```
> criterion(resP2, "BIC")
```

## Picture of BIC criterion



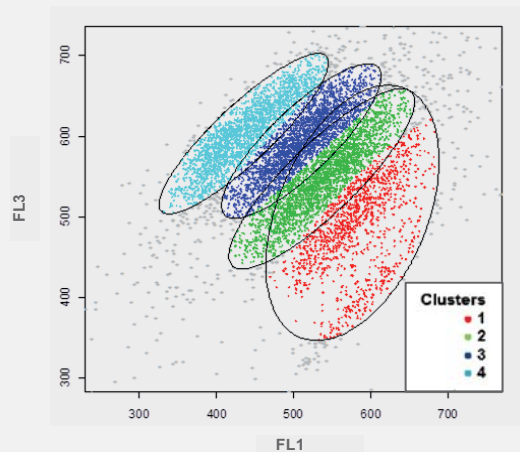
## Visualization

# Plot clustered data with outliers and legend is visualized.

```
> plot(resP2[[4]], data=P12, pch.outliers="+", xlab="FL1", ylab="FL3",
pch=20, xlim=c(250,750), ylim=c(300,720))
```

```
> legend("bottomright", col=2:5, legend=1:4, title="Clusters", pch=20)
```

## Picture of cluster analysis



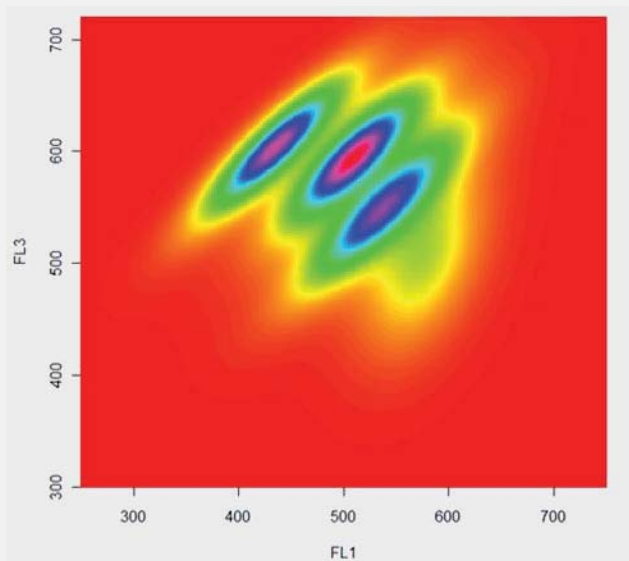


# The plot clustered data is visualized as a density plot where “npoints” is numeric vector specifying the number of grid points in x (horizontal) and y (vertical) directions.

```
> resP2.den <- density(resP2[[4]], data = P12, npoints=c(1000,1000))

> plot(resP2.den, type = "image", nlevels=100, xlim=c(250,750),
ylim=c(300,720))
```

**Picture of density analysis**



# The command “summary” provides information about the experiment, clustering, transformation, information criteria and data quality.

```
> summary(resP2[[4]])
```

# The “summary” output looks as follows.

```
** Experiment Information **
Experiment name: Flow Experiment
Variables used: FL1 FL3
** Clustering Summary **
Number of clusters: 4
Proportions: 0.1883078 0.2788811 0.2873053 0.2455058
** Transformation Parameter **
```

## # The parameter for box-cox transformation $\lambda$ .

```
lambda: 0.9899544
** Information Criteria **
BIC: -189824.7
** Data Quality **
Rule of identifying outliers: 85% quantile
Number of outliers: 607 (7%)
Uncertainty summary:
```

# The uncertainty is defined as 1 minus the posterior probability that a data point belongs to the cluster to which it is assigned. All uncertainty values for each data point were determined and based on this data minimum, 1<sup>st</sup> quantile, median, mean, 3<sup>rd</sup> quantile and maximum values were calculated.

Min.	1st Qu.	Median	Mean	3rd Qu.	Max.
4.671e-03	4.421e-02	1.104e-01	1.557e-01	2.358e-01	6.738e-01

## # Retrieving data from particular cluster populations by first splitting data;

```
> sub4 <- split(P12,resP2[[4]], population=list(A1=c(1), A2=c(2),
A3=c(3), A4=c(4)))
```

## # The output of particular cluster data is provided by the command “summary”.

### # summary cluster I

```
> summary(sub4$A1)
```

	SS	EV	FL1	FL2	FL3
Min.	373.0	7.00	470.0	561	347.0
1st Qu.	394.0	35.00	554.0	660	450.0
<b>Median</b>	414.0	54.00	<b>582.0</b>	688	<b>492.0</b>
<b>Mean</b>	417.3	67.93	<b>582.3</b>	688	<b>488.5</b>
3rd Qu.	436.0	85.00	613.0	717	529.0
Max.	523.0	284.00	682.0	794	621.0



### # summary cluster II

```
> summary(sub4$A2)
```

	SS	EV	<b>FL1</b>	FL2	<b>FL3</b>
Min.	373.0	7.00	419.0	411.0	443
1st Qu.	399.0	34.00	502.0	656.0	514
<b>Median</b>	422.0	50.00	<b>537.0</b>	691.0	<b>547</b>
<b>Mean</b>	425.2	65.03	<b>536.8</b>	689.5	<b>547</b>
3rd Qu.	447.0	81.00	571.0	722.0	579
Max.	526.0	277.00	651.0	839.0	657

### # summary cluster III

```
> summary(sub4$A3)
```

### # summary cluster IV

```
> summary(sub4$A4)
```

## 3.21.2 Production intensity assay (FL1, FL3) (FL1, FL3, SS, EV)

# The *FlowClust* analysis of production intensity data is done as previously described with some exceptions. First clustering is done at FL1 and FL3 values to remove outliers.

```
> resB1<- flowClust(B1, varNames = c("FL1", "FL3"), K = 1, B = 100)
> B12 <- B1[B1 %in% resB1, ]
```

# The second clustering is done as an multidimensionality approach to better exploit data sets at clustering according FL1, FL3, SS and EV.

```
> resB12 <- flowClust(B12, varNames = c("FL1", "FL3", "SS", "EV"), K= 1:6,
B = 100, trans=1)
```

### 3.22 Central composite design

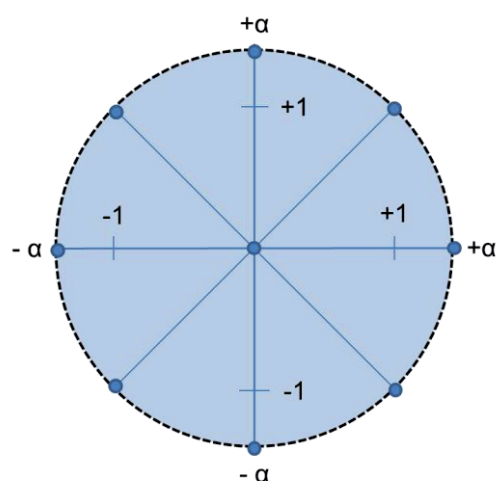
A CCD was used to estimate the effect of  $\text{MgSO}_4 \times 7\text{H}_2\text{O}$  and  $(\text{NH}_4)_2\text{SO}_4$  on the functional production and secretion respectively of ABF D1.3 scFv by *B. megaterium* [164, 181]. Therefore different concentrations of these two components were tested (**Tab. 4**) and analysed by Stat-Ease Design Expert Software 7 to predict optimal parameters.

**Table 4:** (A) Combinations of  $\text{MgSO}_4 \times 7\text{H}_2\text{O}$  and  $(\text{NH}_4)_2\text{SO}_4$  concentrations according a central composite design, (\*) centre points experiments were done twice for statistical reasons. (B) CCD principle with particular coding values.

(A)

experiment	$\text{MgSO}_4 \times 7\text{H}_2\text{O}$ (g/L)	$(\text{NH}_4)_2\text{SO}_4$ (g/L)
1	2.99	25.08
2*	1.88	15.60
3	0.30	15.60
4	1.88	29.00
5	1.88	2.20
6	0.76	6.12
7*	1.88	15.60
8	3.45	15.60
9	2.99	6.12
10	0.76	25.08

(B)



### 3.23 Genetic algorithm

The principle of a genetic algorithm (GA) is first to set up randomly a number of experiments with different media compositions then evaluate these experiments and create, based on the previous results, a new population of media recipes. The best experiments of a parent population are combined among each other accompanied with set mutation and crossover rates, creating a new generation of experiments. This approach of creating new media compositions is realized by coding the parameters to be optimized in bit strings defining the number of concentrations levels in between parameters that can be varied. Detailed methods of using genetic algorithms for media optimization are described elsewhere [182, 183].

Media optimization using genetic algorithms has been proven to be effective in prokaryotic and eukaryotic systems, e. g. for the production of L-lysine, L-isoleucine, ILE/L-valine



*Corynebacterium glutanicum* [184, 185], esterase production in *E. coli* [186],  $\Delta 1$ -dehydrogenase production by *Arthrobacter simplex* cells [183] and cyanobacteria growth [187].

The software “Genetic Algorithms for Optimization of Processes” (GALOP Vers. 2.2, IBT Research Center Jülich, 1998) was used to create new media compositions. To prevent a unidirectional optimization towards production with a possible limitation of growth, a simultaneous maximization of production and biomass formation was followed. This was realized by selecting 15 media towards the aim of maximizing biomass formation and 15 towards optimizing the production of ABF production for each generation. Concretely the multi-objective function was to maximize the amount of functional folded ABF D1.3 scFv in the supernatant measured by ELISA and the biomass yield of *B. megaterium* in parallel deep-well-plate cultivations.

The concentrations of metal ions were varied in ranges in between two decades of selected concentrations adopted from elsewhere [166, 188] (e. g. :  $c_r = 0.3 \text{ g/L MgSO}_4 \times 7\text{H}_2\text{O}$ ;  $c_{\min} = c_r \times 0.1 = 0.03 \text{ g/L}$ ;  $c_{\max} = c_r \times 10 = 3.0 \text{ g/L}$ ). With a population of 30 individuals each measured in triplicates and a binary code length of 63 for the whole variable space optimization was realized with a crossover using a probability of 99% [189]. By choosing a scaling window of one, the previous and the generation before are accounted for creating the following generation of experiments using the method of keep best, ball bearing [190]. According to Bäck et al. (1993) [191] the mutation rate was set to 0.016 and the crossover rate chosen as 0.95 [192].

### 3.24 Prediction of metal-dependent enzymes of *Bacillus megaterium*

To deduce metal-dependent enzymes of *B. megaterium* the comprehensive enzyme database BRENDA [193] [194] was used. EC numbers of metal-dependent enzymes were queried following NCBI Taxonomy [195] for a) the genus *Bacillus* b) *Firmicutes*, and c) for all bacteria from BRENDA. In this order the resulting EC numbers were compared against the current annotation of *B. megaterium* DSM319 [101]. For matching EC numbers all metal ions were summarized and sorted by their dependency (r – required, a – activation). Predictions for the cellular localization of the enzymes were achieved using the PrediSi program [196]. Nearly 400 enzymes with dependencies on metal ions could be predicted.



## 3.25 DNA micro arrays

### 3.25.1 RNA-preparation

For transcriptome analysis 25 OD equivalents ( $2.5 \times 10^{10}$  bacterial cells) were harvested and immediately stopped in sodium azide containing killing buffer (20mM). The RNA was purified as described in [197]. Additionally a RNA Purification Kit (Jena Science, Germany) was used for final purification with an elution volume of 30  $\mu$ L. The RNA concentration and quality was measured using the Nanodrop (Nanodrop1000, Peqlab, software: Nanodrop 1000 V 3.8.9, USA) and the Bioanalyzer technology (Agilent 2100 Bioanalyzer, software: 2100 expert, USA). RNA quality was determined by calculating a RNA integrity number (RIN). RIN numbers larger than 8.5 were decided to be applicable for RNA-Microarrays [198].

### 3.25.2 One colour microarray

The labelling of RNA was done using “ULS Fluorescent Labelling Kit for Agilent arrays” from KREATECH (EA-022//EA-023). The degree of labelling [8] was determined by nanodrop measurements (array-program). Applicable values were defined between 1.0 and 3.6. The fragmentation, hybridization and final processing of 600 ng of labelled sample RNA occurred after the manufacturers’ instruction including a gene expression hybridization kit, an array washer and a hybridization oven (Agilent Technologies, USA). Slides were scanned using the micro array scanner Agilent C Scanner (Agilent Technologies, USA) and the software Agilent Scan Control 8.4.1. Subsequently the results were analysed with “Feature Extraction 10.7.3.1” software (Agilent Technologies USA).

The microarray platform used in this study was provided by Agilent (Agilent technologies, USA). 8 x 15k microarray slides were custom-made using the software array (Agilent technologies, USA) based on the published genome data of *B. megaterium* DSM319 [101]. For each gene three probes were used to ensure a proper binding of labelled mRNA. The normalization and calculation of differential expressed genes differs from two-color data analysis and was performed as described in Bunk 2010 [100]. The data is based on three biological replicates with four sample time points each for the ABF producing strain and the control strain. The heatmap analysis was performed with the software MultiExperimentViewer (MeV).

## 3.26 Chemicals

All chemicals were purchased from Sigma (Steinheim, Germany), Merck (Darmstadt, Germany) or Roth (Karlsruhe, Germany) and are of analytical grade.





## 4 Results and discussion

### 4.1 Aims of the work

ABs and ABFs are most important tools in therapeutic and diagnostic applications. An increasing demand of these high potential drugs makes less cost intensive production systems most desirable. Microbial production platforms are beneficial compared to mammalian cell cultures in reaching high production titers, scale up approaches, regulatory aspects and reduced COG. Among these, production systems having the ability of an additional product secretion are most advantageous as the downstream processing costs are decisively reduced.

The aim of this work is to characterize and maximize the production and secretion of recombinant anti-lysozyme ABF D1.3 scFv using *B. megaterium* as an alternative production host with high secretion capacities. This is done following a holistic bioprocess development approach ranging from micro titer to pilot bioreactor scale. As a first step a defined medium for ABF D1.3 scFv production is developed by means of statistical design of experiments and using a genetic algorithm for particular medium screening. Secondly, an appropriate bioprocess is designed to reach both, high cell densities with at the same time high productivities. The method of flow cytometry is used to gain deeper insights into the microbial physiology of ABF producing *B. megaterium* cells. This knowledge is implemented for further process development and optimization. A subsequent transcriptome analysis is used to gain a deeper process understanding to uncover potential bottlenecks of production and secretion of ABF D1.3 scFv.

The project was part of the Collaborative Research Center (SFB 578) "From Gene to Product" holding a key position assigning ABF production from the lab-scale to industrial bioprocesses with the focus on a holistic bioprocess development. Based on intensive collaborations with particular project partners upstream processing approaches like specific strain designs as well as strategies for efficient purification methods were successfully realized.

## 4.2 Medium design

### 4.2.1 Carbon source screening

The ABF D1.3 scFv was shown before to be successfully secreted by *B. megaterium* using complex media compositions [46, 199]. Based on cultivation media suggested by Yang et al. (2007) [166] for Hydrolase production with *B. megaterium* different carbon sources were tested considering growth and ABF D1.3 scFv production properties each with the same amount of molar carbon concentration supplemented with 1 g/L yeast extract. Cultivations were carried out for 25 h and samples were taken every hour to gain appropriate insights into growth and production processes. Maximal corresponding specific growth rates, maximal product values measured by ELISA and achieved biomass concentrations were determined (Fig. 16).

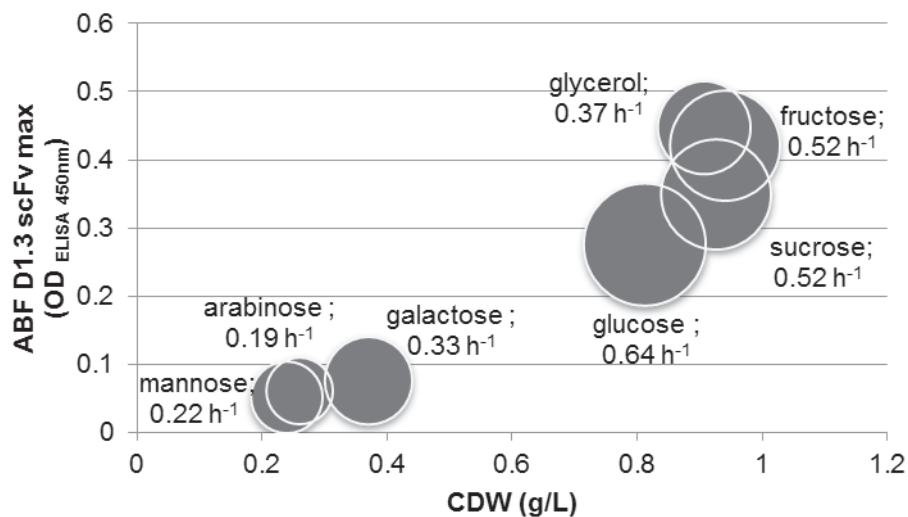


**Figure 16:** Different carbon sources were screened for biomass formation (cell dry weight (CDW) (g/L)) and production of ABF D1.3 scFv secreted by *B. megaterium* YYBm1 (EJBmD1.3scFv) in minimal medium with 4 g/L of same amount of molar carbon concentration and supplemented with 1 g/L yeast extract. The spot diameter represents particular maximal growth rates reached as indicated.

In this case fructose, glycerol, sucrose and glucose were the favored carbon sources. Growth on maltose, arabinose and galactose is probably related to the supplemented yeast extract. A closer look on the growth behavior and production trends when using glucose and fructose revealed that the depletion of glucose is somehow a precondition for the beginning of ABF production (data not shown) whereas utilization of fructose led to a growth coupled production of ABFs. This seems to be surprising as the regulatory element (catabolite responsive element, *cre*) in the *xyIA* promotor region has previously been removed by adapted expression plasmid design [119, 200]. Under these circumstances



another mechanism most probably takes place, since glucose-6-phosphate, e. g. produced at glucose uptake, can function as an additional repressor of transcription by competing with xylose for the binding site at the xylose repressor (XylR) [201] (section 1.3). Glucose-6-phosphate has a higher binding affinity to the XylR protein which still remains at the *xyA*-promotor region and blocks transcription of the ABF D1.3 scFv gene until glucose is depleted. Additionally when glycerol was used as carbon source it was shown to be related to high production rates but to lower growth rates. Therefore, fructose was chosen as favorable carbon source and applied for further medium optimization.

#### 4.2.2 Inducer screening

Different concentrations of xylose for inducing ABF D1.3 scFv production ranging from 0.1% to 2% were tested in particular shaking flask experiments (section 3.9). The experiments were carried out in minimal medium for 23 h and the induction was done 1 h after inoculation with an OD of 0.1. An increase in the inducer concentration clearly shows a negative effect on the maximal specific growth rate (**Fig. 17 A**) and on the overall ABF D1.3 scFv concentrations reached in the underlying shaking flask cultivations (**Fig. 17 B**).

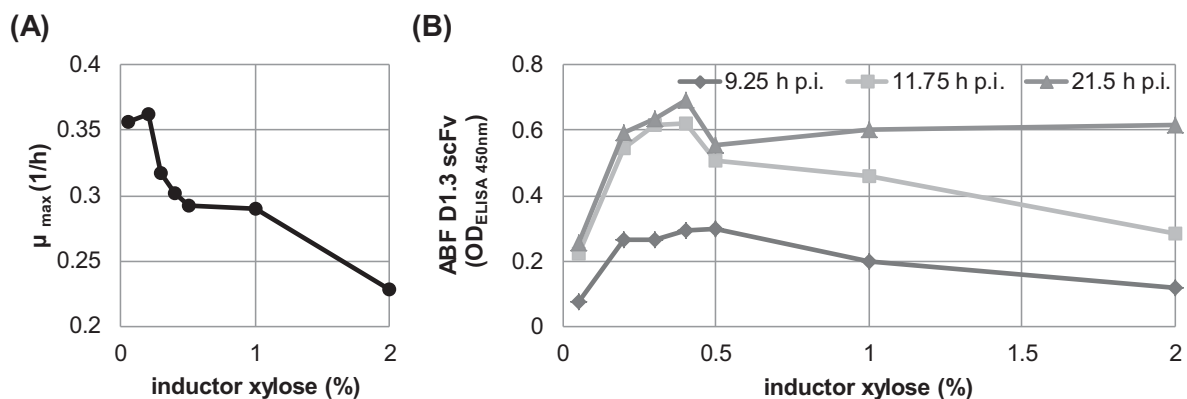


**Figure 17:** Different inducer concentrations (0.1% to 2%) were tested and **(A)** the effect on the specific growth rate and **(B)** ABF production was determined at different time points after induction (p.i.) at *B. megaterium* YYBm1 (EJBmD1.3scFv) shaking flask cultivations.

This is most probable due to the over-expression of genes related to the xylose catabolism. As only the *xyA* gene is not functional in the used strain YYBm1 [166] other genes like xylose transporters and related genes on the operon e. g. *xyB* are still expressed without the actual degradation of xylose taking out internal resources for biomass formation. It was found that when xylose concentrations were used lying above the actual fructose concentration of 5 g/L the particular maximal growth rate is reduced. Here, the organism is probably more adapted to degrade xylose than fructose and therefore is inhibited in growth due to *xyA* deficiency. Finally this led to lesser biomass generation and



lower overall product formation. Consequently 0.5% of xylose was chosen as an optimal inducer concentration.

#### 4.2.3 Genetic algorithm approach – optimization of metal ion concentrations

The next aim was to totally replace the yeast extract used as supplement to create a defined minimal medium. Here, different metal ion compositions were tested using micro titer deep well plates as cultivation platform. A genetic algorithm was used to vary concentrations of calcium (Ca), cobalt (Co), molybdenum (Mo), magnesium (Mg), copper (Cu), zinc (Zn), boron (B) and manganese (Mn) for simultaneous maximization of biomass and ABF D1.3 scFv formation using *B. megaterium* [172].

To give an overview of all performed generations of experiments the mean values of concerning biomass formation and production of ABF D1.3 scFv were calculated. **Figure 18** illustrates the best results of each generation of experiments and the mean value of all individuals for biomass formation (**Fig. 18 A**) as well as for ABF production (**Fig. 18 B**). The mean values of ABF titers increased until the fourth generation with the exception of the third generation. Here the lower product formation is possibly related to the general work mechanism of the genetic algorithm relying on a stochastic method for creating new media compositions. This particular behaviour has been shown before using genetic algorithms for media optimization [187]. Except for generations 3 and 7 the best medium of each generation always reached higher values than the originally used medium. The best medium tested showed a 2.2 times higher production of ABF D1.3 scFv compared to the original medium used. In addition, generation 2 and generation 5 also featured 1.34 and 1.57 times higher product formation for best media compositions respectively. For the biomass formation an increase up to a 1.6 times could be reached in comparison to the control medium for all generations. It became obvious that almost no changes appeared in the mean values of biomass formation which may be due to the fact that the originally used metal ion compositions were already close to the optimal composition for biomass generation. The fact that the composition of the particular metal ion concentration was more essential for the production and secretion of ABF D1.3 scFv than for the biomass formation itself may be related to the evolutionary adaptation and distinctive robustness of *B. megaterium* being a soil bacterium adjusted to a variety of habitats [99].

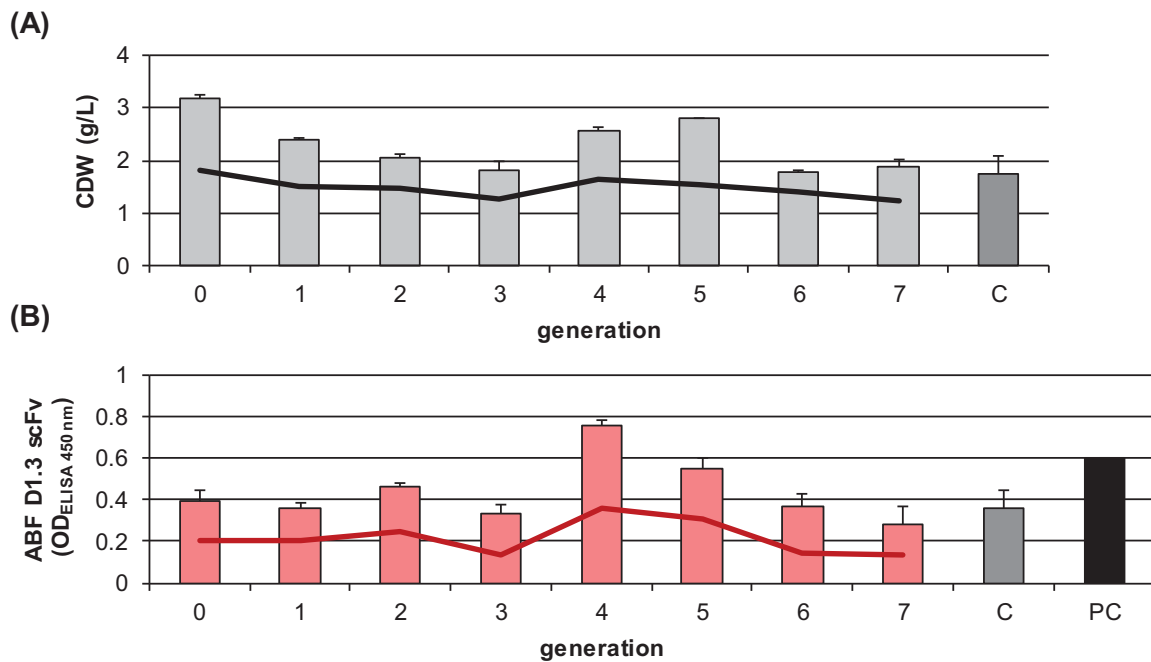


**Figure 18: (A)** Best results concerning biomass formation (CDW (g/L)) and **(B)** ABF production (OD<sub>ELISA 450 nm</sub>) of *B. megaterium* YYBm1 (EJBmD1.3scFv) producing ABF D1.3 scFv of each generation and the mean value of the 30 media compositions tested in each generation (—). Each medium composition was measured in triplicates as indicated by the particular standard deviation. The control medium (C) [166] was also measured in each generation and is shown as an average value of all generations (■). PC (■) stands for positive control of the ELISA to normalize data sets.

**Figure 19** illustrates the dependencies of the particular fraction of metal ions used related to the production of ABF D1.3 scFv. Thereby the effects of particular metal ions towards production and secretion are highlighted. All experiments were clustered in eight main groups according to their particular amount of ABF or produced biomass. The grouped ABF and biomass values were related to the mean values of the particular fraction of metal ions corresponding to the total metal ion concentration of each particular medium. This correlation gives, in contrast to the consideration of single generations, a more general view on the results, allowing conclusions on certain effects of replacements as fractions of metal ions are considered.

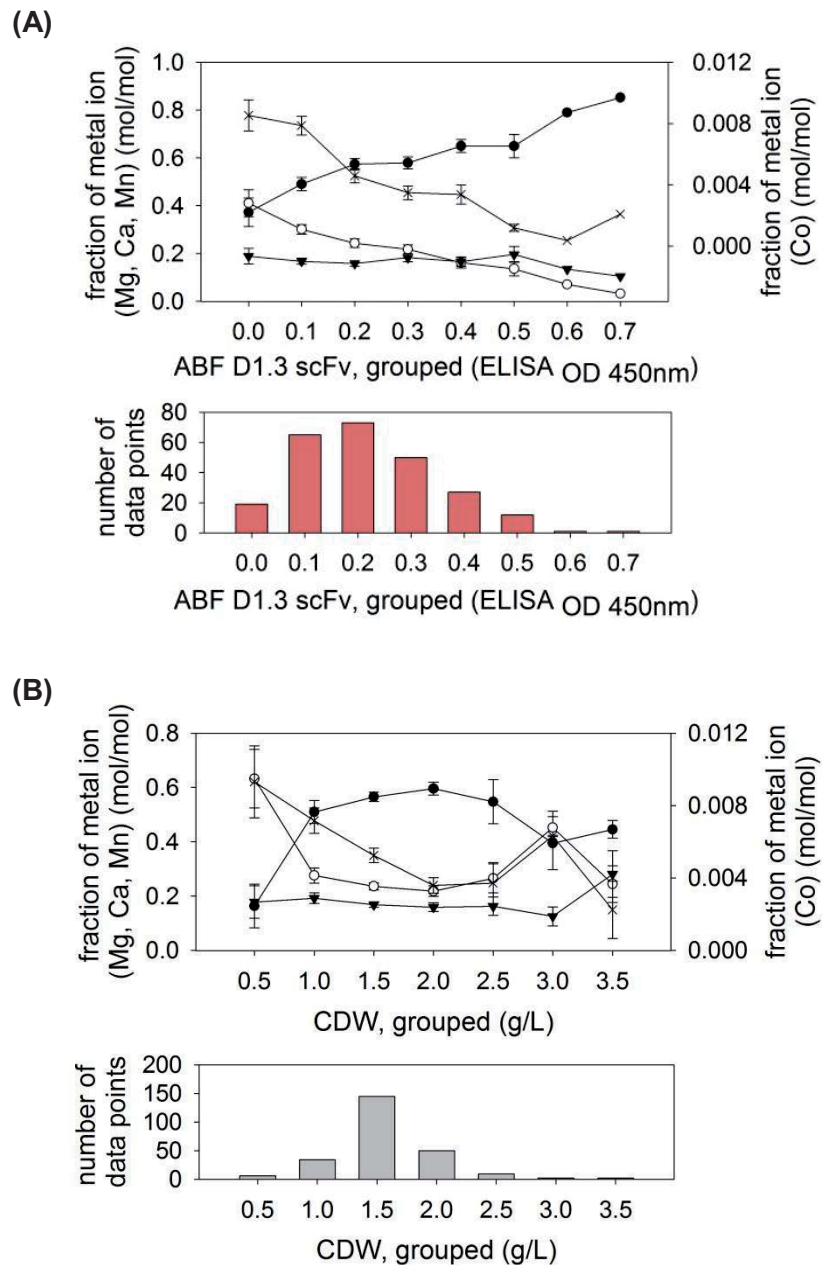


**Figure 19:** Dependencies of the fraction of metal ions: **(A)** Grouped ABF D1.3 scFv values and **(B)** grouped biomass values related to mean values of the particular fraction of metal ion corresponding to total metal ion concentration with standard error of mean and number of data points included in each mean value:  $\text{MgSO}_4 \times 7\text{H}_2\text{O}$  (●),  $\text{CaCl}_2 \times 2\text{H}_2\text{O}$  (○),  $\text{MnCl}_2 \times 4\text{H}_2\text{O}$  (▼),  $\text{CoCl}_2(\text{x})$ .

It can be seen that high Mg-fractions and low Co-fractions respectively (**Fig. 19**) favour an increased production of ABF D1.3 scFv. Fe, Cu, Zn, B and Mo are not taken into account in this context as no clear correlation could be observed. A decrease of the Ca-fraction accompanied by an increase of the Mg-fraction at higher ABF D1.3 scFv production may be related to the natural antagonism of Mg and Ca ions [202]. This highlights the importance of Mg for the production/secretion process and the possible unfavourable effect or replacement of this ion by Ca ions. Interestingly, Fe and Ca could not be determined as positive effectors of secretion which has been shown elsewhere for other proteins



secreted by *B. subtilis* [203]. Low Co-fractions showed both higher biomass formations accompanied with increased product formation (**Fig. 19 A, B**). This indirectly implies that the effect of Co is more global since the gain in biomass is probably directly linked to an increased product formation or secretion. In contrast to the global effect of Co ions, Ca and Mg ions seem to have a more specific effect on production and/or secretion efficiency as, quite interestingly, no clear dependencies of these metal ions can be found concerning biomass formation (**Fig. 19 B**). The particular Mn-fractions show no dependencies to either production intensity (**Fig. 19 A**) or biomass formation (**Fig. 19 B**) revealing that this ion is not limiting or favouring the product or biomass formation for the tested concentration ranges. Most of the data points considered in this context are related to medium rated values of ABF production and biomass formation as illustrated at the lower bar diagram (**Fig. 19 A, B**). This may be due to the fact that both biomass and product formation were optimized at once, leading to an optimization approach of one at the expense of the other. The best medium for the highest production of ABF D1.3 scFv was not simultaneously the best medium for biomass formation and vice versa. **Figure 20** summarizes all 240 tested media compositions and their related biomass and product formation in one Pareto plot. The media tested can be grouped according to the control medium relating to higher and lower product and biomass formation. It becomes obvious that most of the media compositions tested exhibit a lower product formation and approximately the same biomass concentration when compared to the control medium. In addition, media with production and biomass formation higher than the control medium were successfully achieved.

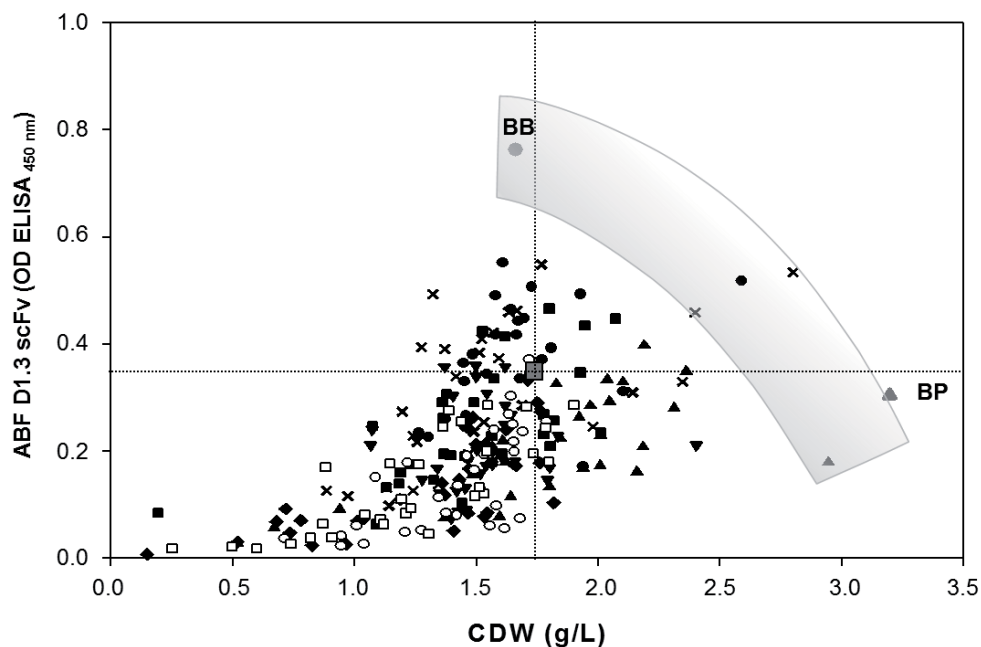


**Figure 20:** Pareto plot for the multi-objective optimization of biomass formation and ABF D1.3 scFv (240 tested media compositions): 0 gen. (▲), 1 gen. (▼), 2 gen. (■), 3 gen. (◆), 4 gen. (●), 5 gen. (x), 6 gen. (○), 7 gen. (□), previously used medium as control (■) (averaged by values of all generations), ● BP = medium with best ABF D1.3 scFv production, ▲ BB = medium with best biomass formation, shadowed area (Pareto-optimal solution space, (PP)).



Interestingly the optimal medium for biomass formation (BB) had decreasing effects on the production and differed completely in its metal composition from the optimal production medium (BP) or even the control medium (**Tab. 5**). In parallel, the medium with the best production of ABF showed no increase in biomass formation compared to the control medium. This coherency highlights the problem of optimizing two competing target functions. In general, the aim of reaching high production titers is usually related to a reduced biomass formation. The target function “production” can be optimized only at the expense of biomass formation, which is not required for all cases. As can be seen in **Figure 20** at least two of the media compositions show a higher product formation as well as an equal or higher biomass formation compared to the control medium. These media are the best for relatively high production combined with high biomass formation and can be described as Pareto optimal scores of the solution space being a compromise between production and growth (shadowed area in **Fig. 20**). To avoid an optimization towards higher production at the expense of biomass formation finally leading to lower production, both strategies of increasing biomass and production of ABF should be considered. If either a high product or a high biomass formation is desired, the compositions of BP (+117% product) and BB (+84% biomass) are the favoured media. **Table 5** summarizes the compositions of best media for product (BP) and biomass formation (BB) separately and in parallel (Pareto optimal scores (PP)).

**Table 5:** Best media compositions regarding production of ABF D1.3 scFv (BP), biomass formation (BB) and both aims combined (PP) concerning metal ion concentration. Result B (P) shows the gain respectively loss in biomass formation or production compared to the control medium.

			BB	BP	PP		
<b>Generation</b>			0	1	5	2	4
<b>Result B</b>			84%	-1%	28 %	31 %	53 %
<b>Result P</b>			-13%	117 %	19 %	38 %	61 %
<b>Concentration of metal ions</b>	MnCl <sub>2</sub> x 4H <sub>2</sub> O	(mg/L)	428.0	312.0	776.0	432.0	424.0
	CaCl <sub>2</sub> x 2H <sub>2</sub> O	(mg/L)	684.0	95.4	206.7	227.9	678.4
	FeSO <sub>4</sub> x 7H <sub>2</sub> O	(mg/L)	29.5	5.5	35.3	13.3	16.8
	CoCl <sub>2</sub>	(mg/L)	1.4	6.2	4.7	1.2	1.4
	CuSO <sub>4</sub> x 5H <sub>2</sub> O	(µg/L)	7.5	16.0	20.5	10.3	8.0
	H <sub>3</sub> BO <sub>3</sub>	(µg/L)	155.0	155.0	193.8	181.3	124.0
	MgSO <sub>4</sub> x 7H <sub>2</sub> O	(g/L)	1.1	2.6	2.2	2.1	3.0
	ZnSO <sub>4</sub> x 7H <sub>2</sub> O	(µg/L)	15.0	15.0	1.1	13.8	25.0
	(NH <sub>4</sub> ) <sub>6</sub> Mo <sub>7</sub> O <sub>24</sub> x 4H <sub>2</sub> O	(mg/L)	2.6	21.6	12.2	18.4	2.6

As seen from the results above, the metal ion concentrations have a great influence on cell growth as well as on production, and respectively secretion. Metal ions play a critical role in several catalytic enzymes. To therefore allow a deeper analysis of the impact of



metal ions, annotated genome data from *B. megaterium* parental strain DSM319 was used to screen for metal-dependent enzymes and their particular function (section 3.24).

It was shown that approximately 400 enzymes being 40% of all annotated enzymes are metal-ion related. First they were grouped according to their association with the corresponding metal ions and again subdivided into the corresponding enzyme classes related by EC-nomenclature (**Fig. 21**).

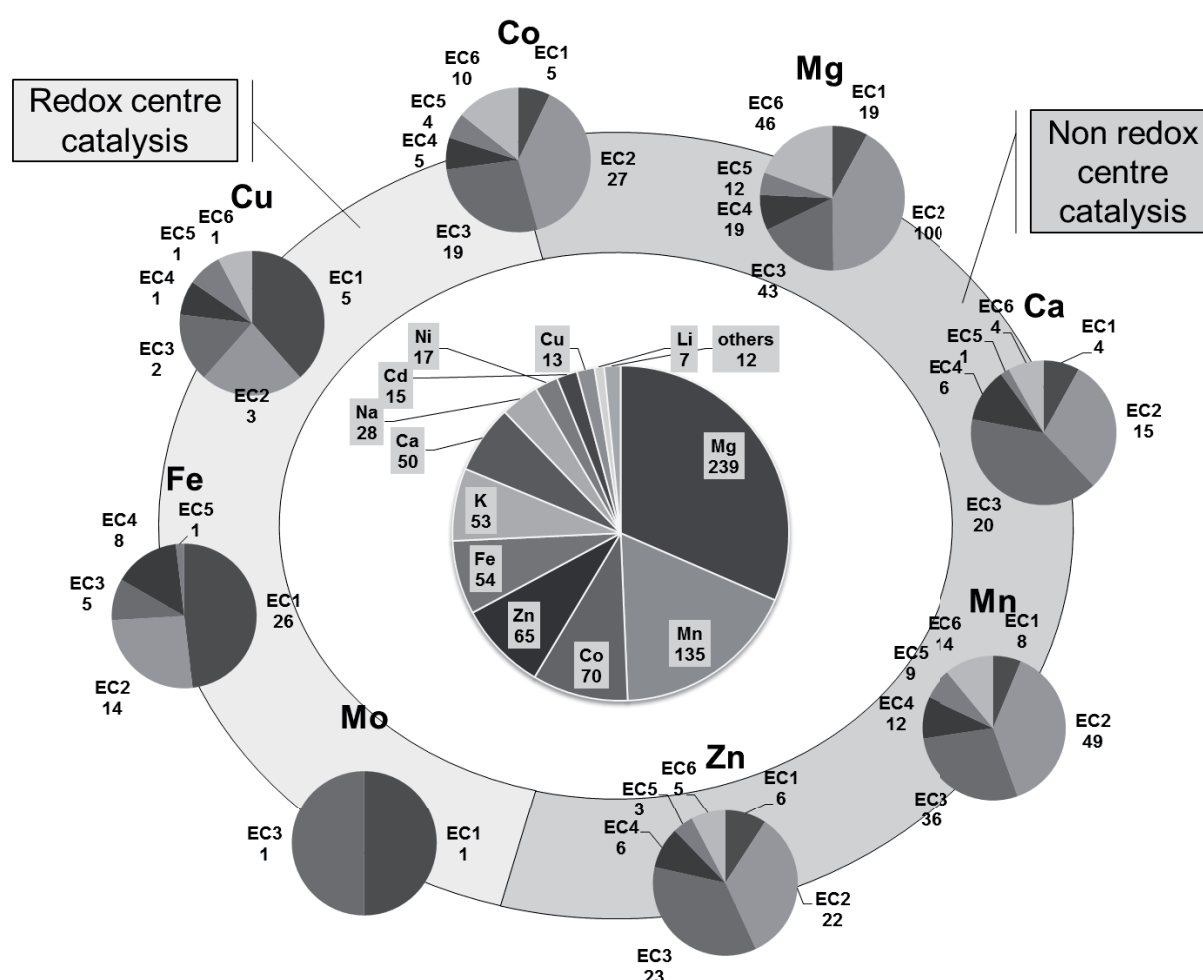


**Figure 21:** Catalytic metal ions occurrence in *B. megaterium* according to predicted enzymes from annotated genome data, subdivision into enzyme classes according to EC nomenclature and catalytic mode of action. Numbers directly refer to quantity of particular enzymes. EC1: Oxidoreductases, EC2: Transferases, EC3: Hydrolases, EC4: Lyases, EC5: Isomerases, EC6: Ligases.

The different effector ions are on the one hand required for function and/or may also act by activating and increasing certain enzyme functions, therefore each single enzyme may be counted more than once. The metal ions themselves can again be divided in two main subclasses: redox centre catalysis and non-redox centre catalysis. Being directly involved in the catalytic reaction through performing electron transfer by changing their oxidation state Fe, Cu and Mo are typical metal ions which are necessary for redox centre catalysis [204]. In this study oxidoreductases (EC1) which catalyze redox reactions dominate the pie charts (**Fig. 21**). Other ions such as Mn, Zn, Mg and Ca mainly act by stabilizing negative charges and activate substrates by acting as a Lewis acid shown at the electrophilic activation of P-O and C-P bonds [204]. At this non-redox centre catalysis transferases (EC2) and hydrolases (EC3) dominate the particular pie charts having a demand for electrostatic stabilizers and activators such as Mn, Zn, Ca and Mg. These are directly involved in the function of kinases and phosphatases. Quite interestingly Co acts in both: catalysis of redox reactions (e. g. at Vitamin B12-generating and -dependent enzymes) and also functions as Lewis acid by binding and activating particular substrates. By scanning for secretion signals and transmembrane domains in the protein sequence data of metal-dependent enzymes, an additional subdivision into cytosol-associated enzymes as well as membrane and extracellular enzymes becomes possible (**Fig. 22**). Here Ca and Co seem to play an important role at the extracellular level, illustrated by the increased fraction in membrane associated/extracellular enzymes. Possible interactions and functional sites of metal ions concluded from literature [205] in combination with these results from genome annotated data are finally summarized (**Fig. 22**).

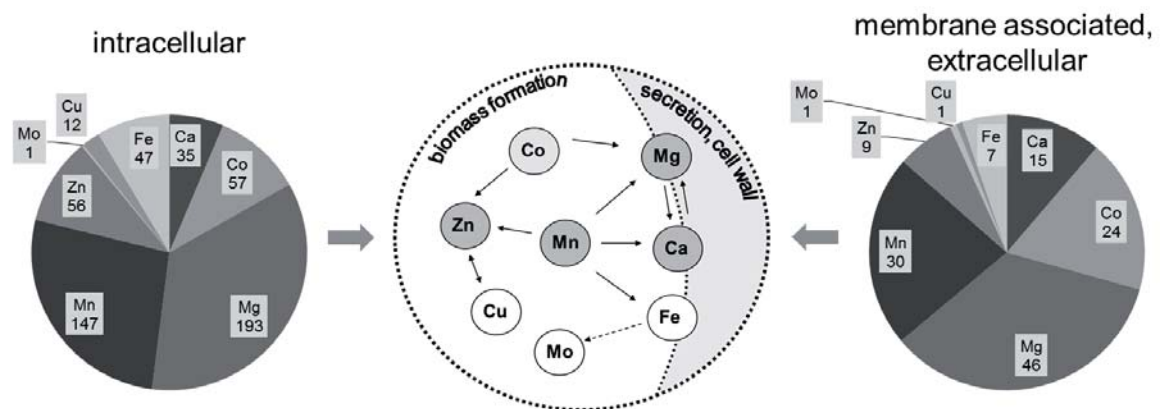


**Figure 22:** Occurrence of catalytic metal ions according to the cellular localization of particular metal associated enzymes related to predictions from sequence data summarized in an overview of interactions and present functional sites of metal ions (Redox (●) and non-redox center dependent catalytic activity (○)).

From experimental and genome analysis derived data, Mg was shown to be the key component of the metal ions tested for biomass generation and especially for production and secretion of ABFs. **Figure 21** demonstrates that one third of all metal-dependent



enzymes require Mg for activity. The demand for Mg is clearly demonstrated by its essential role in protein biosynthesis consuming approximately 90% of the energy of a growing bacterial cell. As an example all known aminoacyl tRNA-synthetases (EC 6.1.1) and also tRNA methyl- and formyltransferases (EC 2.1.1.31/33, EC 2.1.2.9) require Mg ions. Furthermore the phosphate complexing activity of Mg ions is important for all nucleotide- and ATP-dependent reactions of the central metabolism.

In addition to these metabolic functions and protein synthesis related effects of Mg, this ion may also directly affect the production and secretion processes of ABFs. From *B. subtilis* it is known that the cell wall takes up metal ions up to 8.226  $\mu\text{mol Mg/mg}$  cell wall. This is quite a lot compared to other metal ions with particular adsorption quantities (Na: 2.697, K: 1.944, Ca: 0.399, Mn: 0.801,  $\text{Fe}^{\text{III}}$ : 3.581, Ni: 0.107, Cu: 2.990  $\mu\text{mol/mg}$  cell wall [206]). This binding occurs due to anionic polymers (teichonic and teichuronic acids) which are covalently attached to peptidoglycan [207]. By undergoing this attachment, the concentration of metal ions in the medium directly affects the net cell wall charge and supports or hinders the release of secreted proteins through the cell wall, depending on the individual charge distribution. Certain cations like  $\text{Ca}^{2+}$ ,  $\text{Fe}^{2+}$  and  $\text{Mg}^{2+}$  are known to be required as folding factors for a variety of secreted proteins including alpha amylase and levansucrase produced by *B. subtilis* [208]. Beyond that, Mg plays a critical role in the secretion process itself. It binds directly to the SecA protein, a part of the secretion machinery with ATPase activity that is also affected by interaction with other components of the bacterial protein translocation system such as the protein channel SecYEG, lipids and the secreted pre-protein itself [209]. Mg was found to have a powerful effect on the binding affinity and turnover of ATP attached to SecA, making this metal ion an indispensable component of the secretion apparatus [210].

For all these reasons Mg is not only a key component for the generation of biomass but is also needed for the secretion process, functional folding and release through the cell wall of secreted proteins. When optimizing metal ion concentrations in media compositions the replacement of metal ions amongst each other also has to be considered. This replacement may result in a decreased activity of the particular enzyme and or even change the specificity of enzymatic system. Ca and Mg are for instance known as natural antagonists [202]. The question of why such small amounts of ions may have such a big effect on the production and generation of biomass may be due to their ability to concentrate ions in the cell wall [205]. According to specific Mg transport systems which are also present in *B. megaterium* (CorA and MgtE), no interactions or competitions related to different metal ions were reported [211], so that inhibitory effects among the ions according to transport can be neglected.

#### 4.2.4 Statistical DoE – optimization of $\text{MgSO}_4$ and $(\text{NH}_4)_2\text{SO}_4$ concentrations

Beside different carbon sources, metal ion and inducer concentrations,  $(\text{NH}_4)_2\text{SO}_4$  as a primary nitrogen source was also a major focus of media optimization. Therefore shaking flask experiments were carried out according to a CCD varying  $\text{MgSO}_4 \times 7\text{H}_2\text{O}$  and  $(\text{NH}_4)_2\text{SO}_4$  concentrations with different combinations (**Tab. 4**). By direct comparison of the maximal achieved product titers distinct effects of Mg and  $\text{NH}_4$  concentrations on ABF production became observable. Based on these data sets, a quadratic model was fitted and an optimal media composition for ABF D1.3 scFv production was predicted by applying 25 g/L  $(\text{NH}_4)_2\text{SO}_4$  and 2.78 g/L  $\text{MgSO}_4 \times 7\text{H}_2\text{O}$  (**Fig. 23**).

Related to ABF production both components seem to complement each other which is illustrated by the fact that for higher Mg concentrations maximal product titers can easily be achieved at lower  $\text{NH}_4$  concentrations (**Fig. 23**). This may indicate that Mg and  $\text{NH}_4$  ions have the same site of action.  $\text{NH}_4$  is only less metabolized during growth and production (data not shown), so that the nitrogen source cannot be considered as a limiting component for production but rather for secretion of ABFs.

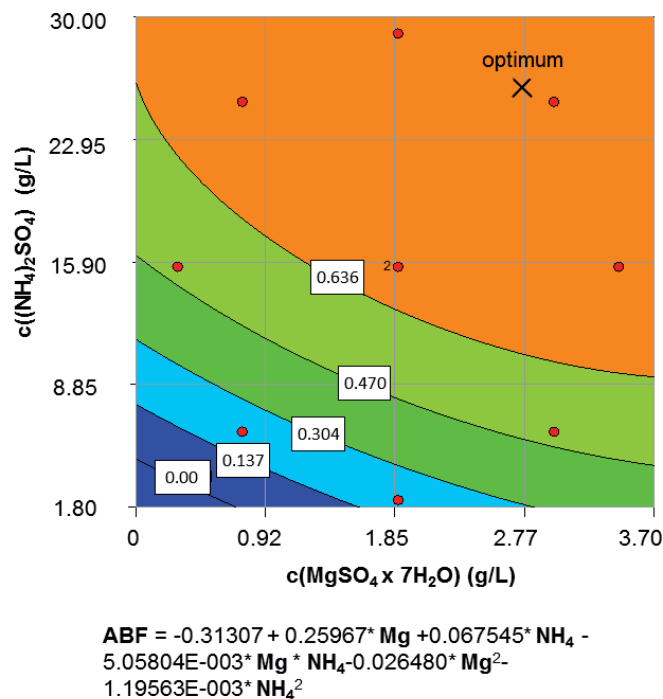


**Figure 23:** Central Composite Design (CCD) of different concentrations of  $\text{MgSO}_4 \times 7\text{H}_2\text{O}$  (g/L) and  $(\text{NH}_4)_2\text{SO}_4$  (g/L) (**Tab. 4**). Different colors and numbers represent the amount of ABF D1.3 scFv produced ( $\text{OD}_{\text{ELISA } 450 \text{ nm}}$ ) and fitted according to a full quadratic model. The experimental setup in the center point was carried out twice for statistical considerations.

Studies regarding cell wall composition and properties of *B. megaterium* demonstrated that the overall stability of the cell wall is affected by changes in environmental ionic strength and pH [212]. Electrostatic attractions seem to play a major role in determining



the compactness of highly contracted walls. It was shown that the walls responded to increased environmental ionic strength by expansion [212]. Therefore the increased concentration of  $\text{NH}_4$  and also Mg ions in the cultivation medium may lead to a shift in the ionic charge distribution resulting in the expansion of cell wall structures. These more porous structures may at least favor a more efficient ABF secretion and release through the cell wall. Beside these considerations of wall porosity, the charge and ion distribution of the cell wall may also directly affect the secretion efficiency. Another reason might be that an increased osmolarity in the culture medium triggers a certain stress response leading to favorable folding conditions. This was e. g. shown for *P. pastoris* where the unfolded protein response (UPR) was a result of higher present osmolarity [213].

## 4.3 Single cell analysis

### 4.3.1 Membrane potential

For microbial bioprocess development it is most important to monitor cellular stress response related to cell viability as such information can directly correlate to the overall process efficiency [214]. This can be realized by measuring MP and membrane integrity. The MP is primary coupled to the  $[\text{H}^+]$  gradient of a cell, which itself is a direct parameter for the essential ATP generation capacity. The underlying  $[\text{H}^+]$  gradient is generated by the electron transport through the electron transport chain. This again is related to the  $\text{NADH}_2$  availability and is therefore directly associated with the metabolic activity of every single cell. Changes in MP are consequently the most sensitive indicators for culture status estimation whereas cell membrane integrity measurements relate to more distinctive parameters like compromised cell membrane and cell wall structures.

To estimate particular MPs diverse approaches were followed by using different fluorescent probes such as 3,3'-diethyloxacarbocyanine iodide ( $\text{DiOC}_2(3)$ , [173]), 3,30-dihexyloxacarbocyanine iodide ( $\text{DiOC}_6(3)$ , [214]) and bis-(1,3-dibutylbarbituric acid) trimethine oxonol ( $\text{DiBAC}_4(3)$ , [215]).  $\text{DiOC}_6(3)$  and  $\text{DiOC}_2(3)$  are positively charged lipophilic fluorescent probes which bind to the membrane of actively growing cells and were already used to successfully estimate the MP of Gram positive bacteria [216].  $\text{DiBAC}_4(3)$  provides lipophilic properties as well as an anionic charge therefore not being able to pass through polarized membranes of living bacteria. Instead the dye was shown to only enter cells when the MP is depleted where it can bind either specifically to positively charged proteins or less specifically to hydrophobic regions [216].

#### 4.3.1.1 Validation of used fluorescence dyes

Different dyes used to estimate MP measurements like  $\text{DiOC}_2(3)$ ,  $\text{DiOC}_6(3)$ ,  $\text{DiBAC}_4(3)$  were tested considering their applicability for optimized concentration and incubation times (**Tab. 6**). MPs were evaluated according to the maximal signal difference between carbonyl cyanide m-chlorophenylhydrazone (CCCP) treated cells from exponential phase



(control for depolarized cells) [173] and exponential growing cells (polarized) at particular combinations of incubation time and applied dye concentration. The higher the difference the more precise was the final resolution of MP estimations. Here the resulting mean values of the specific fluorescence concentrations (FL-FC) of particular fluorescence distributions or regions respectively were taken into account. When staining the cells with DiOC<sub>2</sub> the ratio between red and green fluorescence was analyzed as described before (section 3.15). In the underlying dye evaluation DiOC<sub>2</sub>(3) and DiOC<sub>6</sub>(3) were shown to increasingly stain polarized cells whereas DiBAC<sub>4</sub>(3) instead predominantly stained depolarized cells.

**Table 6:** Dye screening for MP estimation; overview of different dyes used to estimate MP of *B. megaterium* cells, optimized concentration ranges and incubation times with their particular effect on sideways scatter (SS) and electronic volume (EV); the mean values and particular standard deviations are based on all samples throughout a bioreactor cultivation.

Dye	DiOC <sub>2</sub> (3)	DiOC <sub>6</sub> (3)	DiBAC <sub>4</sub> (3)
Increasing fluorescence according to cell status	Red (675 nm) / green (525 nm) ratio, polarized	Green (525 nm), polarized	Green (675 nm), depolarized
Concentration range (μM)	4-80	0.015-0.4	0.02-3
Incubation time range (min)	0-43	0-36	0-43
Maximum difference to depolarized cells with CCCP	Concentration (μM)	14	0.365
	Incubation time t (min)	5 < t < 27	2 < t < 4
Influence on	SS (%±SD)	-18 (±8)	-14 (±6)
	EV(%±SD)	-19 (±5)	-54 (±5)

Interestingly the signal intensity over time was stable for DiOC<sub>2</sub>(3) and DiOC<sub>6</sub>(3) staining (5 < t < 28 min) whereas is the case of DiBAC<sub>4</sub>(3) the staining of depolarized cells decreased during the incubation time and remained stable only for a short time period (2 < t < 4 min). This may be due to the different chemical properties of DiBAC<sub>4</sub>(3) as an oxonol stain (negatively charged) compared to DiOC<sub>2</sub>(3) and DiOC<sub>6</sub>(3), which are carbocyanides (positively charged) [173]. Optimal dye concentrations and incubation times were tested in bioreactor cultivations with multiple sample points throughout different growth phases. The effects on SS, granularity respectively and EV, shown in **Table 6**, were estimated from a bioreactor cultivation comparing the SS and EV values of all dyed samples to non-dyed samples. The mean value of the particular difference and its standard deviation were determined. This direct application revealed dye dependent effects on single cell properties like the EV and SS. Although DiBAC<sub>4</sub>(3) and DiOC<sub>6</sub>(3) were most efficient in distinguishing polarized from depolarized (CCCP treated) cells the dyes showed no





explicit application on bioreactor cultivations samples. This may be due to the fact that these dyes both change SS and EV signals up to 84% leading to non-significant measurements. On the contrary, DiOC<sub>2</sub>(3) could be easily applied to estimate MP and was at the same time the dye with minimal influence on single cell properties like EV and SS. It should be stressed that it is indispensable to individually develop protocols and assays for the particular organism of interest. Although DiBAC<sub>4</sub>(3) and DiOC<sub>6</sub>(3) were capable of measuring MP in calibration experiments they were found not to be effective for physiological cell characterization in bioreactor cultivations. This may be due to changes in cell properties related to cell wall and membrane structures caused by an increased shear stress in bioreactors compared to shaking flask experiments. Cell wall and membrane structures may influence the characteristics of dye binding [216]. However DiOC<sub>2</sub>(3) was found to be most applicable dye in describing the status of cell membrane polarization under bioreactor culture conditions (**Tab. 6**). This better applicability may be related to the applied higher concentrations of the DiOC<sub>2</sub>(3) dye. The main staining principle which is based on the saturation and agglomeration at polarized membranes probably results in a more robust assay [216]. DiOC<sub>2</sub>(3) was chosen for the following experiments as the optimal dye to estimate MPs with indicated concentration and incubation times guaranteeing sensitive and robust measurements.

#### 4.3.1.2 MP estimation

For cell viability measurements it is most important to have appropriate and efficient controls to ensure data reliability and consistency. **Figure 24** illustrates the reproducible measurements of DiOC<sub>2</sub>(3) stained cells which were evaluated according to the FL3/FL1 ratio method as described in section 3.15.

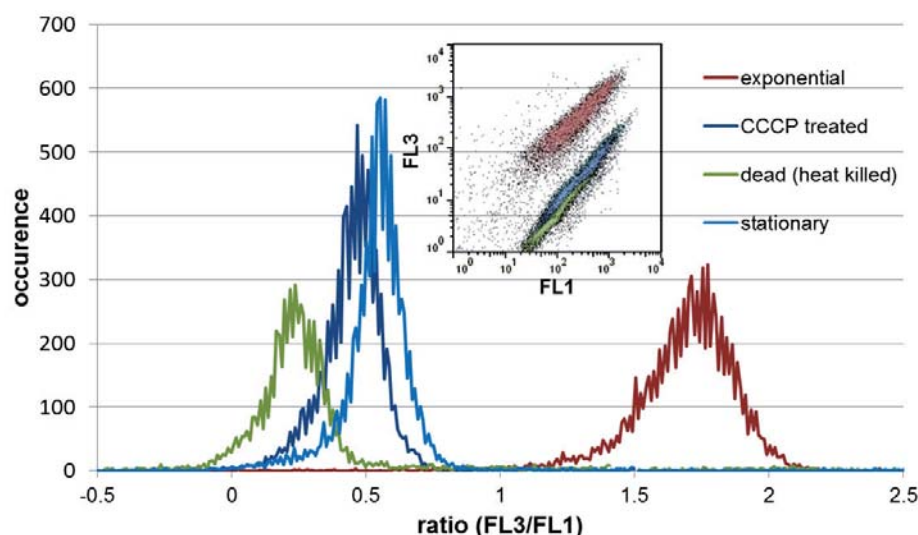


**Figure 24:** Membrane potential measurements of *B. megaterium* cells producing ABF D1.3 scFv. DiOC<sub>2</sub>(3) staining and subsequent FL3/FL1 ratio analysis regarding different growth stages (exponential and stationary) and treatment with heat and CCCP as negative controls.



Cells from the exponential growth phase compared to dead cells (heat treated) and as controls for the depolarized status stationary cells as well as CCCP treated exponential phase cells were being used. The DiOC<sub>2</sub>(3) dye is assumed to enter polarized cells in such an amount, that the normally green fluorescence dye exhibit increased red fluorescence properties most likely due to agglomeration of dye molecules [173]. Therefore an increased red fluorescence directly reflects the state of optimal membrane polarization and the enhanced metabolic activity of the corresponding cell population. Intensity values are normalized to the green fluorescence signal according to cellular size. Stationary cells show the same fluorescence pattern as CCCP treated cells thus verifying the applicability of the staining method for MP estimation. Moreover a distinct separation of polarized versus depolarized cells is also illustrating the high sensitivity level of this detection method. As no real MP has been estimated so far for *B. megaterium*, a calibration between the measured fluorescence intensities and the existing MPs was performed.

The calibration with different potassium [K<sup>+</sup>] ion concentrations accompanied with valinomycin treatment was carried out to artificially emulate certain MPs according to the method of Novo et al. (1999) [173]. These calculated MPs were correlated to measured DiOC<sub>2</sub>(3) fluorescence signal intensities of *B. megaterium* cells which were producing ABF D1.3 scFv. From the applied [K<sup>+</sup>] concentrations, the particular MP was determined using the Nernst Equation and related to the measured FL3/FL1 ratio values of particular samples. A strong linear correlation could be observed for a wide range including saturation values on both sides of polarized and depolarized cells showing a sigmoidal curve trend (**Fig. 25**). At the maximum a membrane polarization of -50 mV could be determined which may be due to the fact that ABF producing cells were measured (other cell types showed MP of -120 mV [174]). Despite this the observed linear correlation clearly shows that the staining intensity of DiOC<sub>2</sub>(3) can be directly correlated to the MP created by the applied [K<sup>+</sup>] concentrations thus again highlighting the sensitivity and applicability of the method.

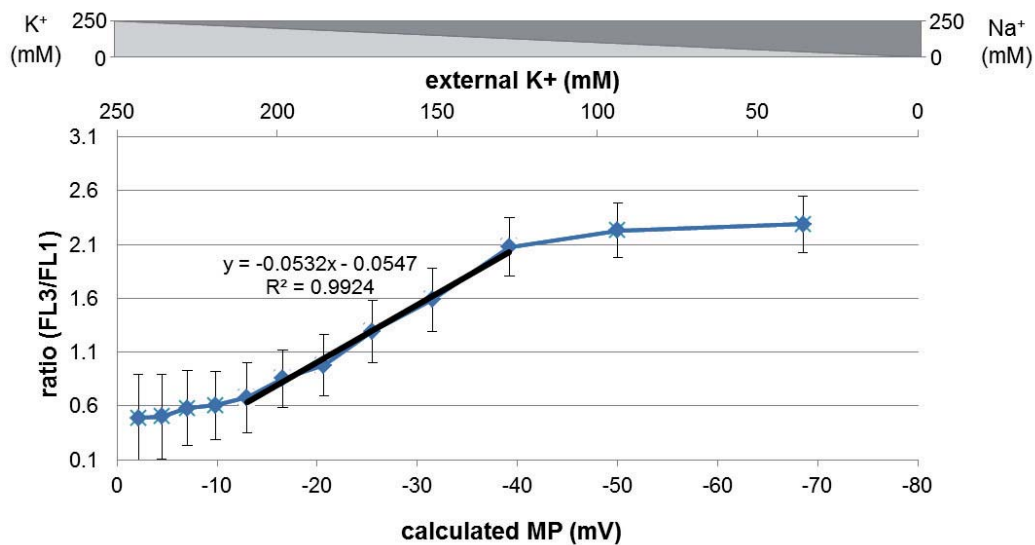


**Figure 25:** MP calibration related to DiOC<sub>2</sub>(3) stain FL3/FL1 ratio analysis of *B. megaterium* YYBm1 (EJBmD1.3scFv) producing ABF scFv D1.3. MP was simulated by valinomycin and potassium [ $K^+$ ] addition and calculated by the Nernst equation. Error bars representing the coefficient of variation values of particular FL3/FL1 distributions.

#### 4.3.2 Cell integrity

Apart from MP estimation the cell integrity is also an important parameter for bioprocess evaluation especially during long-term starvation periods. Here the differentiation between dormant depolarized cells and dead cells indicated by a compromised cell membrane is most desirable. Dye combinations of DiBAC<sub>4</sub>(3) and PI were tested in *B. megaterium* cells which were taken from exponential growth phase and either untreated or heat-inactivated (**Fig. 26**). Different mixtures of these cells were investigated and could be directly correlated to the resulting clusters representing the differentiated populations. **Figure 26** clearly shows the applicability of the dye combination for the correlated data. Here the fluorescence concentration (FL-Fc) was considered to ensure accurate measurements of fluorescence intensities related to the particular cell volume.

In case of heat-inactivated cells PI should be able to enter the cell and intercalate into nucleic acid structures due to porous membrane and cell wall structures thereby increasing its fluorescence intensity. Such treated cells are also expected to show a higher green fluorescence due to DiBAC<sub>4</sub>(3) staining related to the depolarized MP. However only an increased red fluorescence was measurable probably related to the PI dye showing certain quenching properties towards the green fluorescence of DiBAC<sub>4</sub>(3).

When using PI as an indicator for cell membrane integrity it has to be taken into account, that even highly reproductive cells show an increased PI-staining besides dead cells [217]. Furthermore significant variability in uptake patterns of nucleic acid binding dyes by Gram positive bacteria were shown before [218].

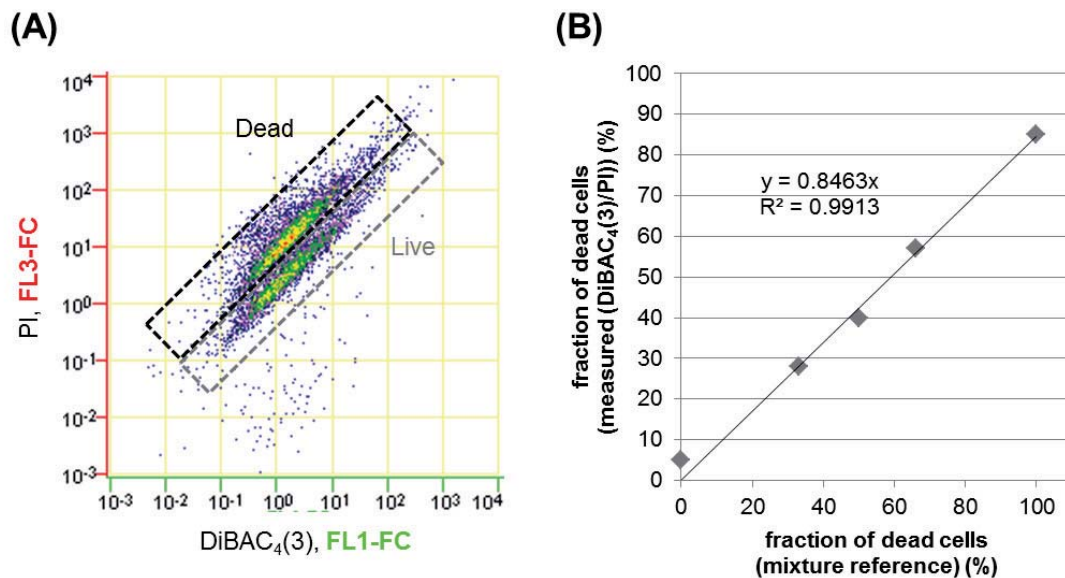


**Figure 26:** Live/dead test of *B. megaterium* YYBm1 (EJBmD1.3scFv) producing ABF D1.3 scFv with dye combination of DiBAC<sub>4</sub>(3)/PI. (A) DiBAC<sub>4</sub>(3)/PI stain: 50% dead cell, 50% live cell mixture, (B) calibration curve determined via different mixtures of dead (heat killed) and live (exponential phase) cells after particular gate analysis.

#### 4.3.3 Production intensity

Further process relevant methods focus on discriminating distinct information which are related to single cell productivity e. g. to develop a reliable method for differentiation high producing from low or non-producing cells. It has to be clarified whether a reduced productivity is due to less effective production in every single cell or to differentiated cell populations of producing and non-producing cells. Under normal circumstances only average values are taken into account. Especially for high cell density cultivations, population analysis may lead to totally new insights into reduced specific productivities revealing the actual bottleneck of production and/or secretion.

To gain deeper insights in single cell production intensities of *B. megaterium* cells which were secreting ABF D1.3 scFv, a specific detection assay was developed. As shown in **Figure 27 A** the lysozyme treatment is indispensable to make the ABF accessible for detection ABs. After fixing the cells with paraformaldehyde the secreted AB is stuck to the cell surface making it accessible for immunohistochemical detection by specific ABs. Detection of secreted ABF D1.3 scFv is done by using an anti-penta His AB followed by a species-specific anti-mouse AB which is coupled to the fluorochrome Alexa Fluor 488. With this detection protocol ABF-producing cells can be detected using different methods such as FCM or CLSM.

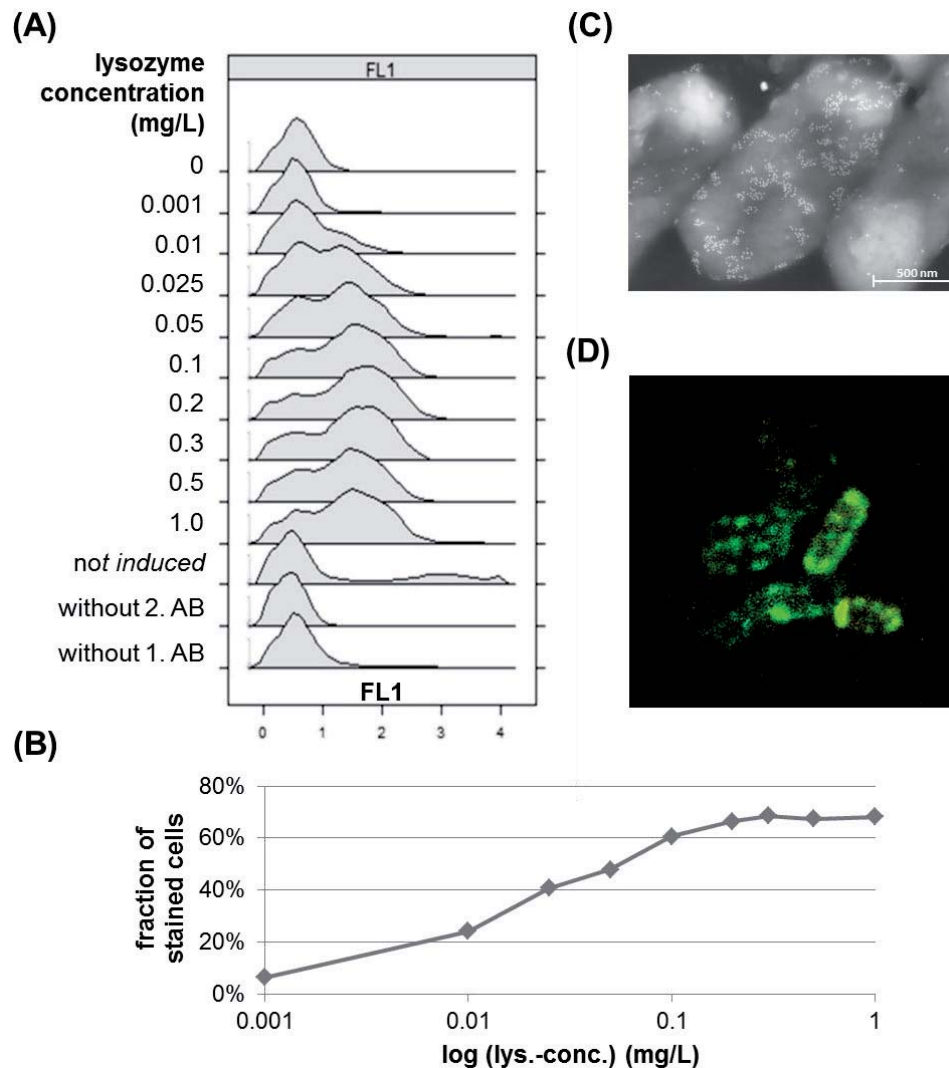


**Figure 27:** Production intensity assay-validation; lysozyme treatment of *B. megaterium* YYBm1 (EJBmD1.3scFv) producing ABF D1.3 scFv for assay evaluation distinguishing between producing and non-producing cells; **(A)**, **(B)** different lysozyme concentrations and their effect on staining intensities with second Alexa Fluor 488 coupled AB; **(C)** Immuno-FESEM picture of ABF D1.3 scFv secreting, lysozyme treated *B. megaterium* cells incubated with a second gold coupled detection AB; **(D)** Confocal Laser Scanning Microscopy (CLSM) picture of *B. megaterium* cells, lysozyme treatment combined with second Alexa Fluor 488 coupled detection AB.

In the experimental screening with different lysozyme concentrations not all cells were secreting ABFs, a phenomenon which is shown by the two overlapping distributions (**Fig. 27 A**). These distributions were even separated when applying higher lysozyme concentrations, where a saturation of the fraction of stained cells was reached (**Fig. 27 B**). Control treatments were carried out to check for unspecific binding of first or second detection ABs which were at least negligible and could further be reduced by additional wash steps. The CLSM technique was used to illustrate the specific labeling of ABF D1.3 scFv producing cells by fluorochrome Alexa Fluor 488 coupled detection ABs (**Fig. 27 D**). ABFs were detected in the space between cell membrane and cell wall indicated by green



ring structures. In addition, immuno field emission scanning electron microscopy (Immuno-FESEM) was used to detect certain regions of secretion on the cell surface in detail (**Fig. 27 C**). Here a second AB coupled to gold particles was used to make these regions visible. For *B. subtilis* similar investigations showed that the Sec apparatuses are located at specific multiple sites by being organized in spiral like cluster structures along the cell [104]. Both presented methods reveal cells with higher labeling or less labeling patterns therefore giving hints on production and secretion heterogeneities within the bacterial population.

When further examining the production intensities of ABF producing *B. megaterium* two different lysozyme concentrations (0.5; 0.25 mg/L) were being applied to check for accumulation of ABFs at the cytoplasmatic membrane and within the cell wall structures as well. Based on the microscopy data, the used detection ABs can be considered as surface markers and, as such, a quantitative fluorescence surface density (FSD) can be estimated from the raw data of EV and FL1 values.

The interpretation of estimated FSD is done by differentiated region analysis. As shown in **Figure 28**, two regions were clearly defined. The first region included all measured cells whereas the second region comprised only cells which were labeled with detection ABs and therefore had an ABF producing status. The ratio of the particular fractions of cells was taken and weighted with the mean fluorescence value of the second region. Thereby a quantitative parameter which stands for the production intensity (*Prod\_Inten*) of the whole cell population was defined and used as a parameter for bioprocess monitoring (*Equation 8*).

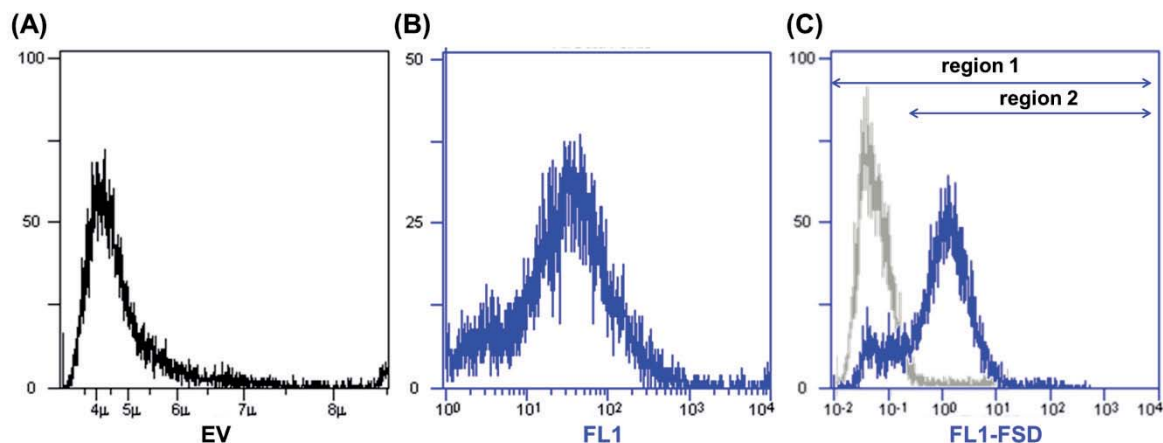


**Figure 28:** Production Intensity evaluation; FL1 Fluorescent Surface Density (FL1-FSD) distributions combined from electronic volume (EV) (**A**) and FL1 (**B**) data sets. Direct comparison of ABF D1.3 scFv producing (blue) and non- producing cells (grey) (**C**). Different region (1, 2) settings to calculate production/secretion intensities of *B. megaterium* cells as shown in *equation (8)*.



$$Prod\_Inten = \frac{\% cell\ reg2}{\% cells\ reg1} \times mean\ FL1\ (reg2) \quad (8)$$

To determine the secretion rates of yeast cells several other methods which relied mostly on artificially created affinity matrices have been developed before [219, 220]. However the developed method displays a simple and robust technique which is simply based on fixation and lysozyme treatment of *B. megaterium* cells. Although cells have to be considered as dead after paraformaldehyde treatment they could be sorted by a FACS and subsequently be analyzed on transcriptome or proteome level [221, 222]. Even plasmid banks of *B. megaterium* could be used for screening for high producers similar to library screens of scFv libraries e. g. in yeast systems [223, 224].

## 4.4 Process development

### 4.4.1 Batch culture

Based on the optimized minimal medium, batch cultivations were carried out and single cell analysis was performed under controlled bioprocess conditions to study the D1.3 scFv ABF production and secretion with *B. megaterium* at different cultivation stages.

The established methods for MP measurements, viability considerations and specific investigation regarding the production status of *B. megaterium* cells producing and secreting ABF D1.3 scFv were applied on samples of a bioreactor cultivation showing the potential of at-line flow cytometric data analysis on a single cell level for bioprocess state estimation.

As depicted in **Figures 29 A** and **B** the estimated MP by staining with DiOC<sub>2</sub>(3) could be clearly assigned to different growth phases of the particular *B. megaterium* cultivation. Especially during the exponential growth phase the polarization status of the cells reached a maximum indicated by the FL3/FL1 ratio analysis. As soon as the carbon source fructose was depleted the DO concentration immediately started to increase (**Fig. 29 B**) paralleled by a remarkable decrease in FL3/FL1 ratio which directly reflected the reduced MP of the cells. During the next 10 hours of starvation phase the MP further decreased to low constant values which correlated with cells in the stationary phase as shown before (**Fig. 24**).

Interestingly the measured FL3/FL1 ratio values and corresponding MPs (**Fig. 29 C, D**) showed a linear correlation between the specific CO<sub>2</sub> production (qCO<sub>2</sub>) and O<sub>2</sub> consumption rates (qO<sub>2</sub>). This illustrates a direct relationship between the cellular MP and the microbial metabolic activity represented by CO<sub>2</sub> production and O<sub>2</sub> consumption. The correlation holds for any growth phase as the proportionality constant is equal for both qO<sub>2</sub> and qCO<sub>2</sub> variables.



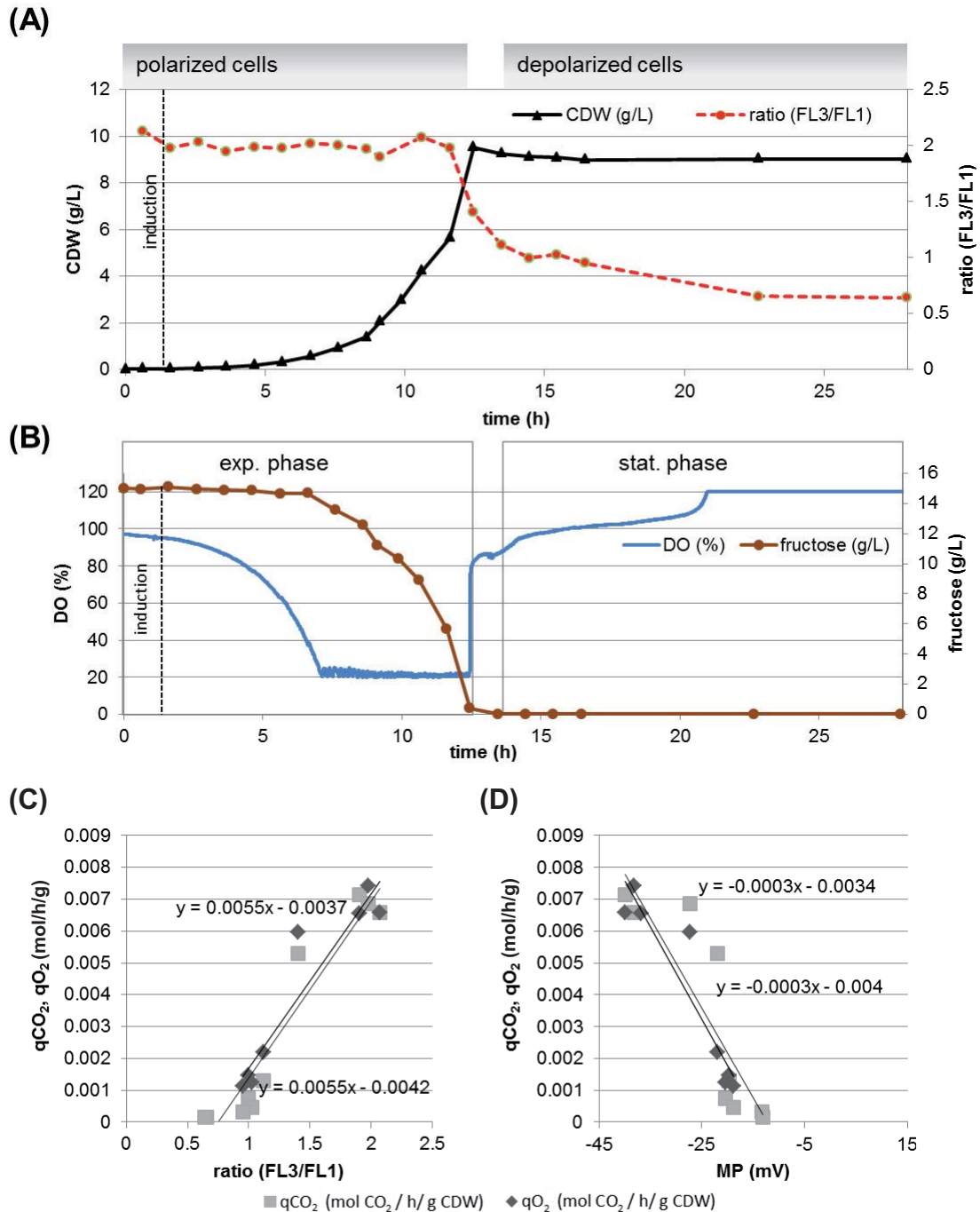


**Figure 29:** MP investigations of *B. megaterium* (YYBm1 (EJBmD1.3scFv)) cells producing/secreted ABF D1.3 scFv in a bioreactor cultivation (15 g/L fructose, DO>20%, 1L). **(A)** DiOC<sub>2</sub>(3) stain of cells analyzed with ratio analysis of FL3/FL1 values, related to cell dry weight biomass measurements, **(B)** dissolved oxygen (DO), fructose concentration and resulting growth phases, **(C)**, **(D)** correlation between specific CO<sub>2</sub> production ( $qCO_2$ ), specific O<sub>2</sub> consumption rate ( $qO_2$ ) with MP measurement deduced from MP calibration and FL3/FL1 ratio analysis.



Another important factor which was also measured for the same bioprocess were changes in cellular membrane integrity of *B. megaterium*. The applicability of the live/dead assay as a sensitive method for detecting changes in membrane integrity has already been verified in this study and was thus used to analyze differences in particular cell populations, especially in the late stationary phase (**Fig. 30 A**). It also had to be taken into account that cell characteristics of unstained cells like SS and EV were remarkably affected throughout the cultivation (**Fig. 30 B**). Especially the EV decreased to about 50% when the culture developed from exponential to stationary phase. Keeping this in mind distinctive effects regarding staining intensity and behavior might occur. Changes of the physiological status of a cell can have an effect on cell size and granularity. For instance protein or polyhydroxybutyrate (PHB) cell content has been shown to depend on particular growth phases [140, 225-228]. In addition, a growth phase dependent behavior of *B. megaterium* cell size arises from cell chain formation and disintegration. In case of chain formation, it is not possible to know if these chains are further separated into single cells through the hydrodynamical focusing of the flow cytometer. In the device used here, the equivalent size and fluorescence are estimated for every "event", i.e. for every counted particle regardless of it being a single bacterium or a chain of bacteria. Therefore normalization of fluorescence was performed for each "counted" event either belonging to a single cell or cell-cell conglomerates. In this case EV values were used to normalize the different data sets by calculating the fluorescence concentration (FL-FC). Region analysis of dot plots (FL1-FC vs. FL3-FC) was done and percentages of cells in particular regions were determined for all sample points (**Fig. 30 A, C**). For the exponential and stationary phases an increase of cells with higher red fluorescence could be detected. The fraction of PI-positive cells of the exponential phase might be due to loosened cell wall structures of fast dividing cells, which has been shown to be the case for other bacteria before [217]. During the stationary phase the higher amount of PI-positive cells was possibly a result of reduced and permeated cell wall/membrane structures caused by enhanced autolysin activity [218, 229].

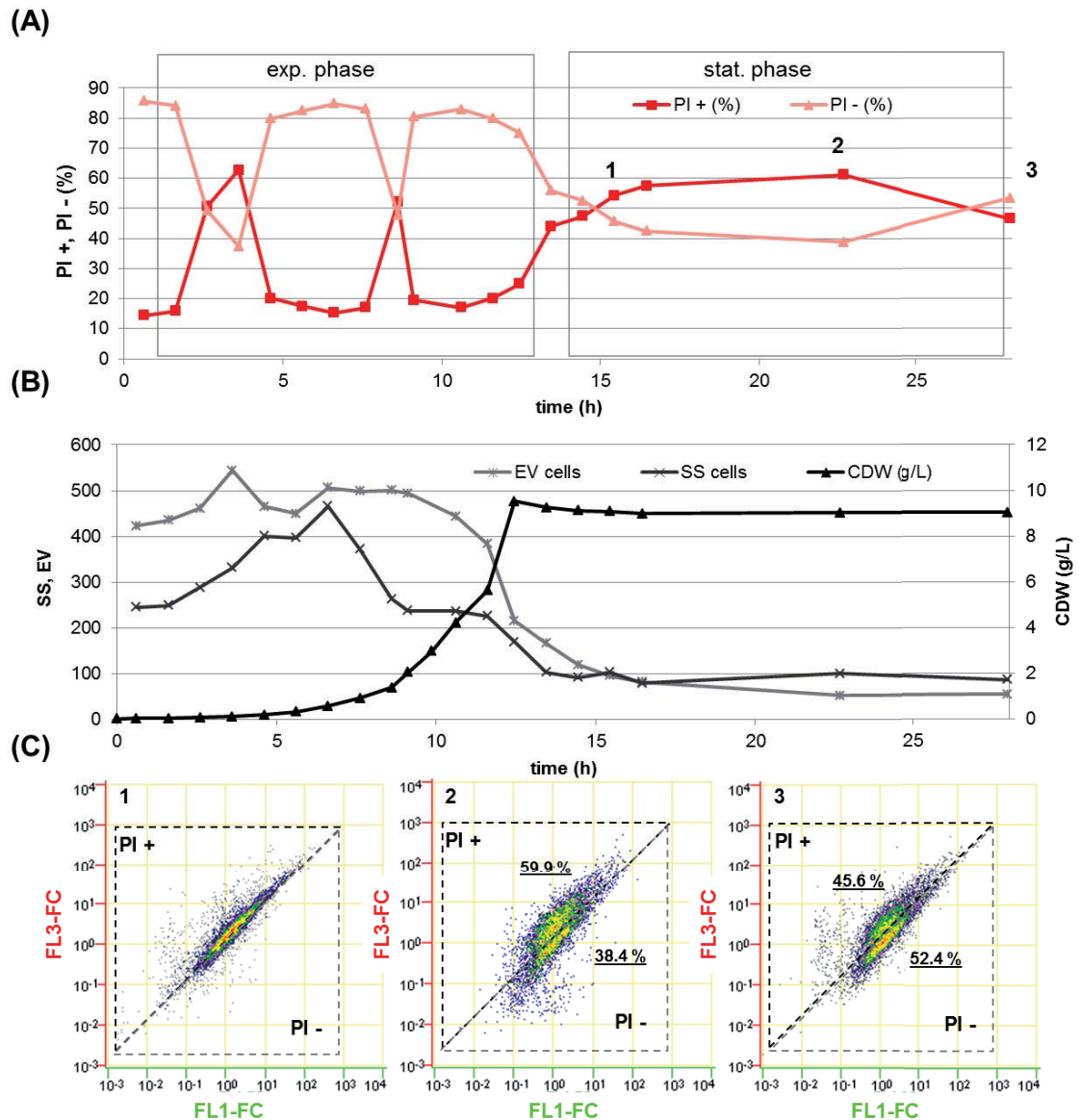


**Figure 30:** Viability investigations of a bioreactor cultivation of *B. megaterium* cells (YYBm1 (EJBmD1.3scFv)) producing/secreting ABF scFv D1.3 (15 g/L fructose, DO>20%, 1L). **(A)** DiBAC<sub>4</sub>(3)/PI stain of samples, percentages of PI+ and PI- cells according gate analysis of FL1-FC and FL3-FC dot plots. **(B)** Sideways scatter (SS), electronic volume (EV) mean values related cell dry weight characteristics at different growth phases of unstained cells. **(C)** Population analysis of DiBAC<sub>4</sub>(3)/PI stain related increased red fluorescence at late cultivation time points.

In the last two sample points a separation into different populations became observable (**Fig. 30 C; 2, 3**). An original homogenous population transformed into two distinct fractions which may be related to a population dynamic behavior of long term starvation cultures. Therefore detected PI-positive cells which reached the stationary phase should rather be considered as dormant or partially damaged (PI permeable) than as totally dead cells.



This bioprocess was also analyzed in terms of ABF D1.3 scFv production regarding the efficiency of secretion of single cells and the overall product yield. Therefore the previously defined production intensity was determined via fluorescence labeling. The functionally secreted and folded ABF D1.3 scFv was measured in the supernatant by an ELISA assay and normalized to the measured cellular dry weight (yield coefficient,  $Y_{P/X}$ ). These two calculated parameters “production intensity” and “ $Y_{P/X}$ ” were directly compared (**Fig. 31**). To get an idea of the secretion efficiency of ABFs through the cell wall, different lysozyme concentrations were applied after cell fixation. By using a high concentration of lysozyme it can be assumed that the measured values directly reflect the total amount of ABFs accumulated behind the cell membrane. In contrast when applying low concentrations of lysozyme only a part of generated ABFs within the cell wall structures might be detected due to a only partially degradation of cell wall components.

In the investigated batch process, different phases of production could be clearly distinguished. The first phase right after induction showed a remarkably increase in the production intensity at both 0.025 g/L and 0.5 g/L lysozyme treatment (**Fig. 31**). The product yield remained low and has to be carefully interpreted as the detected concentrations of the secreted ABF were in the range of the lowest detection limit. During exponential growth both the production intensity as well as the product yield remained constant which was related to growth coupled production behavior. Here the increase in biomass directly favored higher concentrations of functional folded ABFs in the supernatant in the same range (**Fig. 31 B**). A detailed view reveals higher production intensities during the late phase of exponential growth. Of particular importance is the time shift observed for this phenomenon in case of different concentrations of lysozyme treatment. At lower lysozyme concentrations the shift to higher production intensities was delayed for one hour compared to lysozyme treatment with higher concentration. A possible explanation for this fact might be that the generated ABFs first accumulated behind the cell membrane before they were secreted. This delay of the secretion process could also be seen during the stationary phase. Here a sudden increase in production intensity of both lysozyme treatment approaches was paralleled by a delayed increase in the production yield. A definite decrease in production intensity related to single cell analysis was shown for the late stationary phase, which was most possibly due to starvation and cell inactivation. However the ABF concentration as well as the biomass concentration were not affected and remained at a constant level.

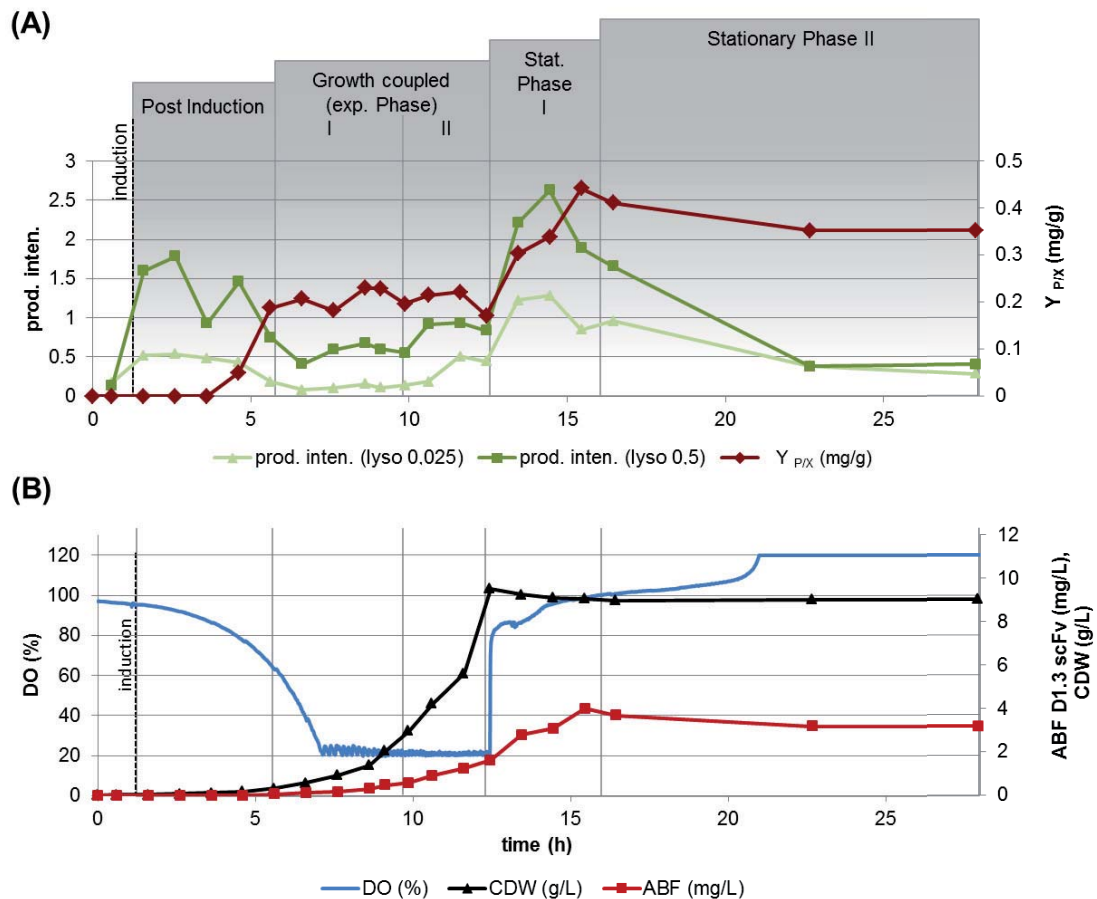


**Figure 31:** Product yield ( $Y_{P/X}$ ) and production intensity measurements of *B. megaterium* cells producing/secreting ABF D1.3 scFv in a bioreactor cultivation (15 g/L fructose, DO>20%, 1 L). **(A)** Growth phase dependent product yield ( $Y_{P/X}$ ) and production intensity of ABF D1.3 scFv production and secretion. Production intensities were determined by applying different lysozyme concentrations; **(B)** relation to growth phase dependent dissolved oxygen (DO), absolute ABF D1.3 scFv and cell dry weight (CDW) concentration.

As the time courses of the product yield  $Y_{P/X}$  and the production intensity are both coupled for most of the cultivation time, it can be concluded that the processes of biosynthesis and membrane associated secretion of ABFs inside the cell are directly related to the final secretion and functional appearance outside the cell in the supernatant. Interestingly the measured production intensities of the particular lysozyme treatments showed more distinctive differences at phases of higher production. This stresses that the cell wall itself is a barrier which has to be overcome by secreted ABFs. Therefore, especially for states with high production, the cell wall may be regarded as a bottleneck concerning the observed overall process productivity, since it delays the product transport thus increasing the secretion time at single cell level.

Through analysis of MP and production intensities no population heterogeneities within the different growth and production phases became observable. This is most probably due to the well-controlled bioprocess parameters guaranteeing ideal mixing conditions with optimal temperature, pH-control and no oxygen limitation.



Cell integrity, MP and production intensity measurements revealed clear changes in the particular cell states at the transition from exponential to stationary phase. Here the question arises if depolarization of cells during the stationary phase which was accompanied by a decrease in membrane integrity may be directly related to the gain in production and secretion of ABF D1.3 scFv. It was shown before that by decreasing the polarization status of a cell a better secretion performance of proteins may occur. This was due to changes in cell structure caused by a higher autolysin activity which resulted from changes in the cell wall charge distribution [229]. Therefore the MP can be indirectly used to estimate enhanced production and secretion of ABF D1.3 scFv by *B. megaterium* and might therefore be a relevant parameter for further process control. By the analysis done it was discarded that cells in the early stationary phase 2-3 h after fructose depletion should be considered as dead and, therefore, lyse and release ABFs in a high amount. It was shown that entirely depolarized cells in a dormant status are totally recovered by fructose addition after starving periods of up to 4 h (results not shown).

This key experiment of a typically batch process with its increased stationary phase coupled production and secretion of ABF D1.3 scFv was taken as a basis for an advanced process control of an adapted fed-batch process which will be further explained in the following section.

#### 4.4.2 Fed-batch culture

The generation of an appropriate bioprocess control for reaching high cell densities with guaranteed high productivities was the main focus of the subsequent investigations. For improving the production of ABF D1.3 scFv by *B. megaterium* several common methods of fed-batch control principles were tested (**Tab. 7**). Although high cell densities were reached, the production rates decreased right after starting the feeding. The cells were also less productive at the stationary phase which might have been expected differently from former batch experiments. Therefore an adapted feeding strategy based on a time-dependent oscillating growth rate strategy was developed.



#### 4.4.2.1 Process strategies - overview

Multiple process strategies for ABF D1.3 scFv production were tested. The particular yield coefficients and kinetic parameters were calculated and are summarized in **Table 7**.

**Table 7:** Overview of different scales and cultivation strategies applied for production of ABF D1.3 scFv by *B. megaterium* YYBm1.

	shaking flask	batch		fed batch					
feed strategy	-	-		constant	DO controlled	$\mu_{\text{set}} = 0.15$	$\mu_{\text{set}} = 0.3$	$\mu_{\text{set}} \approx \cos(t)$	
								$\mu_{\text{max}} = 0.3$	$\mu_{\text{max}} = 0.4$
volume scale (L)	0.1	1.0	1.0	3.3	3.0	3.4	3.1	3.1	57.4
fructose conc. batch (g/L)	5.0	15.0	50.0	5.0	5.0	5.0	5.0	2.7	2.7
fructose conc. feed (g/L)	-	-		80.0	10 (50)	20.0	30.0	225.0	225.0
CDW (g/L)	2.2	8.0	20.0	25.4	17.4	5.5	10.0	4.4	4.5
ABF D1.3 scFv (mg/L)	0.80	3.00	1.00	3.00	0.75	1.10	0.65	11.90	5.14
ABF D1.3 scFv (mg)	0.08	3.00	1.00	9.90	2.25	3.74	2.02	36.89	295.04
$Y_{X/S}$ (g/g)	0.45	0.53	0.40	0.55	0.61	0.41	0.61	0.45	0.34
$Y_{P/X}$ (mg/g)	0.36	0.38	0.05	0.12	0.04	0.20	0.06	2.70	1.13
$Y_{P/S}$ (mg/g)	0.16	0.20	0.02	0.06	0.03	0.08	0.04	1.21	0.39
duration (h) (p.i.)	15.0	14.0	19.0	18.5	16.0	26.0	17.0	26.0	28.0
productivity (mg/h)	0.01	0.21	0.05	0.54	0.14	0.14	0.12	1.42	10.54
specific productivity (mg/g/h)	0.024	0.027	0.003	0.006	0.003	0.008	0.004	0.104	0.040





Batch cultivations in bioreactors were shown to be more effective in production of ABF D1.3 scFv compared to shaking flask cultivations which was probably due to the optimized process control of constant pH and DO regulation. The batch mode is yet limited in reaching high cell densities as overflow metabolites like acetate were produced which made the process less efficient and was leading to inhibition of growth and production (**Tab. 7**, batch with 50 g/L initial fructose concentration). Therefore fed-batch techniques based on exponential feeding profiles of constant growth rates of 0.3 (1/h) and 0.15 (1/h) were tested. It could be shown that for lower specific growth rates an overall higher specific productivity could be reached. This indicates a less growth associated production and secretion behavior of ABF D1.3 scFv production. A DO adapted controlled feeding strategy and constant feeding rates were also less successful in reaching higher productivities. In contrast the established  $\mu$  oscillating feeding profile, explained in detail in the following, was found to be most effective in production and secretion of ABF D1.3 scFv with a specific production rate of 0.104 mg/g/h.

#### 4.4.2.2 Ratio screening: growth phase – production phase

Based on the coupled increased production and secretion properties during the stationary phase a fed-batch process with different durations of growth phases and starving phases was tested. This was realized by the addition of appropriate amounts of nutrients guaranteeing a distinctive time spend of unlimited growth combined with different durations of starvation phases. The particular specific productivity was related to the actual ratio of growth and production times as shown in **Figure 32**. An optimal ratio of growth (1.5 h) to starving phase (0.5 h) with a value of 3 was calculated and used for subsequent bioprocess control.

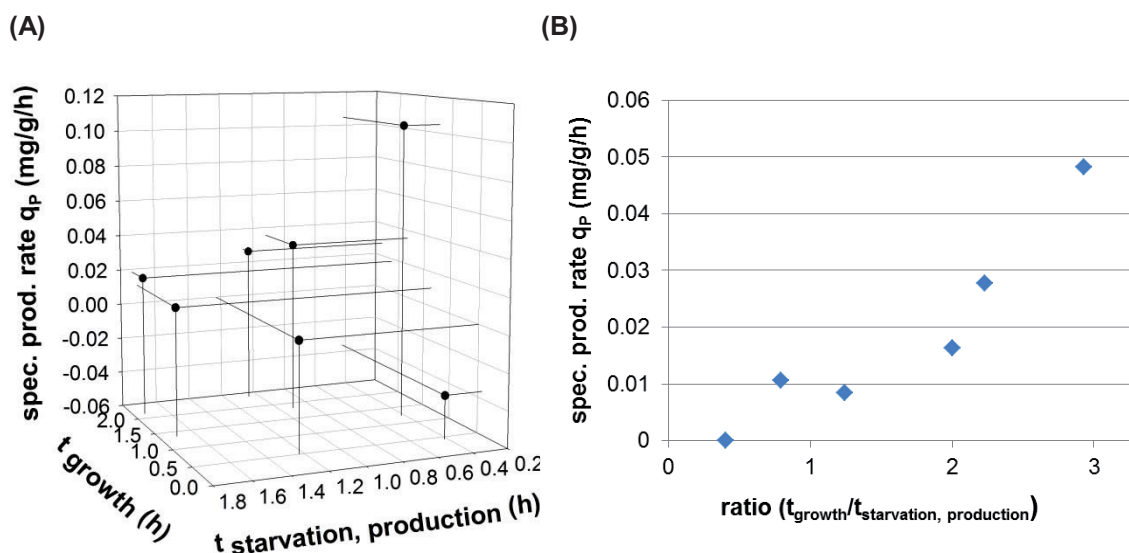


**Figure 32:** Screening of different time spends of growth phase and starving phase related to specific production rate of ABF D1.3 scFv ( $q_p$ ) in *B. megaterium* YYBm1 (EJBmD1.3scFv). **(A)**  $q_p$  related to absolute duration, **(B)**  $q_p$  related to ratio of growth and starvation time spends.

#### 4.4.2.3 Oscillating fed-batch

To ensure high productivity during the stationary phases together with suitable cell proliferation and sufficient nutrient supply, a fed-batch strategy with time-dependent  $\mu$ -oscillating feed control was established. A brief overview of the control strategy is given in **Figure 33**. Its principle is based on an exponential feed control algorithm with a time dependent specific growth rate control which is based upon two cosine functions (section 3.12, *equation 3*). This function was chosen to avoid abrupt feed changes causing over-feeding or sudden increase in overflow metabolites like acetate.

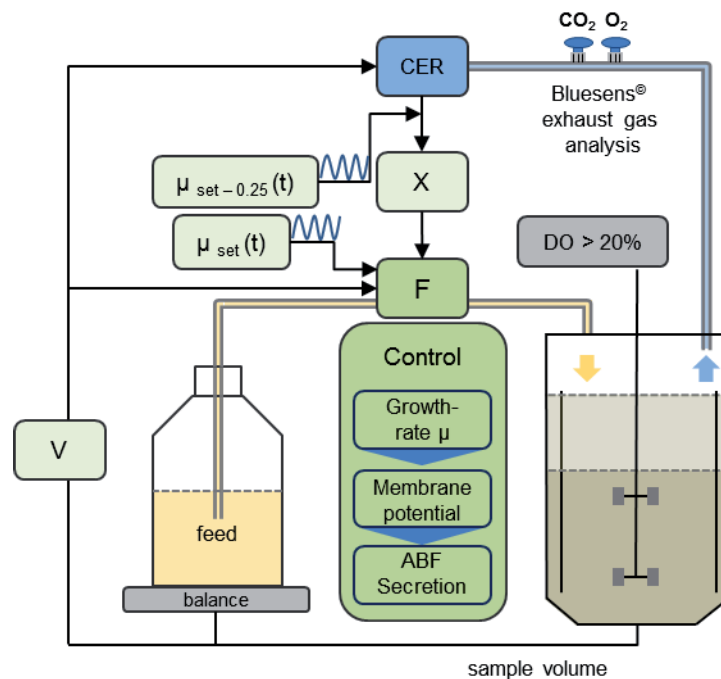


**Figure 33:** Overview of the control mechanism to create a  $\mu$ -oscillating feeding (F) strategy adapted to the particular biomass concentration (X) present. The biomass is estimated via the exhaust gas analysis related to CER ( $\text{CO}_2$  evolution rate) and to the current growth rate  $\mu_{\text{set}-0.25}$ .  $\mu_{\text{set}}$  is time dependent and based on two cosine functions with a defined maximal growth rate  $\mu_{\text{max}}$ . The underlying cultivation volume (V) in the bioreactor is corrected by sample and feed volume.

The current biomass was estimated by CER and the particular time dependent growth rate (**Fig. 34 A**). This growth rate was back shifted due to the adaptation delay of the active growth rate and was taken from former experiments. As shown in **Figure 34 A**, the cosine function was modified to ensure a well-defined ratio of growth and production/starving phases, respectively. A growth phase of 1.5 h with a maximal growth rate of 0.3 (1/h) was followed by a starving phase of 0.5 h.

This strategy could successfully be implemented into the process represented by measured DO concentrations and exhaust gas analysis ( $\text{O}_2$ ,  $\text{CO}_2$ ) based CER and OUR plots (**Fig. 34 B**). As shown in **Figure 34 C** measured CDW values were directly comparable to the online CER-based estimated data. Based on this process information, a feed



profile was successfully adapted (**Fig. 34 D**) ensuring an automated robust control of the process guaranteeing comparable starving and growth phases. Measured fructose and acetate concentrations were negligible as the applied carbon limiting feeding strategy avoided over-feeding. As expected, xylose was not metabolized and its concentration was kept around 5 g/L (data not shown).

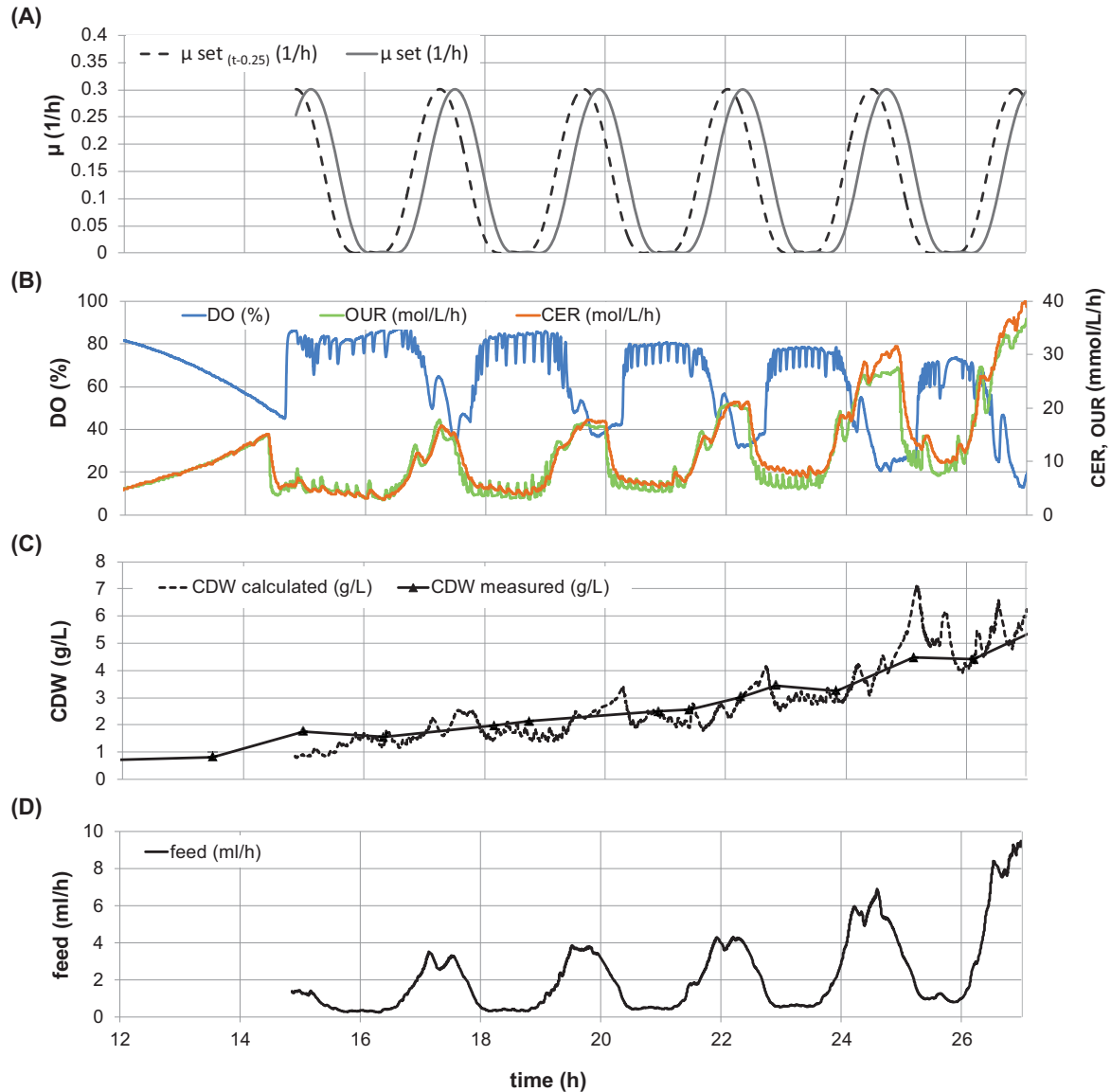


**Figure 34:** Process control of  $\mu$  oscillating fed-batch strategy of a *B. megaterium* YYBm1 (EJBmD1.3scFv) cultivation; Overview of process control variables during the oscillating fed-batch. **(A)**  $\mu_{\text{set}}$  and  $\mu_{\text{set}-0.25}$  were given by a cosine function with a defined  $\mu_{\text{max}}$  value of 0.3 (1/h). **(B)** Dissolved oxygen (DO) concentration and calculated oxygen uptake rate (OUR) and carbon dioxide evolution rate values (CER) were measured online and show clear trends in growth and starvation phases. **(C)** Biomass was calculated based on  $\mu_{\text{set}-0.25}$  and CER and was related to the biomass concentration measured. **(D)** The feeding rate was successfully adapted and was the direct control parameter for particular phases of growth and starvation.

Having a closer look at the absolute biomass and ABF amounts during the oscillating fed-batch, certain dependencies become observable as shown in **Figure 35**. While the biomass increases steadily, the specific production rate is mostly boosted during the controlled starving phases of the process (**Fig. 35 A**).

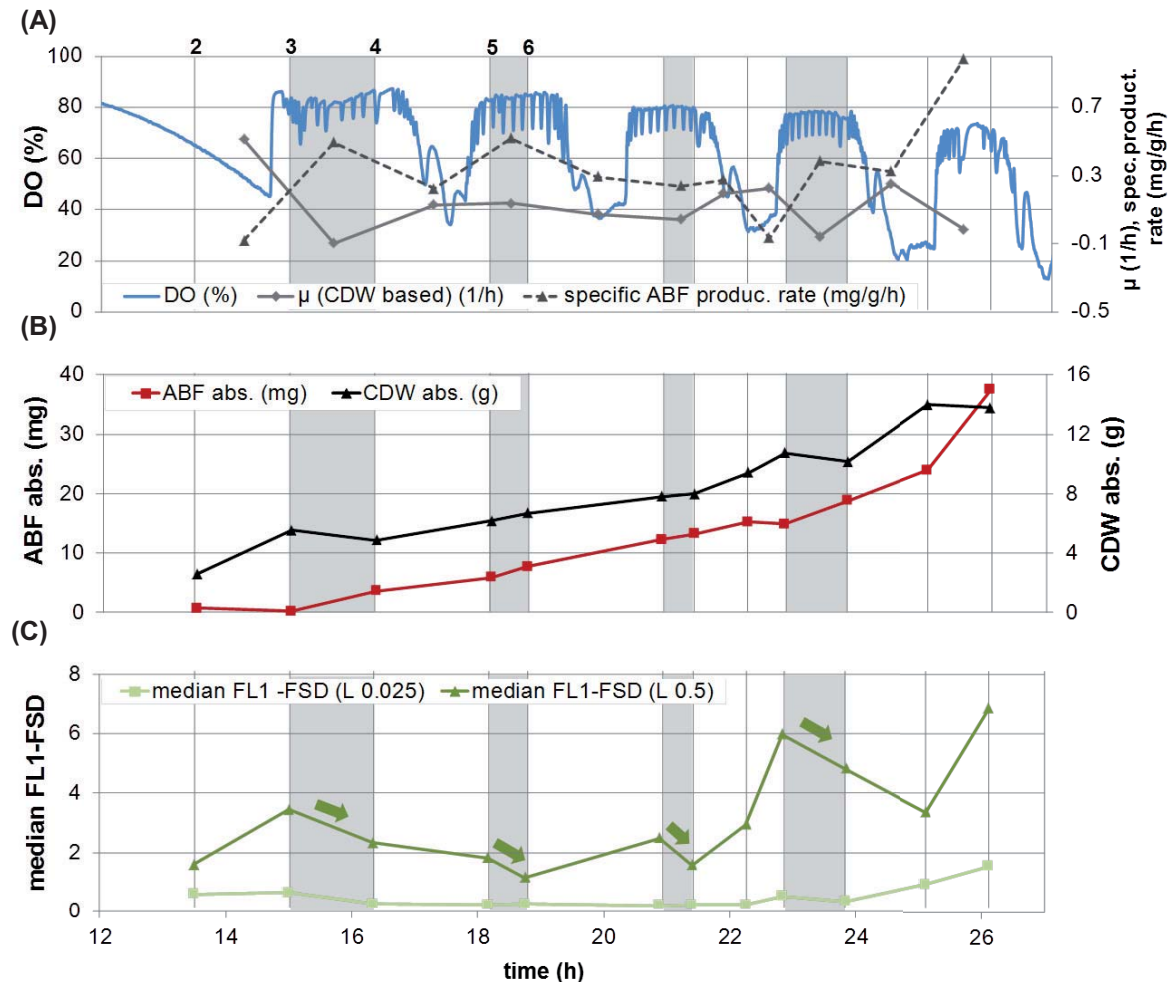


**Figure 35:** Production and biomass formation at  $\mu$  oscillating fed-batch strategy of a *B. megaterium* YYBm1 (EJBmD1.3scFv) cultivation; **(A)** Specific growth rate and production rate of ABF D1.3 scFv in the  $\mu$  oscillating fed-batch at growth and starvation phases (grey shaded). Numbers correspond to particular flow cytometric analysis of MP measurements and production intensity measurements shown in **Figure 36** and **37**; **(B)** absolute concentration of ABF D1.3 scFv (mg) and CDW (g) throughout the cultivation; **(C)** single cell analysis of ABF production status of cells done by immune labeling (production intensity assay), median analysis of particular fluorescence distributions of FL1-FSD at low (0.025 mg/mL) and high (0.5 mg/mL) applied lysozyme concentrations.

Another assessed parameter during the cultivation was the polarization status of the cells using the established fluorescence labeling assay based on DiOC<sub>2</sub> staining (**Fig. 36**). CCCP-treated cells which feature a total collapse of MP were used as a control. As shown in **Figure 36**, cells originating from a polarized cell status from the exponential batch phase were clearly depolarized at the transition from exponential to the stationary phase.



The depolarization increased significantly during the starving phase and could be timewise correlated to an increased secretion of ABFs.

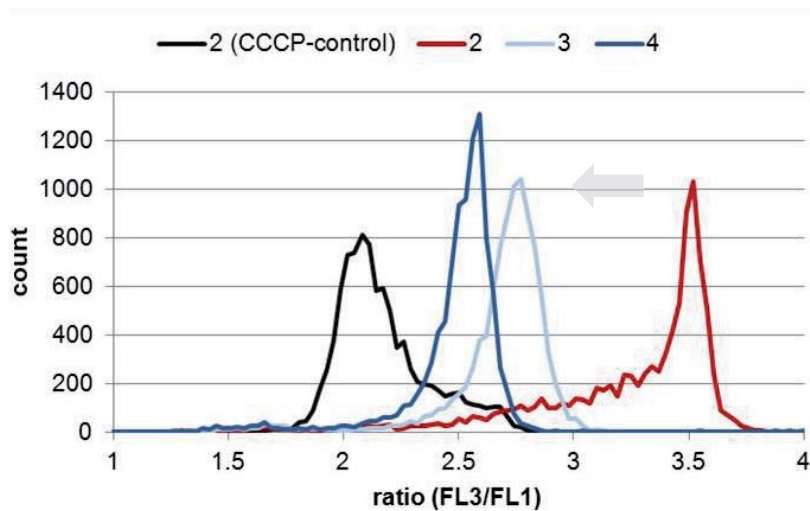


**Figure 36:** MP estimation at  $\mu$  oscillating fed-batch strategy. Single cell analysis of the MP of *B. megaterium* cells (YYBm1 (EJBmD1.3scFv)) secreting ABF D.13 scFv at different cultivation time points corresponding to particular sample numbers (**Fig. 35**). Cells were stained with DiOC<sub>2</sub> and analyzed by FCM in parallel to the cultivation. Data analysis was done by FL3/FL1 ratio calculation. CCCP was used as negative control to depolarize cells. The arrow indicates the shift from a polarized to a depolarized cell status.

Immune fluorescent labeling of producing cells shown in **Figure 37** clearly illustrated a fluorescent shift of the cell population towards decreased fluorescence intensities during the time course of the stationary phase. It was shown that for increased secretion the cell population developed a wider distribution characteristic. This illustrates that the behavior of particular cells differs distinctively from each other and highlights the big advantage of this single cell approach compared to average value measurements.

It can be assumed that ABFs produced during the growth phase are increasingly secreted throughout the stationary starving phase. These findings could also be confirmed by analyzing median-values of particular FL1-FSD distributions using different lysozyme concentrations (**Fig. 35 C**). The decrease in fluorescence intensity was mostly paralleled by an increased secretion of ABFs (specific productivity) during the late stationary phases. By applying different lysozyme concentrations, a dynamic pattern of secretion became observable (**Fig. 35 C**). The fluorescence intensities measured when applying low lysozyme concentrations may correspond to the release efficiency through the cell wall as mentioned before (section 4.4.1). On the contrary, investigations made at higher lysozyme concentrations relate to the amount of ABFs between cell wall and cell membrane. These measurements may give an idea about the secretion efficiency through the cell membrane itself. Beside the increased secretion of ABFs in the stationary phase it could also be shown that the overall secretion was intensified during late stages of the whole cultivation



indicated by an overall higher fluorescent labeling when applying both lysozyme concentrations (**Fig. 35 C**).

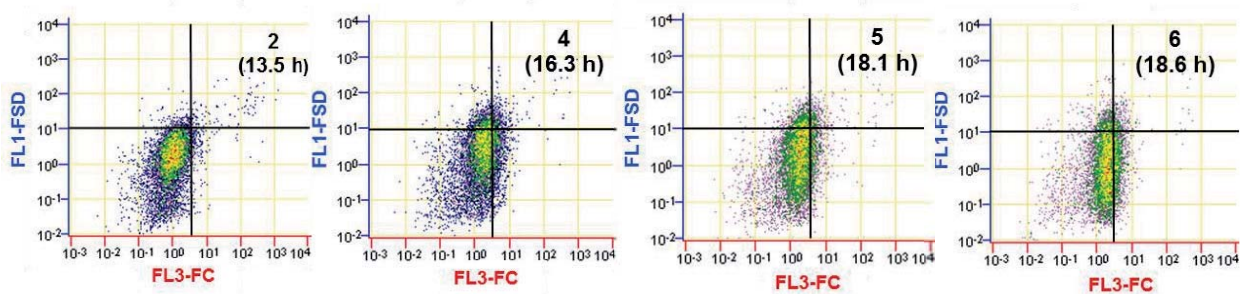


**Figure 37:** Single cell analysis of production intensity at  $\mu$  oscillating fed-batch strategy; *B. megaterium* cells secreting ABFs at different cultivation time points applying a high lysozyme concentration of 0.5 mg/mL. ABF D1.3 scFv producing cells were labeled with detection ABs (AlexaFluor 488) and counter stained with PI. Fluorescence surface density of green fluorescence (FL1-FSD) and fluorescence concentration of red fluorescence (FL3-FC) were determined and displayed in a dot plot.

In the following the possible reasons for an increased secretion of ABF D1.3 scFv coupled to the stationary phase of starvation are summarized.

First it should be taken into account that natural secretion processes are coupled to starvation conditions. Beside other phenomena like competence development and sporulation, the boost in secretion can be regarded as an adaptive mechanism to unfavorable growth conditions [230] making new sources of nutrients available by e. g. secreting enzymes for decomposition. This effect is exploited by numerous bioprocesses for industrial generation of proteases and lipases by *Bacillus* species like *B. subtilis* [231], *B. licheniformis* [232] and *B. clausii* [233]. As shown for the ABF secretion the production of these degradative enzymes also exhibits a specific growth rate and growth phase-dependent behavior in fed-batch processes which cannot solely be explained by different gene expression profiles of particular secreted enzymes. Further global regulating mechanisms must be involved which might also be enhancing the analyzed production and secretion of ABF D1.3 scFv. Probable mechanisms boosting protein secretion in general are illustrated in the following.

During the starvation phases with increased secretion properties the MP is depolarized as no proton motive force is built up due to the lack sufficient energy supply by  $\text{NADH}_2$  as electron donor. Increasing depolarization was directly measured during starvation phase of the applied fed-batch profile by single cell analysis (**Fig. 36**). This depolarization was shown to have a direct effect on the autolysin activity in *B. subtilis* [218, 229]. At exponential growth, secreted protons probably neutralize negative charges in the cell wall, resulting in a relatively low pH value surrounding the protoplast [234]. This acidic pH can inhibit autolysin activity which under normal conditions becomes more active at the outer parts of the cell wall resulting in wall turnover promoting growth processes. In this phase a kind of steady state must exist between energized membrane, wall thickness and wall



turnover [235]. When cells depolarize the proton gradient collapses and the inhibitory effect of the local low pH is abolished. Thereby autolysin activity is enhanced and the cell wall can partially be degraded, thus being loosened and facilitating the release of ABFs as well as other proteins more easily into the supernatant. Supporting these findings, the autolytic enzyme N-acetylmuramoyl-L-alanine amidase CwlB (BMD\_3062 autolysin) was also found in proteomic analysis of secreted proteins of underlying cultivations of *B. megaterium* in the stationary phase (data not shown).

Despite these considerations the Sec translocation pathway may also play a key role in increased secretion during the stationary phase as was shown for *B. subtilis* [236]. Some components of the secretion machinery were shown to be temporarily controlled which resulted in a maximal level of expression in the onset of protein secretion in the early and ongoing stationary growth phase. The increased demand for protein secretion is related to higher *secA* [236], *sipS* and *sipT* transcription levels [103]. The SipS and SipT proteins are responsible for the removal of the signal peptides from non-lipoprotein precursor proteins and are potential rate limiting factors for the secretion process. This cell behavior of boosting protein secretion throughout the stationary phase was exploited in the newly developed cultivation strategy, where online controlled growth phases of cell proliferation were followed by starving phases with increased secretion. The underlying process control was successfully applied, based on a biomass estimation by exhaust gas analysis [237]. Depolarization measurements by single cell analysis, and especially negligible fructose and acetate concentrations showing an optimal carbon substrate uptake and no by-product formation illustrating the general applicability of the underlying method for a robust *B. megaterium* process control.

#### 4.4.3 Up-scale approach

After establishing the oscillating fed-batch control at the lab scale, the strategy was successfully transferred to a pilot plant. For scaling up the process to a 100 L bioreactor several parameters had to be taken into account in advance and thus were adapted. The  $\text{MgSO}_4 \times 7\text{H}_2\text{O}$  concentration was reduced from an optimal concentration of about 2.7 g/L to a concentration of 0.3 g/L. This was necessary due to precipitation of  $\text{MgNH}_4\text{PO}_4$  throughout the process. Therefore  $\text{MgSO}_4 \times 7\text{H}_2\text{O}$  concentration was increased in the feed, where no phosphate was present, and no precipitation occurred. The reduction of Mg ions was probably not that essential for ABF production under these circumstances as it was compensated by the increased  $(\text{NH}_4)_2\text{SO}_4$  concentration as shown in the CCD (section 4.2.4). Besides, the initial fructose concentration was adapted to 2.7 g/L maximizing the number of growth/starvation cycles while simultaneously guaranteeing a sufficient change in  $\text{CO}_2$  exhaust gas to ensure exact biomass estimation at the feed start. For comparable cultivation conditions the lab scale approach previously described was carried out with the same varied parameters as used for the large scale production (section 3.10). The only difference was the maximum specific growth rate at oscillating  $\mu$ -control which was set to 0.4 (1/h) to reach higher cell densities in shorter time periods. This probably led





to lower overall productivities compared to the lab scale process with a maximum growth rate of 0.3 (1/h) (**Tab. 7**). The decrease in production was based on the fact that when applying higher maximal growth rates the starving phases are less pronounced due to possible appearance of overfeeding in the growth phases. However the control strategy itself was most successfully implemented on the large scale. The used control parameters like CER for biomass estimation were not scale dependent and guaranteed a reliable process control.

The applied adaptations clearly illustrated that optimizations being derived from small scale cultivations such as micro titer plates or shaking flasks cannot be directly transferred to a pilot scale using classic methods like keeping the volumetric power input throughout the scaling procedure constant, stressing the fact that when improving a process up to the pilot scale, GMP standards should be considered right from the start of optimization to avoid later process design problems.



## 4.5 Transcriptome analysis

In the previous section it was shown that an increased ABF D1.3 scFv production and secretion was related to the stationary phase under starving conditions. This was exploited by an appropriate process design based on an oscillating fed-batch profile. But what actually happens inside the cells and why under these circumstances an increased ABF production and secretion is favored is yet not fully understood.

Therefore the effect of heterologous production and secretion of ABF D1.3 scFv by *B. megaterium* YYBm1 carrying pEJBmD1.3scFv was investigated on the transcriptome level by using DNA microarray technology. The aim was to uncover potential bottlenecks and limitations of ABF production and secretion providing the basis for a rational strain and process design.

The main goal was to investigate the specific gene expression pattern related to the general effects of ABF production and secretion in the particular growth phases of a batch process. For this approach an appropriate control strain is most important to ensure reliable and meaningful data sets. The *B. megaterium* strain YYBm1 carrying the plasmid p3Stop1623 was used as a control. This plasmid is equal to the ABF expression plasmid pEJBmD1.3scFv but lacks the ABF coding gene.

Both strains were cultivated in biological triplicates and equally treated regarding pre-culture, inoculation, induction with xylose, medium composition and process control. During the cultivation, four time points were chosen for transcriptome sampling. This should give representative insights into gene expression dependencies regarding different growth phases and simultaneously investigating the effects of the heterologous gene expression of ABFs. The first two samples from the exponential phase were set according measured OD values, followed by a sample from the beginning of stationary phase indicated by a sudden increase in DO and a final sample from stationary phase two hours after the previous DO peak. **Figure 38** gives a representative view on the investigated batch cultivations.

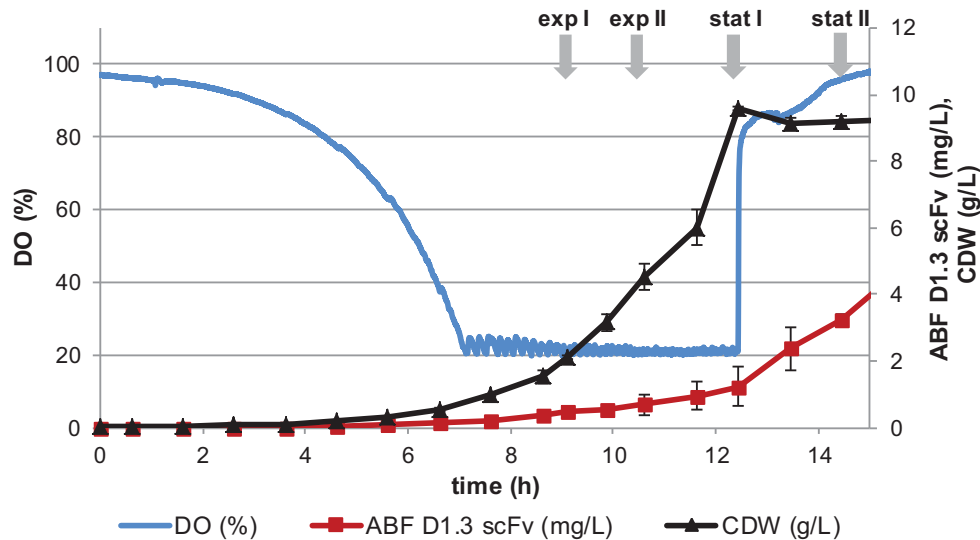


**Figure 38:** Batch experiments of *B. megaterium* YYBm1 (EJBmD1.3scFv) bioreactor cultivations producing and secreting ABF D1.3 scFv (minimal medium (15 g/L fructose), DO control (> 20%)). The ABF concentration was determined by quantitative ELISA. Samples for transcriptome analysis were taken as indicated; data sets are based on biological triplicates.

Based on four sample points each taken from the ABF production strain and the control strain an appropriate transcriptome assay had to be chosen to ensure both, investigations of differentially expressed genes dependent on different growth phases and related to ABF production. Therefore, a one color assay was used to potentially ensure the direct comparison of all samples to determine differentially expressed gene patterns. **Table 8** gives an overview on the matched samples with the particular aim of investigation. These samples were analyzed in detail in the following approach with means of gene cluster analysis according to TIGR role categories [100]. Specific fold changes based on triplicate analysis were illustrated in a heat map analysis either of median values or particular probe intensities. The data analysis was not solely focused on single high regulated genes but furthermore a cluster analysis according to role categories also including less regulated genes was performed. Thereby potential relationships between regulated genes, operon structures and dominant overlapping responses are more likely to be revealed.

**Table 8:** Overview on the matched samples with the particular aim of investigation.

Comparison	Question
Control_exp_I vs. ABF_exp_I Control_exp_II vs. ABF_exp_II Control_stat_I vs. ABF_stat_I Control_stat_II vs. ABF_stat_II	<i>Which genes are differentially expressed in ABF producing cells compared to the control strain independent from the current growth phase? (4.5.1)</i>
ABF_stat_I vs. ABF_stat_II	<i>Which genes are differentially expressed comparing stationary phase I with stationary phase II for ABF producing cells? (4.5.2)</i>
Control_stat_I vs. Control_stat_II	<i>Which genes are differentially expressed comparing stationary phase I with stationary phase II for the control strain? (4.5.2)</i>
Match (ABF_stat_I vs. ABF_stat_II) with (Control_stat_I vs. Control_stat_II)	<i>Which genes are specifically solely up- or down-regulated in the ABF producing strain at transition from stationary phase I to stationary phase II? (4.5.3)</i>

#### 4.5.1 Differential gene expression dependent on recombinant ABF D1.3 scFv production/secretion in *Bacillus megaterium*

The heterologous expression of the *ABF D1.3 scFv* gene was expected to have an effect on the differential gene expression compared to the control strain in *B. megaterium*. To gain a first insight into differential gene expression patterns genes regulated in at least two of the four growth phases investigated were clustered according TIGR role categories. The fold changes cut-off was set at a minimum of 1.75 times for up and down-regulation, respectively.

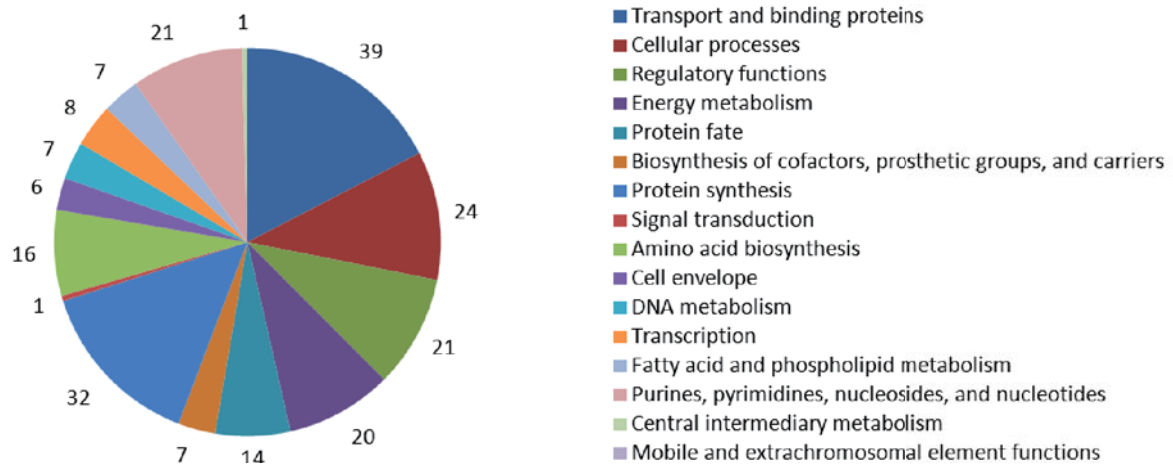


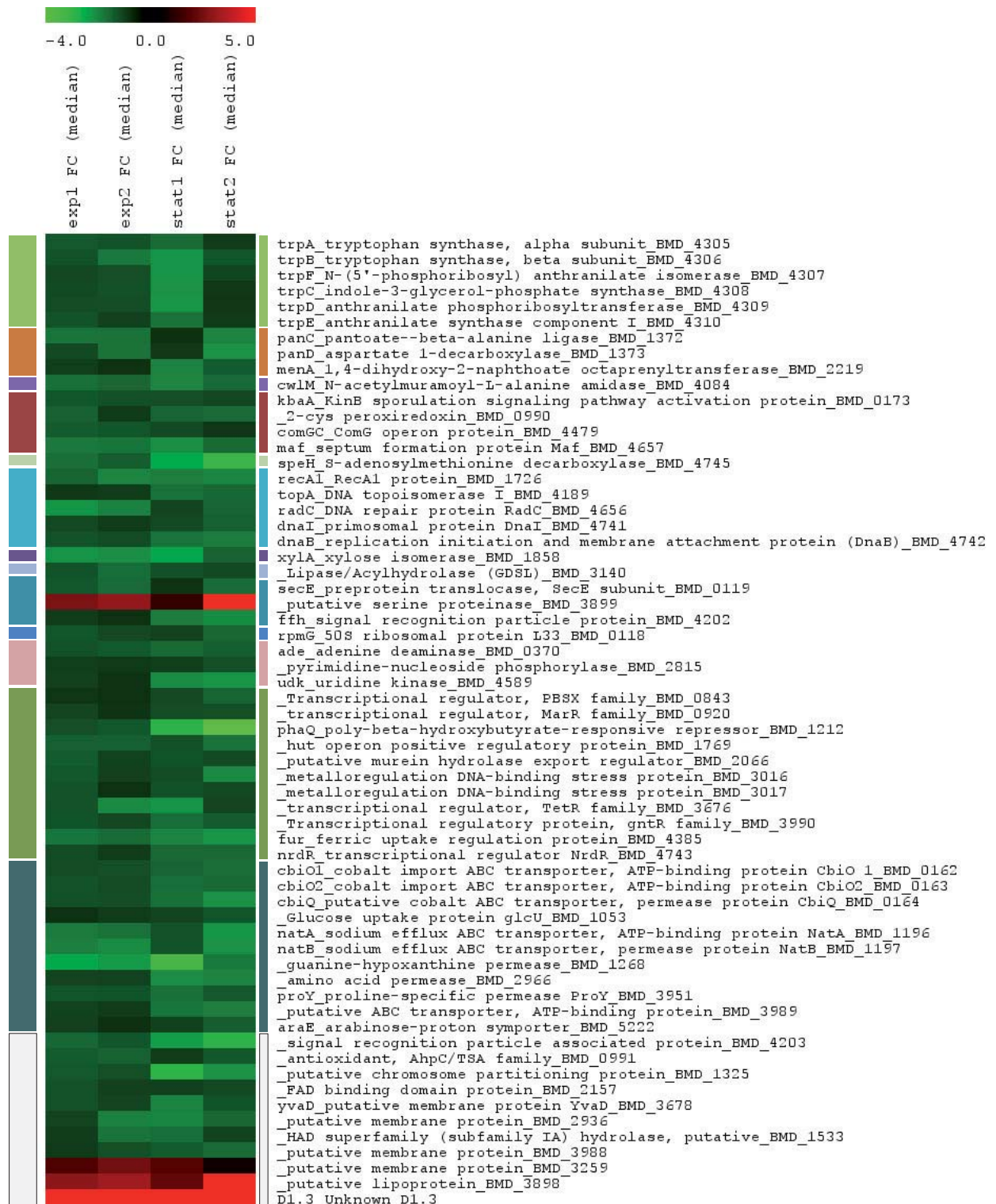
**Figure 39:** Genes regulated in at least two of the four growth phases investigated with a fold change cutoff of minimal 1.75 times up and down-regulation clustered according TIGR role categories.

**Figure 39** illustrates which gene categories are affected by recombinant ABF D1.3 scFv production and secretion by *B. megaterium* throughout the four investigated growth phases. Here, it has to be mentioned that only explicitly identified *B. megaterium* genes were taken into account for the analysis. Regulated genes with just a hypothetical function comprised about 140 possible candidates but were not considered for further investigations.

Most distinctive regulated gene groups were related to transport and binding proteins, cellular processes, protein fate and synthesis, energy metabolism and amino acid synthesis. Especially for the recombinant ABF production, genes related to protein fate may play a predominant role. These are regulated in areas of protein and peptide secretion and trafficking, folding, repair and degradation in particular.

In the following, the most prominent differences in gene expression pattern were taken into account showing regulation throughout all 4 growth phases. Displayed fold changes of at least three times up or down regulated genes were highlighted in particular by a heat map analysis.

At first glance, it is clearly illustrated in **Figure 40** that most differentially expressed genes of the ABF producing strain were down-regulated compared to the control strain lacking heterologous gene expression. Up-regulated genes did encode for at least three putative proteins as well as the ABF D1.3 scFv which was expected to be highly expressed compared to the control. The mRNA coding for the ABF D1.3 scFv was indeed highly up-regulated during all observed growth phases, thus suggesting that biosynthesis of ABFs is not restricted on transcriptional level. Via NCBI conserved domain analysis [238] of underlying putative proteins was carried out [239]. Here the putative lipoprotein BMD\_3898 was found to have high similarities in domain function to the extracellular chaperone *prsA* [240-242] exhibiting potential folding adding functions for ABF secretion.



Amino acid biosynthesis ■; Biosynthesis of cofactors prosthetic groups and carriers ■; Cell envelope ■; Cellular processes ■; Central intermediary metabolism ■; DNA metabolism ■; Energy metabolism ■; Fatty acid and phospholipid metabolism ■; Protein fate ■; Protein biosynthesis ■; Purines, pyrimidines, nucleosides and nucleotides ■; Regulatory functions ■; Transport and binding proteins ■; Hypothetic/putative genes ■

**Figure 40:** Genes regulated in all four samples points at particular growth phases (Control\_strain compared to ABF\_producing\_strain) with a fold change cutoff of minimal 3 times up and down-regulation clustered according TIGR role categories. Fold changes are presented as log<sub>2</sub> (FC) colored data sets of median values of particular samples based on triplicates.





The putative serine proteinase BMD\_3899 was found to possess a PDZ domain [243] of trypsin like serine proteases. This domain is known for the HtrA protein which is involved in heat-shock response, chaperone function and apoptosis and was thereby related to the "protein fate" sub cluster category [244, 245]. A closer look on the domain structure of the putative membrane protein BMD\_3259 revealed regions with a potential protease inhibitory function generally found in the PepsSY superfamily as well as an iron regulation side, respectively [246].

In the following, only the most down-regulated genes are further being discussed in detail. In the amino acid synthesis cluster, the operon encoding for the tryptophan biosynthesis was shown to be most decreased. From *B. subtilis* the translation of the tryptophan operon is known to be regulated by its own mRNA [247]. Genes related to cofactor synthesis of vitamin K<sub>2</sub> (*menA*, menaquinone) and coenzym A (*panC*, *panD*, pantothenate) were also shown to have diminished mRNA expression levels. Furthermore, the expression of the genes encoding for the enzyme CwlM N-acetylmuramoyl-L-alanine amidase (BMD\_4084, EC: 3.5.1.28) and a putative murein hydrolase export regulator (BMD\_2066) which is in charge of controlling the CwlM export itself were also reduced throughout all growth phases. The main function of CwlM is to hydrolyse the link between N-acetylmuramoyl residues and L-amino acid residues in certain cell-wall glycopeptides [248]. Besides the gene expression related to cellular processes like competence (*comGC*) and septum formation for cell division (*maf*) were also down-regulated under heterologous ABF gene expression. The regulation of the competence-associated *comK* gene was shown to also be related to the regulation of the *radC* gene. It probably encodes for a DNA repair protein which was also down-regulated in this case [249]. In terms of transport related proteins the guanine-hypoxanthine permease revealed distinct regulation patterns. The enzymes' functions include transportation of various substrates such as xanthine, uracil, and vitamin C.

Some of the regulated genes could be directly correlated to the secretion process itself. Here, down-regulation of the *secE* gene coding for a preprotein translocase as a part of the Sec-pathway, the signal recognition particle protein Ffh (BMD\_4202) and its associated protein (BMD\_4203) could be detected. This is quite interesting as they display very important parts of the pre-secretory protein translocation and the secretion process as possible bottlenecks for an efficient ABF secretion [250].

#### 4.5.2 Growth phase dependent gene expression

From cultivation data it was previously observed that production and secretion of ABFs were increased during the stationary phase (**Fig. 38**, section 4.4.1). Therefore changes in gene expression patterns on the transition to the stationary phase may provide a deeper understanding of ongoing processes inside the cell which may favor higher secretion intensities in the end. Here differential gene expression was determined between the first and the second stationary phase samples. These differential expression patterns from the ABF producing strain were opposed to regulated genes from the control strain. Thereby





two main clusters of differentially expressed genes at the transition from stationary phase I to stationary phase II became observable (**Fig. 41**). Some genes were regulated in both the control and ABF producing strain, whilst others were only regulated in case of ABF producing strain. Differential gene expression from the control strain was only mildly observable and thus not further considered.

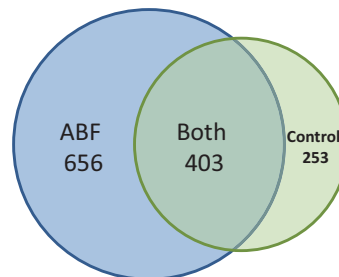


**Figure 41:** Number of genes with a differential gene expression profile from stat I to stat II for recombinant ABF producing strain and for the control strain with a fold change cutoff of minimal 1.75 times up- and down-regulation.

At first genes that were regulated in both strains were analyzed as their expression pattern was independent from heterologous ABF production. These data sets may give a more general overview about which genes changed in their expression pattern during the transition from stationary phase I to stationary phase II. However the effects seen may also favor the production and secretion of ABF in an unspecific way by activation of the general stress response caused by starving conditions and redirected amino acid supply.

All genes with a fold change of minimal 1.75 times up- and down-regulation were further used for cluster analysis according to TIGR role categories (**Fig. 42**). The main classes of transport and binding proteins, energy metabolism and protein synthesis showed a distinctive number of regulated genes involved in the adaptation to stationary growth conditions. To drive more explicit conclusions, a closer look at differentially expressed genes with minimal fold changes of 3 were taken into account and data was illustrated as a heat map analysis (**Fig. 43**). Here, all three hybridized probes for each gene are presented and give a more detailed view on experimental data sets. At first glance, it was obvious that under ABF producing conditions the affected genes were rather down-regulated in comparison to the control strain. This may be due to the additional stress which occurs during recombinant ABF production and secretion leading to a more pronounced response for particular gene expression patterns which are related to nutrient depletion and amino acid availability. These possibly stress-activated genes as well as some other differentially expressed genes are being explained in more detail in the next paragraphs and being put in context with already published data sets from *B. subtilis*.

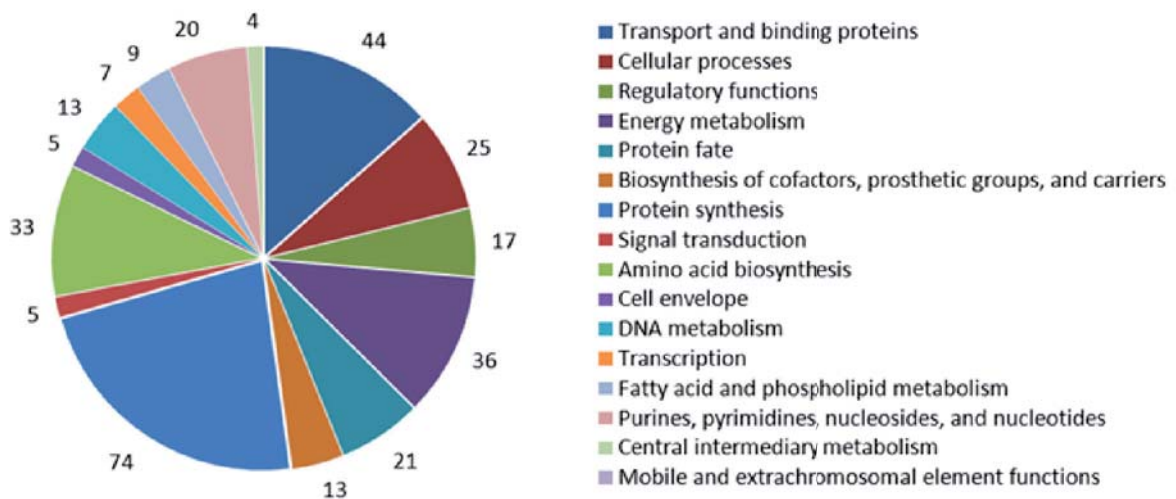
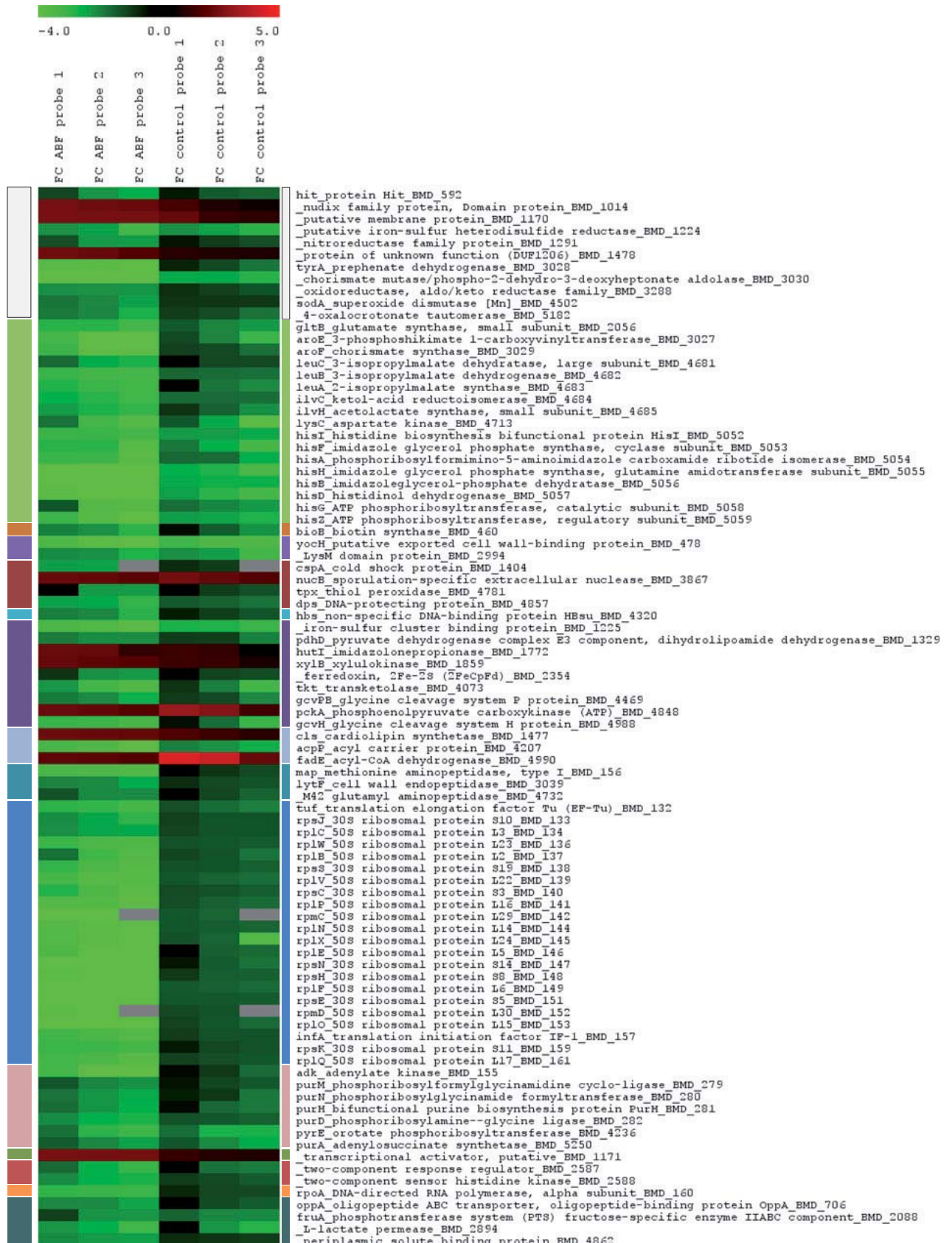


**Figure 42:** Genes regulated comparing first and secondary stationary phase in both ABF producing and the control strain. All genes with a fold change of minimal 1.75 times up- and down-regulation are considered and clustered according to TIGR role categories.

At a functional genomics approach of *B. subtilis* [251] it was shown on proteome and transcriptome level that differentially expressed genes during the transition to the stationary phase are related to the so-called “stringent response”. This is a stress response which occurs due to different types of limitations related to amino-acid starvation, fatty acid limitation [252], iron limitation [253], heat shock [254] and other stress conditions. Here it was shown that genes related to growing cells were switched off and adaptive responses to nutrient starvation like an increased protein turnover [255] were induced. In this case of stationary *B. megaterium* cells some genes which were related to protein modifications (*map*), nucleotide metabolism (*adk*), energy metabolism (*pdhD*) and protein biosynthesis (*infA*, *tuf*, *rpl* (50S), *rpm* (50S) and *rps* (30S)) were equally down-regulated as shown before for the stringent response of *B. subtilis* [251].





Hypothetic putative genes ■; Amino acid biosynthesis ■; Biosynthesis of cofactors, prosthetic groups and carriers ■; Cell envelope ■; Cellular processes ■; DNA metabolism ■; Energy metabolism ■; Fatty acid and phospholipid metabolism ■; Protein fate ■; Protein biosynthesis ■; Purines, pyrimidines, nucleosides and nucleotides ■; Regulatory functions ■; Signaltransduction ■; Transcription ■; Transport and binding proteins ■

**Figure 43:** Genes regulated during transition from stationary phase I to stationary phase II for both the ABF producing strain and the control strain with a fold change cut-off of minimal 3 times up- and down-regulation and clustered according to TIGR role categories. Fold changes are presented as  $\log_2$  (FC) data of particular probes.

Another approach of *B. subtilis* transcriptome and proteome analysis from Mader et al. (2002) [256] could demonstrate that the particular amino acid availability has a distinctive effect on the actual gene expression patterns. The addition of amino acids was responsible for the downregulation of certain genes. In case of *B. megaterium* cells switching to the stationary phase the same regulatory principles may take place as the metabolism changes from a carbon source supply of fructose to an amino acid supply based on proteolytic products provided from the surrounding medium. Similar patterns of down-regulated gene expression as already reported for *B. subtilis* were shown for genes related to amino acid biosynthesis (*aroE*, *aroF*, *hisA*, *hisB*, *hisD*, *hisF*, *hisG*, *hisH*, *hisI*, *hisZ*, *ilvC*, *ilvH*, *leuA*, *leuB*, *leuC*, *lysC*) and energy metabolism (*gcvPB*, *gcvH*).

The up-regulation of certain genes like *nucB* encoding for an extracellular nuclease and *cIs* encoding for a cardiolipin synthetase again illustrate the adaptation of the microorganism towards starving conditions and resulting changes in membrane compositions.

#### 4.5.3 Growth phase dependent gene expression related to recombinant ABF D1.3 scFv production

The next step was to compare specifically regulated genes from the ABF D1.3 scFv production strain during the transition from stationary phase I to stationary phase II. By categorizing the different expression patterns into TIGR role functions (**Fig. 44**) it was apparent that most regulated genes belonged to the groups of proteins involved in transport mechanisms, protein binding, cellular processes and energy metabolism. For the heat map analysis only genes which were at least 3 times up- or down-regulated were taken into account (**Fig. 45**). As the ABF production and secretion can be regarded as an additional stress factor during the stationary phase it may be assumed that some genes are related to a more distinctive stringent response. A closer look at the regulation patterns revealed additional down-regulation of ribosomal genes (*rpl* (50S), *rps* (30S), *rpm* (50S)) and genes related to protein synthesis (*fusA*).



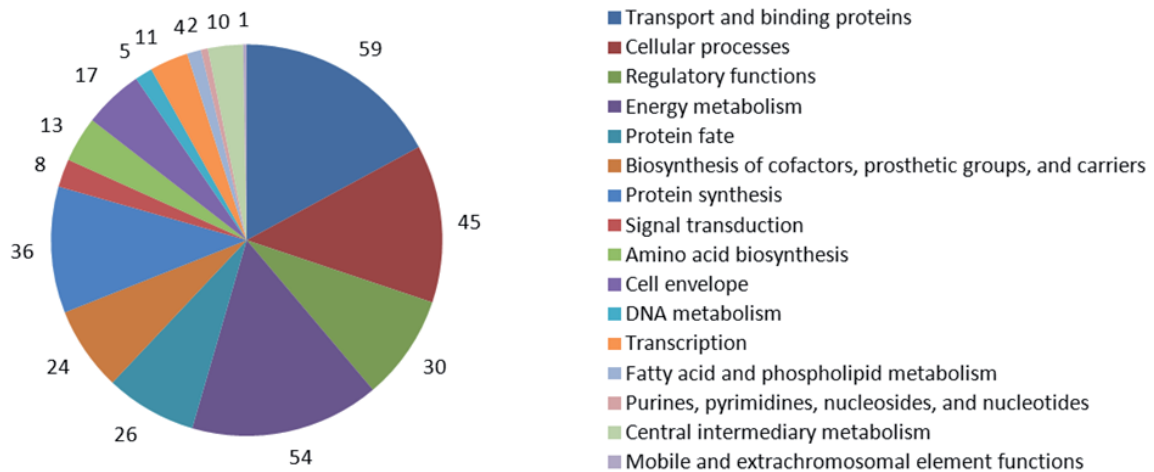
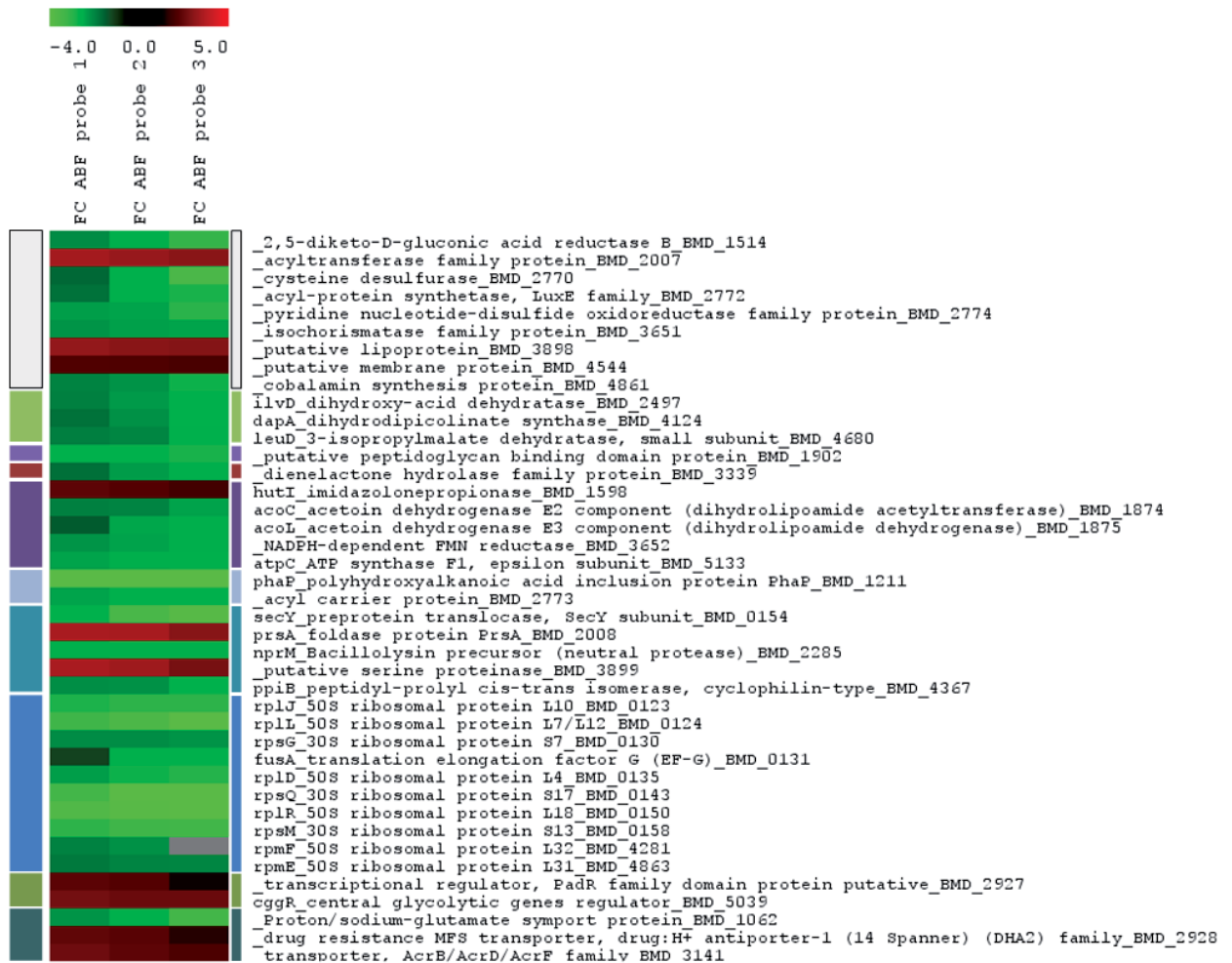


**Figure 44:** Genes regulated comparing first and second stationary phase solely at ABF producing strain. All genes with a fold change of minimal 1.75 times up and down-regulation are considered.

Most important for a sufficiently increased secretion of ABFs may be the up-regulation of certain genes encoding for proteins related to protein fate as discussed before. Here, PrsA can be regarded as a key component for secretion and functional folding of ABFs. Another gene encoding for the putative lipoprotein BMD\_3898 was also shown to be up-regulated during the stationary phase. A closer look at the potential domain structure of the BMD\_3898 gene revealed PrsA similar function. Therefore it can also be regarded as a helper protein for more efficient secretion of ABFs. Quite interestingly the gene encoding BMD\_3898 was also found to be up-regulated in all growth phases compared to the control strain (**Fig. 40**). Another up-regulated gene encodes for the putative serine proteinase BMD\_3899 which is also known to be regulated throughout all growth phases (**Fig. 40**). Here the domain analysis revealed similarities to the *htrA* gene, which encodes for a protein having both chaperone and protease functions [245]. HtrA was shown to act as a chaperone at low temperatures refolding misfolded proteins and as a protease at elevated temperatures [244]. Furthermore HtrA is usually responsible for the decomposition of unfolded, damaged or abnormal membrane or secreted recombinant proteins [257] which might be also true in case of increased ABF production and accumulation. The *secY* gene which encodes for a main component of secretory SecA pathway however is down-regulated also known in context of the stringent response [251]. Another interestingly down-regulated gene is *ppiB* coding for a peptidyl-prolyl cis-trans isomerase. This protein displays potential chaperone functions of the cyclophilin-type, was shown to catalyze protein folding *in vitro* and was found to be necessary for cell viability under starvation conditions [258].



Hypothetic putative genes ■; Amino acid biosynthesis ■; Cell envelope ■; Cellular processes ■; Energy metabolism ■; Fatty acid and phospholipid metabolism ■; Protein fate ■; Protein biosynthesis ■; Regulatory functions ■; Transport and binding proteins ■.

**Figure 45:** Genes regulated at transition from stat I to stat II solely for the ABF D1.3 scFv producing strain with a fold change cutoff of minimum 3 times up and down-regulation and clustered according to TIGR role categories. Fold changes are presented as log<sub>2</sub> (FC) data of particular probes.

#### 4.5.4 Summary

The underlying transcriptome analysis revealed a detailed fingerprint of changes in gene expression patterns of *B. megaterium* cells depending on particular growth phases and under ABF D1.3 scFv producing and secreting conditions. In both approaches distinctive genes were found to be regulated thus providing new ideas for rational process and strain optimization which are further being explained in the following paragraphs.

At the first glance, genes found to be regulated at ABF D1.3 scFv producing cells may be seen as a cell response towards an increased secretion stress. However, particular regulation of genes might not necessarily be a primary effect of heterologous gene expression of ABFs. It can also be a secondary effect caused by ABF production somehow limiting or even inhibiting its own production. For instance an increased



secretion of the ABF may be related to a higher amount of miss-folded proteins causing a higher cell membrane and cell wall associated protease activity. It is possible that certain feedback mechanisms may be in place to avoid overproduction of heterologous secreted proteins and to redirect energy and nutrient resources rather towards cell growth than towards production. This might explain genes being down-regulated at ABF producing cells related to secretion, cell wall hydrolysis and amino acid supply. These genes in particular may display important bottlenecks for the ABF production as they directly interfere with the production, secretion and the release process of ABFs.

For *E. coli* fed-batch production of recombinant proteins it was postulated that overproduction of heterologous proteins also results in the induction of the stringent response as an effect of carbon/energy or precursor limitation [259]. A general down-regulation of rRNA synthesis was observed which is also true for other production systems [260]. Cells were shown to rather degrade ribosomes thereby obtaining building blocks and energy than to degrade the product.

Besides at higher synthesis rates of ABFs, e. g. at exponential growth, it is more likely that the actual folding reaction is limited by the insufficient supply of folding supporting helper proteins like foldases or chaperones. Therefore a rational strain improvement by genetic optimization strategies can be done by coexpression of particular genes on appropriate plasmids under the control of e. g. the xylose inducible promotor system or genome based knock out of certain genes by homologue recombination based techniques [166].



**Figure 46** gives an overview on possible target sites for genetic optimization of production and secretion by gene coexpression (+) and/or deletion (-) which are illustrated in detail as follows.

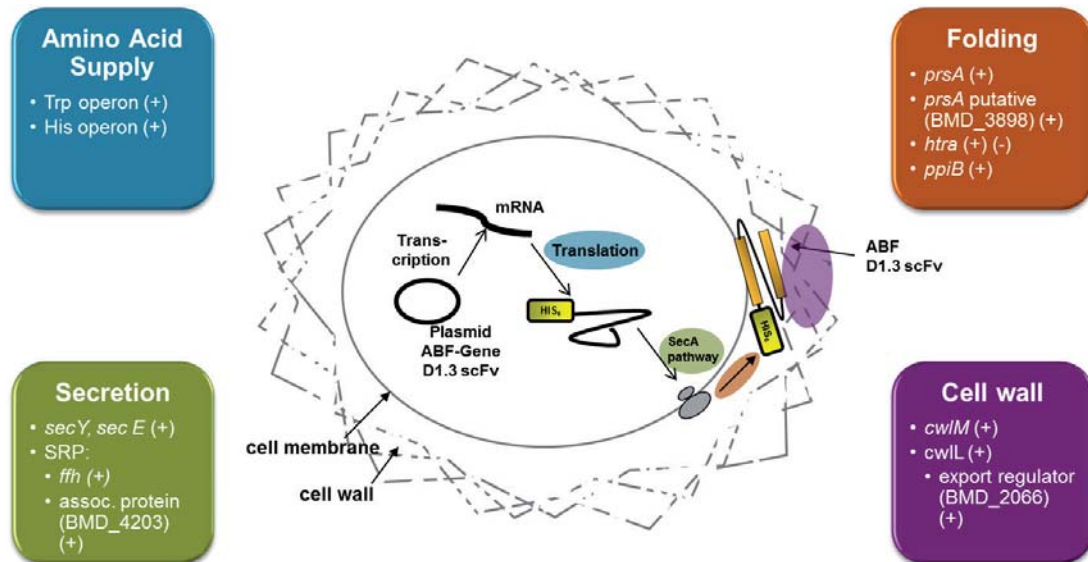


**Figure 46:** Potential targets sites for genetic optimization of *B. megaterium* producing recombinant ABFs by gene coexpression (+) and/or deletion (-).

The building process of fully functional ABFs demands several essential production steps displaying possible genetic target sites for rational strain improvement. Starting at protein synthesis and translation of mRNA the sufficient supply of amino acids may play an important role for efficient ABF peptide generation. Therefore a coexpression of genes from the histidine or the tryptophan pathway which were down-regulated may increase ABF propeptide generation. Additionally specific amino acids could be included into the cultivation medium. As a second step the generated peptide is guided to the membrane associated secretion apparatus by the help of signal recognition complexes (SRP). Here the *fhh* gene coding for a SRP protein and another gene coding for an SRP associated protein (BMD\_4203) were shown to be down-regulated and therefore provide also potential targets for particular coexpression. Similar strategies were shown to be effective for enhancing heterologous protein secretion in *E. coli* cells [261]. In a third step, the peptide is secreted through the cell membrane mediated by the Sec apparatus. Interestingly, the proteins encoded by *secE* and *secY* genes being some of the most important parts of the secretion machinery were shown to be decreased in case of ABF producing cells which may be related to a feedback control to decrease exceeding secretion. Therefore they also display a potential target for further strain optimization by increased coexpression. After release of the ABF peptide through the Sec-pathway, a fourth step of functional protein folding is most important. Proteins with chaperone and foldase functions



which are related to extracellular protein folding may play a key role for sufficient ABF secretion. Potential candidates of this gene class were differentially increased through all phases (putative *prsA* BMD\_3898) and especially up-regulated during stationary phase (*prsA*). The PrsA foldase protein was already shown to have a positive effect on recombinant protein secretion in *B. subtilis* before [262, 263]. The potential *htra* gene encoding BMD\_3899 was also differentially up-regulated. Its possible functions comprise both protease and foldase properties. Here, both strategies of coexpression and gene knock out may lead to a successful increase of ABF secretion. As a last step the functional folded ABF has to be released through the cell wall which may function as barrier. This problem may be overcome by loosening the cell wall structure by coexpression autolysin genes. These were already shown to be activated during stationary phase potentially favoring an alleviated release of ABFs [218, 229]. Here, *cwIM* and *cwIL* combined with a gene encoding for the export regulator BMD\_2066 under the control of a weak promoter to avoid cell lysis are possible candidates.

Modifications of these targets sites may lead to overall higher growth associated productivities comparable to the stationary phase. Additionally, the productivity may be further increased as the drawbacks of the stationary phase which were related to carbon source depletion, insufficient nutrient supply and a predominant stringent response have not to be taken into account during the exponential phase of unlimited growth.

## 4.6 Culture heterogeneity

Heterogeneities in bacterial populations may arise due to a variety of reasons (section 2.2.3). In general changes in environmental conditions trigger distinctive stress responses which are forcing bacterial cells to differentiate. Here the development of subpopulations can be regarded as an evolutionary mechanism to cope with challenging conditions.

In the following, two examples for population dynamics of *B. megaterium* cells producing ABF D1.3 scFv are presented. In the first case heterologous ABF production was induced at a late cultivation time point causing a stress response leading to the development of distinct cell populations. In a second example a batch cultivation was carried out with a high carbon source concentration also promoting a separation into subpopulations.

### 4.6.1 Late induction of ABF D1.3 scFv production

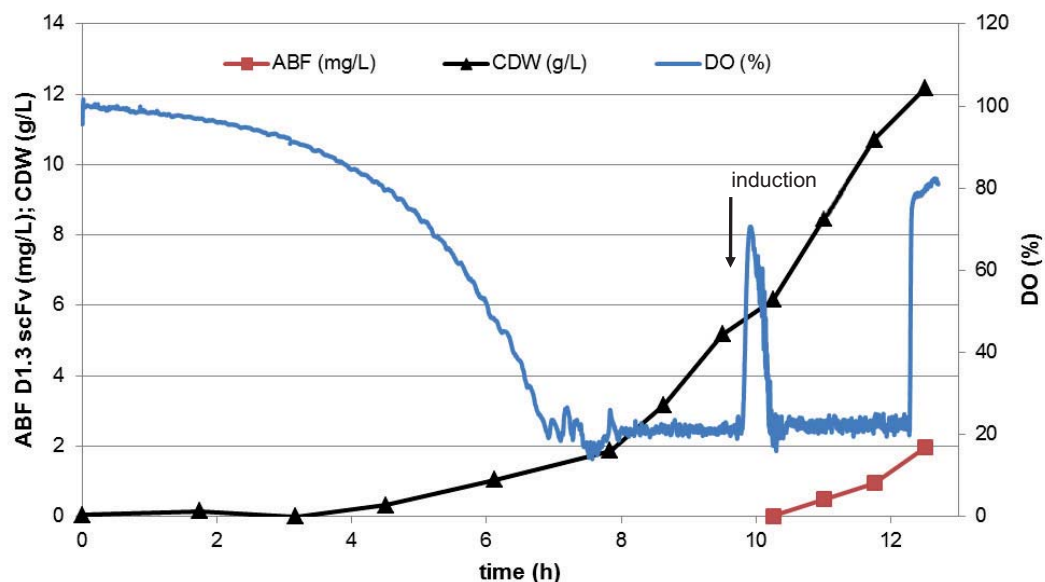


**Figure 47:** Batch cultivation, *B. megaterium* YYBm1 (pEJBmD1.3scFv), bioreactor (1L, DO > 20%, pH 6.3, 15 g/L fructose), late induction.

The underlying bioprocess was carried out with the previously used minimal medium for batch cultivation under controlled DO and pH process conditions. The heterologous ABF D1.3 scFv production was induced by adding 0.5% xylose 9.5 h after inoculation. Shortly after induction a sudden increase in DO (**Fig. 47**) was detectable paralleled by a decrease in OUR and CER (**Fig. 48 B**). The RQ value increased indicating an overflow metabolism in this case linked to enhanced acetate accumulation (**Fig. 48 B, C**). Right after the DO peak detectable amounts of functional ABF D1.3 scFv could be measured in the superna-



tant (**Fig. 47**). Starting from these data only rough assumptions can be made that induction of ABF production at late time points leads to some kind of disturbance in cell growth also reflected by whole cell culture parameters of DO, CER and OUR measurements. What actually happened on the single cell level is so far unknown. Therefore FCM analysis was done for particular time points (**Fig. 48, A-E**) using the previously developed protocols for MP (section 4.3.1) and production intensity estimation (section 4.3.3) to gain deeper insights on single cell level.

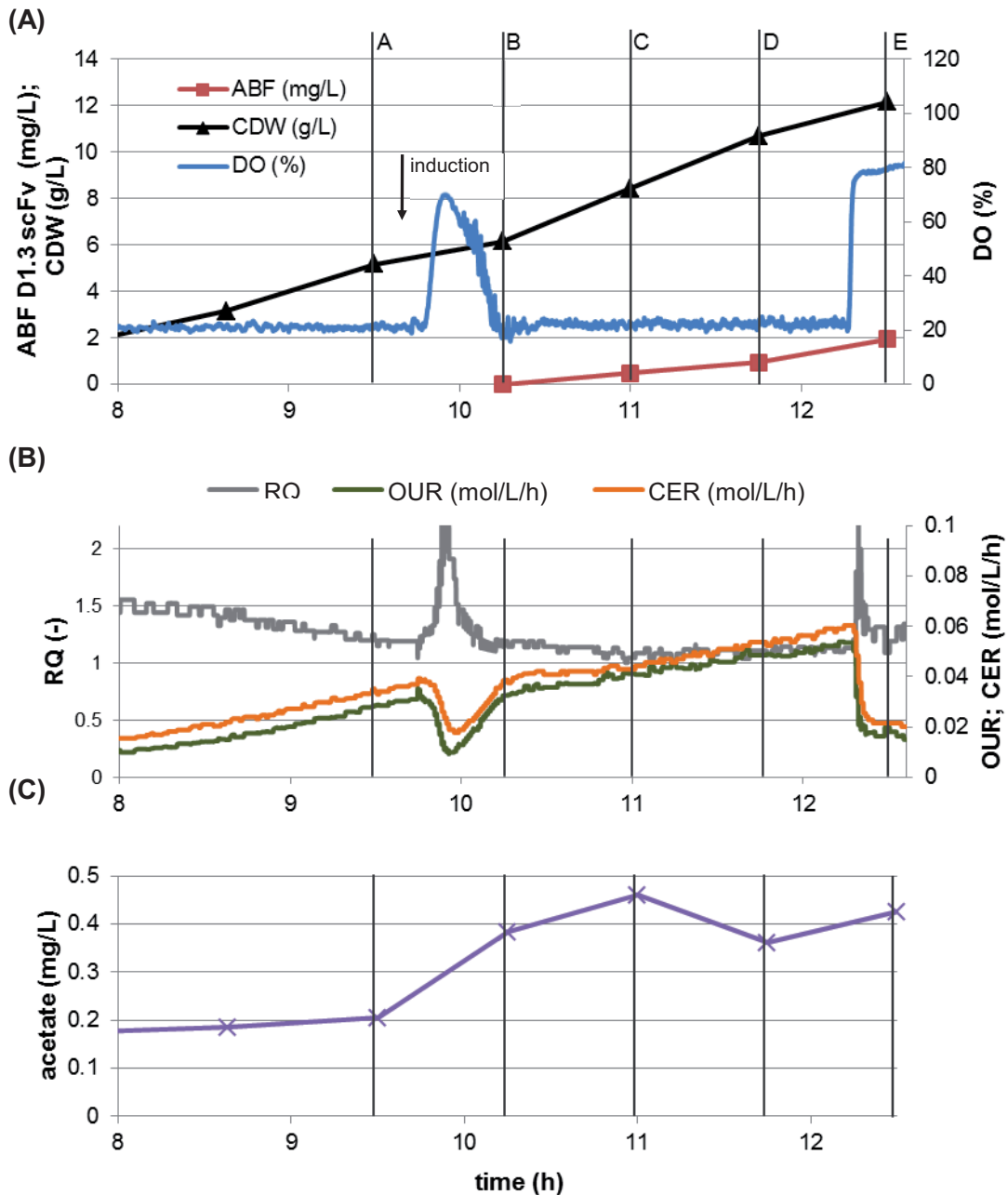


**Figure 48:** Batch cultivation, *B. megaterium* YYBm1 (EJBmD1.3scFv) bioreactor (1L, DO > 20%, pH 6.3, 15 g/L fructose), late induction. **(A)** Sample time points for FCM analysis, **(B)** OUR, CER, RQ, **(C)** acetate accumulation.

Analysis of FCM data was done with R software tools for population analysis (section 3.21). Particular data sets are summarized by presenting cluster proportions, statistics of outliers and uncertainty median and mean values of fluorescence data.

At the first measured time point (**Fig. 49, A\_MP**) the cells were in a highly polarized state of an exponential growing culture indicated by a high red fluorescence with a mean value of 423.2 (**Tab. 9**). Right after induction the homogenous population splitted into diverse subpopulations characterized by four different clusters. Here the main cluster 1 of 42.8% remained highly polarized ( $FL3_{mean}$ : 459.8, **Tab. 9**) whereas the two others (cluster 2, 3;  $\Sigma$  38%; **Tab. 9**) showed a decrease in red fluorescence indicating depolarization of these cells. This decrease of MP was at least coupled to a reduction of metabolic cell activity which again was related to a reduced  $O_2$  consumption. This explains the increase in DO as agitation and aeration cultivation parameters remained constant. Quite interestingly the fourth cluster containing 19.3% of cells even showed an increase in polarization ( $FL3_{mean}$ : 512; **Tab. 9**) compared to the cells from the first sample (**Fig. 49, A\_MP**). Although the process parameters of DO, CER and OUR were again restored at the third time point (**Fig. 49, C\_MP**) distinctive population heterogeneities concerning MP on single cell level still remained present. Here a small proportion of only 13.3% of cells was still in a high polarization status represented by cluster 3. A variety of four other clusters showed decreased MP down to a red fluorescence less than 160 of up to 30% of cells (cluster 1, 5; **Tab. 9**).

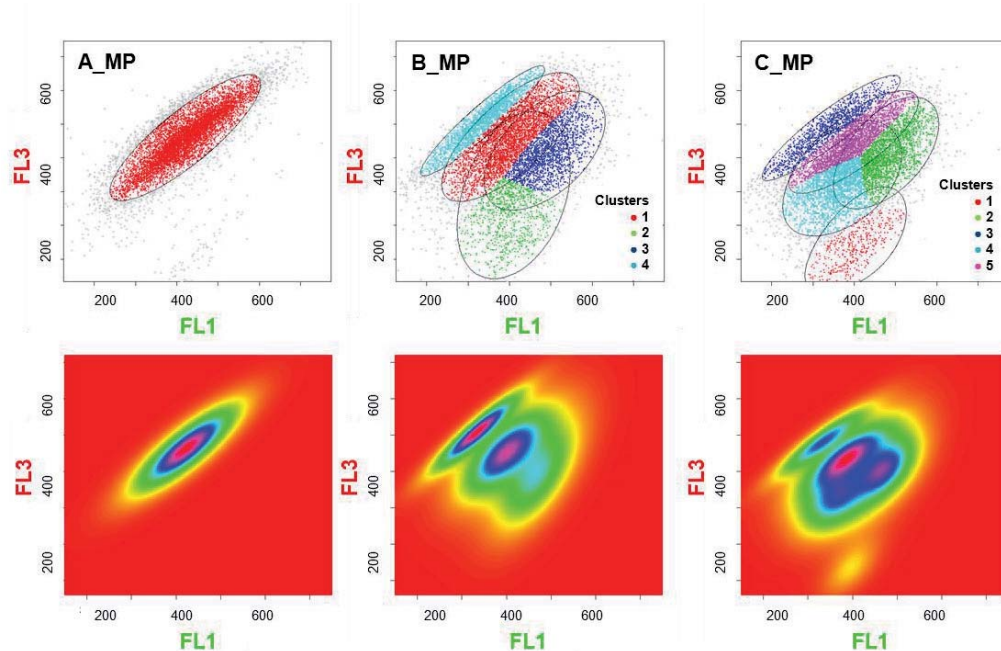


**Figure 49:** Population and cluster analysis of MP measurements with R statistic tools at different sample points (A, B, C); upper row: dot plot image of predicted clusters, lower row: density plots based on previous cluster analysis.



**Table 9:** Data collection of cluster analysis of MP assay (sample A, B, C): particular proportions, mean values of FL1, FL3 measurements and statistics of outliers and uncertainty median and mean values of clustered data sets.

	number of clusters	proportions (%)	mean FL1	mean FL3	outliniers (%)	statistics; uncertainty	
						median	mean
<b>A-MP</b>	1	100.0	423.2	461.8	14.12	0.00	0.00
<b>B-MP</b>	1	42.8	402.1	459.8	6.11	0.19	0.23
	2	12.9	397.5	230.9			
	3	24.9	495.4	416.1			
	4	19.3	334.6	512.0			
<b>C-MP</b>	1	4.9	402.7	135.9	5.65	0.27	0.29
	2	27.1	485.5	412.6			
	3	13.3	336.1	487.0			
	4	29.0	354.0	307.0			
	5	25.7	375.0	161.4			

At the fourth sample point (**Fig. 50, D\_MP**) cells somehow synchronized back to a homogenous population with high MP of polarized cells. Subsequently after fructose depletion, indicated by a sudden DO increase (**Fig. 48**) the cells depolarized which is verified by a distinctive population shift towards less red fluorescence at sample point E (**Fig. 50, E\_MP**).

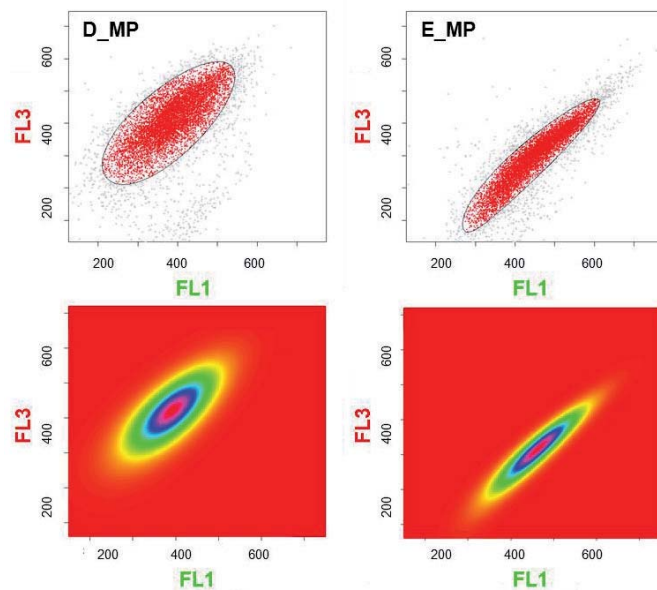


**Figure 50:** Population and cluster analysis of MP measurements with R statistic tools at different sample points (D, E); upper row: dot plot image of predicted clusters, lower row: density plots based on previous cluster analysis.



**Table 10:** Data collection of cluster analysis of MP assay (sample D and E): particular proportions, mean values of FL1, FL3 measurements and statistics of outliers and uncertainty median and mean values of clustered data sets.

	number of clusters	proportions (%)	mean FL1	mean FL3	outliners (%)	statistics; uncertainty	
						median	mean
D-MP	1	100.0	387.1	415.2	12.10	0.00	0.00
E-MP	1	100.0	550.1	399.5	11.53	0.00	0.00

Besides the presented MP estimations the underlying production intensities on single cell level were determined as well. Therefore the developed Alexa Fluor based detection assay (section 4.3.3) was performed and a subsequent cluster analysis by R statistic tools was done. Here an increase in green fluorescence directly correlates to a higher production status of cells as described before. For sample A low fluorescence properties were measured as it was expected for non-induced cells. As soon as the heterologous gene expression of ABF D1.3 scFv is induced the cells differentiate into four overlapping clusters of higher fluorescence corresponding to increased ABF production/secretion intensities (**Fig. 51, B\_ABf**). As indicated by the density plot two main regions of highly productive (cluster 4,  $FL1_{mean}$ : 359.8, 25.4%; **Tab. 11**) and less productive cells ( $\sum$  cluster 1, 2, 3; 75%; **Tab. 11**) become observable. At the next sample point (**Fig. 51, C\_ABf**) the cluster analysis revealed five different cluster regions. Here up to 41.2% ( $\sum$  cluster 1, 2; **Tab. 11**) of the cells showed increased ABF production intensities indicated by a gain in FL1 fluorescence mean values. Other clusters (cluster 3-5; **Fig. 51**) demonstrated less intensive productivity properties.

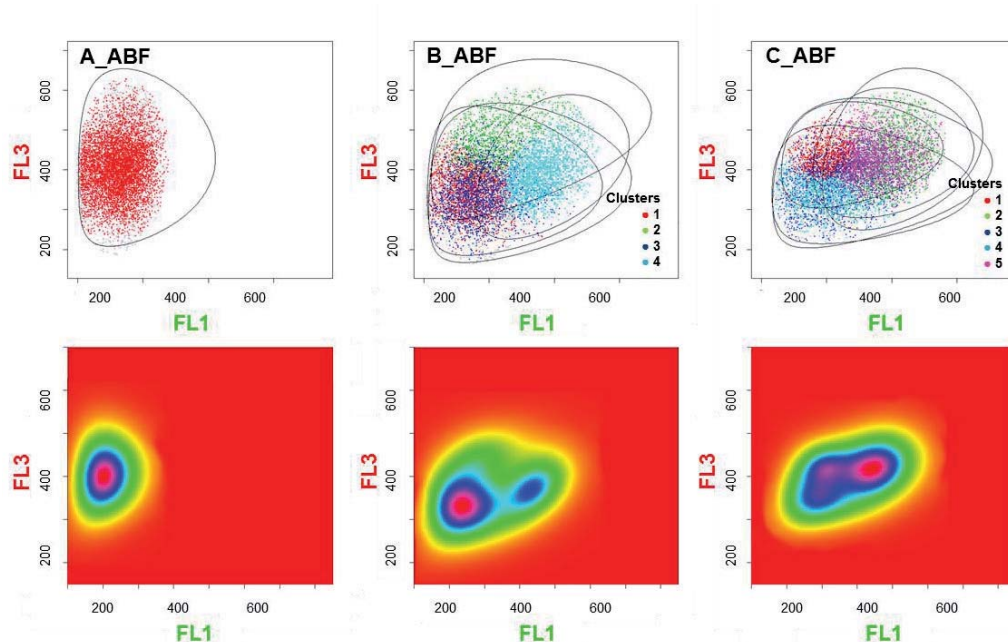


**Figure 51:** Population and cluster analysis of the production intensity assay with R statistic tools at different sample points (A, B, C); upper row: dot plot image of predicted clusters, lower row: density plots based on previous cluster analysis.





**Table 11:** Data collection of cluster analysis of production intensity assay (sample A to C): particular proportions, mean values of FL1, FL3 measurements and statistics of outliers and uncertainty median and mean values of clustered data sets.

	number of clusters	proportions %	mean FL1	mean FL3	outliners (%)	statistics; uncertainty median	mean
A-ABF	1	100.0	49.0	518.5	7.13	0.00	0.00
B-ABF	1	31.4	141.4	446.9	5.16	0.24	0.27
	2	18.2	223.8	576.7			
	3	24.9	179.9	437.5			
	4	25.4	359.8	490.7			
C-ABF	1	20.1	402.7	135.9	3.94	0.31	0.32
	2	21.1	485.5	412.6			
	3	19.2	336.1	487.0			
	4	16.3	354.0	307.0			
	5	23.3	375.0	161.4			

Sample points D and E each revealed two clusters for production intensities as presented in both dot plots and density plots analysis (**Fig. 52**, D\_ABf, E\_ABf). Half of the cells showed less production and the other half increased production intensities as presented in **Table 12**.

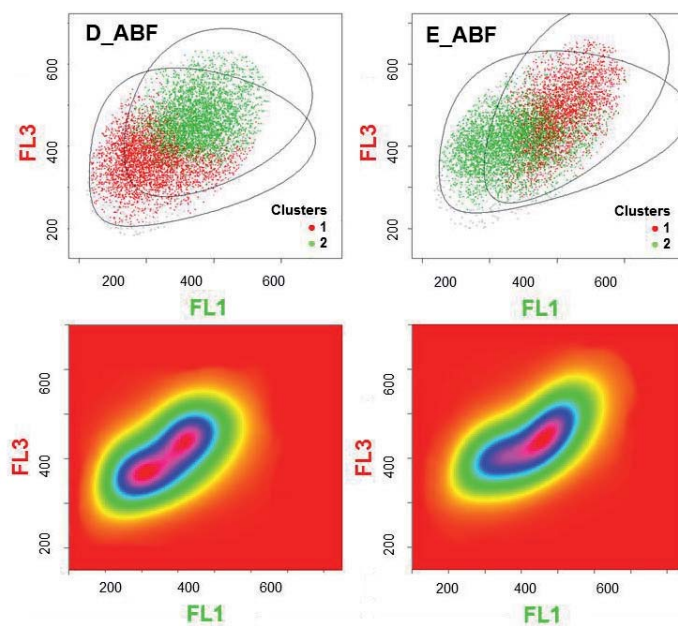


**Figure 52:** Population and cluster analysis of production intensity assay with R statistic tools at different sample points (D, E); upper row: dot plot image of predicted clusters, lower row: density plots based on previous cluster analysis.

**Table 12:** Data collection of cluster analysis of production intensity assay (sample D and E): particular proportions, mean values of FL1, FL3 measurements and statistics of outliers and uncertainty median and mean values of clustered data sets.

	number of clusters	proportions %	mean FL1	mean FL3	outliniers (%)	statistics; uncertainty median	mean
D-ABF	1	53.5	154.2	478.5	5.50	0.11	0.16
	2	46.5	376.1	593.8			
E-ABF	1	49.0	172.5	503.5	5.54	0.11	0.16
	2	51.0	340.0	522.7			

At both measurements of MP and ABF D1.3 scFv production intensities a highly dynamic process of heterogeneity development of late induced ABF producing *B. megaterium* becomes observable. A certain differentiation into several subpopulation right after induction was followed by a synchronization to a single (MP) or double population (production intensities) respectively. Quite interestingly these effects were observable on both levels of MP and production status of cells highlighting a certain correlation between both parameters. As indicated by some colored examples in **Table 13** cluster proportions from particular assays may directly be related. As an example at sample point B the proportion of 42.83% polarized cells is comparable to the 31.45% of less productive cells (dark blue shaded). Right after induction probably not all cells immediately start to produce and secrete ABFs but remain in the metabolic state of exponentially dividing cells as measured at the sample point before (A\_MP). The sudden induction of heterologous ABF production and secretion may be directly related to a certain stress response being coupled to the MP. It is known that the synthesis of foreign proteins at high concentrations exerts a severe metabolic stress on the host cell [148]. The consumption of essential substrates (e. g. carbohydrates, amino acids) and energy is redirected from normal cellular functions, resulting in a transient reduction of the cells' energy status directly related to the current MP. Therefore clusters of higher production intensity may relate to clusters with reduced MP as indicated by red colors in **Table 13**. The proportion of cells with a highly increased MP of 19% may be associated with cells producing acetate as an overflow metabolite. Besides metabolizing fructose as a carbon source through the citric acid cycle further NADH and ATP may be generated by acetate generation through overflow metabolism. The gain in NADH may directly favor higher polarization states of the cell membrane.

Sandén et al. (2002) proposed two different mechanisms leading to an increased acetate accumulation after induction of heterologous proteins at high growth rates [259]. 1) The produced heterologous protein deviates from the mean amino acid composition of the host proteins. Therefore after induction a distinctive amount of some amino acids is less needed, leading to a redirection of the flux to the formation of acetic acid. 2) Another mechanism might be a general imbalance of mRNA, protein synthesis and metabolite production after induction leading to a temporary block of the citric acid cycle resulting in an increased acetate accumulation.



**Table 13:** Data collection of cluster analysis of MP and production intensity assay (sample A to E): particular proportions, ratio analysis of FL3/FL1 mean values estimating MP, FL1 mean values related to production intensity; different clusters are colored according to similar proportions in both assays.

sample	MP			ABF production intensity		
	cluster	proportions (%)	FL3/FL1	cluster	proportions (%)	FL1 mean
<b>A</b>	1	100.00	1.09	1	100.00	49.01
<b>B</b>	1	42.83	1.14	1	31.45	141.4
	2	12.94	0.58	2	18.20	223.8
	3	24.89	0.84	3	24.92	179.9
	4	19.34	1.53	4	25.43	359.8
<b>C</b>	1	4.94	0.34	1	20.11	402.7
	2	27.06	0.85	2	21.06	485.5
	3	13.29	1.45	3	19.21	336.1
	4	29.05	0.87	4	16.32	354
	5	25.66	0.43	5	23.30	375
<b>D</b>	1	100.00	1.07	1	53.54	154.2
				2	46.46	376.1
<b>E</b>	1	100.00	0.73	1	48.98	172.5
				2	51.02	340

The distinctive phenotypic variations of cells at both MPs and production intensities are likely to be related to the stress factor of inducing ABF production and secretion at a late induction time point. This effect was shown before in *E. coli* cells producing a heterologous expressed protein [148]. Here it was proposed that the particular effect of the induction time point is related to the inducer concentration per cell. When the inducer xylose is added its amount per individual cell is dependent on the particular cell concentration at the time point of addition. Therefore at low cell densities the induction effect may be stronger than at higher cell concentrations. The individual stress for every single cell is more pronounced and consistent at lower cell densities making heterogeneities less likely to occur as at higher cell concentrations.

#### 4.6.2 Batch process with 50 g/L initial carbon source

Another interesting example for population dynamics was investigated in detail at a batch process approach with an initial carbon concentration of 50 g/L fructose. This cultivation was again carried out with previously designed minimal medium in a 1L bioreactor under DO (>20%) and pH control (pH 6.3). The ABF D1.3 scFv production was induced immediately from the start by adding 0.5% xylose. The acetate concentration was determined via HPLC and the ABF concentration was measured in the supernatant by functional ELISA assay. The process itself was stable with controlled DO at 20% until a sudden increase of DO with oscillating behavior under constant aeration and agitation control became observable (**Fig. 53**). Again these oscillations were also present at CER and OUR at exhaust gas analysis. MPs were estimated by means of FCM to gain deeper insights into the cell behavior on single cell level.

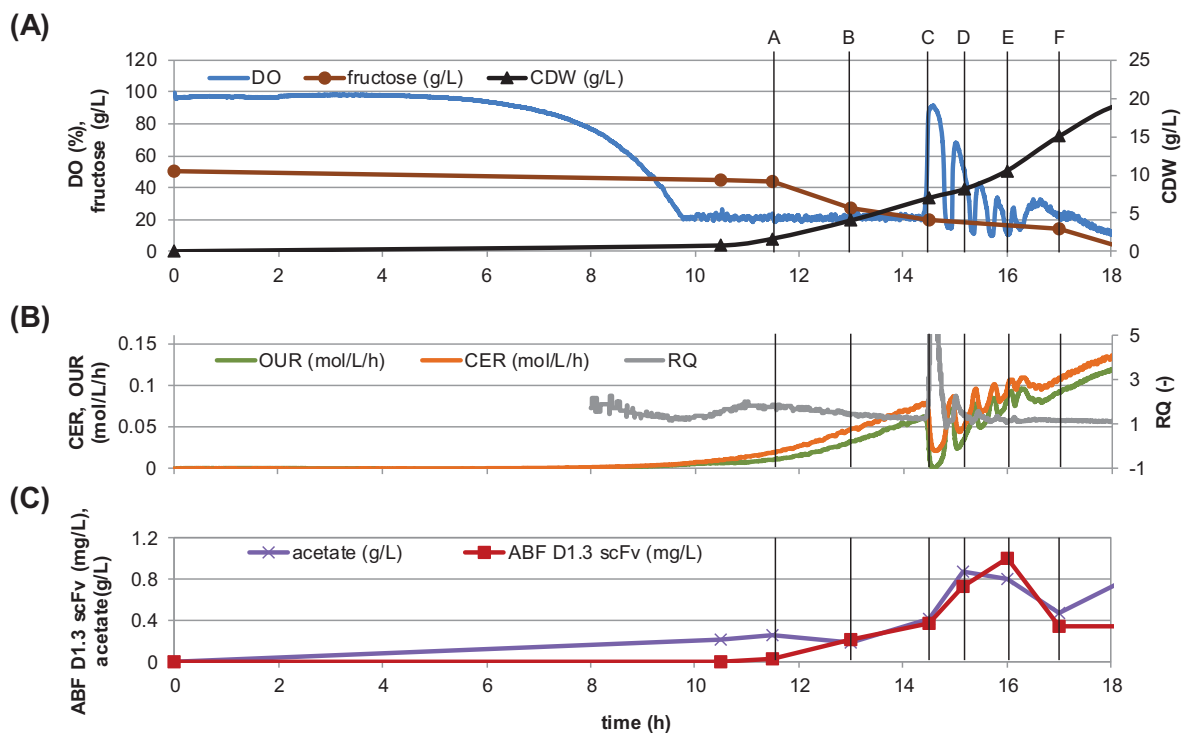


**Figure 53:** Batch cultivation of *B. megaterium* YYBm1 (EJBmD1.3scFv), bioreactor (1L, DO > 20%, pH 6.3, 50 g/L fructose), induction from the start (0.5% xylose). **(A)** DO, fructose concentration and CDW, sample time points for FCM analysis, **(B)** OUR, CER, RQ, **(C)** acetate accumulation and functional ABF D1.3 scFv concentration in the supernatant.

Measurements at different time points clearly showed the splitting from a homogenous population at sample point A to several subpopulations (sample points B to D) (**Fig. 54**). Again a reduction in MP of certain subpopulations is directly correlated with an increase in the DO concentration. Considering the MP certain population dynamics on single cell level were observed until the cells synchronized again to a single homogenous cluster (**Fig.**



54). This particular behavioral pattern might be explained by the accumulation of acetate throughout the cultivation as an overflow metabolite. Having reached a certain concentration range the produced acetate becomes toxic to the bacterial cells and might lead to a so-called acetate switch. This effect is well described for *E.coli* cultivations where under certain conditions acetate is metabolized as a primary carbon source [264]. In this case *B. megaterium* populations are differentiating during this DO oscillating time period of about 2 h where both acetate and fructose are metabolized in parallel, possibly by different cell populations. Quite interestingly the ABF concentration was also reduced which may be related to some increased protease activities and/or secretion. This experiment is another important example for the occurrence of heterogeneities in bioreactor cultivations induced by a distinctive stress factor. Disadvantages of a batch process with high initial carbon source concentrations are here highlighted from a single cell point of view. The accumulation of acetate, less product formation and the tendency towards culture heterogeneities favor unstable and not reproducible process conditions and should be avoided. However the ability of cell populations to cope with changing environmental conditions by the development of various cell populations was remarkably illustrated.

It could be demonstrated that multi-parameter FCM analysis for measuring MP and production intensities is a valuable tool for a detailed monitoring of bioprocesses on a single cell level. Parameters like reactor inoculation, induction time and substrate concentration may have a major influence on stabilization of distinct metabolic and production cell states.

The detailed reasons for the development of such heterogeneities are manifold as illustrated in the introduction (section 2.2.3). Generally speaking the history of each single cell is decisive for its particular reaction on environmental trigger factors like the induction of heterologous protein production or increased acetate concentrations. Thereby stochastic effects should not be underestimated as they can have crucial effects if a whole cell population develops distinctive heterogeneity pattern or not.

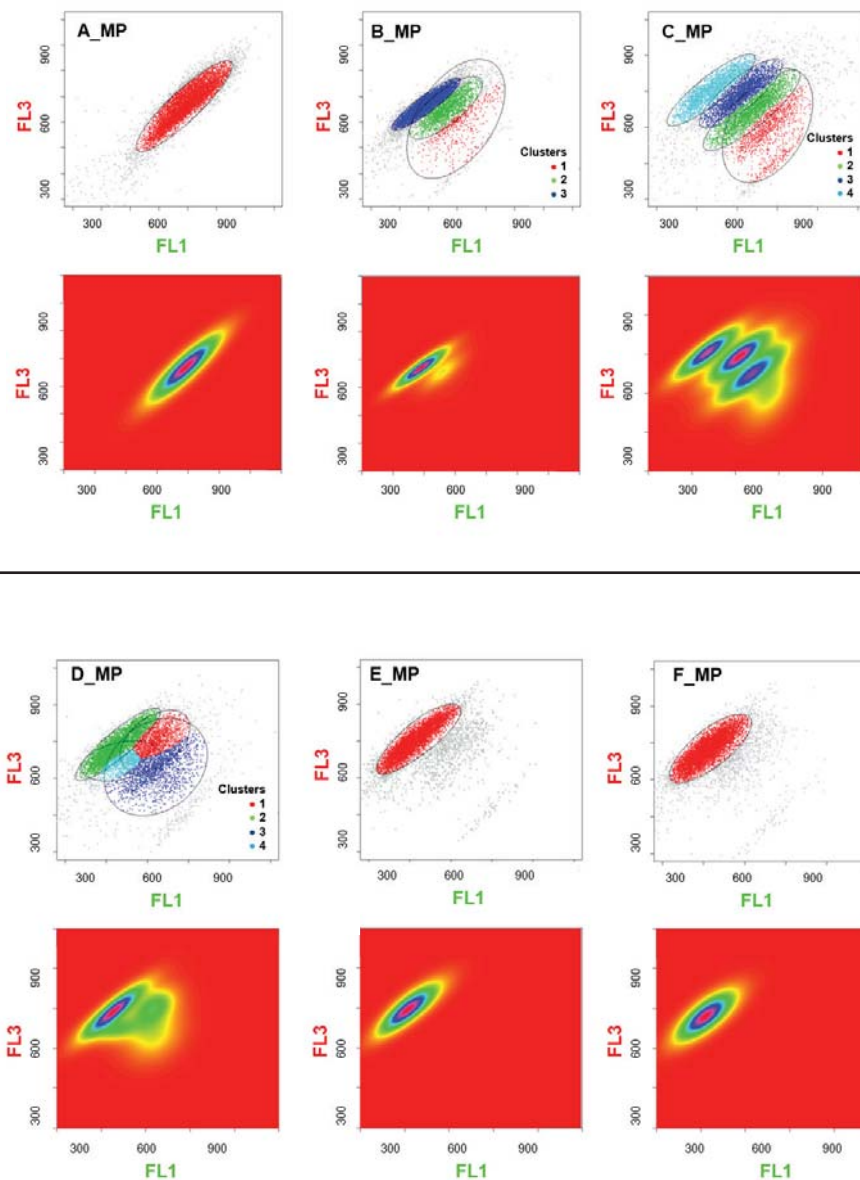


**Figure 54:** Population and cluster analysis with R statistic tools for MP estimation array at different sample points (A-F); upper row: dot plot image of predicted clusters, lower row: density plots based on previous cluster analysis.

#### 4.6.3 Process relevance of heterogeneities

In biotechnological production processes subpopulations may have a distinctive impact on the process productivity and reproducibility. Therefore knowledge about the heterogeneity regulation can be directly used for adequate online process control, optimization strategies and rational strain design. However the ability to adapt to changing environmental conditions is at least based on this variability development so that the total avoidance of heterogeneity might finally lead to less robust strains. As described before heterogeneous populations show increased fitness compared with homogenous populations.





Current knowledge of network motifs regulating the epigenetic inheritance and culture heterogeneities mechanism are promising tools for biotechnological and medical applications. In the field of synthetic biology invented networks were already used to improve bioprocess performances [265, 266]. Also the combinatorial promotor design was shown to be effective in engineering noisy gene expression. Instead of direct enzyme or pathway engineering another approach of global transcription machinery engineering (gTME) was used for metabolic engineering efforts. By reprogramming of the transcription machinery e. g. elevated ethanol tolerance and increased production performances in yeast could be achieved [267].

Quite interestingly mutations in biotechnological processes are considered to have less influence on product synthesis. This is due to the fact that the outgrowth of such mutations requires a higher growth rate of the particular individual and many replication rounds for competing with originally inoculated organism [128]. In contrast to genetically engineered microorganisms the engineered capacity (e. g. of the plasmid) is often lost and accompanied by prevailing of the wild type strain [128]. Nevertheless these quiescent mutations have a high potential to support selective strain creations e. g. mutants that channel carbon and energy from proliferation to metabolic processes to improve productivity [268]. It is most desirable to efficiently separate these high producers and adapt the process to their favorable conditions.

In the area of “omics” techniques and fast sampling, the insurance that a homogeneous cell population is characterized is also a very important issue [222]. Here at-line MP measurements could be an adequate tool for quantitatively analyzing the particular culture status. The implementation of cytomics and proteomics techniques regarding bacterial cells was recently proven to be successful [269] and has great potential for future applications in revealing totally new insights on single cell level and population dynamics related to cellular heterogeneity.



## 5 Conclusions and outlook

Microbial platforms for antibody fragment (ABF) production are beneficial compared to mammalian cell cultures regarding higher specific productivities, established scale up approaches, less regulatory aspects and reduced cost of goods (COGs). Among these, *B. megaterium* which was used as a model organism has the big advantage to directly secrete the product into the supernatant which is remarkably reducing the downstream processing costs.

The aim of this work was to optimize the production and secretion of recombinant anti-lysozyme ABF D1.3 scFv using *B. megaterium* as an alternative production host. This was done by first developing an appropriate minimal medium for production and, secondly, designing a high productive bioprocess resulting in a successful upscale approach. Advanced methods for bioprocess monitoring like flow cytometry (FCM), revealing insights on a single cell level, and transcriptome analysis were used to gain a deeper process understanding and uncovering potential bottlenecks of production and secretion of ABF D1.3 scFv.

### 5.1 Medium design

The aim of developing new defined media compositions with increased production and biomass formation is not trivial. When more than ten components are involved a simple optimization strategy by changing one parameter at one time is simply not practical due to the huge number of necessary experiments. Therefore experimental approaches using a genetic algorithm and statistical design of experiments like Central Composite Design (CCD) were applied. It was shown that an appropriate medium design is most important for *B. megaterium* to produce and functionally secrete the ABF D1.3 scFv. A minimal medium with defined components is indispensable for an adequate process control and investigations on the level of metabolome, transcriptome and proteome to ensure meaningful conclusions.

Based on a screening for a suitable carbon source, fructose was chosen as an ideal substrate for growth associated production of ABF D1.3 scFv. An inducer concentration of 0.5% xylose was found to be optimal and less influencing the maximal growth rate whilst guaranteeing a high ABF D1.3 scFv production.

Regarding a further screening of medium components it has to be considered that certain interactions between these components with a direct effect on growth and production may



take place. It is for instance known that metal ions themselves can replace each other thus leading to an increase or decrease of enzyme functions [205]. Therefore, for optimization purposes “changes one at a time” methods were not applicable as, in this case, the possible interactions between different metal ion concentrations would not be considered. By using a genetic algorithm approach a large parameter space was investigated and the possibility of finding just a local maximum was reduced. Thereby several media compositions for high functional secretion of ABF D1.3 scFv and slightly increased biomass formation were developed. It was highlighted that certain trends in changing metal ions fractions related to an increased production of ABFs were followed through the generations of experiments made. From these particular dependencies it could be concluded that an increased Mg-fraction and lower Co- and Ca-fractions directly favored higher product formation and secretion. These results were interpreted by annotated genome data associated to metal dependent enzyme classes where Mg was one of the most important metal ions for biomass generation and the ABF production and secretion process. In addition the interaction, activation and replacement of certain metal ions became obvious from annotated genome data combined with enzyme database research.

By screening different  $(\text{NH}_4)_2\text{SO}_4$  concentrations in a CCD experiment it was found that higher concentrations directly favored an increased ABF D.1.3 scFv production. This may be related to the enhanced osmolality due to a higher overall salt concentration having a direct effect on the compactness of cell wall structures [212] and the particular charge distribution inside the cell wall favoring or hindering an efficient protein secretion [208]. Additionally this change in osmotic environments may cause an unfolded protein response as shown before in yeast systems finally supporting functional protein folding [213].

Based on a originally complex medium for ABF D1.3 scFv production a defined minimal medium with an increased productivity was successfully developed being most important for an appropriate process design, control and investigations on the transcriptome level made.

## 5.2 Advanced process control

Microorganisms in industrial processes are conventionally considered to behave as uniform populations and therefore are thought to be sufficiently described by average values [128]. However for instance at high cell density *E. coli* cultivations a reduction of up to 20% of cell viability was observed by FCM measurements [270]. Standard bioprocess control techniques could not provide this kind of information as they only measure average biomass concentrations. It is most desirable to have reliable methods available to adequately monitor bioprocesses for production intensities of single cells and reveal population dynamics, e. g. under substrate limited conditions or high cell densities.



The technique of FCM was successfully used to reveal deeper insights on single cell level of *B. megaterium* secreting ABFs. By this method it became possible to distinguish between viable, metabolic active, depolarized, dormant, and dead cells and to discriminate between high and low productive cells. Batch related ABF production intensities of single cells revealed certain dynamics within the process. It was shown that the secretion through the membrane coupled Sec-pathway [40] and subsequent delayed release from the cell wall structures predominantly increased in the stationary phase. These investigations were based on a newly developed production intensity assay where the single cell productivity was determined by a specific fluorescence detection antibodies (AB). Besides the descriptive function of measuring and characterizing heterogeneities concerning the productivity the method also opens up the possibility to selectively screen for high producers.

Whole cell culture based process parameters like dissolved oxygen (DO), carbon dioxide evolution rate (CER) and oxygen uptake rate (OUR) characteristics could directly be correlated to single cell based measurements as shown for membrane potential (MP) correlations. Abrupt changes in DO concentrations with an oscillating behavior could be attributed to MP population heterogeneities at late induction of ABF production and processes with a high initial carbon concentration. The methods were shown to be suitable tools for at-line monitoring of processes allowing a better process understanding, increasing robustness and forming a firm basis for physiology-based analysis and optimization with the general application for bioprocess development.

Comparing both at-line methods for the evaluation of a current cell status (cell viability (MP) and cell integrity), it was clearly obvious, that MP measurements were far more sensitive in describing cell properties than the presented assays for cell integrity measurements. The latter are more accurate for measuring extreme effects like cell lysis after heat treatment or long term starvation. As both parameters of cell viability and integrity are important, they should be monitored simultaneously during bioreactor cultivations and can be most helpful in describing population dynamics and changes in cell physiology. Especially in deciding whether a process is operating in a stable condition or not, the MP estimation is an optimal and very sensitive parameter to adapt process conditions or even to abort the cultivation at early stage when heterogeneities appear or critical physiological values are reached. Therefore a tool for online single cell characterization is most desirable. Measurements based on an impedance microfluidic chip technique (Leister Process Technologies, Axetris Division) were recently shown to be feasible for single cell MP characterization directly comparable to fluorescence based techniques used in this approach [271]. Single cell online analysis for bioprocess characterization and control has already been applied for processes using *Saccharomyces cerevisiae* or mammalian cell cultures [272]. Here the automated control on single cell level could be successfully used for scale-up and fed-batch processes [273].

As suggested by the initiative for Process Analytical Technologies (PAT) new techniques of bioprocess monitoring on a single cell level can be regarded as suitable tools to gain additional knowledge-based data to better control bioprocesses and assure product



quality. Limitations of models arising from insufficient online data quantity and quality may thereby be overcome.

### 5.3 Process development and limitations

The investigated bioprocess is both a production process and at the same time a secretion process of ABF D1.3 scFv. Secreted products have the big advantage of reducing the purification efforts as the product of interest is already functionally folded in the supernatant with less other contaminating proteins. Secretion processes in general are coupled to particular conditions and are affected by a variety of parameters like the current specific growth rate [233]. In this case it could be demonstrated that the secretion of ABF D1.3 scFv increased when cells entered into the stationary phase. Based on these investigations an adequate process strategy was newly developed. By an adapted online feeding profile controlled growth and starving phases with increased ABF D1.3 scFv production were successfully established. The control algorithm used guaranteed comparable growth and starvation phases as the feeding profile was based on online estimated parameters of the particular biomass concentration and the cultivation volume. Other strategies like exponential, linear or DO controlled feedings were not found to promote production or secretion. This may be related to the fact that cells have to undergo a certain time of starvation stress to develop improved secretion properties.

The aim of increasing the overall process performance can also be followed by optimizations based on genetic modifications of the production host. Therefore transcriptome analyses were done to reveal potential candidates for optimizing ABF production and secretion. It is most important that the experiments are done under the controlled conditions of a bioreactor cultivation to have a firm basis for industrial process related optimizations strategies.

Starting from the transcriptome experiments it became obvious that the effects of stationary phase coupled increased secretion were not due to a changed expression pattern of ABF D1.3 scFv mRNA but may be related to certain genes which are being regulated during the stationary phase. These include for instance proteins exhibiting folding aiding functions like PrsA or HtrA. Besides, global effects enhancing secretion processes at starvation conditions which are actually favoring the secretion of degradative enzymes like proteases, lipases or nucleases may at the same time also further promote the secretion of ABFs. However it also has to be considered that the ABF has complete different folding properties and protein structure compared to naturally secreted proteins being evolutionary adapted for secretion. Here the protein charge distribution may play a critical role, having a direct effect on the release efficiency through the cell wall [274]. The Sec-pathway is also coupled to the folding process itself e. g. the generation of disulfide bonds may also display a process limiting step making folding supporting conditions and acquisition of helper proteins as foldases important factors for promoting ABF secretion. For further process development a rational optimization of the production strain should be



a major goal. Coexpression of the genes encoding for the foldase PrsA and cell wall lyases like CwIM and CwIL are promising candidates to boost secretion also during the exponential growth phase. These may lead to a tremendous increase in ABF secretion as the actual process of secretion would not anymore be limited to the stationary phase. Disadvantages of nutrient limitation as a pre-condition for an effective secretion may thereby be overcome.

## 5.4 Era of cytomics and data modeling

The possibility of investigating a single cell finger print of a whole cell culture by FCM has a high potential to be combined with cutting-edge “omics” technologies [221, 269]. The sensitivity of these techniques increased in many ways within the past few years. Based on a sufficient cluster analysis different microbial populations can be disintegrated, further be characterized and unravel the heterogeneities on a detailed molecular level. Transcriptome, Proteome, Fluxome and Metabolome data sets have the potential to give totally new insights into regulatory and enzymatic networks of different populations. Main goals are here to develop more robust, energy, time and resource efficient bioprocesses. By “omics” data sets insufficient information from fluorescence based assays can be completed on an intracellular level [221, 269]. This combination of technologies is most important to uncover possible bottlenecks of production processes regarding culture heterogeneities. These can be related to the expression or suppression of distinct pathways. Furthermore the information can also be used to rationally design approaches in the area of directed evolution to gain more robust and particularly adapted production strains. The approach of characterizing microbial cultures by combining cytomics and proteomics was recently successfully established [269]. Also for non-cultivable bacteria from microbial communities this technique has a high potential to give totally new insights on the molecular level.

FCM measurements are an ideal instrument to monitor cell properties on single cell level to gain additional information for appropriate bioprocess modeling and control. For this approach five essential issues must be addressed: 1) the development of suitable methods to measure cell heterogeneities on single cell level, 2) appropriate data analysis based on standardized statistical methods like automated clustering approaches, 3) appropriate reproducible experimental designs, 4) single cell “omics” to reveal process dependencies on the molecular level, 5) formulation and solution of computationally tractable models. These models accounting for cell heterogeneity are used in order to develop better bioprocess control strategies. They are divided into structured approaches [275] and segregated models [276] and most are population balanced approaches [277]. To use these models the cellular phenomena as well as their mathematical applicability have to be fully understood [278]. Delay differential equations were used to selectively describe population dynamics of age distribution in bacterial cultivations [279]. In this case the particular experimental design of a phased cultivation was adapted to selectively





create distinct population dynamics and synchronization of the individual cell cycle [153]. Particular stages of cell cycle were characterized by the particular DNA content of the cells measured by means of flow cytometry. These artificially created experiments give insights into the work mechanisms of cell cycle synchronization but are difficult to transfer to industrial relevant processes like batch and fed-batch designs with constantly changing conditions of nutrient availability, cell density and environmental parameters. Therefore a predictive modeling approach can only be realized in case of well controlled conditions e. g. for a phased [153] or continuous cultivations [280] to reduce stochastic effects [279]. A population model as a basis for an adapted online bioprocess control has not been implemented so far due to the complex mechanisms associated with the development of culture heterogeneities. Sitton and Srien (2008) proposed an online control of a fed-batch process relying on automated flow cytometry measurements [273]. This was done for a scale up approach of a mammalian cell culture. Here samples were automatically taken, diluted and measured via flow cytometry. The feeding was controlled according to the measured percentage of non-viable cells and thereby an easy online control was established.

The complex interplay between environmental changes and cellular responses is not yet fully understood and the integration of this new single cell knowledge into the strategies for design, operation and control of bioprocesses remains challenging [278]. In order to attain a reliable quantitative description of cell heterogeneity suitable for control of bioprocesses it is highly important to specifically coordinate between experimental and modeling effort.

However the aim to implement single cell measurements, single cell “omics” combined with an appropriate model approach has a great potential to understand the complex cellular mechanisms behind the generation of heterogeneity development.

## **5.5 Antibodies – a future perspective**

### **5.5.1 Potential of microbial systems**

Today most recombinant monoclonal antibodies (mAB) are produced in mammalian cell culture systems like chinese hamster ovary (CHO) [281] and murine myeloma cells, usually being NSO [282] and HEK293 cells [10]. The biggest advantages of these systems are the correct folding and glycosylation pattern of whole size IgG ABs, displaying effector function paralleled by generation of high product titers. Currently for high cell density mammalian cell cultivation processes 5 g/L AB concentrations are achieved [84]. In the next 5 years productivity levels may be extended up to 10-20 mg/L/h for a 21-day process based on further host cells and bioprocess engineering [283]. The actual bottleneck of the process is the purification of this highly concentrated products due to limiting purification columns capacities. However mammalian processes are very expensive due to long process times and high media costs. Nowadays serum free media



are available but this prolongs generation time and results in higher COG for the overall process. Establishing stable high producer cell lines is also a time-dependent step. A particular screening has to be done as the gene of interest randomly integrates into the chromosome after transfection of the cells [31]. Here the site and number of integrations is crucial and determines the production efficiency. Furthermore when cultivating mammalian cells a lot of regulatory concerns have to be followed. Due to the evolutionary relatedness of all mammalian species, the probability of transmission of unknown genetic material e. g. viruses is higher when using a hamster derived cell line than when using microbial hosts [31]. Quite interestingly when it comes to ABFs like Fv and scFv fragments expression yields in mammalian cell lines like CHO and myeloma cells were quite low [284, 285]. For these purposes microbial system can be more advantageous.

Microbial systems display a bunch of advantages compared to mammalian expression systems. Rapid process times due to higher growth rates, high cell densities favoring an increased volumetric productivity, simple serum free media, and easy scale-up up to five fold larger compared to mammalian cells making the production process far more economical. The absences of human related pyrogenic compounds such as toxin or viral contaminations are other advantages of microbial expression systems. As an example a typical production process with *E. coli* cells lasts for 1-3 days whereas typical mammalian cell culture takes up to 10 to 12 days limited to 20 000 liter scale [31]. For yeast systems the current volumetric productivity of 5-10 mg/L/h exceeds that of mammalian cells being 1-2 mg/L/h [286].

Most microbial systems are limited to the production of ABFs where posttranslational modifications like galactolysations or glycosylations are not required. However recently a human-like glycosylated IgG AB (rituximab) was successfully produced with a human N-glycosylation in glycoengineered *P. pastoris* cell line [287]. As a big advantage in the underlying humanized yeast system uniform glycosylations are created in contrast to most mammalian systems which produce mixtures of glycoforms.

Other advantages for microbial systems are the established techniques for stable genetic modifications and shorter overall development times to gain an efficient production strain. A time-consuming screening for high producers is not necessary as the ABs are expressed from an extrachromosomal replicating plasmids. However when using antibiotics as selection markers a validation of removal during purification has to be done and may increase downstream processing costs.

*B. megaterium* is a good alternative to *E. coli* as an expression host, as generated ABFs are directly being secreted into the surrounding medium avoiding problems like formation of inclusion bodies or subsequent intensive *in vitro* refolding or proteolytic degradation by intracellular proteases. The oxidative extracellular environment also enables the formation of disulfide bonds being important for functional ABF domain folding. In contrast to Gram negative bacteria Gram positive bacteria exhibit no endotoxins and therefore facilitate an easier downstream processing. Additionally *B. megaterium* has not been used for industrial ABF production so far so that no restrictions due to patents have to be consid-



ered. Despite these advantages the specific productivity of *B. megaterium* producing and secreting ABFs compared to other production systems remains relatively low.

However the optimization strategies for ABF production in *B. megaterium* are not yet to be exploited. Until now only the expression plasmid e. g. promotor region and ribosomal binding site (RBS) design were extensively optimized. This optimization approach has to be extended to particular strain design done by overexpression or deletion of certain genes. Potential candidates like foldases, proteases, lyases were revealed by the transcriptome analysis done in this work. Especially for gene deletion it has to be considered that transformation efficiencies for *B. megaterium* are still very low being based on protoplast transformation. Therefore the generation of mutant strains is yet a challenging task. Transcriptome analysis done with the ABF secreting and GFP overproducing strains (data not shown) revealed fewer genes as expected being highly regulated under production conditions. This may be a hint on a distinctive robustness of *B. megaterium* as a production host being able to compensate the production stress caused by heterologous protein overproduction. This ability of tending towards homeostatic conditions may be a natural evolutionary mechanism of *B. megaterium* being able to grow under various conditions e. g. at metabolizing a variety of carbon sources.

The demand for AB therapeutics increases the pressure on the production processes to be more effective related to economic reasons. Therefore in the future simple and cost effective production systems such as yeast and bacteria will be favored over mammalian systems facilitating rapid development times to the clinic and market.

### 5.5.2 Most promising antibody formats

Monoclonal AB-based approvals continue to dominate the biopharmaceutical market with today 240 mAB products being in clinical trials [295]. In the future genomic research and “omics” technologies will reveal totally new target sites for AB based therapeutic applications for unmet medical needs. The situation on the global market with growing competition between companies and products, economic problems of health care systems and higher quality demands are the main driving forces for highly efficient and productive processes with reduced COG [31]. These production processes have to be easily scalable and robust in manufacturing operations with high expression rates, optimized production yield and reduced downstream processing comprising 80% of today’s production costs.

The challenge nowadays is not discovering of new ABs but rather focusing on the development of new highly specific and stable formats, their design and the reduction of production costs [31]. As an example in 2009 the first bispecific mAB (Removab) was approved in the EU. This AB binds to the tumor cell is subsequently attracting both accessory cells and T-cells which is the reason for a multiple highly specific tumor destruction response [288]. In general mAB-dependent, cells mediated, cytotoxicity-optimized and glycoengineered ABs have a great future. The aim to increase AB affinity will lead to a reduction of administered AB amounts to generate the therapeutic effect thereby lowering the prizes for medical treatment.



Other promising ABFs are so-called “single domain ABs”. They consist of single domains derived from human VH libraries, camelid HCAs and Ig-NARs derived from sharks [289]. These fragments can be efficiently expressed in bacteria as active, soluble, and robust proteins. Due to their small size and single domain structure, they are capable to reach epitopes buried in clefts and grooves which cannot be accessed by larger ABFs [289]. They exhibit effective and fast organ permeability and can also enter in dense tissues like tumors [290]. Other AB formats like dimeric, tetrameric, diabodies or Fv fragments fused to toxins, cytotoxic antibiotics, radionucleotides or RNAses may also play a major role in future applications for specific tissue targeting. Besides protein engineering approaches post translation modification (PTM) engineering will be in the focus of prospective optimization strategies. Recently a knockout CHO cell line was developed that was able to produce defucosylated ABs displaying improved cancer killing abilities [291].

### 5.5.3 Future – application

Nowadays and in the future mAB and ABFs will be applied in areas of therapy and diagnostics like tumor treatment, allergic disorders, disease characterization, chronic inflammation, autoimmune and infectious diseases.

A key for rational AB drug design lies in the field of pharmacogenomics where potential disease targets are redefined and newly developed. Clinical trials will be adapted focusing on certain subsets of patients with particular genetic profiles. Specific diagnostic tests screening for an overexpressed target receptor have to be developed in parallel to the actual therapeutic. Thereby rational therapies can be directed towards patient populations with high response rates [32, 33]. Also in the field of basic research and diagnostic approaches ABs and ABFs will gain in importance. They are key detection reagents for the “postgenomic” analysis e. g. of the ~ 90.000 proteins of the human proteome [292-294].

An increased market for ABs is also seen in industrial areas like catalytic and immuno purification reagents and also as therapeutic agents in commodities such as toothpaste and shampoos [8, 9].

From discovering a potential disease target until the final launch of the product into the market it still takes about 10-15 years. The investigations and developments made do not rely anymore on trial and error principles but show systematic and automated approaches. However gaining deeper insights into biological processes may also lead to more complex and time lasting developments of new therapeutics.



## 6 References

- [1] Li, J., Zhu, Z., Research and development of next generation of antibody-based therapeutics. *Acta Pharmacologica Sinica* 2010, 31, 1198-1207.
- [2] Witkop, B., Bernhard, C. G., Crawford, E., Sörbom, P., Paul Ehrlich: His Ideas and His Legacy'. *Science, Technology and Society in the Time of Alfred Nobel (Editors CG Bernhard, E. Crawford & P. Sörbom)*. Oxford: Pergamon 1982.
- [3] Jeong, K. J., Jang, S. H., Velmurugan, N., Recombinant antibodies: Engineering and production in yeast and bacterial hosts. *Biotechnology Journal* 2010.
- [4] BCC, <http://www.bccresaerch.com/report/BIO016G.html> (28.04.2011)
- [5] Group, T. B. C., Medizinische Biotechnologie in Deutschland 2009; Wirtschaftsdaten von Biopharmazeutika und Therapiefortschritt durch Antikörper. *BCG Report* 2009.
- [6] Schirrmann, T., Al-Haiabi, L., Dübel, S., Hust, M., Production systems for recombinant antibodies. *Frontiers in Bioscience* 2008, 13, 4576-4594.
- [7] Krüger, C., Hu, Y., Pan, Q., Marcotte, H., *et al.*, In situ delivery of passive immunity by lactobacilli producing single-chain antibodies. *Nature biotechnology* 2002, 20, 702-706.
- [8] Krüger, C., Hultberg, A., van Dollenweerd, C., Marcotte, H., Hammarström, L., Passive immunization by lactobacilli expressing single-chain antibodies against *Streptococcus mutans*. *Molecular biotechnology* 2005, 31, 221-231.
- [9] Wycoff, K. L., Secretory IgA antibodies from plants. *Current pharmaceutical design* 2005, 11, 2429-2437.
- [10] Rodrigues, M. E., Costa, A. R., Henriques, M., Azeredo, J., Oliveira, R., Technological progresses in monoclonal antibody production systems. *Biotechnol. Prog* 2010, 26, 332–351.
- [11] Jerne, N. K., The immune system. *Scientific American* 1973, 229, 52.
- [12] Behring, S., Kitasato, S., *Deutsch. med. Wochenschr.* 16: 1113, 1890; Behring, E., and Wernicke, E. E., *Deutsch. med. Wochenschr* 1892, 12, 10-45.
- [13] Edelman, G. M., Antibody structure and molecular immunology. *Science* 1973, 180, 830.
- [14] Tonegawa, S., The molecules of the immune system. *Scientific American* 1985, 253, 104-113.
- [15] Padlan, E. A., Anatomy of the antibody molecule. *Molecular Immunology* 1994, 31, 169-217.
- [16] Hulett, M. D., Hogarth, P. M., Molecular basis of Fc receptor function. *Advances in immunology* 1994, 57, 1-56, 56a, 57-127.
- [17] Janeway, C., Immunobiology: The Immune System in Health and Disease. *Taylor & Francis Group; Garland Science; 6th edition* 2005.
- [18] Köhler, G., Milstein, C., Continuous cultures of fused cells secreting antibody of predefined specificity. *Nature* 1975, 256, 495-497.





- [19] Brüggemann, M., Caskey, H. M., Teale, C., Waldmann, H., *et al.*, A repertoire of monoclonal antibodies with human heavy chains from transgenic mice. *Proceedings of the National Academy of Sciences of the United States of America* 1989, 86, 6709.
- [20] Hust, M., Dübel, S., Human Antibody Gene Libraries. *Antibody Engineering* 2010, 65-84.
- [21] Schirrmann, T., Hust, M., Construction of human antibody gene libraries and selection of antibodies by phage display. *Methods in Molecular Biology (Clifton, NJ)* 2010, 651, 177-209.
- [22] Ostendorp, R., Frisch, C., Urban, M., Generation, engineering and production of human antibodies using HuCAL®. *Antibodies, Novel Technologies and Therapeutic Use*, 2.
- [23] Hudson, P. J., Kortt, A. A., High avidity scFv multimers; diabodies and triabodies. *Journal of immunological methods* 1999, 231, 177-189.
- [24] Bird, R. E., Hardman, K. D., Jacobson, J. W., Johnson, S., *et al.*, Single-chain antigen-binding proteins. *Science* 1988, 242, 423.
- [25] Huston, J. S., Levinson, D., Mudgett-Hunter, M., Tai, M. S., *et al.*, Protein engineering of antibody binding sites: recovery of specific activity in an anti-digoxin single-chain Fv analogue produced in *Escherichia coli*. *Proceedings of the National Academy of Sciences of the United States of America* 1988, 85, 5879.
- [26] Pack, P., Plueckthun, A., Miniantibodies: use of amphipathic helices to produce functional, flexibly linked dimeric Fv fragments with high avidity in *Escherichia coli*. *Biochemistry* 1992, 31, 1579-1584.
- [27] Hust, M., Jostock, T., Menzel, C., Voedisch, B., *et al.*, Single chain Fab(scFab) fragment. *BMC biotechnology* 2007, 7, 14.
- [28] Kufer, P., Lutterbuse, R., Baeuerle, P. A., A revival of bispecific antibodies. *Trends in biotechnology* 2004, 22, 238-244.
- [29] Nguyen, V. K., Desmyter, A., Muyldermans, S., Functional heavy-chain antibodies in Camelidae. *Advances in Immunology* 2001, 79, 261-296.
- [30] Batra, S. K., Jain, M., Wittel, U. A., Chauhan, S. C., Colcher, D., Pharmacokinetics and biodistribution of genetically engineered antibodies. *Current opinion in biotechnology* 2002, 13, 603-608.
- [31] Glover, D., Humphreys, D., Antibody Fragments. Production, purification and formatting for therapeutic applications. *Antibodies, Volume 1, Production and Purification*, G. Subramanian (Ed.), Kluwer Academic New York 2004.
- [32] Gottschalk, U., K., M., Thirty years of Monoclonal Antibodies: A long way to pharmaceutical and commercial success. *Modern Biopharmaceuticals: Design, Development and Optimization, Volume 3* 2005.
- [33] Gutjahr, T., Reinhardt, C., The Development of Herceptin: Paving the Way for Individualized Cancer Therapy. *Modern Biopharmaceuticals: Design, Development and Optimization; Volume 1* 2004.
- [34] Owens, M. A., Horten, B. C., Da Silva, M. M., HER2 amplification ratios by fluorescence in situ hybridization and correlation with immunohistochemistry in a cohort of 6556 breast cancer tissues. *Clinical breast cancer* 2004, 5, 63-69.
- [35] Ross, J. S., Fletcher, J. A., Bloom, K. J., Linette, G. P., *et al.*, Targeted therapy in breast cancer. *Molecular & Cellular Proteomics* 2004, 3, 379.
- [36] De Santes, K., Slamon, D., Anderson, S. K., Shepard, M., *et al.*, Radiolabeled antibody targeting of the HER-2/neu oncoprotein. *Cancer research* 1992, 52, 1916.



- [37] Carter, P., Presta, L., Gorman, C. M., Ridgway, J. B., *et al.*, Humanization of an anti-p185HER2 antibody for human cancer therapy. *Proceedings of the National Academy of Sciences* 1992, 89, 4285.
- [38] Burgess, A. W., Cho, H. S., Eigenbrot, C., Ferguson, K. M., *et al.*, An open-and-shut case? Recent insights into the activation of EGF/ErbB receptors. *Molecular cell* 2003, 12, 541-552.
- [39] Holbro, T., Beerli, R. R., Maurer, F., Koziczak, M., *et al.*, The ErbB2/ErbB3 heterodimer functions as an oncogenic unit: ErbB2 requires ErbB3 to drive breast tumor cell proliferation. *Proceedings of the National Academy of Sciences of the United States of America* 2003, 100, 8933.
- [40] Grabenstein, J., ImmunoFacts, Vaccines and Immunologic Drugs. 2011.
- [41] Choy, E. H. S., Hazleman, B., Smith, M., Moss, K., *et al.*, Efficacy of a novel PEGylated humanized anti TNF fragment (CDP870) in patients with rheumatoid arthritis: a phase II double blinded, randomized, dose escalating trial. *Rheumatology* 2002, 41, 1133.
- [42] Pant, N., Hultberg, A., Zhao, Y., Svensson, L., *et al.*, Lactobacilli expressing variable domain of llama heavy-chain antibody fragments (lactobodies) confer protection against rotavirus-induced diarrhea. *Journal of Infectious Diseases* 2006, 194, 1580.
- [43] Van der Vaart, J. M., Pant, N., Wolvers, D., Bezemer, S., *et al.*, Reduction in morbidity of rotavirus induced diarrhoea in mice by yeast produced monovalent llama-derived antibody fragments. *Vaccine* 2006, 24, 4130-4137.
- [44] Pelat, T., Hust, M., Hale, M., Lefranc, M., *et al.*, Isolation of a human-like antibody fragment (scFv) that neutralizes ricin biological activity. *BMC Biotechnology* 2009, 9.
- [45] Pelat, T., Hust, M., Laffly, E., Condemine, F., *et al.*, High-affinity, human antibody-like antibody fragment (single-chain variable fragment) neutralizing the lethal factor (LF) of *Bacillus anthracis* by inhibiting protective antigen-LF complex formation. *Antimicrobial agents and chemotherapy* 2007, 51, 2758.
- [46] Jordan, E., Hust, M., Roth, A., Biedendieck, R., *et al.*, Production of recombinant antibody fragments in *Bacillus megaterium*. *Microbial Cell Factories* 2007, 6, 2.
- [47] Jordan, E., Al-Halabi, L., Schirrmann, T., Hust, M., Dübel, S., Production of single chain Fab (scFab) fragments in *Bacillus megaterium*. *Microbial Cell Factories* 2007, 6, 38.
- [48] Jordan, E., Al-Halabi, L., Schirrmann, T., Hust, M., Antibody production by the gram-positive bacterium *Bacillus megaterium*. *Methods Mol Biol* 2009, 525, 509-516, xiv.
- [49] Humphreys, D. P., Glover, D. J., Therapeutic antibody production technologies: Molecules, applications, expression and purification. *Current opinion in drug discovery & development* 2001, 4, 172.
- [50] Skerra, A., Pluckthun, A., Assembly of a functional immunoglobulin Fv fragment in *Escherichia coli*. *Science* 1988, 240, 1038.
- [51] Sletta, H., Tondervik, A., Hakvag, S., Vee Aune, T. E., *et al.*, The presence of N-terminal secretion signal sequences leads to strong stimulation of the total expression levels of three tested medically important proteins during high-cell-density cultivations of *Escherichia coli*. *Applied and Environmental Microbiology* 2007, 73, 906-912.
- [52] Tachibana, H., Takekoshi, M., Cheng, X. J., Nakata, Y., *et al.*, Bacterial Expression of a Human Monoclonal Antibody-Alkaline Phosphatase Conjugate Specific for *Entamoeba histolytica*. *Clinical and Diagnostic Laboratory Immunology* 2004, 11, 216-218.
- [53] Rusch, S. L., Kendall, D. A., Interactions that drive Sec-dependent bacterial protein transport. *Biochemistry* 2007, 46, 9665-9673.

- [54] Lauer, B., Ottleben, I., Jacobsen, H. J., Reinard, T., Production of a single-chain variable fragment antibody against fumonisin B1. *Journal of Agricultural and Food Chemistry* 2005, 53, 899-904.
- [55] Mi, J., Yan, J., Guo, Z., Zhao, M., Chang, W., Isolation and characterization of an anti-recombinant erythropoietin single-chain antibody fragment using a phage display antibody library. *Analytical and Bioanalytical Chemistry* 2005, 383, 218-223.
- [56] Simmons, L. C., Reilly, D., Klimowski, L., Shantha Raju, T., *et al.*, Expression of full-length immunoglobulins in *Escherichia coli*: Rapid and efficient production of aglycosylated antibodies. *Journal of Immunological Methods* 2002, 263, 133-147.
- [57] Shiroza, T., Shinozaki-Kuwahara, N., Hayakawa, M., Shibata, Y., *et al.*, Production of a single-chain variable fraction capable of inhibiting the *Streptococcus mutans* glucosyltransferase in *Bacillus brevis*: Construction of a chimeric shuttle plasmid secreting its gene product. *Biochimica et Biophysica Acta - Gene Structure and Expression* 2003, 1626, 57-64.
- [58] Wu, S. C., Yeung, J. C., Duan, Y., Ye, R., *et al.*, Functional production and characterization of a fibrin-specific single-chain antibody fragment from *Bacillus subtilis*: effects of molecular chaperones and a wall-bound protease on antibody fragment production. *Applied and environmental microbiology* 2002, 68, 3261.
- [59] Jordan, E., Hust, M., Roth, A., Biedendieck, R., *et al.*, Production of recombinant antibody fragments in *Bacillus megaterium*. *Microb Cell Fact* 2007, 6, 2.
- [60] Chancey, C. J., Khanna, K. V., Seegers, J. F. M. L., Zhang, G. W., *et al.*, Lactobacilli-expressed single-chain variable fragment (scFv) specific for intercellular adhesion molecule 1 (ICAM-1) blocks cell-associated HIV-1 transmission across a cervical epithelial monolayer. *Journal of Immunology* 2006, 176, 5627-5636.
- [61] Marcotte, H., Koll-Klais, P., Hultberg, A., Zhao, Y., *et al.*, Expression of single-chain antibody against RgpA protease of *Porphyromonas gingivalis* in *Lactobacillus*. *Journal of Applied Microbiology* 2006, 100, 256-263.
- [62] Fish, B., Concepts in development of manufacturing strategies for monoclonal antibodies. *Antibodies, Volume 1, Production and Purification*, G. Subramanian (Ed.), Kluwer Academic New York 2004.
- [63] Daßler, T., Wich, G., EP 1 903 115 B1: Process for the fermentative production of antibodies. *European patent* 2006.
- [64] Yoon, S. H., Kim, S. K., Kim, J. F., Secretory production of recombinant proteins in *Escherichia coli*. *Recent Patents on Biotechnology*, 4, 23-29.
- [65] Economou, A., Following the leader: bacterial protein export through the Sec pathway. *Trends in Microbiology* 1999, 7, 315-320.
- [66] Stammen, S., Muller, B. K., Korneli, C., Biedendieck, R., *et al.*, High-Yield Intra-and Extracellular Protein Production Using *Bacillus megaterium*. *Applied and environmental microbiology* 2010, 76, 4037.
- [67] Schallmeyer, M., Singh, A., Ward, O. P., Developments in the use of *Bacillus* species for industrial production. *Canadian journal of microbiology* 2004, 50, 1-17.
- [68] Buckholz, R. G., Gleeson, M. A. G., Yeast systems for the commercial production of heterologous proteins. *Bio/Technology* 1991, 9, 1067-1072.
- [69] Ridder, R., Schmitz, R., Legay, F., Gram, H., Generation of rabbit monoclonal antibody fragments from a combinatorial phage display library and their production in the yeast *Pichia pastoris*. *Bio/Technology* 1995, 13, 255-260.

- [70] Eldin, P., Pauza, M. E., Hieda, Y., Lin, G., *et al.*, High-level secretion of two antibody single chain Fv fragments by *Pichia pastoris*. *Journal of Immunological Methods* 1997, 201, 67-75.
- [71] Frenken, L. G. J., Van Der Linden, R. H. J., Hermans, P. W. J. J., Bos, J. W., *et al.*, Isolation of antigen specific Llama V(HH) antibody fragments and their high level secretion by *Saccharomyces cerevisiae*. *Journal of Biotechnology* 2000, 78, 11-21.
- [72] Frenken, L. G. J., Hessing, J. G. M., Van Den Hondel, C. A. M. J. J., Verrips, C. T., Recent advances in the large-scale production of antibody fragments using lower eukaryotic microorganisms. *Research in Immunology* 1998, 149, 589-599.
- [73] Horwitz, A. H., Chang, C. P., Better, M., Hellstrom, K. E., Robinson, R. R., Secretion of functional antibody and Fab fragment from yeast cells. *Proceedings of the National Academy of Sciences of the United States of America* 1988, 85, 8678-8682.
- [74] Liu, J., Wei, D., Qian, F., Zhou, Y., *et al.*, pPIC9-Fc: A Vector System for the Production of Single-Chain Fv-Fc Fusions in *Pichia pastoris* as Detection Reagents in Vitro. *Journal of Biochemistry* 2003, 134, 911-917.
- [75] Shusta, E. V., Raines, R. T., Plückthun, A., Wittrup, K. D., Increasing the secretory capacity of *Saccharomyces cerevisiae* for production of single-chain antibody fragments. *Nature Biotechnology* 1998, 16, 773-777.
- [76] Hamilton, S. R., Davidson, R. C., Sethuraman, N., Nett, J. H., *et al.*, Humanization of yeast to produce complex terminally sialylated glycoproteins. *Science* 2006, 313, 1441-1443.
- [77] Joosten, V., Gouka, R. J., Van Den Hondel, C. A. M. J. J., Verrips, C. T., Lokman, B. C., Expression and production of llama variable heavy-chain antibody fragments (VHHs) by *Aspergillus awamori*. *Applied Microbiology and Biotechnology* 2005, 66, 384-392.
- [78] Nyysönen, E., Penttilä, M., Harkki, A., Saloheimo, A., *et al.*, Efficient production of antibody fragments by the filamentous fungus *Trichoderma reesei*. *Bio/Technology* 1993, 11, 591-595.
- [79] Schirrmann, T., Al-Halabi, L., Dübel, S., Hust, M., Production systems for recombinant antibodies. *Frontiers in Bioscience* 2008, 13, 4576-4594.
- [80] Kretzschmar, T., Aoustin, L., Zingel, O., Marangi, M., *et al.*, High-level expression in insect cells and purification of secreted monomeric single-chain Fv antibodies. *Journal of Immunological Methods* 1996, 195, 93-101.
- [81] Liang, M., Dübel, S., Li, D., Queitsch, I., *et al.*, Baculovirus expression cassette vectors for rapid production of complete human IgG from phage display selected antibody fragments. *Journal of Immunological Methods* 2001, 247, 119-130.
- [82] Ailor, E., Betenbaugh, M. J., Modifying secretion and post-translational processing in insect cells. *Current Opinion in Biotechnology* 1999, 10, 142-145.
- [83] Reavy, B., Ziegler, A., Diplexito, J., Macintosh, S. M., *et al.*, Expression of functional recombinant antibody molecules in insect cell expression systems. *Protein Expression and Purification* 2000, 18, 221-228.
- [84] Wurm, F. M., Production of recombinant protein therapeutics in cultivated mammalian cells. *Nature Biotechnology* 2004, 22, 1393-1398.
- [85] Fussenegger, M., Bailey, J. E., Molecular regulation of cell-cycle progression and apoptosis in mammalian cells: Implications for biotechnology. *Biotechnology Progress* 1998, 14, 807-833.
- [86] Jones, D., Kroos, N., Anema, R., Van Montfort, B., *et al.*, High-level expression of recombinant IgG in the human cell line PER.C6. *Biotechnology Progress* 2003, 19, 163-168.

- [87] Cho, M. S., Yee, H., Brown, C., Mei, B., *et al.*, Versatile expression system for rapid and stable production of recombinant proteins. *Biotechnology Progress* 2003, 19, 229-232.
- [88] Robinson, D. K., Chan, C. P., Ip, C. C. Y., Seamans, C., *et al.*, Product consistency during long-term fed-batch culture. *Animal Cell Technology: Products of Today, Prospects for Tomorrow* 1994, 763-767.
- [89] Daniell, H., Streatfield, S. J., Wycoff, K., Medical molecular farming: Production of antibodies, biopharmaceuticals and edible vaccines in plants. *Trends in Plant Science* 2001, 6, 219.
- [90] Hiatt, A., Cafferkey, R., Bowdish, K., Production of antibodies in transgenic plants. *Nature* 1989, 342, 76-78.
- [91] Peeters, K., De Wilde, C., Depicker, A., Highly efficient targeting and accumulation of a Fab fragment within the secretory pathway and apoplast of *Arabidopsis thaliana*. *European Journal of Biochemistry* 2001, 268, 4251-4260.
- [92] Bary, A., DE 1884 Vergleichende Morphologie und Biologie der Pilze, Mycetozen und Bakterien. *Wilhelm Engelmann, Leipzig*.
- [93] Clarke, N. A., Studies on the host-virus relationship in a lysogenic strain of *Bacillus megaterium*: The Growth of *Bacillus megaterium* in Synthetic Medium. *Journal of Bacteriology* 1952, 63, 187.
- [94] Robinow, C. F., Observations on the nucleus of resting and germinating spores of *Bacillus megaterium*. *Journal of Bacteriology* 1953, 65, 378.
- [95] De Carlo, M. R., Sarles, W. B., Knight, S. G., Lysogenicity of *Bacillus megaterium*. *Journal of Bacteriology* 1953, 65, 53.
- [96] Levinson, H. S., Sevag, M. G., Manganese and the proteolytic activity of spore extracts of *Bacillus megaterium* in relation to germination. *Journal of Bacteriology* 1954, 67, 615.
- [97] Lemoigne, M., Peaud, L. C., Croson, M., 1950, p. 705.
- [98] Rohde, M., Biedendieck, R., David, F., SEM images; Ultra thin section. 2010.
- [99] Vary, P. S., Prime time for *Bacillus megaterium*. *Microbiology* 1994, 140 ( Pt 5), 1001-1013.
- [100] Bunk, B., Comparative and Functional Genomics of *Bacillus megaterium* DSM319. *Dissertationsschrift* 2010.
- [101] Eppinger, M., Bunk, B., Johns, M. A., Edirisinghe, J. N., *et al.*, Genome sequences of the industrial vitamin B12-producers *B. megaterium* QM B1551 and DSM319 reveal new insights into the *Bacillus* genome evolution and pan-genome structure  
[http://www.ncbi.nlm.nih.gov/nuccore/NC\\_014103](http://www.ncbi.nlm.nih.gov/nuccore/NC_014103). *NCBI* 2010.
- [102] Biedendieck, R., Yang, Y., Deckwer, W. D., Malten, M., Jahn, D., Plasmid system for the intracellular production and purification of affinity-tagged proteins in *Bacillus megaterium*. *Biotechnol Bioeng* 2007, 96, 525-537.
- [103] Tjalsma, H., Noback, M. A., Bron, S., Venema, G., *et al.*, *Bacillus subtilis* contains four closely related type I signal peptidases with overlapping substrate specificities. *Journal of Biological Chemistry* 1997, 272, 25983.
- [104] Campo, N., Tjalsma, H., Buist, G., Stepniak, D., *et al.*, Subcellular sites for bacterial protein export. *Molecular microbiology* 2004, 53, 1583-1599.
- [105] Kim, J. Y., Overproduction and secretion of *Bacillus circulans* endo-  $\alpha$ -1, 3-1, 4-glucanase gene (bgIBC1) in *B. subtilis* and *B. megaterium*. *Biotechnology letters* 2003, 25, 1445-1449.

- [106] Priest, F. G., Extracellular enzyme synthesis in the genus *Bacillus*. *Microbiology and Molecular Biology Reviews* 1977, 41, 711.
- [107] Martín, L., Prieto, M. A., Cortes, E., García, J. L., Cloning and sequencing of the *pac* gene encoding the penicillin G acylase of *Bacillus megaterium* ATCC 14945. *FEMS microbiology letters* 1995, 125, 287-292.
- [108] Takasaki, Y., Novel maltose-producing amylase from *Bacillus megaterium* G-2. *Agricultural and Biological Chemistry* 1989, 53, 341-347.
- [109] Wang, W., Hollmann, R., Fürch, T., Nimtz, M., *et al.*, Proteome analysis of a recombinant *Bacillus megaterium* strain during heterologous production of a glucosyltransferase. *Proteome Science* 2005, 3, 4.
- [110] Wang, W., Hollmann, R., Deckwer, W. D., Comparative proteomic analysis of high cell density cultivations with two recombinant *Bacillus megaterium* strains for the production of a heterologous dextranucrase. *Proteome Science* 2006, 4, 19.
- [111] Raux, E., Lanois, A., Warren, M. J., Rambach, A., Thermes, C., Cobalamin (vitamin B12) biosynthesis: identification and characterization of a *Bacillus megaterium* *cobI* operon. *Biochemical Journal* 1998, 335, 159.
- [112] Biedendieck, R., Malten, M., Barg, H., Bunk, B., *et al.*, Metabolic engineering of cobalamin (vitamin B12) production in *Bacillus megaterium*. *Microbial Biotechnology* 2010, 3, 24-37.
- [113] He, J. S., Fulco, A. J., A barbiturate-regulated protein binding to a common sequence in the cytochrome P450 genes of rodents and bacteria. *Journal of Biological Chemistry* 1991, 266, 7864.
- [114] Bäumchen, C., Roth, A. H. F. J., Biedendieck, R., Malten, M., *et al.*, D Mannitol production by resting state whole cell biotransformation of D fructose by heterologous mannitol and formate dehydrogenase gene expression in *Bacillus megaterium*. *Biotechnology journal* 2007, 2, 1408-1416.
- [115] Burger, S., Tatge, H., Hofmann, F., Genth, H., *et al.*, Expression of recombinant *Clostridium difficile* toxin A using the *Bacillus megaterium* system. *Biochemical and biophysical research communications* 2003, 307, 584-588.
- [116] Fürch, T., Hollmann, R., Wittmann, C., Wang, W., Deckwer, W. D., Comparative study on central metabolic fluxes of *Bacillus megaterium* strains in continuous culture using <sup>13</sup> C labelled substrates. *Bioprocess and biosystems engineering* 2007, 30, 47-59.
- [117] Furch, T., Wittmann, C., Wang, W., Franco-Lara, E., *et al.*, Effect of different carbon sources on central metabolic fluxes and the recombinant production of a hydrolase from *Thermobifida fusca* in *Bacillus megaterium*. *J Biotechnol* 2007, 132, 385-394.
- [118] Biedendieck, R., Beine, R., Gamer, M., Jordan, E., *et al.*, Export, purification, and activities of affinity tagged *Lactobacillus reuteri* levansucrase produced by *Bacillus megaterium*. *Applied microbiology and biotechnology* 2007, 74, 1062-1073.
- [119] Rygus, T., Hillen, W., Catabolite repression of the *xyl* operon in *Bacillus megaterium*. *Journal of bacteriology* 1992, 174, 3049.
- [120] Rygus T., Hillen W., Catabolite Repression of the *xyl* Operon in *Bacillus megaterium*. *Journal of Bacteriology* 1992, 174, 3049-3055.
- [121] Gernaey, K. V., Woodley, J. M., Sin, G., Introducing mechanistic models in Process Analytical Technology education. *Biotechnology Journal* 2009, 4, 593-599.
- [122] Gucker, F. T., O'Konski, C., Electronic Methods of Counting Aerosol Particles. *Chemical Reviews* 1949, 44, 373-388.



- [123] Kamentsky, L. A., Melamed, M. R., Derman, H., Spectrophotometer: new instrument for ultrarapid cell analysis. *Science* 1965, 150, 630.
- [124] Seo, J. H., Srienc, F., Bailey, J. E., Flow cytometry analysis of plasmid amplification in *Escherichia coli*. *Biotechnology Progress* 1985, 1, 181-188.
- [125] Scheper, T., Hitzmann, B., Rinas, U., Schugerl, K., Flow cytometry of *Escherichia coli* for process monitoring. *Journal of biotechnology* 1987, 5, 139-148.
- [126] Slater, M. L., Sharrow, S. O., Gart, J. J., Cell cycle of *Saccharomyces cerevisiae* in populations growing at different rates. *Proceedings of the National Academy of Sciences* 1977, 74, 3850.
- [127] Hutter, K. J., Rapid test methods for dead-or-alive analysis of yeast cells. *Brauwelt International* 1993, 300-300.
- [128] Müller, S., Harms, H., Bley, T., Origin and analysis of microbial population heterogeneity in bioprocesses. *Current opinion in biotechnology* 2010, 21, 100-113.
- [129] Reis, A., da Silva, T. L., Kent, C. A., Kosseva, M., *et al.*, Monitoring population dynamics of the thermophilic *Bacillus licheniformis* CCMI 1034 in batch and continuous cultures using multi-parameter flow cytometry. *Journal of biotechnology* 2005, 115, 199-210.
- [130] Wållberg, F., Sundström, H., Ledung, E., Hewitt, C. J., Enfors, S. O., Monitoring and quantification of inclusion body formation in *Escherichia coli* by multi-parameter flow cytometry. *Biotechnology letters* 2005, 27, 919-926.
- [131] Gauthier, C., St-Pierre, Y., Villemur, R., Rapid antimicrobial susceptibility testing of urinary tract isolates and samples by flow cytometry. *Journal of medical microbiology* 2002, 51, 192.
- [132] Suller, M. T. E., Lloyd, D., Fluorescence monitoring of antibiotic-induced bacterial damage using flow cytometry. *Cytometry Part A* 1999, 35, 235-241.
- [133] Bunthof, C. J., Bloemen, K., Breeuwer, P., Rombouts, F. M., Abee, T., Flow cytometric assessment of viability of lactic acid bacteria. *Applied and environmental microbiology* 2001, 67, 2326.
- [134] Rault, A., Béal, C., Ghorbal, S., Ogier, J. C., Bouix, M., Multiparametric flow cytometry allows rapid assessment and comparison of lactic acid bacteria viability after freezing and during frozen storage. *Cryobiology* 2007, 55, 35-43.
- [135] Boyd, A. R., Gunasekera, T. S., Attfield, P. V., Simic, K., *et al.*, A flow-cytometric method for determination of yeast viability and cell number in a brewery. *FEMS yeast research* 2003, 3, 11-16.
- [136] Czechowska, K., Johnson, D. R., van der Meer, J. R., Use of flow cytometric methods for single-cell analysis in environmental microbiology. *Current opinion in microbiology* 2008, 11, 205-212.
- [137] Hewitt, C. J., Nebe-Von-Caron, G., An industrial application of multiparameter flow cytometry: assessment of cell physiological state and its application to the study of microbial fermentations. *Cytometry Part A* 2001, 44, 179-187.
- [138] Coulter, W. B., Google Patents 1953.
- [139] Díaz, M., Herrero, M., García, L. A., Quirós, C., Application of flow cytometry to industrial microbial bioprocesses. *Biochemical Engineering Journal* 2010, 48, 385-407.
- [140] Steen, H. B., Boye, E., Skarstad, K., Bloom, B., *et al.*, Applications of flow cytometry on bacteria: cell cycle kinetics, drug effects, and quantitation of antibody binding. *Cytometry Part A* 1982, 2, 249-257.



- [141] Looser, V., Hammes, F., Keller, M., Berney, M., *et al.*, Flow-cytometric detection of changes in the physiological state of *E. coli* expressing a heterologous membrane protein during carbon-limited fedbatch cultivation. *Biotechnology and bioengineering* 2005, 92, 69-78.
- [142] Nebe-von Caron, G., Stephens, B., Assessment of bacterial viability status by flow cytometry and single cell sorting. *Journal of applied microbiology* 1998, 84, 988-998.
- [143] Lewis, K., Persister cells, dormancy and infectious disease. *Nature Reviews Microbiology* 2006, 5, 48-56.
- [144] Kærn, M., Elston, T. C., Blake, W. J., Collins, J. J., Stochasticity in gene expression: from theories to phenotypes. *Nature Reviews Genetics* 2005, 6, 451-464.
- [145] Kaufmann, B. B., Yang, Q., Mettetal, J. T., Van Oudenaarden, A., Heritable stochastic switching revealed by single-cell genealogy. *PLoS biology* 2007, 5, e239.
- [146] Avery, S. V., Microbial cell individuality and the underlying sources of heterogeneity. *Nature Reviews Microbiology* 2006, 4, 577-587.
- [147] Lara, A. R., Galindo, E., Ramírez, O. T., Palomares, L. A., Living with heterogeneities in bioreactors. *Molecular biotechnology* 2006, 34, 355-381.
- [148] Lewis, G., Taylor, I. W., Nienow, A. W., Hewitt, C. J., The application of multi-parameter flow cytometry to the study of recombinant *Escherichia coli* batch fermentation processes. *Journal of Industrial Microbiology and Biotechnology* 2004, 31, 311-322.
- [149] Veening, J. W., Smits, W. K., Kuipers, O. P., Bistability, epigenetics, and bet-hedging in bacteria. *Annu. Rev. Microbiol.* 2008, 62, 193-210.
- [150] Stewart, E. J., Madden, R., Paul, G., Taddei, F., Aging and death in an organism that reproduces by morphologically symmetric division. *PLoS Biology* 2005, 3, e45.
- [151] Fredriksson, A., Nystrom, T., Conditional and replicative senescence in *Escherichia coli*. *Current opinion in microbiology* 2006, 9, 612-618.
- [152] Lindner, A. B., Madden, R., Demarez, A., Stewart, E. J., Taddei, F., Asymmetric segregation of protein aggregates is associated with cellular aging and rejuvenation. *Proceedings of the National Academy of Sciences* 2008, 105, 3076.
- [153] Fritsch, M., Starrau, J., Loesche, A., Mueller, S., Bley, T., Cell cycle synchronization of *Cupriavidus necator* by continuous phasing measured via flow cytometry. *Biotechnology and bioengineering* 2005, 92, 635-642.
- [154] Müller-Hill, B., *The lac operon: A short history of a genetic paradigm*, de Gruyter 1996.
- [155] Smits, W. K., Kuipers, O. P., Veening, J. W., Phenotypic variation in bacteria: the role of feedback regulation. *Nature Reviews Microbiology* 2006, 4, 259-271.
- [156] Veening, J. W., Igoshin, O. A., Eijlander, R. T., Nijland, R., *et al.*, Transient heterogeneity in extracellular protease production by *Bacillus subtilis*. *Molecular systems biology* 2008, 4.
- [157] Torkelson, J., Harris, R. S., Lombardo, M. J., Nagendran, J., *et al.*, Genome-wide hypermutation in a subpopulation of stationary-phase cells underlies recombination-dependent adaptive mutation. *The EMBO Journal* 1997, 16, 3303-3311.
- [158] Balaban, N. Q., Merrin, J., Chait, R., Kowalik, L., Leibler, S., Bacterial persistence as a phenotypic switch. *Science* 2004, 305, 1622.
- [159] Casadesús, J., Low, D., Epigenetic gene regulation in the bacterial world. *Microbiology and molecular biology reviews* 2006, 70, 830.

- [160] Verma, R., Boleti, E., George, A. J. T., Antibody engineering: comparison of bacterial, yeast, insect and mammalian expression systems. *Journal of immunological methods* 1998, 216, 165-181.
- [161] Ferrer-Miralles, N., Domingo-Espín, J., Corchero, J. L., Vázquez, E., Villaverde, A., Microbial factories for recombinant pharmaceuticals. *Microbial Cell Factories* 2009, 8, 17.
- [162] Junker, B. H., Wang, H. Y., Bioprocess monitoring and computer control: Key roots of the current PAT initiative. *Biotechnology and bioengineering* 2006, 95, 226-261.
- [163] Services, U. S. D. o. H. a. H., Guidance for Industry, Process validation: General principles and Practices. 2011.
- [164] Montgomery, D. C., Runger, G. C., Gauge capability analysis and designed experiments. Part II: experimental design models and variance component estimation. *Quality Engineering* 1993, 6, 289-305.
- [165] Afnan, A., PAT-A Framework for Innovative Pharmaceutical Development, Manufacturing and Quality Assurance. *Guidance for Industry*. 2004.
- [166] Yang, Y., Malten, M., Grote, A., Jahn, D., Deckwer, W. D., Codon optimized *Thermobifida fusca* hydrolase secreted by *Bacillus megaterium*. *Biotechnol Bioeng* 2007, 96, 780-794.
- [167] Wittchen, K. D., Meinhardt, F., Inactivation of the major extracellular protease from *Bacillus megaterium* DSM319 by gene replacement. *Applied microbiology and biotechnology* 1995, 42, 871-877.
- [168] Hames, B. D., *Gel electrophoresis of proteins: a practical approach*, Oxford University Press, USA 1998.
- [169] Akerstrom, B., Nilson, B. H. K., Hoogenboom, H. R., Bjorck, L., On the interaction between single chain Fv antibodies and bacterial immunoglobulin-binding proteins. *Journal of immunological methods* 1994, 177, 151-163.
- [170] Ritchie, D. G., Nickerson, J. M., Fuller, G. M., Two simple programs for the analysis of data from enzyme-linked immunosorbent (ELISA) assays on a programmable desk-top calculator. *Analytical Biochemistry* 1981, 110, 281-290.
- [171] Yang, Y., Biedendieck, R., Wang, W., Gamer, M., *et al.*, High yield recombinant penicillin G amidase production and export into the growth medium using *Bacillus megaterium*. *Microb Cell Fact* 2006, 5, 36.
- [172] David, F., Westphal, R., Bunk, B., Jahn, D., Franco-Lara, E., Optimization of antibody fragment production in *Bacillus megaterium*: the role of metal ions on protein secretion. *Journal of Biotechnology* 2010, 150, 115-124.
- [173] Novo, D., Perlmutter, N. G., Hunt, R. H., Shapiro, H. M., Accurate flow cytometric membrane potential measurement in bacteria using diethyloxacarbocyanine and a ratiometric technique. *Cytometry Part A* 1999, 35, 55-63.
- [174] Shapiro, H. M., Membrane potential estimation by flow cytometry. *Methods* 2000, 21, 271-279.
- [175] Panchuk-Voloshina, N., Haugland, R. P., Bishop-Stewart, J., Bhalgat, M. K., *et al.*, Alexa dyes, a series of new fluorescent dyes that yield exceptionally bright, photostable conjugates. *Journal of Histochemistry and Cytochemistry* 1999, 47, 1179.
- [176] Gottardo, R., Lo, K., flowClust Bioconductor package. 2008.
- [177] Hahne, F., LeMeur, N., Brinkman, R. R., Ellis, B., *et al.*, flowCore: a Bioconductor package for high throughput flow cytometry. *Bmc Bioinformatics* 2009, 10, 106.

- [178] Kyongryun, L., Florian, H., Deepayan, S., Robert, G., iflow: A graphical user interface for flow cytometry tools in bioconductor. *Advances in bioinformatics* 2009, 2009.
- [179] Lo, K., Brinkman, R. R., Gottardo, R., Automated gating of flow cytometry data via robust model based clustering. *Cytometry Part A* 2008, 73, 321-332.
- [180] Lo, K., Hahne, F., Brinkman, R. R., Gottardo, R., flowClust: a Bioconductor package for automated gating of flow cytometry data. *BMC bioinformatics* 2009, 10, 145.
- [181] Ibrahim, H. M., Yusoff, W. M. W., Hamid, A. A., Illias, R. M., *et al.*, Optimization of medium for the production of [beta]-cyclodextrin glucanotransferase using Central Composite Design (CCD). *Process Biochemistry* 2005, 40, 753-758.
- [182] Freyer, S., Weuster-Botz, D., Wandrey, C., Medium Optimization Using Genetic Algorithms. *BioEng* 1992, 8, 16-25.
- [183] Weuster-Botz, D., Pramatarova, V., Spassov, G., Wandrey, C., Use of a genetic algorithm in the development of a synthetic growth medium for *Arthrobacter simplex* with high hydrocortisone-dehydrogenase activity. *Journal of Chemical Technology & Biotechnology* 1995, 64, 386-392.
- [184] Weuster-Botz D, K. R., Frantzen M, Wandrey C, Substrate Controlled Fed-Batch Peroduction of L-Lysine with *Corynebacterium glutanicum*. *Biotechnol Prog* 1997, 13, 387-393.
- [185] Weuster-Botz D, K. M., Joksche B, Schärtges D, Wandrey C, Integrated Developement of Fermentation and Downstream Proessing of L-Isoleucin Production with *Corynebacterium glutanicum*. *Appl Microbiol Biotechnol* 1996, 46, 209-219.
- [186] Böhling, H., Voss, H., Optimization of Protein-Synthesis in Recombinant E.coli BL21. *BIOforum Int* 1997, 2/97, 86-91.
- [187] Havel, J., Link, H., Hofinger, M., Franco-Lara, E., Weuster-Botz, D., Comparison of genetic algorithms for experimental multi-objective optimization on the example of medium design for cyanobacteria. *Biotechnol J* 2006, 1, 549-555.
- [188] Neidhardt, F. C., Bloch, P. L., Smith, D. F., Culture medium for enterobacteria. *J Bacteriol* 1974, 119, 736-747.
- [189] Reeves, C. R., Using Genetic Algorithms with small populations. *Proceedings of the Fifth International Conference on Genetic Algorithms* 1993, Morgan Kaufmann Publ. San Mateo, California, 92 – 99.
- [190] Möllney, M., Freyer, S., Wichert, W., D., W.-B., GmbH, F. J., Programmdokumentation für das Programm GALOP (Vers. 2.2). 1998.
- [191] Bäck, T., Optimal Mutation Rates in Genetic Search. *Forest S (ed) Proceedings of the Fifth Conference on Genetic Algorithms. Morgan Kaufmann Publ. San Mateo, California: 1993, 2-8.*
- [192] Grefenstette, J., Optimization of Control Parameters for genetic Algorithms. *IEEE Transactions on Systems, Man and Cybernetics* 1986, SMC-16(1), 122-128.
- [193] BRENDA, [www.brenda-enzymes.info](http://www.brenda-enzymes.info) (05.05.2011).
- [194] Chang, A., Scheer, M., Grote, A., Schomburg, I., Schomburg, D., BRENDA, AMENDA and FRENDA the enzyme information system: new content and tools in 2009. *Nucleic acids research* 2009, 37, D588.
- [195] Taxonomy, <http://www.ncbi.nlm.nih.gov/Taxonomy> (05.05.2011).
- [196] Hiller, K., Grote, A., Scheer, M., Münch, R., Jahn, D., PrediSi: prediction of signal peptides and their cleavage positions. *Nucleic acids research* 2004, 32, W375.

- [197] Biedendieck R., Borgmeier C., Bunk B., Stammen S., *et al.*, Systems biology of recombinant protein production using *Bacillus megaterium*. *Methods in Enzymology* 2011, *In press*.
- [198] Mueller, O., Lightfoot, S., Schroeder, A., RNA integrity number (RIN)–standardization of RNA quality control. *Agilent Application Note, Publication* 2004, 1-8.
- [199] Lüders, S., David, F., Steinwand, M., Jordan, E., *et al.*, *Applied microbiology and biotechnology* 2011.
- [200] Malten, M., Hollmann, R., Deckwer, W. D., Jahn, D., Production and secretion of recombinant *Leuconostoc mesenteroides* dextranucrase DsrS in *Bacillus megaterium*. *Biotechnol Bioeng* 2005, 89, 206-218.
- [201] Dahl, M. K., Schmiedel, D., Hillen, W., Glucose and glucose-6-phosphate interaction with Xyl repressor proteins from *Bacillus* spp. may contribute to regulation of xylose utilization. *Journal of bacteriology* 1995, 177, 5467.
- [202] Walker, G. M., The roles of magnesium in biotechnology. *Critical Reviews in Biotechnology* 1994, 14, 311-354.
- [203] Petit-Glatron, M. F., Grajcar, L., Munz, A., Chambert, R., The contribution of the cell wall to a transmembrane calcium gradient could play a key role in *Bacillus subtilis* protein secretion. *Mol Microbiol* 1993, 9, 1097-1106.
- [204] Andreini, C., Bertini, I., Cavallaro, G., Holliday, G. L., Thornton, J. M., Metal ions in biological catalysis: from enzyme databases to general principles. *J Biol Inorg Chem* 2008, 13, 1205-1218.
- [205] Dedyukhina, E. G., Eroshin, V. K., Essential metal ions in the control of microbial metabolism. *Process Biochemistry* 1991, 26, 31-37.
- [206] Beveridge, T. J., Murray, R. G., Sites of metal deposition in the cell wall of *Bacillus subtilis*. *J. Bacteriol.* 1980, 141, 876-887.
- [207] Chambert, R., Petit-Glatron, M. F., Anionic polymers of *Bacillus subtilis* cell wall modulate the folding rate of secreted proteins. *FEMS microbiology letters* 1999, 179, 43-47.
- [208] Haddaoui, E., Chambert, R., Petit-Glatron, M. F., Lindy, O., Sarvas, M., *Bacillus subtilis* alpha-amylase: the rate limiting step of secretion is growth phase-independent. *FEMS microbiology letters* 1999, 173, 127-131.
- [209] Gold, V. A., Robson, A., Clarke, A. R., Collinson, I., Allosteric regulation of SecA: magnesium-mediated control of conformation and activity. *J Biol Chem* 2007, 282, 17424-17432.
- [210] Robson, A., Gold, V. A. M., Hodson, S., Clarke, A. R., Collinson, I., Energy transduction in protein transport and the ATP hydrolytic cycle of SecA. *Proceedings of the National Academy of Sciences* 2009, 106, 5111.
- [211] Papp, K. M., Maguire, M. E., The CorA Mg<sup>2+</sup> Transporter Does Not Transport Fe<sup>2+</sup>. *J. Bacteriol.* 2004, 186, 7653-7658.
- [212] Marquis, R. E., Salt-induced contraction of bacterial cell walls. *Journal of Bacteriology* 1968, 95, 775.
- [213] Dragosits, M., Stadlmann, J., Graf, A., Gasser, B., *et al.*, The response to unfolded protein is involved in osmotolerance of *Pichia pastoris*. *BMC genomics*, 11, 207.
- [214] Lopes da Silva, T., Piekova, L., Mileu, J., Roseiro, J. C., A comparative study using the dual staining flow cytometric protocol applied to *Lactobacillus rhamnosus* and *Bacillus licheniformis* batch cultures. *Enzyme and Microbial Technology* 2009, 45, 134-138.

- [215] Hewitt, C. J., Onyeaka, H., Lewis, G., Taylor, I. W., Nienow, A. W., A comparison of high cell density fed batch fermentations involving both induced and non induced recombinant *Escherichia coli* under well mixed small scale and simulated poorly mixed large scale conditions. *Biotechnology and bioengineering* 2007, 96, 495-505.
- [216] Sträuber, H., Müller, S., Viability states of bacteria-Specific mechanisms of selected probes. *Cytometry Part A* 2010, 77, 623-634.
- [217] Shi, L., Günther, S., Hübschmann, T., Wick, L. Y., *et al.*, Limits of propidium iodide as a cell viability indicator for environmental bacteria. *Cytometry Part A* 2007, 71, 592-598.
- [218] Kemper, M. A., Urrutia, M. M., Beveridge, T. J., Koch, A. L., Doyle, R. J., Proton motive force may regulate cell wall-associated enzymes of *Bacillus subtilis*. *Journal of bacteriology* 1993, 175, 5690.
- [219] Frykman, S., Srienc, F., Quantitating secretion rates of individual cells: design of secretion assays. *Biotechnology and bioengineering* 1998, 59, 214-226.
- [220] Manz, R., Assenmacher, M., Pflüger, E., Miltenyi, S., Radbruch, A., Analysis and sorting of live cells according to secreted molecules, relocated to a cell-surface affinity matrix. *Proceedings of the National Academy of Sciences of the United States of America* 1995, 92, 1921.
- [221] Müller, S., Cytomics reaches microbiology-population heterogeneity on the protein level caused by chemical stress. *Cytometry. Part A: the journal of the International Society for Analytical Cytology* 2008, 73, 3.
- [222] Schädel, F., Franco-Lara, E., Rapid sampling devices for metabolic engineering applications. *Applied microbiology and biotechnology* 2009, 83, 199-208.
- [223] Feldhaus, M., Siegel, R., Flow cytometric screening of yeast surface display libraries. *METHODS IN MOLECULAR BIOLOGY-CLIFTON THEN TOTOWA-* 2004, 263, 311-332.
- [224] Mattanovich, D., Borth, N., Applications of cell sorting in biotechnology. *Microbial Cell Factories* 2006, 5, 12.
- [225] Ackermann, J., Müller, S., Lösche, A., Bley, T., *Methylobacterium rhodesianum* cells tend to double the DNA content under growth limitations and accumulate PHB. *Journal of Biotechnology* 1995, 39, 9-20.
- [226] James, B. W., Mauchline, W. S., Dennis, P. J., Keevil, C. W., Wait, R., Poly-3-hydroxybutyrate in *Legionella pneumophila*, an energy source for survival in low-nutrient environments. *Applied and environmental microbiology* 1999, 65, 822.
- [227] Maskow, T., Müller, S., Lösche, A., Harms, H., Kemp, R., Control of continuous polyhydroxybutyrate synthesis using calorimetry and flow cytometry. *Biotechnology and bioengineering* 2006, 93, 541-552.
- [228] Steen, H. B., Boye, E., *Escherichia coli* growth studied by dual-parameter flow cytophotometry. *Journal of Bacteriology* 1981, 145, 1091.
- [229] Jolliffe, L. K., Doyle, R. J., Streips, U. N., The energized membrane and cellular autolysis in *Bacillus subtilis*. *Cell* 1981, 25, 753-763.
- [230] Strauch, M. A., Regulation of *Bacillus subtilis* gene expression during the transition from exponential growth to stationary phase. *Progress in nucleic acid research and molecular biology* 1993, 46, 123-123.
- [231] Ferrari, E., Jarnagin, A. S., Schmidt, B. F., Commercial production of extracellular enzymes. *Bacillus subtilis and other gram-positive bacteria. American Society for Microbiology, Washington, DC* 1993, 917-937.



- [232] Frankena, J., Verseveld, H. W., Stouthamer, A. H., A continuous culture study of the bioenergetic aspects of growth and production of exocellular protease in *Bacillus licheniformis*. *Applied microbiology and biotechnology* 1985, 22, 169-176.
- [233] Christiansen, T., Michaelsen, S., Wümpelmann, M., Nielsen, J., Production of savinase and population viability of *Bacillus clausii* during high cell density fed batch cultivations. *Biotechnology and bioengineering* 2003, 83, 344-352.
- [234] Calamita, H. G., Ehringer, W. D., Koch, A. L., Doyle, R. J., Evidence that the cell wall of *Bacillus subtilis* is protonated during respiration. *Proceedings of the National Academy of Sciences of the United States of America* 2001, 98, 15260.
- [235] Kirchner, G., Koch, A. L., Doyle, R. J., Energized membrane regulates cell pole formation in *Bacillus subtilis*. *FEMS Microbiology Letters* 1984, 24, 143-147.
- [236] Herbort, M., Klein, M., Manting, E. H., Driessen, A. J. M., Freudl, R., Temporal expression of the *Bacillus subtilis* secA gene, encoding a central component of the preprotein translocase. *Journal of bacteriology* 1999, 181, 493.
- [237] Jenzsch, M., Simutis, R., Eisbrenner, G., Stückerath, I., Lübbert, A., Estimation of biomass concentrations in fermentation processes for recombinant protein production. *Bioprocess and biosystems engineering* 2006, 29, 19-27.
- [238] NCBI, <http://www.ncbi.nlm.nih.gov/a> (15.05.2011).
- [239] Marchler-Bauer, A., Anderson, J. B., Cherukuri, P. F., DeWeese-Scott, C., *et al.*, CDD: a Conserved Domain Database for protein classification. *Nucleic acids research* 2005, 33, D192.
- [240] Williams, R. C., Rees, M. L., Jacobs, M. F., Prágai, Z., *et al.*, Production of *Bacillus anthracis* protective antigen is dependent on the extracellular chaperone, PrsA. *Journal of Biological Chemistry* 2003, 278, 18056.
- [241] Vitikainen, M., Pummi, T., Airaksinen, U., Wahlstrom, E., *et al.*, Quantitation of the capacity of the secretion apparatus and requirement for PrsA in growth and secretion of {alpha}-amylase in *Bacillus subtilis*. *Journal of Bacteriology* 2001, 183, 1881.
- [242] Vitikainen, M., Hyryläinen, H. L., Kivimäki, A., Kontinen, V. P., Sarvas, M., Secretion of heterologous proteins in *Bacillus subtilis* can be improved by engineering cell components affecting post translocational protein folding and degradation. *Journal of applied microbiology* 2005, 99, 363-375.
- [243] Cowburn, D., Peptide recognition by PTB and PDZ domains. *Current opinion in structural biology* 1997, 7, 835-838.
- [244] Schumann, W., Function and regulation of temperature-inducible bacterial proteins on the cellular metabolism. *Influence of Stress on Cell Growth and Product Formation* 2000, 1-33.
- [245] Pallen, M. J., Wren, B. W., The HtrA family of serine proteases. *Molecular microbiology* 1997, 26, 209-221.
- [246] Yeats, C., Rawlings, N. D., Bateman, A., The PepSY domain: a regulator of peptidase activity in the microbial environment? *Trends in biochemical sciences* 2004, 29, 169-172.
- [247] Otridge, J., Gollnick, P., MtrB from *Bacillus subtilis* binds specifically to trp leader RNA in a tryptophan-dependent manner. *Proceedings of the National Academy of Sciences of the United States of America* 1993, 90, 128.
- [248] Kuroda, A., Sugimoto, Y., Funahashi, T., Sekiguchi, J., Genetic structure, isolation and characterization of a *Bacillus licheniformis* cell wall hydrolase. *Molecular and General Genetics* MGG 1992, 234, 129-137.



- [249] Berka, R. M., Hahn, J., Albano, M., Draskovic, I., *et al.*, Microarray analysis of the *Bacillus subtilis* K state: genome wide expression changes dependent on ComK. *Molecular microbiology* 2002, 43, 1331-1345.
- [250] Bunai, K., Yamada, K., Hayashi, K., Nakamura, K., Yamane, K., Enhancing Effect of *Bacillus subtilis* Ffh, a Homologue of the SRP54 Subunit of the Mammalian Signal Recognition Particle, on the Binding of Sec A to Precursors of Secretory Proteins In Vitro. *Journal of biochemistry* 1999, 125, 151.
- [251] Eymann, C., Homuth, G., Scharf, C., Hecker, M., *Bacillus subtilis* functional genomics: global characterization of the stringent response by proteome and transcriptome analysis. *Journal of bacteriology* 2002, 184, 2500.
- [252] Gallant, J. A., Stringent control in *E. coli*. *Annual Review of Genetics* 1979, 13, 393-415.
- [253] Miethke, M., Westers, H., Blom, E. J., Kuipers, O. P., Marahiel, M. A., Iron starvation triggers the stringent response and induces amino acid biosynthesis for bacillibactin production in *Bacillus subtilis*. *Journal of bacteriology* 2006, JB. 01049-01006v01041.
- [254] Grossman, A. D., Taylor, W. E., Burton, Z. F., Burgess, R. R., Gross, C. A., Stringent response in *Escherichia coli* induces expression of heat shock proteins\* 1. *Journal of molecular biology* 1985, 186, 357-365.
- [255] Mandelstam, J., The intracellular turnover of protein and nucleic acids and its role in biochemical differentiation. *Microbiology and Molecular Biology Reviews* 1960, 24, 289.
- [256] Mader, U., Homuth, G., Scharf, C., Buttner, K., *et al.*, Transcriptome and proteome analysis of *Bacillus subtilis* gene expression modulated by amino acid availability. *Journal of bacteriology* 2002, 184, 4288.
- [257] Wülfing, C., Plückthun, A., Protein folding in the periplasm of *Escherichia coli*. *Molecular microbiology* 1994, 12, 685-692.
- [258] Göthel, S. F., Scholz, C., Schmid, F. X., Marahiel, M. A., Cyclophilin and Trigger Factor from *Bacillus subtilis* Catalyze In Vitro Protein Folding and Are Necessary for Viability under Starvation Conditions. *Biochemistry* 1998, 37, 13392-13399.
- [259] Sandén, A. M., Prytz, I., Tubulekas, I., Förberg, C., *et al.*, Limiting factors in *Escherichia coli* fed batch production of recombinant proteins. *Biotechnology and bioengineering* 2003, 81, 158-166.
- [260] Dong, H., Nilsson, L., Kurland, C. G., Gratuitous overexpression of genes in *Escherichia coli* leads to growth inhibition and ribosome destruction. *Journal of bacteriology* 1995, 177, 1497.
- [261] Puertas, J. M., Nannenga, B. L., Dornfeld, K. T., Betton, J. M., Baneyx, F., Enhancing the secretory yields of leech carboxypeptidase inhibitor in *Escherichia coli*: Influence of trigger factor and signal recognition particle. *Protein expression and purification*, 74, 122-128.
- [262] Wu, S. C., Yeung, J. C., Duan, Y., Ye, R., *et al.*, Functional production and characterization of a fibrin-specific single-chain antibody fragment from *Bacillus subtilis*: Effects of molecular chaperones and a wall-bound protease on antibody fragment production. *Applied and Environmental Microbiology* 2002, 68, 3261-3269.
- [263] Wu, S. C., Ye, R., Wu, X. C., Ng, S. C., Wong, S. L., Enhanced secretory production of a single-chain antibody fragment from *Bacillus subtilis* by coproduction of molecular chaperones. *Journal of bacteriology* 1998, 180, 2830.
- [264] Epps, D. E., Wolfe, M. L., Groppi, V., Characterization of the steady-state and dynamic fluorescence properties of the potential-sensitive dye bis-(1, 3-dibutylbarbituric acid) trimethine oxonol (Dibac4 (3)) in model systems and cells. *Chemistry and physics of lipids* 1994, 69, 137-150.

- [265] Alper, H., Moxley, J., Nevoigt, E., Fink, G. R., Stephanopoulos, G., Engineering yeast transcription machinery for improved ethanol tolerance and production. *Science* 2006, 314, 1565.
- [266] Gardner, T., Collins, J. J., Google Patents 2001.
- [267] Craig, V., J, Adams, M.D, *et al.*
- [268] Dauner, M., Sonderegger, M., Hochuli, M., Szyperski, T., *et al.*, Intracellular carbon fluxes in riboflavin-producing *Bacillus subtilis* during growth on two-carbon substrate mixtures. *Appl Environ Microbiol* 2002, 68, 1760-1771.
- [269] Jehmlich, N., Hübschmann, T., Gesell Salazar, M., Völker, U., *et al.*, Advanced tool for characterization of microbial cultures by combining cytomics and proteomics. *Applied microbiology and biotechnology* 2010, 1-10.
- [270] Hewitt, C. J., Nebe-Von Caron, G., Nienow, A. W., McFarlane, C. M., The use of multi-parameter flow cytometry to compare the physiological response of *Escherichia coli* W3110 to glucose limitation during batch, fed-batch and continuous culture cultivations. *Journal of biotechnology* 1999, 75, 251-264.
- [271] David, F., Hebeisen, M., Schade, G., Franco-Lara, E., Di Berardino, M., Viability and metabolic activity analysis of *Bacillus megaterium* cells by impedance flow cytometry. *Biotechnology and Bioengineering* 2011 109 (2), 483-492.
- [272] Kacmar, J., Zamamiri, A., Carlson, R., Abu-Absi, N. R., Srienc, F., Single-cell variability in growing *Saccharomyces cerevisiae* cell populations measured with automated flow cytometry. *Journal of biotechnology* 2004, 109, 239-254.
- [273] Sitton, G., Srienc, F., Mammalian cell culture scale-up and fed-batch control using automated flow cytometry. *Journal of biotechnology* 2008, 135, 174-180.
- [274] Petit-Glatron, M. F., Monteil, I., Benyahia, F., Chambert, R., *Bacillus subtilis* levansucrase: amino acid substitutions at one site affect secretion efficiency and refolding kinetics mediated by metals. *Mol Microbiol* 1990, 4, 2063-2070.
- [275] Gernaey, K. V., Lantz, A. E., Tufvesson, P., Woodley, J. M., Sin, G., Application of mechanistic models to fermentation and biocatalysis for next-generation processes. *Trends in biotechnology* 2010, 28, 346-354.
- [276] Ramkrishna, D., ScienceDirect, *Population balances: theory and applications to particulate systems in engineering*, Academic Press San Diego 2000.
- [277] Fredrickson, A. G., Population balance equations for cell and microbial cultures revisited. *AIChE journal* 2003, 49, 1050-1059.
- [278] Lencastre Fernandes, R., Nierychlo, M., Lundin, L., Pedersen, A. E., *et al.*, Experimental methods and modeling techniques for description of cell population heterogeneity. *Biotechnology Advances* 2011.
- [279] Noack, S., Klöden, W., Bley, T., Modeling synchronous growth of bacterial populations in phased cultivation. *Bioprocess and biosystems engineering* 2008, 31, 435-443.
- [280] Mantzaris, N. V., Srienc, F., Daoutidis, P., Nonlinear productivity control using a multi-staged cell population balance model. *Chemical Engineering Science* 2002, 57, 1-14.
- [281] Wood, C. R., Dorner, A. J., Morris, G. E., Alderman, E. M., *et al.*, High level synthesis of immunoglobulins in Chinese hamster ovary cells. *The Journal of Immunology* 1990, 145, 3011.
- [282] Bebbington, C. R., Renner, G., Thomson, S., King, D., *et al.*, High-level expression of a recombinant antibody from myeloma cells using a glutamine synthetase gene as an amplifiable selectable marker. *Nature Biotechnology* 1992, 10, 169-175.

- [283] Farid, S. S., Process economics of industrial monoclonal antibody manufacture. *Journal of Chromatography B* 2007, 848, 8-18.
- [284] King, D. J., Byron, O. D., Mountain, A., Weir, N., *et al.*, Expression, purification and characterization of B72. 3 Fv fragments. *Biochemical Journal* 1993, 290, 723.
- [285] Dorai, H., McCartney, J. E., Hudziak, R. M., Tai, M. S., *et al.*, Mammalian Cell Expression of Single-Chain Fv (sFv) Antibody Proteins and Their C-terminal Fusions with Interleukin-2 and Other Effector Domains. *Nature Biotechnology* 1994, 12, 890-897.
- [286] Gerngross, T. U., Advances in the production of human therapeutic proteins in yeasts and filamentous fungi. *Nature biotechnology* 2004, 22, 1409-1414.
- [287] Li, H., Sethuraman, N., Stadheim, T. A., Zha, D., *et al.*, Optimization of humanized IgGs in glycoengineered *Pichia pastoris*. *Nature biotechnology* 2006, 24, 210-215.
- [288] Seimetz, D., Novel Monoclonal Antibodies for Cancer Treatment: The Trifunctional Anti-body Catumaxomab (Removab®). *Journal of Cancer* 2011, 2, 309-316.
- [289] Saerens, D., Ghassabeh, G. H., Muyldermans, S., Single-domain antibodies as building blocks for novel therapeutics. *Current Opinion in Pharmacology* 2008, 8, 600-608.
- [290] Wu, A. M., Senter, P. D., Arming antibodies: prospects and challenges for immunoconjugates. *Nature biotechnology* 2005, 23, 1137-1146.
- [291] Yamane Ohnuki, N., Kinoshita, S., Inoue Urakubo, M., Kusunoki, M., *et al.*, Establishment of FUT8 knockout Chinese hamster ovary cells: An ideal host cell line for producing completely defucosylated antibodies with enhanced antibody dependent cellular cytotoxicity. *Biotechnology and bioengineering* 2004, 87, 614-622.
- [292] Hust, M., Dubel, S., Schirrmann, T., Selection of recombinant antibodies from antibody gene libraries. *Methods In Molecular Biology-Clifton Then Totowa-* 2007, 408, 243.
- [293] Hust, M., Meyer, T., Voedisch, B., Rülker, T., *et al.*, A human scFv antibody generation pipeline for proteome research. *Journal of Biotechnology* 2011.
- [294] Hust, M., Mersmann, M., Phage Display and Selection in Microtitre Plates. *Antibody Engineering* 2010, 139-149.
- [295] Walsh, G., Biopharmaceutical benchmarks 2010, *Nat Biotechnol*, 28(9), 917-924.



## 7 Nomenclature

### 7.1 Abbreviations

AB	antibody
ABF	antibody fragment
ADCC	AB-dependent cellular cytotoxicity
ATP	adenosine triphosphate
BB	best biomass
BHK	Baby Hamster Kidney
BIC	Baysian Information Criterion
BMD	<i>Bacillus megaterium</i> DSM 319
BP	band pass
BP	best production
BRENDA	Braunschweig Enzyme Database
CAGR	compound annual growth rate
CCCP	carbonyl cyanide m-chlorophenylhydrazone
CCD	central composite design
CcpA	catabolite control protein A
CDC	complement-dependent cellular cytotoxicity
CDR	complementarity determining region
CDW	cell dry weight
CER	carbondioxide evolution rate
cGMP	current Good Manufacturing Practise
CHO	Chinese Hamster Ovary
CLSM	confocal laser scanning microscopy
COG	cost of goods
conc.	concentration
cre	catabolite response element
CRP	c reactive proteine
CV	coefficient of variation
Dibac4(3)	bis-(1,3-dibutylbarbituric acid) trimethine oxonol
DiOC2	3,3'-diethyloxacarbocyanine iodide

DiOC6	3,3'-dihexyloxacarbocyanine iodide
DNA	Desoxyribonucleic acid
DO	dissolved oxygen
DoE	Design of Experiments
DOL	degree of labeling
DSB	double strand break
ELISA	enzyme-linked-immunosorbent-assay
EU	European Union
EV	electronic volume
exp I	first exponential phase
exp II	second exponential phase
FACS	fluorescence-activated cell sorting
FC	fluorescence concentration
FC	fold changes
FCM	flow cytometry
FDA	Food and Drug Administration
FESEM	Immuno field emission scanning electron microscopy
FL	fluorescence
FSD	fluorescence surface density
GA	Genetic Algorithm
GALOP	Genetic Algorithms for Optimization of Processes
GFP	green fluorescence protein
GRAS	generally regarded as safe
gTME	global transcription machinery engineering
HEK	Human Embryonic Kidney
HER2	human epidermal growth factor receptor 2
HMS	hyper mutable subpopulation
HPLC	high performance liquid chromatography
HRP	horse radish peroxidase
Ig	immunoglobulin
ITEM	Institut für Toxikologie und Experimentelle Medizin
LP	long pass
mAB	monoclonal antibody
MP	membrane potential
mRNA	messenger RNA
NAD	Nicotinamide adenine dinucleotide
NCBI	National Center for Biotechnology Information



OD	optical density
OUR	oxygen uptake rate
p.i.	post induction
PAT	Process Analytical Technologies
PBS	phosphat buffered saline
PBST	phosphat buffered saline tween
PEG	polyethylene glycol
PHB	polyhydroxybutyrate
PI	propidium iodide
PMT	photomultiplier
PP	pareto optimal scores
Prod_Iten	production intensity
PTM	post translational modifications
RIN	RNA integrity number
RNA	ribonucleic acid
rRNA	ribosomal RNA
RT	room temperature
scFV	single chain Fab variable
sdAB	single domain antibody
SDS	sodium dodecyl sulfat
SE	secondary electron
Sec	secretion
SEM	scanning electronic microscope
SFB	Sonderforschungsbereich
SRP	signal recognition particle
SS	sidewards scatter
stat I	first stationary phase
stat II	second stationary phase
TE	Tris-EDTA
TIGR	The Institute for Genomic Research
TMB	tetramethylbenzidine
TNF	tumor necrosis factor
UPR	unfolded protein response
VH	variable heavy
VL	variable light
XylR	Xylose repressor





## 7.2 Symbols

$S$	(g/L)	substrate concentration
$V$	(L)	volume
$X$	(g/L)	biomass concentration
$\mu$	(1/h)	specific growth rate
$Q_P$	(mg/h)	production rate
$q_P$	(mg/g/h)	specific production rate
$Y_{X/S}$	(g/g)	biomass yield
$Y_{P/X}$	(mg/g)	product yield
$Q_{O_2}$	(mg/L/h)	Oxygen Uptake Rate (OUR)
$Q_{CO_2}$	(mg/L/h)	Carbon Dioxide Evolution Rate (CER)
$q_{O_2}$	(mmol/g/h)	specific OUR
$q_{CO_2}$	(mmol/g/h)	specific CER
$RQ$	(-)	respiratory quotient

- 
- Band 1**     **Sunder, Matthias:** Oxidation grundwasserrelevanter Spurenverunreinigungen mit Ozon und Wasserstoffperoxid im Rohrreaktor. 1996. FIT-Verlag · Paderborn, ISBN 3-932252-00-4
- Band 2**     **Pack, Hubertus:** Schwermetalle in Abwasserströmen: Biosorption und Auswirkung auf eine schadstoffabbauende Bakterienkultur. 1996. FIT-Verlag · Paderborn, ISBN 3-932252-01-2
- Band 3**     **Brüggenthies, Antje:** Biologische Reinigung EDTA-haltiger Abwässer. 1996. FIT-Verlag · Paderborn, ISBN 3-932252-02-0
- Band 4**     **Liebelt, Uwe:** Anaerobe Teilstrombehandlung von Restflotten der Reaktivfärberei. 1997. FIT-Verlag · Paderborn, ISBN 3-932252-03-9
- Band 5**     **Mann, Volker G.:** Optimierung und Scale up eines Suspensionsreaktorverfahrens zur biologischen Reinigung feinkörniger, kontaminierter Böden. 1997. FIT-Verlag · Paderborn, ISBN 3-932252-04-7
- Band 6**     **Boll Marco:** Einsatz von Fuzzy-Control zur Regelung verfahrenstechnischer Prozesse. 1997. FIT-Verlag · Paderborn, ISBN 3-932252-06-3
- Band 7**     **Büscher, Klaus:** Bestimmung von mechanischen Beanspruchungen in Zweiphasenreaktoren. 1997. FIT-Verlag · Paderborn, ISBN 3-932252-07-1
- Band 8**     **Burghardt, Rudolf:** Alkalische Hydrolyse – Charakterisierung und Anwendung einer Aufschlußmethode für industrielle Belebtschlämme. 1998. FIT-Verlag · Paderborn, ISBN 3-932252-13-6
- Band 9**     **Hemmi, Martin:** Biologisch-chemische Behandlung von Färbereiabwässern in einem Sequencing Batch Process. 1999. FIT-Verlag · Paderborn, ISBN 3-932252-14-4
- Band 10**    **Dziallas, Holger:** Lokale Phasengehalte in zwei- und dreiphasig betriebenen Blasensäulenreaktoren. 2000. FIT-Verlag · Paderborn, ISBN 3-932252-15-2
- Band 11**    **Scheminski, Anke:** Teiloxidation von Faulschlamm mit Ozon. 2001. FIT-Verlag · Paderborn, ISBN 3-932252-16-0
- Band 12**    **Mahnke, Eike Ulf:** Fluidodynamisch induzierte Partikelbeanspruchung in pneumatisch gerührten Mehrphasenreaktoren. 2002. FIT-Verlag · Paderborn, ISBN 3-932252-17-9
- Band 13**    **Michele, Volker:** CDF modeling and measurement of liquid flow structure and phase holdup in two- and three-phase bubble columns. 2002. FIT-Verlag · Paderborn, ISBN 3-932252-18-7
- Band 14**    **Wäsche, Stefan:** Einfluss der Wachstumsbedingungen auf Stoffübergang und Struktur von Biofilmsystemen. 2003. FIT-Verlag · Paderborn, ISBN 3-932252-19-5
- Band 15**    **Krull Rainer:** Produktionsintegrierte Behandlung industrieller Abwässer zur Schließung von Stoffkreisläufen. 2003. FIT-Verlag · Paderborn, ISBN 3-932252-20-9
- Band 16**    **Otto, Peter:** Entwicklung eines chemisch-biologischen Verfahrens zur Reinigung EDTA enthaltender Abwässer. 2003. FIT-Verlag · Paderborn, ISBN 3-932252-21-7

- Band 17**     **Horn, Harald:** Modellierung von Stoffumsatz und Stofftransport in Biofilmsystemen. 2003. FIT-Verlag · Paderborn, ISBN 3-932252-22-5
- Band 18**     **Mora Naranjo, Nelson:** Analyse und Modellierung anaerober Abbauprozesse in Deponien. 2004. FIT-Verlag · Paderborn, ISBN 3-932252-23-3
- Band 19**     **Döpfens, Eckart:** Abwasserbehandlung und Prozesswasserrecycling in der Textilindustrie. 2004. FIT-Verlag · Paderborn, ISBN 3-932252-24-1
- Band 20**     **Haarstrick, Andreas:** Modellierung millieugesteuerter biologischer Abbauprozesse in heterogenen problembelasteten Systemen. 2005. FIT-Verlag · Paderborn, ISBN 3-932252-27-6
- Band 21**     **Baaß, Anne-Christina:** Mikrobieller Abbau der Polyaminopolycarbonsäuren Propylendiamin-tetraacetat (PDTA) und Diethylentriaminpentaacetat (DTPA). 2004. FIT-Verlag · Paderborn, ISBN 3-932252-26-8
- Band 22**     **Staudt, Christian:** Entwicklung der Struktur von Biofilmen. 2006. FIT-Verlag · Paderborn, ISBN 3-932252-28-4
- Band 23**     **Pilz, Roman Daniel:** Partikelbeanspruchung in mehrphasig betriebenen Airlift-Reaktoren. 2006. FIT-Verlag · Paderborn, ISBN 3-932252-29-2
- Band 24**     **Schallenberg, Jörg:** Modellierung von zwei- und dreiphasigen Strömungen in Blasensäulenreaktoren. 2006. FIT-Verlag · Paderborn, ISBN 3-932252-30-6
- Band 25**     **Enß, Jan Hendrik:** Einfluss der Viskosität auf Blasensäulenströmungen. 2006. FIT-Verlag · Paderborn, ISBN 3-932252-31-4
- Band 26**     **Kelly, Sven:** Fluidodynamischer Einfluss auf die Morphogenese von Biopellets filamentöser Pilze. 2006. FIT-Verlag · Paderborn, ISBN 3-932252-32-2
- Band 27**     **Grimm, Luis Hermann:** Sporenaggregationsmodell für die submerse Kultivierung koagulativer Myzelbildner. 2006. FIT-Verlag · Paderborn, ISBN 3-932252-33-0
- Band 28**     **León Ohl, Andrés:** Wechselwirkungen von Stofftransport und Wachstum in Biofilmsystemen. 2007. FIT-Verlag · Paderborn, ISBN 3-932252-34-9
- Band 29**     **Emmler, Markus:** Freisetzung von Glucoamylase in Kultivierungen mit *Aspergillus niger*. 2007. FIT-Verlag · Paderborn, ISBN 3-932252-35-7
- Band 30**     **Leonhäuser, Johannes:** Biotechnologische Verfahren zur Reinigung von quecksilberhaltigem Abwasser. 2007. FIT-Verlag · Paderborn, ISBN 3-932252-36-5
- Band 31**     **Jungebloud, Anke:** Untersuchung der Genexpression in *Aspergillus niger* mittels Echtzeit-PCR. 1996. FIT-Verlag · Paderborn, ISBN 978-3-932252-37-2
- Band 32**     **Hille, Andrea:** Stofftransport und Stoffumsatz in filamentösen Pilzpellets. 2008. FIT-Verlag · Paderborn, ISBN 978-3-932252-38-9
- Band 33**     **Fürch, Tobias:** Metabolic characterization of recombinant protein production in *Bacillus megaterium*. 2008. FIT-Verlag · Paderborn, ISBN 978-3-932252-39-6

- 
- Band 34**     **Grote, Andreas Georg:** Datenbanksysteme und bioinformatische Werkzeuge zur Optimierung biotechnologischer Prozesse mit Pilzen. 2008. FIT-Verlag · Paderborn, ISBN 978-3-932252-40-120
- Band 35**     **Möhle, Roland Bernhard:** An Analytic-Synthetic Approach Combining Mathematical Modeling and Experiments – Towards an Understanding of Biofilm Systems. 2008. FIT-Verlag · Paderborn, ISBN 978-3-932252-41-9
- Band 36**     **Reichel, Thomas:** Modelle für die Beschreibung des Emissionsverhaltens von Siedlungsabfällen. 2008. FIT-Verlag · Paderborn, ISBN 978-3-932252-42-6
- Band 37**     **Schultheiss, Ellen:** Charakterisierung des Exopolysaccharids PS-EDIV von *Spingomonas pituitosa*. 2008. FIT-Verlag · Paderborn, ISBN 978-3-932252-43-3
- Band 38**     **Dreger, Michael Andreas:** Produktion und Aufarbeitung des Exopolysaccharids PS-EDIV aus *Spingomonas pituitosa*. 1996. FIT-Verlag · Paderborn, ISBN 978-3-932252-44-0
- Band 39**     **Wiebels, Cornelia:** A Novel Bubble Size Measuring Technique for High Bubble Density Flows. 2009. FIT-Verlag · Paderborn, ISBN 978-3-932252-45-7
- Band 40**     **Bohle, Kathrin:** Morphologie- und produktionsrelevante Gen- und Proteinexpression in submersen Kultivierungen von *Aspergillus niger*. 2009. FIT-Verlag · Paderborn, ISBN 978-3-932252-46-2
- Band 41**     **Fallet, Claas:** Reaktionstechnische Untersuchungen der mikrobiellen Stressantwort und ihrer biotechnologischen Anwendungen. 2009. FIT-Verlag · Paderborn, ISBN 978-3-932252-47-1
- Band 42**     **Vetter, Andreas:** Sequential Co-simulation as Method to Couple CFD and Biological Growth in a Yeast. 2009. FIT-Verlag · Paderborn, ISBN 978-3-932252-48-8
- Band 43**     **Jung, Thomas:** Einsatz chemischer Oxidationsverfahren zur Behandlung industrieller Abwässer. 2010. FIT-Verlag · Paderborn, ISBN 978-3-932252-49-5
- Band 45**     **Herrmann, Tim:** Transport von Proteinen in Partikeln der Hydrophoben Interaktions Chromatographie. 2010. FIT-Verlag · Paderborn, ISBN 978-3-932252-51-8
- Band 46**     **Becker, Judith:** Systems Metabolic Engineering of *Corynebacterium glutamicum* towards improved Lysine Production. 2010. Cuvillier-Verlag · Göttingen, ISBN 978-3-86955-426-6
- Band 47**     **Melzer, Guido:** Metabolic Network Analysis of the Cell Factory *Aspergillus niger*. 2010. Cuvillier-Verlag · Göttingen, ISBN 978-3-86955-456-3
- Band 48**     **Bolten J., Christoph:** Bio-based Production of L-Methionine in *Corynebacterium glutamicum*. 2010. Cuvillier-Verlag · Göttingen, ISBN 978-3-86955-486-0
- Band 49**     **Lüders, Svenja:** Prozess- und Proteomanalyse gestresster Mikroorganismen. 2010. Cuvillier-Verlag · Göttingen, ISBN 978-3-86955-435-8

- Band 50**    **Wittmann, Christoph:** Entwicklung und Einsatz neuer Tools zur metabolischen Netzwerkanalyse des industriellen Aminosäure-Produzenten *Corynebacterium glutamicum*. 2010. Cuvillier-Verlag · Göttingen, ISBN 978-3-86955-445-7
- Band 51**    **Edlich, Astrid:** Entwicklung eines Mikroreaktors als Screening-Instrument für biologische Prozesse. 2010. Cuvillier-Verlag · Göttingen, ISBN 978-3-86955-470-9
- Band 52**    **Hage, Kerstin:** Bioprozessoptimierung und Metabolomanalyse zur Proteinproduktion in *Bacillus licheniformis*. 2010. Cuvillier-Verlag · Göttingen, ISBN 978-3-86955-578-2
- Band 53**    **Kiep, Katina Andrea:** Einfluss von Kultivierungsparametern auf die Morphologie und Produktbildung von *Aspergillus niger*. 2010. Cuvillier-Verlag · Göttingen, ISBN 978-3-86955-632-1
- Band 54**    **Fischer, Nicole:** Experimental investigations on the influence of physico-chemical parameters on anaerobic degradation in MBT residual waste. 2011. Cuvillier-Verlag · Göttingen, ISBN 978-3-86955-679-6
- Band 55**    **Schädel, Friederike:** Stressantwort von Mikroorganismen. 2011. Cuvillier-Verlag · Göttingen, ISBN 978-3-86955-746-5
- Band 56**    **Wichter, Johannes:** Untersuchung der L-Cystein-Biosynthese in *Escherichia coli* mit Techniken der Metabolom- und <sup>13</sup>C-Stoffflussanalyse. 2011. Cuvillier-Verlag · Göttingen, ISBN 978-3-86955-750-2
- Band 57**    **Knappik, Irena Isabell:** Charakterisierung der biologischen und chemischen Reaktionsprozesse in Siedlungsabfällen. 2011. Cuvillier-Verlag · Göttingen, ISBN 978-3-86955-760-1
- Band 58**    **Driouch, Habib:** Systems biotechnology of recombinant protein production in *Aspergillus niger*. 2011. Cuvillier-Verlag · Göttingen, ISBN 978-3-86955-808-0
- Band 59**    **Gehder, Matthias:** Systems biotechnology of recombinant protein production in *Aspergillus niger*. 2011. Cuvillier-Verlag · Göttingen, ISBN 978-3-86955-808-0
- Band 60**    **Sommer, Becky:** Systems biotechnology of recombinant protein production in *Aspergillus niger*. 2011. Cuvillier-Verlag · Göttingen, ISBN 978-3-86955-808-0
- Band 61**    **Dohnt, Katrin:** Charakterisierung von *Pseudomonas aeruginosa*-Biofilmen in einem *in vitro*-Harnwegskathetersystem. 2011. Cuvillier-Verlag · Göttingen, ISBN 978-3-86955-852-3
- Band 62**    **Greis, Tillman:** Modelling the risk of chlorinated hydrocarbons in urban groundwater. 2011. Cuvillier-Verlag · Göttingen, ISBN 978-3-86955-970-4







